

UNIVERSITA' DELLA CALABRIA



Dipartimento di Fisica

Università della Calabria

Department of Physics

Astronomia & Astrofisica FIS/05

“Bernardino Telesio”

“Doctorate School of Science and Technique”

Curriculum in “Physics of Complex Systems”

Cycle XXV

Title

SEA LEVEL CHANGES AND VERTICAL MOTION OF THE LAND IN THE
MEDITERRANEAN AT DIFFERENT TIME SCALES

PhD Candidate

Marco Anzidei

Supervisor
Prof. Ignazio Guerra

School Director
Prof. Roberto Bartolino

Curriculum Coordinator
Prof. Vincenzo Carbone

2011-2012

INDEX

Foreword	Pag.5
1. Introduction and research goal	Pag.8
2. Sea level	Pag.10
3. Global scale changes	Pag.15
4. The Mediterranean region	Pag.19
5. The sea level indicators	Pag.25
5.1 The archaeological indicators	Pag.27
5.2 The roman fish tanks	Pag.29
6. Vertical land movements	Pag.32
7. Recent findings for the coast of Calabria	Pag.35
7.1 Tyrrhenian coast	Pag.36
7.2 Ionian coast	Pag.39
7.3 Remarks on the Calabria region	Pag.39
8. Sea level changes at different time scales in the Mediterranean from Tide Gauge data	Pag.42
8.1 The ISPRA tidal network	Pag.43
8.2 Tidal time series 2001-2001 - ISPRA network (Italy)	Pag.46
8.3 The longest tidal records in the Mediterranean	Pag.53
9. Tsunami recordings in the Mediterranean Sea from tidal stations: case studies	Pag.66
9.1 The May 21, 2003, Mw 6.8 Boumerdès earthquake (Algeria)	Pag.67
9.2 The March 11, 2011, M=9.0 Tohoku-Oki earthquake (Japan)	Pag.71
10. Future predictions	Pag.79
11. Concluding remarks	Pag.90
References	Pag.91
List of papers and abstracts published during the Doctorate	Pag. 103
Annexes	Pag. 105

Annex 1 - A. Vecchio, M. Anzidei, V. Capparelli, V. Carbone and I. Guerra. Has the Mediterranean Sea felt the March 11th, 2011, Mw 9.0 Tohoku-Oki earthquake? *EPL*, 98 (2012) 59001. doi: 10.1209/0295-5075/98/59001

Annex 2 - K. Lambeck, F. Antonioli, M. Anzidei, L. Ferranti, G. Leoni, G. Scicchitano, S. Silenzi. Sea level change along the Italian coast during the Holocene and projections for the future. *Quaternary International*, 2010. DOI 10.1016/j.quaint.2010.04.026

Annex 3 - Kurt Lambeck, Fabrizio Antonioli, Marco Anzidei. Sea level change along the Tyrrhenian coast from early Holocene to the present. *Accademia Nazionale dei Lincei, Atti dei convegni Lincei*, 254, IX Giornata mondiale dell'acqua, Il bacino del Tevere, Roma, 2010.

Annex 4 - M. Anzidei, F. Antonioli, A. Benini, K. Lambeck, D. Sivan, E. Serpelloni, P. Stocchi. Sea level change and vertical land movements since the last two millennia along the coasts of southwestern Turkey and Israel. *Quaternary International*, 2010. doi:10.1016/j.quaint.2010.05.005

Annex 5 - M. Anzidei, F. Antonioli, K. Lambeck, A. Benini, M. Soussi. New insights on the relative sea level change during Holocene along the coasts of Tunisia and western Libya from archaeological and geomorphological markers. *Quaternary International*, 2010 DOI: 10.1016/j.quaint.2010.03.01

Annex 6 - Marco Anzidei, Fabrizio Antonioli, Alessandra Benini, Anna Gervasi, Ignazio Guerra (2012). Evidence of vertical tectonic uplift at Briatico (Calabria, Italy) inferred from Roman age maritime archaeological indicators. *Quaternary International*, in press (2012), doi:10.1016/j.quaint.2012.01.019

*The past resembles the future
more than a drop of water resembles another*

Ibn Khaldun

Foreword

The Mediterranean is likely the most amazing sea of the world as it keeps jealously the remnants of the past signs of its geological and archaeological history. The *Mare Nostrum* of the roman is just a little basin with respect to the Oceans, thus favoring the cultural and commercial exchanges through the ancient Mediterranean populations. In this way, besides the aqueducts, the fish tanks built along the coast of the Mediterranean are among the most marvelous exemplary structures built around 2000 years ago by the roman hydraulic engineers. They were built along the shores to embellish the maritime villas of the wealthy Romans and to breed fish as well. These installations had constructional elements, such as tidally controlled channels equipped with sluice gates for water exchange in the basins that bear directly on sea level. Well-preserved remains of these provide a precise measure of the intervening sea-level change because they exactly show the mean sea level at the time of their construction. In addition, they provide information on the vertical motion of the land being sometimes constructed in active tectonics and volcanic zones. These pools allow us to extract from their constructional parts crucial information to understand one of the most critical effects caused by the global changes affecting our planet: the rising sea level.

It is quite funny for me to understand after several years when I was just a young boy that used to spend his summer holidays swimming and fishing in the large roman fish tanks of Torre Astura near Anzio, that in 1976 my colleagues Pirazzoli, Schmiedt, Caputo and Pieri, were in competition to publish their first results on the sea level position in roman times from these same fish tanks. And it was nice for me to swim back again into these fish tanks after years and use them as valuable paleo-sea level indicators, discovering that previous studies did not recognize the right indicators, thus underestimating the changes in sea level.

In the meantime, I had a degree in Geology and an extensively experience in geophysics and geodesy that allow me to understand and appreciate the precious information that we can get from these maritime structures. These considerations induced me to begin new and extensive surveys in Italy and in the Mediterranean, searching for the archaeological evidences of past sea levels, to understand the changes and possibly to estimate the future trends. Therefore, in the frame of research projects, I had the possibility to visit a large number of coastal archaeological structures located in many parts of the Mediterranean. In these research programs I had the opportunity to collaborate with many scientists from different countries.

Mainly I benefit from the collaboration with Kurt Lambeck, Emeritus Professor of the Australian National University and former President of the Australian Academy of Science. Kurt is the most expert geophysicist in sea level and introduced me to the multidisciplinary research including geodesy, geology, geomorphology, topography, biology and archaeology, all joined together to interpret and model the observations. With him, I had long discussions on the high validity of the roman fish tanks as sea level gauges. I am greatly thankful to Kurt, because he opened my mind bringing me toward new limits of geophysics during these years. In 2012 he won the Balzan Prize in the Earth Sciences "*for his exceptional contribution to the understanding of the relationship between post glacial rebound and sea level changes. His findings have radically modified climate science*". I am proud that our common research in the Mediterranean played an important role in these results.

I also had benefit from the long discussions with marine archaeologists like Piero Gianfrotta, Rita Auriemma, Emanuela Solinas and many others. I am particularly thankful

to Alessandra Benini. She introduced me since the beginning into maritime archaeology, providing many historical books and archaeological papers with the description of most of the archaeological sites we have visited. With Alessandra we introduced for the first time the basic concept of “functional elevation”, which is at the basis of our archeological interpretations of roman sea level. I always appreciated her criticism and the great skill during field surveys even in remote and uncomfortable coastal areas of the Mediterranean. We spent together nice and hard times into the fish tanks and other archaeological indicators, sometimes polluted by modern coastal installations. We consumed our hands excavating the seafloor in search of constructional parts crucial for the geophysical interpretations.

I am thankful to Fabrizio Antonioli, of ENEA, for the long discussion on the biological and archaeological markers we had during our field trips and for the long work spent together in the field and in his office, discussing results and preparing papers. Moreover, being an expert photo diver, during our field work he shot beautiful pictures of the fish tanks that clearly show the details of these amazing constructions.

I am grateful to Giovanni Arena at ISPRA, manager of the Italian tidal network, for his precious collaboration to provide the tidal data and for the fruitful technical discussions.

At the University of Calabria, I had fruitful work with Vincenzo Carbone and Antonio Vecchio, both at the Department of Physics of the University of Calabria. With them, we explored new research fields in geophysics and tuned new techniques to analyze tidal data in relationship with tsunamis. In this way we found an unexpected transient signal in sea level variation in the Mediterranean sea, induced by the March 11, 2011, tsunami that followed the giant M=9, Tohoku-Oki earthquake (Japan). We obtained so exciting results that our paper had a worldwide resonance, in the newspapers and in the WEB, as well.

I am particularly thankful to Ignazio Guerra, of the Department of Physics of the University of Calabria for his warm collaboration and welcome. With him, I spent many days during my winter staying in Arcavacata, discussing of geophysics and geodesy. He always supported me with great enthusiasm, appreciating the multidisciplinary studies performed along the coasts of Calabria. In this area I also had a great collaboration with Luigi Cantafora, likely one of the most expert divers I have ever met. With him and Alessandra Benini, I explored a part of the Ionian coast of Calabria, obtaining new crucial data for the geodynamic comprehension of this region.

In Libya I was supported by Luisa Musso, chair professor in archaeology at the University of Roma 3 and director of the Italian archaeological mission in Leptis Magna. I am thankful to Luisa who showed me some of the most amazing maritime roman coastal cities of the Mediterranean from which I obtained new data on the roman sea level.

In Tunisia, I had great collaboration with my friend Mohamed Soussi, chair professor in geology at the University of El Manar, Tunis. With Mohamed I explored about all the coast of Tunisia, observing geological, biological and archaeological evidences of the sea level changes.

In Israel I had the opportunity to work with Dorit Sivan, chair professor at the University of Haifa. With Dorit we re-visited the roman coastal installations in Israel, finding new evidences of recent sea level changes. Here, I had the possibility to have very interesting diving in the submerged harbor of Cesarea, built by Herod's the Great. These observations were important to compare the constructional features of this port with respect to others similar ports in the Mediterranean, like at Torre Astura, to interpret their relationship with past sea levels. I am also thankful to Captain Mustafa Yildir and his brother, who accompanied me on board of a gullet along some hundreds of miles of the amazing coasts

of southwestern Turkey, surveying several submerging cities and coastal installations from Lycia to Byzantine ages.

At least but not last, I am particularly thankful to my wife Paola, my son Luca and my daughter Alessandra, for their patience for all the times I have been away during my frequent field work.

Finally, I feel to dedicate this thesis to my colleague Sergio Silenzi, of ISPRA, who recently died, killed by a cancer. We discussed of our common research in the Mediterranean up to end of his life. Sergio was using biological markers to reconstruct the sea level history and his findings were really exciting. I do hope to be able to complete his unfinished research.



Kurt Lambeck, Marco Anzidei and Fabrizio Antonioli, during the ceremony for the Balzan Prize, won by Kurt Lambeck and awarded by the President of the Italian Republic Giorgio Napolitano, on November 14, 2012 at Quirinale Palace, Rome.

1. Introduction

The recent estimates of global sea level change, based on radar altimetry and tide gauge data, established a global and regional sea level rise, during the 20th century and the last two decades, at rates of 1.7 mm/yr and 3.2 mm/yr respectively, as a result of both increase of ocean thermal expansion and land ice loss (Meysignac and Cazenave). This is one of the most important consequences of climate change that has evident impacts on the coasts and on human activities (Bruun, 1962; Daly, 2004, Woodworth et al., 2010; Nicholls, 2010; Mitchum et al., 2010). The contributing factors, analyzed in the recent IPCC Fourth Assessment Report (IPCC 2007; www.ipcc-wg2.org), are characterized by a broad range of time scales and covers many disciplines and physical sciences of the Earth at the same time (Douglas and Peltier, 2002). In this context, geophysical and geological studies, including the geodetic observing systems, play a key role (Blewitt et al., 2010). The temporal and spatial changes of past sea levels for the last thousands of years in relation to the late Pleistocene glacial cycles, are partially caused by predominant vertical deformation of the Earth's lithosphere and mantle (Peltier, 2000; Lambeck and Chapell, 2001; Lambeck et al., 2002a; Stocchi and Spada, 2009). This process of post-glacial isostatic adjustment (Global Isostatic Adjustment, GIA) is still active on a global scale, including the Mediterranean area and Italy and occurs mainly with slow vertical deformation of the land (Lambeck and Purcell, 2005; Lambeck et al., 2004a). During the '70s, Farrell and Clark (1976) proposed that the deformation of the mantle could be able to produce variations of the geoid. This, in turn, induces changes in the shape of the ocean's surface. These global processes are at the basis of the principles of hydro and glacio-isostasy (Lambeck et al., 2003; Mitrovica et al., 2010). Recent studies have shown that the sum of vertical movements occurring along the coast (caused by GIA, local subsidence, tectonics and volcanism), together with the eustatic rise, can produce large coastal variations in a short time (Lambeck et al. 2011; Dvorak and Mastrolorenzo 1991; Firth et al. 1996; Stiros 2000; Morhange et al. 2006; Tallarico et al., 2003). Climate change superimpose to these phenomena, amplifying the total effects along the coastal plains (Rahmstorf, 2007b; Church et al., 2004). Lambeck et al. (2011), for the first time faced this environmental problem for the Italian area estimating a maximum sea level rise up to 153 cm by the year 2100, as a worst scenario at specific sites. Since the Italian area is subject to vertical tectonic movements, local subsidence and GIA, these effects will mainly affect low elevated coastal areas that presently are at high risk of marine flooding.

In addition, the increase in extreme events observed in recent years (e.g. violent storms), can generate significant flooding of vast coastal areas (Lowe et al., 2010). Recent computations, based on the Empirical Mode Decomposition, from the analysis of historical climate data, have show temperatures fluctuations and presence of significant trends related to global warming, likely related to El Nino oscillations, with direct effect on rising sea level and terrestrial ice dissolution (Capparelli et al., 2011).

Significant constraints to the models have been provided by observations of changes in sea level based on reliable geological and archaeological indicators, capable of giving information for the geological and historical past. Among these, the archaeological data from the Roman period (2.3-1.5 ka BP) and Middle Ages, together with instrumental and tidal data, have provided new valuable information in many parts of the Mediterranean (Flemming and Webb, 1986; Pirazzoli, 1976; Pirazzoli, 1987; Lambeck et al., 2004b; Antonioli et al., 2007; Anzidei et al., 2011a; Anzidei et al., 2011b; Pagliarulo et al., 2012; Mourtzas, 2012). It must be emphasized that the use of archaeological indicators to determine the relative changes in sea level can be successfully applied in the Mediterranean region, since this is the seat of ancient cultures which have developed

along these coasts (Auriemma and Solinas, 2009). In this context, the Italian area is one of the most suitable for such studies due to the large abundance of well preserved coastal archaeological structures and geological and geomorphological signatures that can be found along the coasts (Ferranti et al., 2010). These are crucial to understand and reconstruct the history of the sea-level during the Holocene, thus giving a unique opportunity for such studies. The state of the art on the most recent estimates of sea level rise in Italy, and the Mediterranean as well, is indicating that the relative variations vary from place to place. Along the Tyrrhenian coasts of Italy, was observed a mean sea level rise of about 1.35 m since the last 2 ka (Lambeck et al., 2004b), with the exception of a few uplifting coasts in tectonically active areas, that show a reduced or null relative sea level change (Anzidei et al., 2012). In other areas of the Mediterranean, as in southwest Turkey, were observed negative variations up to several meters due to vertical tectonic movements induced by the Hellenic Arc system, that have lowered the coastline (Anzidei et al., 2011a). The analysis are in agreement in indicating that the purely eustatic variations is about 13 cm, that likely occurred in the last 100±50 years. This period roughly coincides with the beginning of the industrial age and the increase of global temperatures, giving a possible evidence of a direct relationship between sea level rise and recent climate change (Lambeck et al., 2004b). Such changes can be critical in case of extreme events, as for storms and tsunamis, capable to rapidly change the coastline and its morphology (Lowe et al., 2010; Pucci et al., 2011; Pantosti et al., 2008; De Martini et al., 2010; Mastronuzzi and Sansò, 2000; Mastronuzzi and Sansò, 2004). In this Doctorate Thesis, we review the current state of the art, and provide additional results on the sea level change at different time scales in the Mediterranean. Six selected key papers of the twenty I have published on JCR journals during the three years of the Doctorate are annexed to this thesis. In addition to these, further not yet published results are here briefly presented for the Calabria region and for the tidal analysis in relation to the tsunami that followed the Boumerdès earthquake of May 21, 2003. Results can be used for a conscious land planning, because rising sea level will affect the Italian coasts over the next years.

Research goal

The results presented in this Doctoral Thesis originated from the joint efforts of several researchers belonging to several institutions of the Mediterranean countries, conducted by the Istituto Nazionale di Geofisica e Vulcanologia, the Australian National University and ENEA, which have cooperated in the specific topic of the relationships between the reconstruction of the relative sea levels along the coast of the Mediterranean and the post-glacial isostatic adjustment, including tectonics and volcanism. Particularly, this work has substantially benefited since the beginning from the project funded by CNR Agenzia 2000 *“Multidisciplinary Study of maritime villas, harbors and fish tanks of Roman and pre roman age along the coasts of the Italian and Mediterranean Sea, for the evaluation of the crustal, seismic and volcanic deformations and sea level changes during the late Holocene”*, and later by other national research programs and from a cooperation with the Department of Physics of the University of Calabria for this region (Prof. Ignazio Guerra). In this framework were performed archaeological and geological surveys along the coasts of the Mediterranean, analyzed instrumental data and applied glacio-hydro-isostatic geophysical models for the same region.

Observations and descriptions of the sea level change along the coast are crucial for the understanding of the progressive sea level rise in response to the increasing surface temperature of the planet. This phenomenon, caused by past climate changes and accompanied by the melting of the Pleistocene ice sheets, have relevant scientific and

socio-economical implications, because is still active and affecting coastal human settlements, especially when in conjunction with vertical land motion caused by natural and anthropogenic subsidence, tectonics and volcanism.

The present-day sea level rate estimated by the longest available tide-gauge recordings in the Mediterranean, includes vertical movements of the land, that can accelerate (or sometimes decrease) locally the sea level rise, as well as the possible contributions of anthropogenic origin (greenhouse effect, global warming, etc.).

In this work we have measured and analyzed the sea level changes occurring along the coasts in the Mediterranean basin at different time scales, from geological, archaeological data and instrumental observations, and adopting advanced mathematical modeling to constraining deformation mechanisms of the Earth at long temporal scales. Fast sea level oscillations are then analyzed to extract the frequency content of sea level after significant regional or global tsunamis, thus exploring different aspects of the sea level change occurring in the Mediterranean.

2. Sea level

The level of the seas has always changed during the Earth's history with different amplitudes and rates. These changes were dependent on astronomical, climatic and tectonic causes, which vary in space and time (Tab.1). Recent studies have determined that sea-level change is the sum of eustatic, glacio–hydro-isostatic and tectonic factors: the first is global and time dependent, while the other two also vary according to location (Lambeck and Purcell, 2005). Therefore their effects define the sea level in a given area and at a given time. Recent observations suggest that the current global warming may lead to an unprecedented acceleration in the current trend of sea level raise (Church et al., 2010). To understand the cause of the signal we observe along the coasts, which is crucial for coastal planning, it is necessary to define briefly what sea level is.

We can distinguish between absolute sea level and relative sea level. The first one, (η), depends on the mass and density fields, but the combination of different factors that act in time and space determine its changes:

$$\eta = \eta_{mass} + \eta_{density}$$

The η_{mass} is depending from the amount of water in the oceans whose predominant changing factor is the melt or growth of the ice sheets during glacial cycles that vary their extension and thickness in time. The second factor, the $\eta_{density}$, is largely depending by salinity and temperature of the oceans. The latter are changing with global temperatures. Instead, the relative sea level change that can be observed along the coasts can be defined as:

$$\Delta\zeta_{rsl} = \Delta\zeta_e + \Delta\zeta_G + \Delta\zeta_T$$

The first factor $\Delta\zeta_e$ needs global estimates of changes in ice volume, or the eustatic part; the second one $\Delta\zeta_G$, needs understanding of Earth response to changes in surface loads, or isostasy, and knowledge of loads themselves; the last one $\Delta\zeta_T$ needs local knowledge of tectonics of a region, that causes vertical land movements. In Figure 1 is reported a sketch showing the basic concepts of relative sea level change and how it can be

observed along a shore, as resulting from the combination of vertical land movements and ocean volume variation.

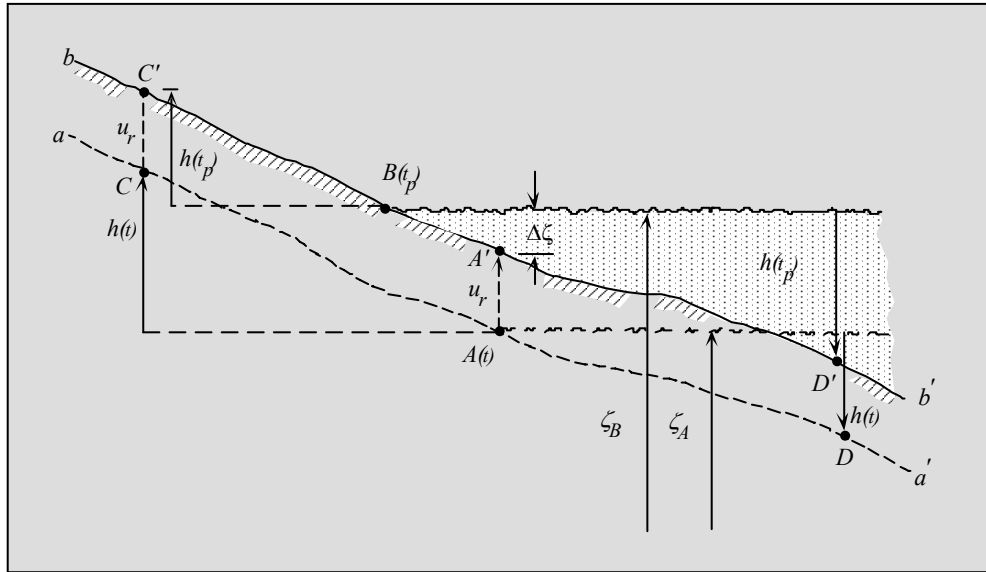


Fig. 1 – The relative sea level change. At present time t_p the shoreline is at $B(t_p)$ and the original shoreline is displaced to $A'(t_p)$. The position of A' relative to B specifies the relative sea level change in the interval $(t-t_p)$. u_r = land uplift. At time t the land surface is at $a-a'$ and shoreline is at $A(t)$. Relative sea level change: $Dz = (z_A - z_B) - u_r$; Elevation at t : $h(t) = h(t_p) - [(z_A - z_B) - u_r] = h(t_p) - Dz(t)$ (from Lambeck et al., 2010)

The main cause of global sea-level change, neglecting tectonics, has been addressed to the growth and decay of ice sheets and the associated deformational and gravitational response of the Earth to the changing surface loads of ice and water. The zero order approximation of sea level change is the average change of the ocean caused by the melting of the ice sheets, defined as (from Nakada & Lambeck, 1989 and Lambeck et al., 2002a):

$$\Delta\zeta_{esl}(t) = -\frac{\rho_i}{\rho_o} \int_t \frac{1}{A_o(t)} \frac{dV_i}{dt} dt$$

Where, V_i is the ice volume at the time t , $A_o(t)$ is the ocean surface area at time t , ρ_i and ρ_o are the average densities of ice and ocean water.

Sea level at any locality φ and time t , is then defined as:

$$\Delta\zeta_{rsl}(\varphi, t) = \Delta\zeta_{esl}(t) + \Delta\zeta_I(\varphi, t) + \Delta\zeta_T(\varphi, t)$$

Where, $\Delta\zeta_{rsl}(\varphi, t)$ is the change of sea surface relative to land at a location φ and time t compared to its present position at time t_p . The second term $\Delta\zeta_I(\varphi, t)$ is the glacio-hydro-isostatic contribution *. The last term $\Delta\zeta_T(\varphi, t)$ is the tectonic contribution for active areas. These terms are functions of positions φ and time t .

* In simple approximation, the isostatic term consists in two parts:

- i) The glacio-isostasy (deformational and gravitational effects on sea level due to changing ice load;

ii) The hydro-isostasy, corresponding to the concomitant changes in the ocean load.

Isostatic corrections are dependent on the rheological model and on assumptions on the ice-volume-equivalent sea level function. Separation of the two can, however, be achieved (Nakada and Lambeck 1989; Lambeck et al., 2002a):

$$\Delta\zeta_I(\varphi, t) = \Delta\zeta_{I-g}(\varphi, t) + \Delta\zeta_{I-h}(\varphi, t)$$

Where, $\Delta\zeta_{I-g}(\varphi, t)$ is the glacio-isostatic part and $\Delta\zeta_{I-h}(\varphi, t)$ is the hydro-isostatic part.

The sea levels at two locations φ_1 and φ_2 , ignoring tectonics, are:

$$\Delta\zeta(\varphi_1, t) = \Delta\zeta_{esl}^0(t) + \delta\Delta\zeta_{esl}^0(t) + \Delta\zeta_{I-g}(\varphi_1, t) + \Delta\zeta_{I-h}(\varphi_1, t)$$

$$\Delta\zeta(\varphi_2, t) = \Delta\zeta_{esl}^0(t) + \delta\Delta\zeta_{esl}^0(t) + \Delta\zeta_{I-g}(\varphi_2, t) + \Delta\zeta_{I-h}(\varphi_2, t)$$

Where, $\Delta\zeta_{esl}^0$ is the contribution to the ice-volume function based on the ice model and $\delta\Delta\zeta_{esl}^0(t)$, is a corrective term to allow for any limitation in the model.

The difference is given by:

$$\begin{aligned} \Delta\zeta(\varphi_1, t) - \Delta\zeta(\varphi_2, t) &= \{\Delta\zeta_{I-g}(\varphi_1, t) - \Delta\zeta_{I-g}(\varphi_2, t)\} + \{\Delta\zeta_{I-h}(\varphi_1, t) - \Delta\zeta_{I-h}(\varphi_2, t)\} \\ &\approx \{\Delta\zeta_{I-h}(\varphi_1, t) - \Delta\zeta_{I-h}(\varphi_2, t)\} \end{aligned}$$

If the two sites are far from ice margins and enough close to each other for glacio-isostatic parts to be small and comparable. This differential observation is primarily a function of the mantle response to the water loading and only to a second order of $\Delta\zeta_{esl}^0(t)$.

Hence it provides an estimate of the rheological parameters which are then used to improve the the $\Delta\zeta_I(\varphi_1, t)$ and the ice-volume-equivalent through:

$$\delta\zeta_{esl}^0(t) = \Delta\zeta(\varphi, t) - \{\Delta\zeta_{esl}^0(t) + \Delta\zeta_I(\varphi_1, t)\}$$

An iterative process is used to obtain the far-field and near-field solutions to yield better ice models and rheological parameters, to estimate the change in the ocean volume through time. Geophysical modeling of the isostatic response of the Earth to surface load redistribution can be undertaken at global or at regional scales. The results here presented are concerning regional and or local analyses for the Mediterranean of the estimates for the ocean volume change during the present interglacial and for the time since that sea levels approached their present level about 7000–6000 years ago. For the analysis has been used the code developed at the Australian National University (www.anu.edu.au).

During the Earth's history, global sea level variations were triggered from geological, astronomical and climatic changes (eustatic changes) and they affected the coasts with different amplitudes at different locations.

The sea level at a point P of coordinates (ω, φ) is the offset between the surface of the geoid and that of the ground surface, as in the following:

$$SL = SL(\omega, \varphi)t = r'g - r's,$$

where the sea level change is given by:

$$S(\omega, \varphi)t = SL - SL_0,$$

where SL_0 is a reference sea level, measured at the same point but at the at a time $t=t_0$ (Fig. 2 A):

$$SL_0 = r_g - r_s.$$

Then, $S(\omega, t) = SL - SL_0$ is the sea level change that can be observed and measured in a point by topographic surveys at P (Fig. 2B).

Combining the previous expressions for $S(\omega, \varphi)t$ we obtain:

$$S(\omega, \varphi)t = N - U,$$

where

$$N(\omega, \varphi)t = r'_g - r_g$$

This is the geoid height change, and

$$U(\omega, \varphi)t = r'_s - r_s.$$

Is the vertical deformation of the land surface. Therefore the sea level change is determined by changes in the shape of the two surfaces that define the geoid and the solid Earth. Sea level change can be then defined on the whole surface of the sphere, since both N and U have precise values across the continents.

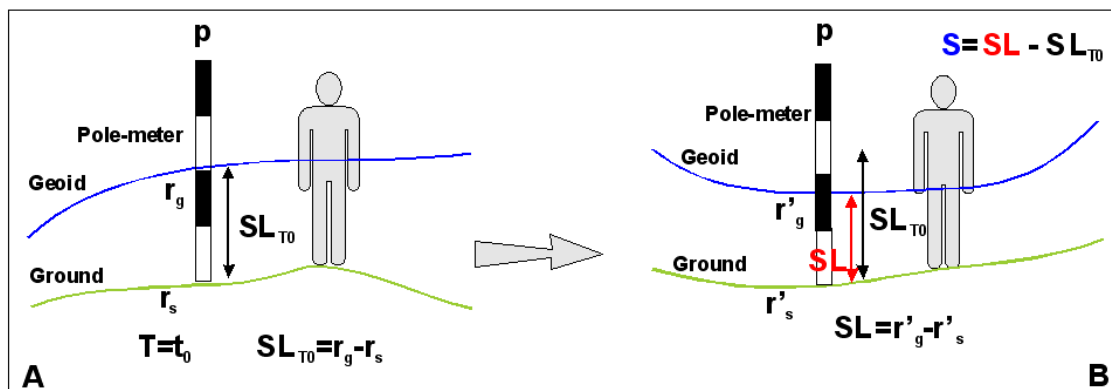


Figure 2 Sea level change measurement S at a point of coordinates (ω, φ) and at a time t along the coast, in relationship with the geoid height change N , and the vertical deformation U (From Stocchi, 2004, modified).

Spatial and temporal scales of sea level change and tectonic and climate causes				
Causes	Time scale	Time window	Spatial scale	Dominant process
Climate	Long term	$10^6 - 10^3$ years	Global	Growth and decay of ice sheets
	Intermediate term	$10^3 - 10^2$ years	Regional	Global change in temperature and ice volume (little ice age, medieval climate optimum)
	Short term	$10^2 - 10$ years	Local	Decadal-scale climate change, wind circulation. Change in thermal state of ocean. Change in ground and surface water storage
Tectonics	Long term	$10^6 - 10^9$ years	Global	Plate tectonics and evolution of ocean basins. Ridge formation
	Intermediate term	$10^6 - 10^3$ years	Regional	Volcanic and sediment loading, changes in stress state of lithosphere
	Short term	$10^3 - 10^2$ years	Local	slow surface response to long term tectonics and volcanism
	Very short term	years -seconds	Local	Rapid surface response to tectonics and volcanism forcing. Earthquakes and eruptions.

Table 1 Spatial and temporal scales of sea level change and tectonic and climate causes

Among the global geological causes, are the drift of the continents, the expansion of the oceanic ridges with the subsequent changes in the shape of the oceans. The predominant astronomical factors that caused the past eustatic fluctuations are the eccentricity of the orbit of the Earth around the sun, the oscillation of the obliquity of the Earth's rotation axis with the motion of precession (change in the orientation of the rotational axis). Continental or regional changes are primarily due to the glacio-hydro-isostatic effects, tectonics, variations in the force of gravity, subsidence and, in recent centuries, anthropogenic. At local scale are also possible short-term changes (daily, monthly, yearly), caused by climatic and meteorological conditions.

Rapid changes are typically caused by tides, winds, atmospheric pressure and tsunamis. These oscillations may cause temporary variations in the elevations of sea level in the range from some decimeters and even up to several meters, as in the case of storms and tsunamis.

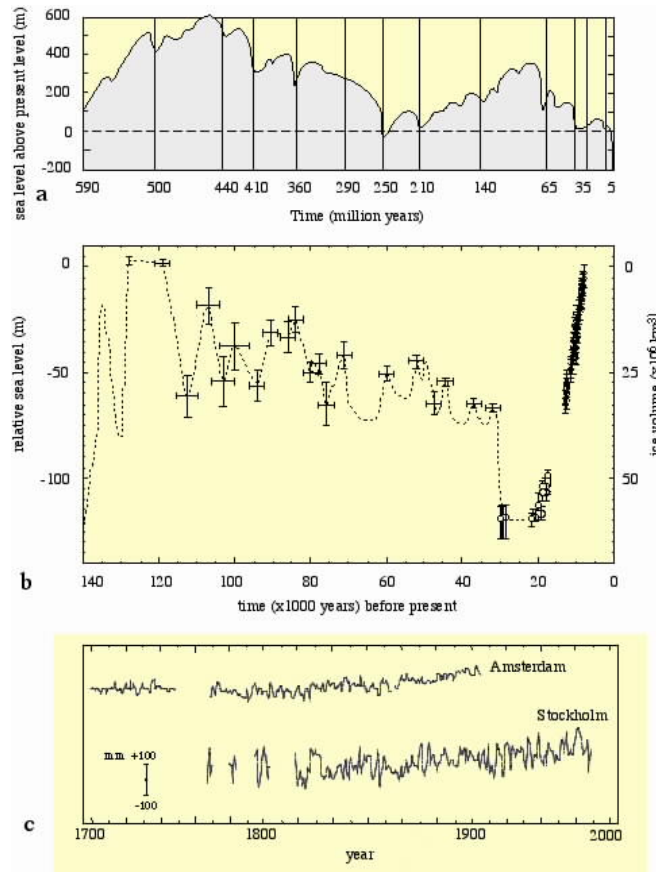


Fig. 3 Sea level reconstruction during the last 600 Million of years. A) Long-term sea levels changes during the past 600 Ma as derived by geological evidence and driven mainly by plate tectonics factors (Hallam, 1984); B) Intermediate-term sea level change from the last glacial cycle from fossil shoreline evidence (last 140 ka, Huon Peninsula, Papua, New Guinea and W-Australia). Signal shows large spatial variability (Lambeck and Chapell, 2001); C) Instrumental record for the last 3 centuries, show high frequency oscillations with longer-term trends (from Church et al., 2001). (set of figures from Lambeck et al., 2010).

3. Global scale changes

The geological phenomena that lead to changes in sea level are mainly related to plate tectonics. The Earth's plate movements and the associated phenomena lead to changes in shape of the oceans and therefore, in the volume of the basins. For example the rapid formation of new oceanic crust causes a decrease in depths of the oceans. Then, the more the lithosphere is young, the more is hot and therefore less dense, generating due to isostasy a lower bathymetry and a lower oceanic volume. This leads to a rise in sea level. In addition, there are the effects of oscillation of the water level on the shape of the submerging land (e.g. coastal subsidence at continental and regional scale, rheological adjustments of the lithosphere, thermo-isostasy, glacio-isostasy, the sediment-isostasy, the accumulation of sediments, etc.).

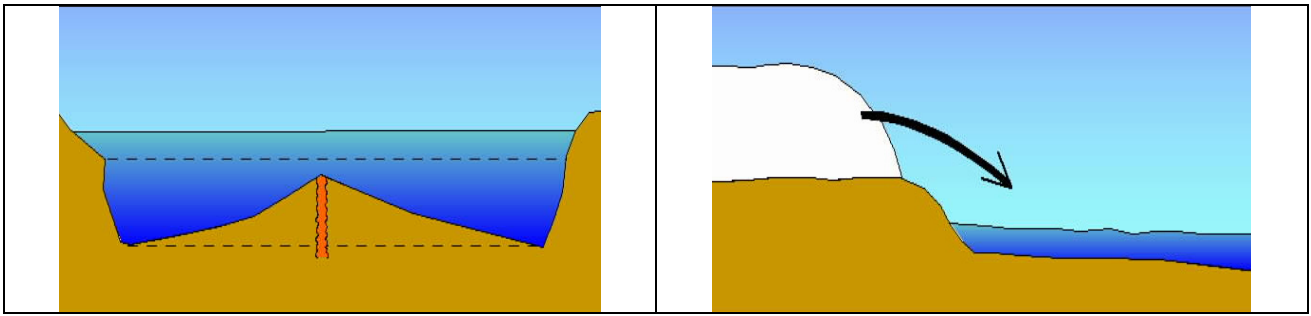


Fig. 4 Left: example of a global scale sea level change caused by ocean ridge formation: the ocean basin changes its shape in relationship to plate tectonics, but with a constant volume of water. Right: Change in ocean volume caused by ice sheets melting in consequence of addition (or removal) of water. Thermal expansion (or contraction) is due to increasing (or decreasing) water temperatures.

The global climatic changes act over tens and hundreds of thousands of years and are mainly triggered by periodic variations of the Earth's orbital parameters (Milankovitch, 1938; Hayas et al., 1976; Adem, 1989). These factors control the intensity of sun radiation that reaches the surface of the planet. The effects of climatic variations on changes in sea level are mainly changes in the relative volumes of water and ice, which occurs by accretion or melting of ice sheets. Changes in sea level have been up to 130 m in 18,000 years (Fig. 3). These oscillations are also defined as glacio-eustatic changes (Maclaren, 1842). Climate change, such as those occurring in glacial and interglacial periods, also involves changes in temperature, salinity and pressure of the ocean water, with relative variations of density and volume. The changes of sea level induced by temperature changes are generally limited (at most a few meters of difference between glacial and interglacial periods), but may be perceptible (some decimeters) if a climate change is produced in a short time, as is happening in recent years because of global warming.

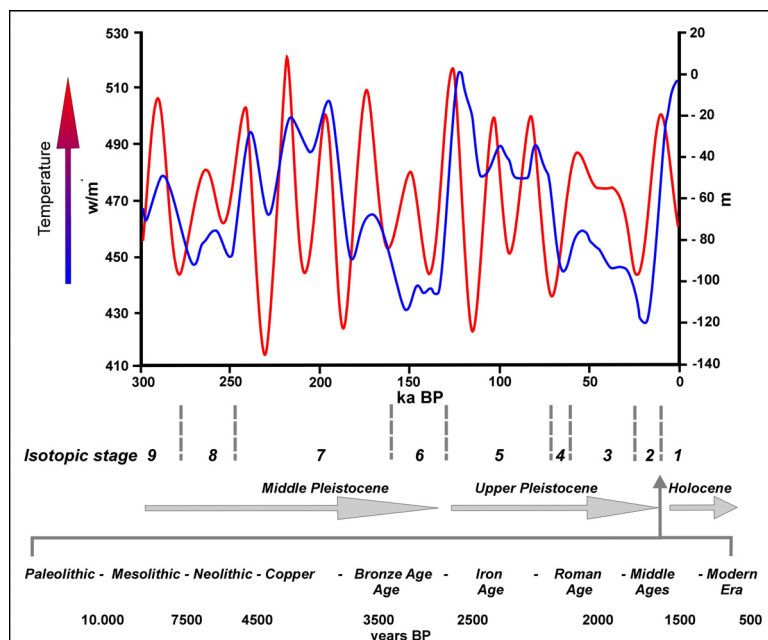


Fig. 5 Sun radiation (red curve) and sea level changes (blue curve) since the Middle Pleistocene. At the bottom are reported the isotopic stages (9-1) and the archaeological ages for the last 10 ka (modified from Silenzi et al., 2004).

The most important climate changes that lead to changes in sea level are related to the glacial cycles. James Croll (1875) was the first to suggest that the climatic fluctuations of the last 2 million years were the result of slow movements that describes the Earth in space during its rotation around the Sun. The theory was elaborated by Milutin Milankovitch around 1930 (Milankovitch, 1930; Milankovitch, 1941) and subsequently discussed and refined by many authors (see eg.: Berger, 1978, Berger, 1988, Berger et al., 1992; Crowley & Kim, 1994; Hays et al., 1976; Imbrie et al., 1984; Imbrie et al., 1992, 1993; Laskar, 1999; Muller & McDonald, 1997; Santer et al., 1993).

According to Milankovitch, because of the gravitational pull exerted by the bodies of the solar system on our planet, the Earth's orbit is constantly modified by the cycles of precession, obliquity of the ecliptic and eccentricity of the orbit. On the basis of astronomical laws that describe these variations and assuming the Earth's atmosphere was stationary, Milankovitch estimated the variation of the solar radiation on the Earth's surface at different latitudes over the past 600,000 years. In this way he explained the past successions of warm and cold periods (Fig. 5). The astronomical cycles determines the transition from glacial to interglacial phases with periods of about 100.000 years. Currently, the Earth is experiencing a warm period or interglacial, named the Holocene. This began about 10.000 years ago after a glacial phase in which, about 22.000 years BP, the sea was about 130 m below the current level.

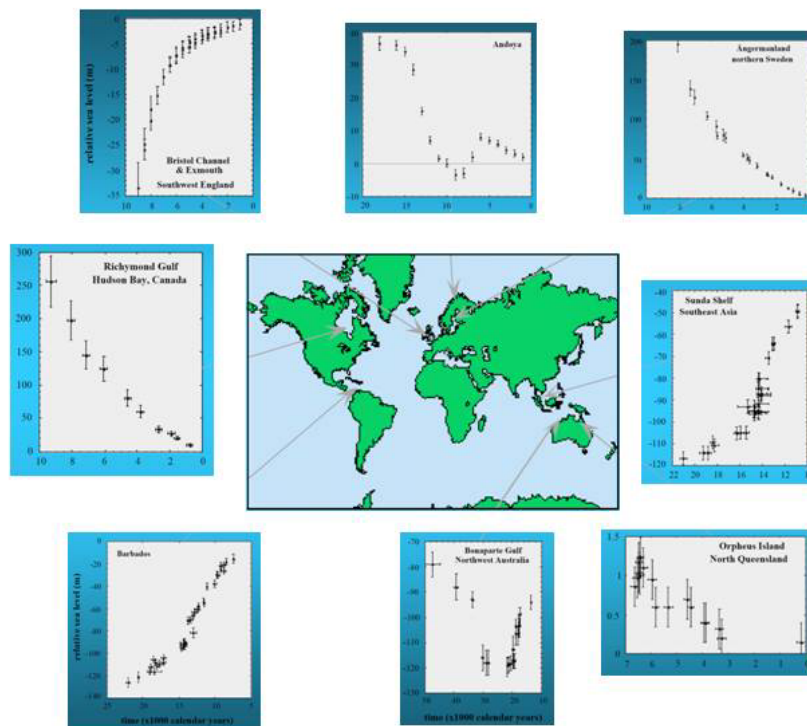


Fig. 6 Sea-level reconstructions at different places round the world. Note the spatial variability caused by the ice-volume changes during the last glacial cycle and the contrasts between, near field (Angerman and Hudson Bay), intermediate field sites (Bristol Channel) and far field sites (Queensland) (From Lambeck et al., 2010).

The earliest evidence of alternation of glacial and interglacial phases was determined by analyzing the ratio of the stable isotopes of oxygen contained in the fossil remains of marine organisms ($\delta^{18}\text{O}$, shows the relative abundance between the isotopes ^{16}O and ^{18}O in carbonatic rocks or in shell of mollusks and foraminifera). Such isotopic ratio is not

random, but is strongly dependent on the temperature (Urey, 1948; Emiliani, 1954, 1977, Shackleton, 1974, 1977, 1988, Shackleton & Opdyke, 1973; Wefer & Berger, 1991), Therefore shells are capable to record the climate of the past times in which they lived. For the above reason, these climatic phases are roughly corresponding to the Milankovitch cycles, or so called isotopic stages. These are indicated by increasing numbers going back in time. Stage 1 corresponds to the Holocene. Similarly, with odd numbers are indicated the past interglacial periods, while even numbers identify the glacial stages. Stage 2 corresponds to the last glacial period whose colder peak occurred 22,000 years ago (LGM: Last Glacial Maximum) (Fig.5).

The changes described by the Milankovitch cycles have brought the Earth 22,000 years ago (during the LGM) to be covered by huge ice sheets, as thick as 4000 meters. In our region, the extent of the ice included a large part of northern Europe and the main mountain ranges of the Alps (Figs. 6 and 7). The formation or melting of the ice sheets causes the Earth's crust vertical movement in response to the loading or unloading by the growth or reduction of the ice sheets.

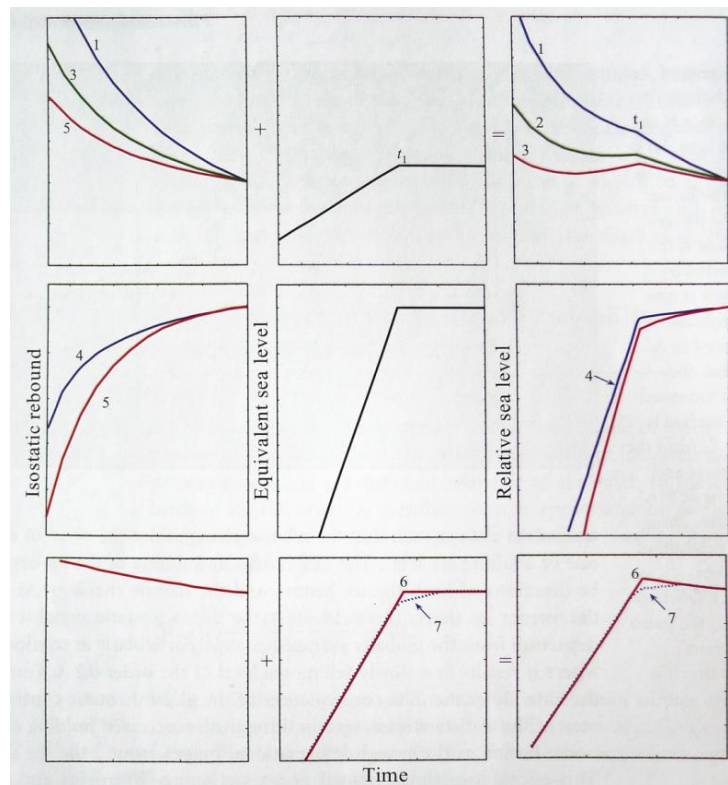


Fig. 7 The Earth's response to deglaciation. Left: crustal rebound. Center: ice-volume-equivalent sea-level (esl). Right: sum of the two. Vertical scales differ. Gravitational effects are not considered, and the melt water is not realistically distributed. (a) sites within the former ice margin: crustal rebound (left) exceeds the esl change (center) and the relative sea level is falling (if the cessation of global melting at time t_1 a small cusp will appear in the relative sea-level curve). The rebound from sites far from the center of rebound will become progressively smaller and near the ice margin the rebound and eustatic signals may be of comparable amplitude but opposite sign. (b) Sites outside the former ice margin: rebound signal is subsidence and isostatic contribution is of the same sign as the esl change. Amplitude depends on distance from the ice margin. (c) Far-field continental margin sites: the dominant signal is a subsidence of the sea floor induced by the water loading of the ocean floor with a concomitant fall in the water surface. The coastal zone is dragged down less than the offshore sea floor and sea level at the coast will appear to be falling. Once major melting has ceased the relaxation of the sea floor dominates and results in the high-stand in relative sea level at ~6000 years ago (From Lambeck et al., 2010).

These phenomena are acting on a global scale and, due to the viscosity of the mantle, persist for a long time even after the end of the cause that led them. The large part of the ice cap that covered once Scandinavia during the last glacial period disappeared since 8000 years, but the Earth's crust in this region is still continuing to rise for glacio-isostatic response, at a rate of about 20 mm/year. At the same time, as the Earth's mass is constant, subsidence occurs in the adjacent regions, such as the Mediterranean, including Italy (Lambeck and Johnston, 1995).

This effect, which tends to be negligible across the equator, is the glacio-isostatic, and has been described among the first by Farrell and Clark in 1976. The hydro-isostatic component is instead connected to changes in the seafloor due to the increase (or decrease) of the water column, in turn caused by the dissolution (or grow) of the ice as a result of the global warming (or cooling). This effect produces a maximum value of subsidence within the ocean basins, and resulting in a rising of the continental lands. All areas are therefore subject to strong circumpolar phenomena of glacio-isostasy, with uplift of up to 200 meters over the past 10,000 years. At mid-latitudes, such as the Mediterranean basin, are added the glacio and hydro components, while at low latitudes (e.g. the equator) the main effects are due to hydro-isostasy

Today we are experiencing a new sea level culmination of a warm interglacial period, which began about 10.000 years ago. During this time sea level has risen dramatically, despite the solar radiance over the Earth's surface decreased (Antonioli and Silenzi, 2007). Recent studies determined that since about 4000 years the melting of the ice caps ceased and therefore their contribution to the eustatism have almost ceased as well. Anyway, the land movements along the coasts are sensitive to the vertical isostatic signal. In this complex framework, the coasts of the Mediterranean underwent to a diffuse subsidence since the end of the last Last Glacial Maximum (LGM), thus experiencing a continuous relative sea level rise (Fig. 6). These movements, which add to the eustatic signal caused by the ice sheets melting in relationship with the recent global warming, will have large effects on most of the coastal areas, especially those at low topographic elevation, like coastal plains, or the river deltas.

4. The Mediterranean region

The indented shores of the Mediterranean Sea run for about 46.000 km along its rocky and sandy shores extending from the Straits of Gibraltar in the west, to the Levant in the east, in southern Europe and North Africa. About 50 sub-aerial and sub-marine volcanoes are still active in this region, which is struck by a continuous seismicity with frequent destructive earthquakes (www.ingv.it).

With its peculiar features, the Mediterranean Sea is a natural laboratory for studying crustal dynamics, volcanism and coastal processes included sea-level changes. Additionally, this region has been settled by ancient populations since Paleolithic times and the archaeological traces of past civilizations are still remaining along the coasts providing valuable information to test geophysical, geodynamic, paleogeographic reconstructions and paleoclimatic models for this region.

The Mediterranean basin is placed in zone of a tectonic convergence between the main African and Eurasian continental plates, although some additionally minor plates, such as the Adriatic and the Arabia, have a key role in the current geodynamic activity (Figs.8 and 9). Therefore, the result is a complex network of tectonic structures that drive the geodynamics of this region, causing seismic and volcanic activity and a diffuse crustal deformation. In the eastern Mediterranean, the Hellenic arc system is the most active and

causes regional deformations, releasing most of the largest earthquakes of the region. In the central Mediterranean, is still active the subduction of the Calabrian arc and the volcanism associated to the Aeolian Islands (Serpelloni et al., 2007 and references therein).

In this geodynamic framework, large scale geological processes cause uplift and subsidence along the shores. The fastest horizontal crustal movements are occurring at rates up to 30–40 mm/yr and often within 1 or 2 mm/yr along the vertical. If we extrapolate back in time these movements, assuming they have continued at constant rates, it means that over the scale of thousands to millions of years their cumulative effects can produce dramatic changes along the coasts. The largest critical effect of these movements, occurred around 6 Ma BP even in conjunction with global climate changes and glacio-eustatic processes: the closure of the Gibraltar strait and of the Atlantic gateway with the subsequent drying event, namely the Messinian Salinity Crisis (Hsu et al. 1973; Clauzon et al. 1996; Hodell et al. 2001; Krijgsman et al. 2001; Warny et al. 2003; Duggen et al. 2003, 2004). During this period, the Mediterranean Sea lost most of its water for evaporation and its level dropped even more than 1.300 m, below the current level (Fig.10). Thick sequences of evaporites deposited in the hyper-saline abyssal plains and today are represented by the salt mines in Sicily (i.e. at Realmonte, near Agrigento).

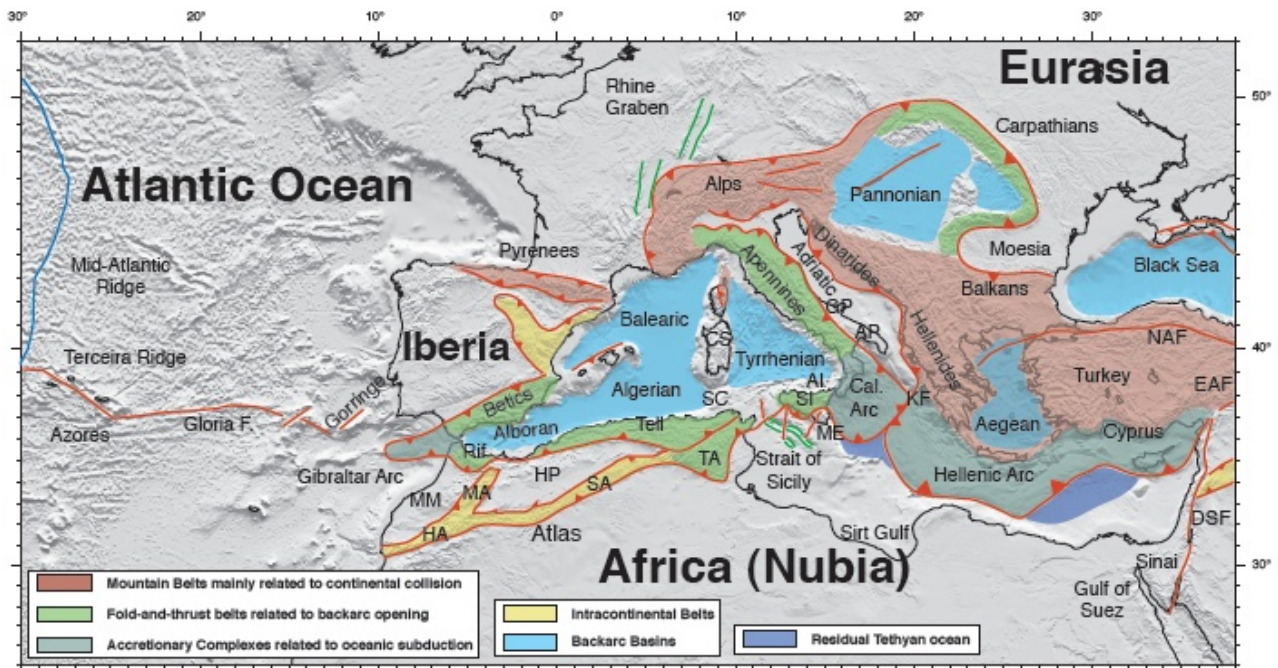


Fig. 8 Simplified tectonic sketch of the Mediterranean region: HA: High Atlas; MM: Moroccan Meseta; MA: Middle Atlas; SA: Saharian Atlas; TA: Tunisian Atlas; HP: High Plateau; SC: Sardinia Channel; ME: Malta Escarpment; SI: Sicily; Al: Aeolian Islands; ET: Mount Etna; PP: Pelagian Plateau; CS: Corsica-Sardinia block; AP: Apulian block; GP: Gargano Promontory; KF: Kephallinia Fault zone (modified from Serpelloni et al., 2007).

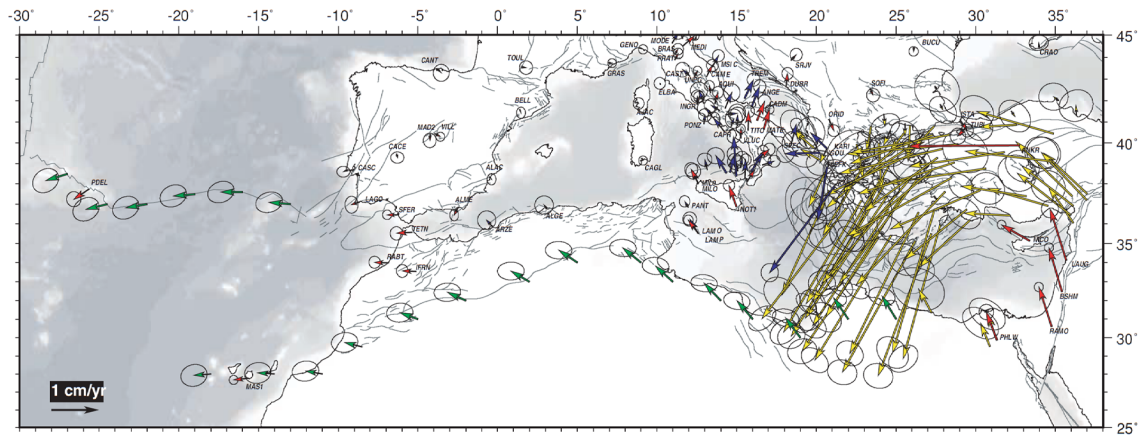


Figure 9. Horizontal velocities (with 95% error ellipses) given with respect to the Eurasian plate. Red arrows: permanent GPS stations; blue arrows: non-permanent GPS stations; yellow arrows: subset of McClusky *et al.* (2000) velocity field transformed into the Eurasian fixed frame. Green arrows display the motion vectors of points south of the seismically active belts in northern Africa predicted by the Nubia-Eurasia Euler vector (From Serpelloni *et al.*, 2007).

The Messinian crisis ended about 5.3 million years ago, when the marine gateway to the Atlantic was restored (Duggen *et al.* 2003) and the present-day straits of Gibraltar formed. Since the Messinian Salinity Crisis, the Mediterranean continuously experienced the effects of tectonics and climate changes, as shown by the stratigraphic sequences in subsiding coastal plains, shallow shelves or in drowned littoral caves, that provided information on Pleistocene sea-level oscillations (Van Andel *et al.* 1989; Fornos *et al.* 2002; Tuccimei *et al.* 2003; Antonioli *et al.* 2004). Flights of marine terraces on emerging coastlines preserved the signatures of sea-level high-stands (Keraudren and Sorel 1987; Goy and Zazo 1988; Dumas *et al.* 1993; Carobene and Dai Pra 2003; Zazo *et al.* 1999, 2003; Rodriguez-Vidal *et al.* 2004; Uluğ *et al.* 2005). These shorelines are used to estimate the geodynamic activity and the most common marker is the shoreline that formed during the Last Interglacial period, 120-130 ka BP, during the climatic optimum of the Marine Isotope Stage (MIS) 5.5.

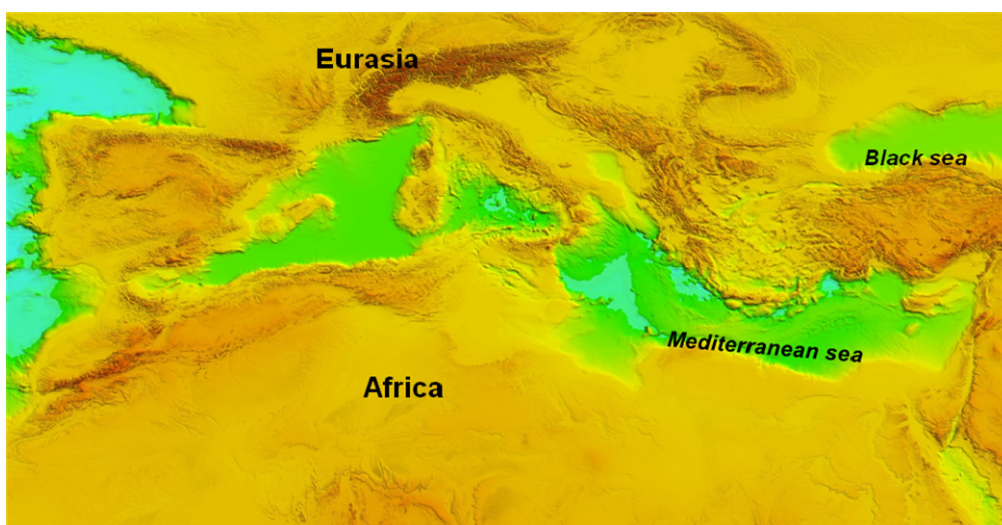


Fig.10 Paleogeographical reconstruction of the Mediterranean basin during the Messinian salinity crisis, about 6 Ma BP, based on SRTM data for surface topography and GEBCO data for bathymetry.

This event has left its traces along a large part of the coast of the Mediterranean, when global sea levels were standing 3–6 m higher than present time, and the warm climatic conditions favored the development of faunal assemblages. The fossilized gastropods of *Strombus bubonius* are valuable sea level indicators of this high-stand (Bordoni and Valensise 1998). Raised MIS 5.5 terraces are found in the Strait of Gibraltar (Zazo et al. 1999). in north-eastern Sicily and south-western Calabria (Miyachi et al. 1994; Bordoni and Valensise 1998; Ferranti et al. 2006). In other parts of the Mediterranean basin, like in Tunisia and Libya, the MIS 5.5 shorelines are roughly at their original elevation. But in other part are missing, such as along the Turkish Aegean coast (Bruckner et al. 2004). Thus, the variability in terrace elevation of the MIS 5.5 highlights the local vertical crustal deformations.

Besides the long term vertical land movements, recent instrumental sea-level data collected along the Mediterranean coast indicate the occurrence of an overall submergence at the rate of 1.2-1.8 mm/yr (Emery et al. 1988). The estimated sea level rates vary with the location, depending on the tectonics and volcanic activity, besides local disturbances. The most active shorelines are those of the Hellenic and Calabrian arc, located in the eastern and central Mediterranean, respectively. These are coinciding with zones at high seismic activity (e.g. Pirazzoli et al. 1986b; Stewart et al. 1996; Anzidei et al., 2011b) or with active volcanic centers (Dvorak and Mastrolorenzo 1991; Firth et al. 1996; Stiros 2000; Morhange et al. 2006; Tallarico et al., 2003). In addition to tectonic deformation, land movements in the Mediterranean are caused by the glacio-hydro-isostatic effect as shown by various competing numerical models developed during the last two decades.

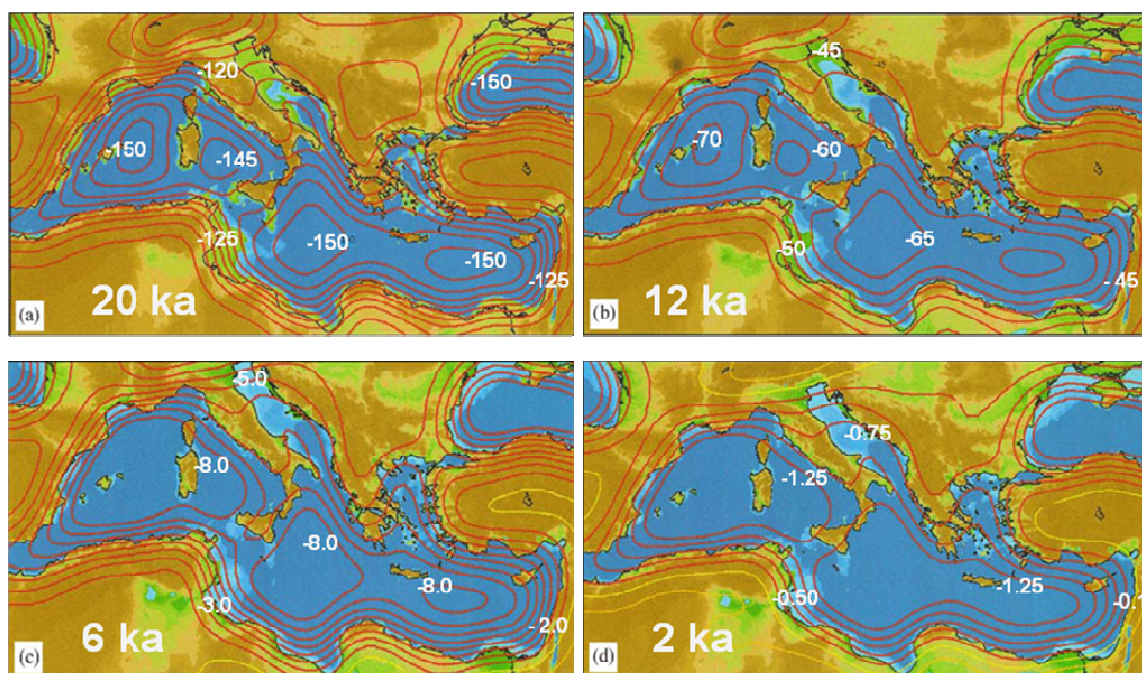


Fig. 11 Predicted relative sea levels and shorelines across the Mediterranean between 20 and 2 ka BP. The green–blue transition is the palaeoshoreline. Contour intervals: 5m for 20 and 12 ka BP; 1m for 6 ka and 0.25m for 2 ka. Red contours are negative values, orange contours are positive values, and yellow contour is zero change (from Lambeck and Purcell, 2005).

They predict the shoreline responses to changes in the ice-ocean loading (Lambeck and Johnston, 1995; Peltier, 2000; Lambeck and Bard 2000; Stocchi and Spada, 2009) originated from the rebound of the former ice-mass centers of Europe and North America. During this global scale deformations, the mantle beneath the Mediterranean crust deformed due to ice-sheet loading and now flows back causing the previously up-warped Mediterranean 'forebulge' to subside. The hydro-isostatic contribution, resulting from the melt water of the ice-sheet decay, increase the water load of the global oceans and seas, down-warping the marine basin floors and up-warping their margins (Lambeck *et al.* 2004a, 2004b). It is worth noting that the glacio-isostatic models are in agreement with field observations and the postglacial Mediterranean sea level has never been higher than today. Therefore eventual Holocene coastal deposit located at elevation above the modern sea level, are the evidence for local vertical tectonic movements.

The Mediterranean Sea is beyond the direct influence of the ice sheets and of the glacio-isostatic signal since the end of the Last Glacial Maximum (Meier *et al.*, 1984). (Fig. 11). For the last 7000 years this signal causes a sea level rise that mostly dominates the hydro-isostatic contribution. Thus, in the absence of tectonics, Late Holocene sea levels for much of the Mediterranean will be characterized by slowly rising values.

The Mediterranean is an area of low tidal amplitudes and restricted wave effect (short fetch). For these features, the records of past sea levels along the coasts are better preserved than in the oceans. Geological, biological, and archaeological indicators represent a good observational database, to address some of the specific issues about Late Holocene sea level. Unfortunately, horizontal and vertical tectonic movements are important in this region due to the still ongoing collision between the African and the Eurasian plates, complicating the pattern of sea-level change expected from glacial cycles alone. Additionally, being the Mediterranean a nearly closed basin, water variations induced by changes in salinity and/or temperatures may be important over decades and centuries. Many studies in the Mediterranean, aimed to establish the sea level rate of change and tectonic uplift rates along the coasts (Flemming 1969; Caputo and Pieri 1976; Van Andel 1989; Laborel *et al.* 1994). But the isostatic contributions were neglected in these studies. Lambeck *et al.* (2004b) and Lambeck and Purcell (2005), introduced the isostatic contribution in the sea level reconstructions and modeled the observed changes across the basin. Anyway, tectonically stable areas within the Mediterranean basin can be identified on geological or geophysical features or from the position of the Tyrrhenian shoreline of the Last Interglacial (MIS 5.5), which is clearly identified by its morphological and litho-stratigraphic markers and the associated Senegalese fauna (Antonioli e Silenzi 2007).

Parts of the Italian peninsula, Sardinia and northwest Sicily can be considered tectonically stable on the Holocene timescale but part of southern Italy, such as Calabria and northeast Sicily are uplifting at rates of up to 2.4 mm/yr (Antonioli e Silenzi 2007). Conversely the north Adriatic area is downliffing at a rate of 0.75 mm/yr in the last two millennia, producing a significant downward displacement of the coastline of ~1.5–1.6m (Antonioli *et al.*, 2007). The evidence of uplifting areas is well given by the erosion notches near Corinth (Figure 21) (Flemming and Webb 1986; Pirazzoli *et al.*, 1994), and their elevations were used to estimate magnitudes and Earthquake recurrence times than for sea level studies. But, in the regions where the Last Interglacial shorelines are absent, uplift and subsidence rates for Holocene can be estimated more precisely when the glacio-hydro-isostatic model has been calibrated against the data from the known tectonically stable areas (Monaco *et al.* 2004; Orrù *et al.* 2004) and then applied to the areas of recognized or supposed tectonic activity (Antonioli *et al.*, 2007).

The assumption of uniform rates of tectonic vertical movement is not always valid for all the areas as shown by the examples of Basiluzzo and Pozzuoli, respectively located in the volcanic arc of the Aeolian Islands and the Phlaegrean Fields volcanic complex. In the latter, the Roman columns of the temple of Serapis show marine borings at elevations up to 7 m above sea level (Morhange et al. 1999). Radiocarbon dating of *in situ* *Lithophaga* and other mollusk shells found in these columns, as well as of *in situ* corals and mollusks from nearby cave and cliff sites, indicates that local sea level reached 7 m above present during three periods since Roman times; in the fifth century AD, early Middle Ages between 700 and 900 AD, between 1300 and 1500 AD, and finally before 1538, when a volcanic eruption created the Monte Nuovo (Morhange et al. 2006) (Fig.12), displacing the coast to a new position.

At other sites there is evidence for long term changes in uplift rates with the average rates for the past approximately 120.000 years up to time larger when compared with those for the past 10.000 years (Antonioli e Silenzi, 2007).

Archaeological evidence provides many records of patterns of change. For example, along the coast of Tunisia (Slim et al. 2004; Anzidei et al., 2011a), in Lybia (Anzidei et al., 2011a), at the buried port of Troy (Kraft et al. 2003), at the ancient harbor of Marseilles (Morhange et al. 2001), or the submerged urban quarters at Tyre where a seawall 3 m high indicates ~3 m of submergence, compared with a submerged quarry indicating relatively little sea-level change at Sidon (Marriner et al. 2006). Along the coast of Israel, sea level rose to reach a level close to present around 2000 years ago (Anzidei et al., 2011b), with evidence of changes of ~30–40 cm (Sivan et al. (2003b; Sivan et al. 2004).

The Roman fish tank data from the more stable areas of the central Mediterranean have provided the most accurate estimates for paleo-sea levels because the relationship between the structural features of the archaeological sites to the tidal range is well established and it indicates an average relative sea-level change along the central Tyrrhenian coast of Italy at $\sim 1.35 \pm 0.07$ m at 2000 years ago (Lambeck et al. 2004b).



Fig. 12 Painting of the 1538 Monte Nuovo eruption (author unknown), that shows the coastline position before the eruption “*Termin del mare de prima*”.

Anyway, in other part of this coast, such as in Calabria, this change is compensated by the tectonic uplift, that has equal value of the glacio-hydro-isostatic signal, but having

opposite direction (Anzidei et al. 2006; Anzidei et al., 2012). Most of this change from the stable region can be attributed to ongoing isostatic signals. When corrected for this and compared with the present rates of change estimated from nearby tide-gauge stations having long enough records to be statistically affordable, the change in sea level attributed to change in ocean volume since the Roman Period is a rise of 0.13 ± 0.09 m. The comparison of the Roman fish tanks and tide gauge results for eustatic sea level indicate that the present-day rate of change can only be representative of a short interval of time unless sea levels in the intervening period were actually lower than the Roman values. In the absence of evidence for this, the comparison indicates that this duration was of the order 100 ± 50 years and, while the uncertainties in this estimate remain large, the results are consistent with an onset of the present sea-level rise in the late nineteenth century or early twentieth century (Lambeck et al. 2004b).

The isostatic response in the Mediterranean basin causes a significant spatial variability due to the variability in the coastline geometry and because of variable distance from the former ice sheets. This is shown from the vermetid and coralline algae data from the French Mediterranean coast between Marseilles and Nice (Laborel et al. 1994) and the well data from Israel (Sivan et al. 2004). The differences can be attributed to the differences in isostatic contribution at the two sites. Thus the differential techniques can be used successfully to separate out the isostatic and ocean-volume contributions. In all cases, the results show an ongoing increase in ocean volume until about 3000 years ago, such as to raise global sea level of about 3 m between ~ 7000 and ~ 3000 years BP, with a near constant ocean volume over the past ~ 2000 years (Lambeck and Purcell 2005).

Therefore, the glacio-hydro-isostatic effect for the Mediterranean, results in a diffuse subsiding process with rates varying from north to south and from west to east, with orders of magnitude between 0.2 and 0.8 mm / yr (Lambeck and Chappel, 2001; Lambeck and Bard, 2000; Lambeck et al., 2004 a; Lambeck et al. 2004b, Antonioli et al., 2007). An exemplary effects of what is happening is given by coastal archaeological structures such as the fish tanks built by the Romans 2000 years ago, along large parts of the Mediterranean coasts that are nowadays often submerged (Lambeck et al., 2004b).

5. The sea level indicators in the Mediterranean

The sea level indicators are natural or anthropogenic structures located along the coast in the tidal range thus directly bearing with the local mean sea level. Particularly valuable, are the paleo-sea-level indicators that are crucial to understand the past positions of sea level. Exist several types of paleo-sea-level indicators: sedimentary (i.e. beachrock), erosional (i.e. notches), ecological (i.e. accretionary biotherms built up by coralline algae), microfossils (i.e. diatoms, testate amoebae, and foraminifera), and archaeological (i.e. harbors, pools, fish tanks).

Anyway, the reconstruction of sea level history (sea level curves) must take into account the uncertainties regarding the determination of vertical relationships between the position of the sea-level indicator and mean sea level and the errors associated with the age determination, considering that their level refer to a position included within the local tidal range. Therefore, is mandatory to define the *functional elevation* or the elevation of the specific the sea level indicators with respect to the estimated local mean sea level at that location and at the time when they were active.

The *functional elevation* depends on the type of the indicator (biological, geomorphological or archaeological, etc.), and the local tide amplitudes. For example, when surveying archaeological indicators, the minimum elevation of particular structures above the local highest tides must be defined on the basis of archaeological interpretations. The main

steps to be followed during surveys and the subsequent interpretation of the results are summarized as follows:

- reduce the measurements to local mean sea level by applying tidal corrections using the available nearby tide gauges (i.e. www.idromare.it; www.pol.ac.uk; <http://www.ioc-sealevelmonitoring.org/>). If tide gauge are unavailable, can be used predicted tidal amplitude (for example using tidal prediction at <http://wxtide.com>), and reducing them for local pressure values;
- estimate measurement errors of topographic elevations (multiple measurements), and ages (instrumental, historical and bibliographical data), of the indicators;
- examine predicted and observed sea levels for the observed locations, by comparing the current elevations of the markers (i.e. relative sea level change measured at each location), against the sea level elevation predicted by the glacio-hydro-isostatic model for the same location;
- in general, and in absence of any further information, during the interpretations can be defined as stable tectonic areas those where the elevations of the indicators are in agreement with the predicted sea-level curve. Conversely, when the elevations of the indicators disagree from the predicted sea-level curve (i.e. they fall below or above the predicted sea-level curve), vertical land movements are expected (due to tectonics, volcanism, subsidence, anthropogenic effects).

it is worth noting that because each area has its own geological and geophysical characteristics, it is not possible to compute a single sea level curve valid to describe the sea level change at regional or global scale. Therefore for each investigated area is necessary to estimate the history of the local sea level curve.

The positions of the sea level indicators can be close to mean high water, as is the case for salt marsh markers (Horton et al. 1999), or mean low water springs, as for coral microatolls (Smithers and Woodroffe 2000; Hopley et al. 2007), or near the mean sea level, as for the sluice gate of the fish tanks (Lambeck et al., 2004b). Often this observation can only gives a limiting value. Positional uncertainties (from survey error or from disturbances of the marker since their existence), and age uncertainties must be taken into account (Woodroffe et al. 2007).

When multiple indicators, such as geological, biological and archaeological are all present in combination in a locality, the observations of the past sea level positions are reinforced (i.e. marine mollusk grown on archaeological structures, as reported in Morhange et al., (2001), or the fish tank complex at Ventotene, with harbor and quarry of the roman age, as in Lambeck et al., (2004b).

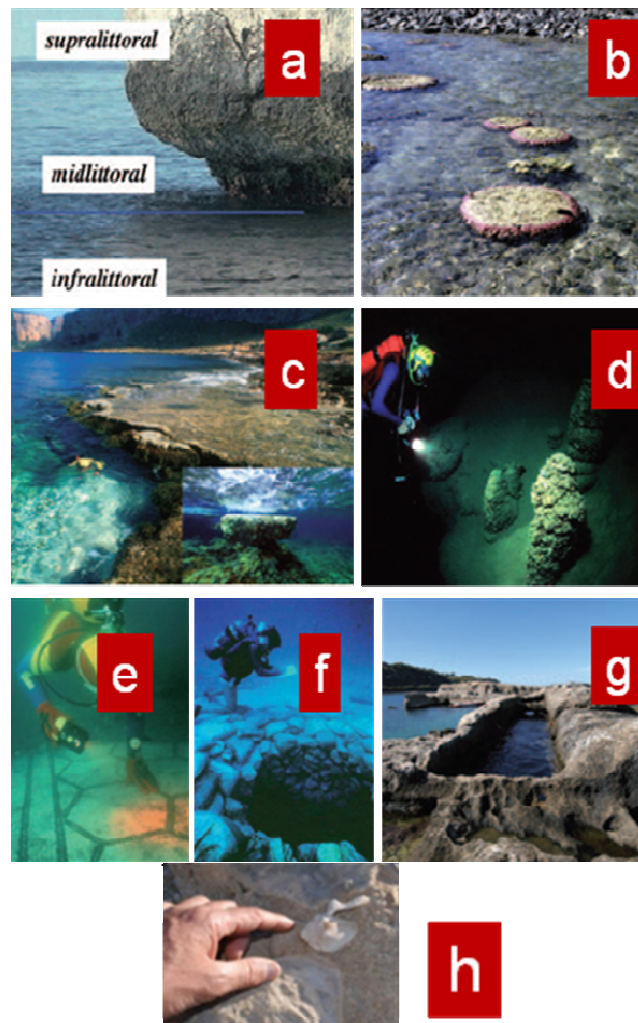


Fig. 13 Sea level indicators: (a) Notches along the rocky coasts of the Mediterranean with organisms characterizing the supralittoral, mid-littoral, and sublittoral environments; (b) coral microatolls (Orpheus island, AU); (c) Vermetid reef; (d) Serpulid overgrowth on submerged stalagmites in Argentarola Cave, Italy; (e) sunken city of Baia (Italy), 2ka BP; (f) Neolithic submerged well at Atlit Yam (9.5 and 8.2 cal/yr BP), at 10 m bsl (Israel); (g) roman age rock-cut fish tank (Briatico, Calabria); (h) *Strombus Bubonius*, fossil of the MIS 5.5 climatic stage of 125 ka BP. (figs. a,b,c,e,f,g from Lambeck et al., 2010; fig.d courtesy of F.Antonioli; fig.e, courtesy A.Benini; fig.g and h by M.Anzidei). (modified from Church et al., 2010)

5.1 The archaeological indicators

Coastal settlements constructed in antiquity provide important insights into sea-level changes during past millennia, and reconstructions of historical sea-level change using archaeological coastal installations have been particularly effective in the Mediterranean Sea, whose coastlines preserve remnants of past human activity since the LGM. The first pioneering results using geophysical interpretations from archaeological indicators for the sea-level change estimation were published by Flemming (1969), Caputo and Pieri (1976), and Pirazzoli (1976). Unfortunately, despite the large number of archaeological remains in the Mediterranean (Figs.13,14 and 16), only a small part of them can be used to obtain precise information on their former relationship to sea level.

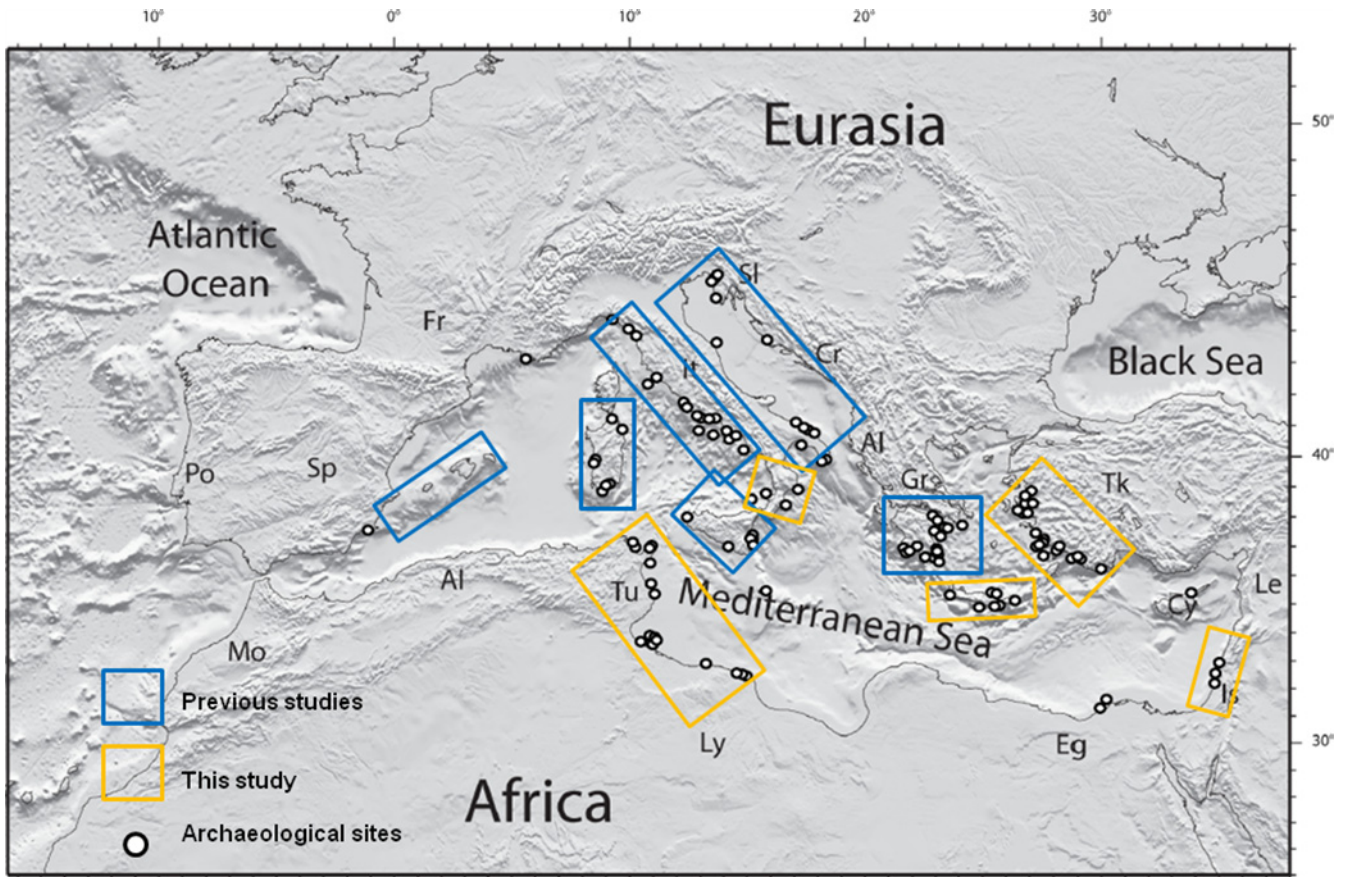


Fig. 14 The archaeological sites in the Mediterranean studied since the last decades. Orange boxes are the areas discussed in this study. Blue boxes are areas previously investigated. Black and white dots are the archaeological sites investigated.

Limitations arise as a result of their uncertain use, poor preservation, or because they were built in geologically unstable areas (for examples soft sediments at the mouth of rivers or near active volcanic centers). The observed intervening sea level change is inferred from those structures or artifacts which must have been terrestrial but have now been flooded, and second those coastal structures that were built with a precise relation to water level and which no longer function because of a change in sea level (either rising or falling). The flooded paintings of Cosquer cave, in Southern France (Clottes et al. 1997), belong to the first category and provide the oldest known archaeological constraints on sea-level change in the Mediterranean (Lambeck and Bard 2000). The second category more precise and includes slipways, fish tanks, piers and harbor constructions generally built between 2500 and 1000 years BP.

The Roman fish tanks, generally dated between the first century B.C. and the first century A.D., are particularly valuable, because they can provide very precise data (Figures 13,14,16,17). Quarries carved along the coastlines and located nearby fish tanks, and harbors or villas of similar age, can provide additional data on past water level, as well as information on their functional elevation above sea level, although these are less precise indicators (Flemming 1969). Wells, such as those submerged off the coast of Israel (Figure 13f), indicate gradual sea-level rise since 8000 years ago (Sivan et al. 2001, 2004). Likewise, now-submerged sites of human activity can provide limiting information.

One example is the Early Neolithic burial site at ~8.5 m in northern Sardinia where the archaeological style of a nearby settlement gives an age of approximately 7600 years BP

at which time local sea level was more than 8.5 m lower than present (Antonioli et al. 1996). Other examples are the submerged buildings of the sunken city of Baia (Fig. 13e) and the submerged breakwater at Capo Malfatano in Sardinia. Functional elevation is defined from the elevation of specific architectural parts of an archaeological structure with respect to the local mean sea level at that location and at the time of its construction, and provides the basis for determining sea-level change. It depends on the type of structure, its use and the local tide amplitudes.

The minimum elevation of particular structures above the local highest tides can be defined. So far, pier surfaces can be estimated at an elevation of at least 1 m above sea level, bollards at 0.7–1.0 m, and up to 2.0 m for large harbors such as at Leptis Magna (Libya), depending on the ship size. Slipways can be found at several sites in the Mediterranean, such as Sicily, Cyprus, and Turkey, and it is apparent that they will function only if they have enough dry length to house the ship out of the water and sufficient depth of water at the bottom of the slipway for the ship to enter (Blackman 1973) (Fig. 15).

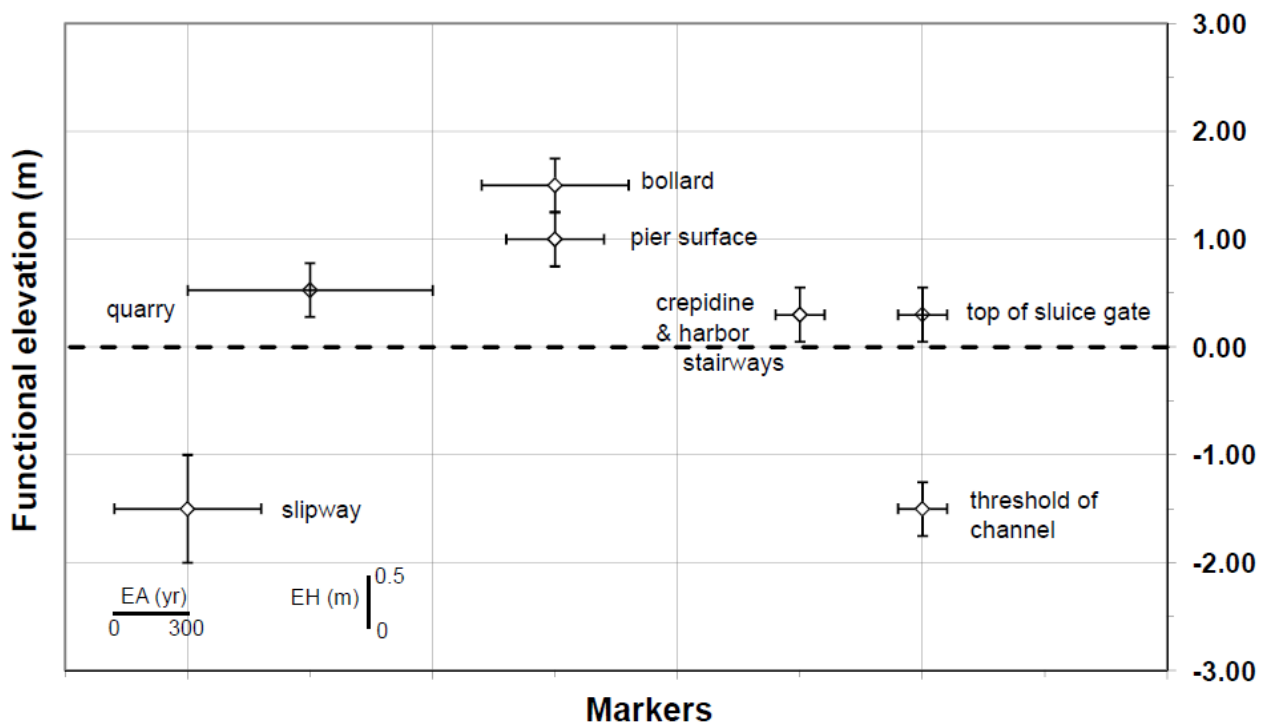


Fig. 15 Sketch of the functional elevation of the archaeological indicators in the Mediterranean. Data derive from the observation of constructional parts in about 100 different coastal archaeological sites distributed along the coasts of the Mediterranean. Vertical bars are the elevation uncertainty; horizontal bars are the age errors.

5.2 The Roman fish tanks

Among the different type of archaeological sea level indicators briefly described before, the Roman fish tanks are the most precise for the past 2 ka (Fig. 16).

These have constructional elements that bear directly on sea level at the time of construction (Columella) and well-preserved remains of these features provide a precise measure of sea-level change (Flemming, 1969; Pirazzoli, 1976; Schmiedt, 1976). According to Plinius and Varro, the use of *piscinae* as holding tanks and fish culture was introduced between the end of the second century and early first century BC. But because

of high construction and maintenance costs, they were used for a relatively short period only and the building of new tanks ceased during the second century AD. Most of the known fish tanks in Italy occur along the Tyrrhenian coastline (Schmiedt, 1976; Giacobini, 1997) near large Roman villas and only two are known along the Adriatic coast, at Ancona and in Apulia (Fouache et al., 2000). Only for a small number of these, precise sea-level markers have been preserved or identified. Remains of piscinae are also found along the Mediterranean coasts beyond the Italian borders (Flemming, 1969; Flemming and Webb, 1986) but these are often lacking in the very features that give the high accuracy for the Tyrrhenian examples, with the exception of a few cases in Cyprus and Tunisia. The Roman fish tanks were often carved into rock up to to a depth of 2.7 m or less “...in pedes novem defondiatu piscine...” depending on fish species. The basins themselves were protected from wave and storm action by exterior walls, “*Mox praeiaciuntur in gyrum moles, ita ut conplectantur sinu suo et tamen excedant stagni modum*”, whose foundations have mostly been preserved but whose relation to sea level is not defined.

From Latin publications and field surveys, were identified the significant sea-level markers and includes foot-walks (crepidines), channels, sluice gates with posts, sliding grooves and, in some cases, the actual sliding gates, and thresholds (Fig. 17) (Lambeck et al., 2004b; Schmiedt, 1976; Fouache et al., 2000). The foot-walks border the internal pools and occur at two or three levels (Flemming, 1969; Caputo and Pieri, 1976; Schmiedt, 1976; Leoni and Dai Pra, 1997). The lowest surface is cut by channels that permit water exchange between the tanks and the open sea, with the flow being controlled by sluice gates. These gates consist of

- a horizontal stone surface that defines the threshold and is cut by a groove to receive the gate;
- two vertical posts with grooves to guide the vertical movement of the gate;
- an upper stone slab with horizontal slot to extract the gate; and
- the gate itself with small holes to permit water exchange and prevent the escape of fish. The base of the channels coincides with the position of the threshold slab.

The top of the sluice gate coincides with the elevation of the lowest level foot-walk and, to keep a safety margin, corresponds, as reported by Columella, “*Spissi deinde clatri marginibus infiguntur, qui super aquam semper emineant, etiam cum maris aestus intumuerit*” to a position above the highest tide level.

From sites with complete preservation of sluice gates, channels and foot-walks, were estimate that the level of the lowest crepidine occurred at ~20 cm above the highest tide level. In the Tyrrhenian Sea the maximum tidal excursion is ~40–45 cm (Istituto Idrografico della Marina; www.pol.ac.uk; www.idromare.it), equal to the observed depths of the channels, and this indicates that the flow of water into the holding tanks was tidally controlled (Fig.17).



Fig. 16 Some of the fish tanks located along the coastlines of the Mediterranean sea, discussed in the text (see also annexes 4,5,6): A) Cesarea (Israel); B) Sidi Daoud (Tunisia); C) Ferma (Crete, Greece); D) Baia (Naples). The photo shows the post and the channel of the fish tank, presently submerged at about -3.4 m; E) Torre Astura (Italy); F) Alicante (Spain); G) Ventotene Island (Italy); H) Briatico (Italy).

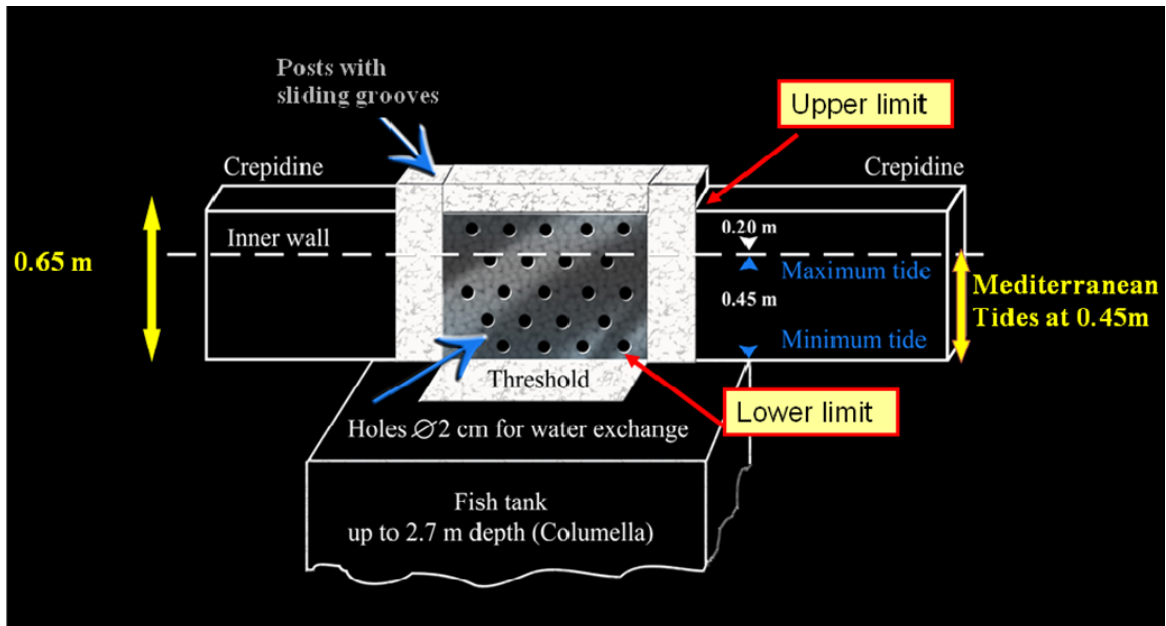


Fig. 17 The sluice gate and channel system for tidally controlled water exchange in a roman age fish tank (tides in the Mediterranean are normally in the range of 0.45 m, with the exception of the Gulf of Gabes (Tunisia) and in the north Adriatic Sea). The sketch corresponds to channels systems that still include sluice gates made of lead or stone, in the fish tanks of Torre Astura – La Banca, Ventotene (Italy), and Akziv (Israel). The complete gate consist of: (i) a horizontal stone surface that defines the threshold with a groove to receive the gate; (ii) two vertical posts with grooves to guide the movement of the gate; (iii) an upper stone slab with horizontal slot to extract the gate; (iv) the gate itself, ~65 cm high, with small holes for water exchange. In this illustration, the gate is partially covered by sand and the bright zone is that part of the gate that has been cleaned of sand and biological growth. The threshold, covered by sand, lies ~10 cm below the measuring rod that is calibrated at 10-cm intervals. (B) Sketch of the channel sluice gate with sliding posts, threshold and lowest level crepidine as viewed from within the fish tank. The top of the sluice gates coincides with the elevation of the lowest level footwalks and corresponds to a position above the highest tide. In this example, the lowest foot-walk is now 0.72 m below the sea surface at the time of measurement and the threshold is 1.37 m below present sea level.

6. Vertical land movements

A crucial point in the estimation of the relative sea level changes at local scale is provided by the active tectonic movements along the vertical, that may modify the coastlines (Pirazzoli, 1991) (Figs. 18, 19, 20, 21). In studies of coastal vertical movements in the Mediterranean are traditionally used geological and biological markers of the last interglacial period of the isotopic stage 5.5 (the Tyrrhenian layer of MIS 5.5 dated at ~125 ka BP). Their elevation corresponds to the eustatic sea level during this period, at 7 ± 1 m above present sea level. Therefore it is possible to determine the value and extent of the long term vertical coastal movements by measuring the elevation of this deposit of the Tyrrhenian age outcropping along the coast (the difference in elevation between the current elevation of the MIS 5.5 layer and its corresponding palaeo-eustatic position at +7 meters, quantitatively defines the mean vertical dislocation occurred in the last 125 ka BP) (Antonioli et al., 2000; Bordoni and Valensise, 1998; Nisi et al., 2003a, Ferranti et al., 2006; Ferranti et al., 2010).

The Mediterranean region is a tectonically active area that suffers of seismicity and volcanism due to the dynamics of the African and the Eurasian plates. Because these plates are still colliding up to several mm/yr (Serpelloni et al., 2007), we can deduce that coastal areas located in this active region can experience, besides the horizontal motion, tectonic uplift or subsidence. Recent studies estimated the rates of the vertical land

movements in the range of -1 and 2.4 mm/year (Amorosi et al., 2004; Doglioni, 1994; Carminati et al., 2003a,b; Ferranti et al., 2007; Figs. 19 and 20). These vertical movements occur at different rates for different locations. The coast of northern Africa facing the Mediterranean, displays an overall tectonic stability and the elevation of the MIS 5.5 is generally at 3-7 m above sea level and in one case within 32 m. In the Levant region, the large part of Tunisia and Libya, part of Italy, the MIS 5.5 is within 5 and 7 m. But along the coasts of SW Turkey is missing, due to the large tectonic coastal subsidence recently estimated at 1.48 mm/yr, and related to the intense seismic activity of the Hellenic Arc, causing the dramatic relative sea level rise for this part of the coast (Anzidei et al., 2011b). In Greece, France, Spain, Slovenia and Croatia, data are sparse and with various elevations. In Italy, the coastal areas of Tuscany, Sardinia, southern Lazio, western Sicily and Apulia are stable with MIS 5.5 elevations generally within 10 m, with the exception of part of the coasts of Lazio, where MIS 5.5 is up to 30 m (Ferranti et al., 2010). Calabria is the area of the Mediterranean with the highest uplift rates. Here, the MIS 5.5 is up to about 200 m of elevation. The Eastern Sicily is also uplifting, but with minor rates. Conversely, the Friuli, Veneto and Emilia-Romagna regions are in tectonic subsidence (Ferranti et al., 2006).

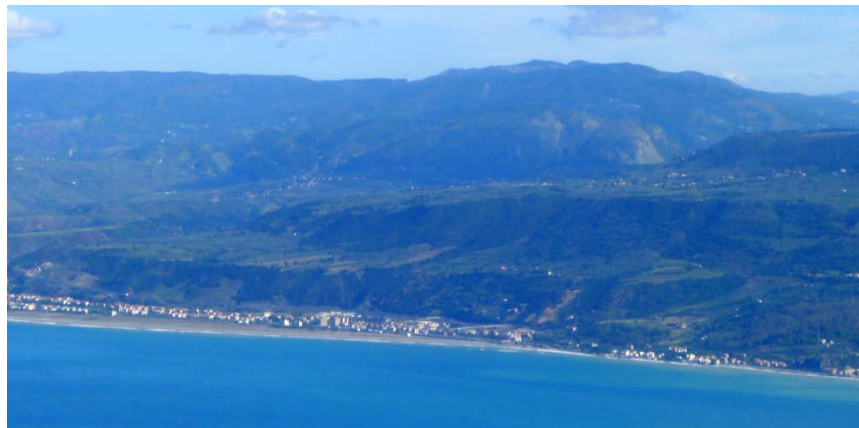


Fig. 18 Elevated marine terraces along the Tyrrhenian coast of Calabria, near Lamezia Terme.

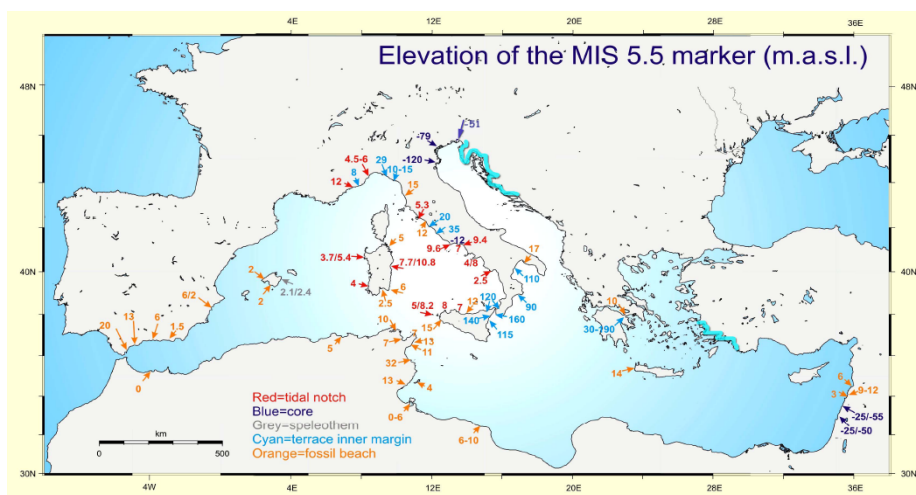


Fig.19 Elevation of the MIS 5.5 marker in the Mediterranean region (From Ferranti et al., 2006). The blue lines mark the absence of MIS 5.5.

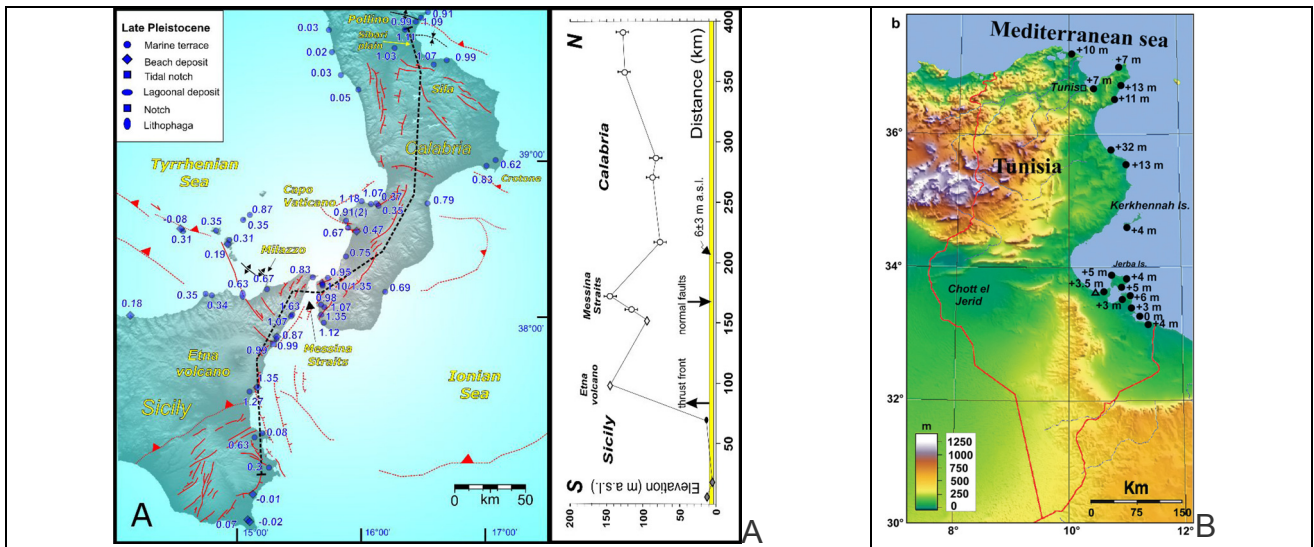


Figure 20 Two key areas of the Mediterranean that highlight the large differences in vertical land movement from the elevation of geological and geomorphological indicators. A) Vertical displacement rates in the Calabrian Arc, which is the most uplifting region in the Mediterranean (From Ferranti et al., 2010); B) Map of the elevation of the MIS 5.5 in Tunisia that reaches 32 m at one location (from Anzidei et al., 2011a). (The black triangle is the position of the Lithophaga at El Grine, dated at 5846-5700 calibrated age, related to a possible high-stand of ~5ka BP) (see annex 5 for details).

The subsidence in coastal lowlands is also caused by natural (e.g. soil compaction), or anthropogenic causes (land reclamation, extraction of fluids). An example is the coast of Emilia-Romagna near the Po delta, where the subsidence rate is up to 70 mm/yr (Carminati and Martinelli, 2002), including those caused to human activities due to fluid extraction, that are of 10-30 mm/year (Bonsignore and Vicari, 2000). Therefore, the use of land resources, are also considered among the causes of the recent sea level change, besides the thermal expansion of the oceans and the melting of glaciers, likely due to the massive release of greenhouse gases in the atmosphere.

In addition, the over-exploitation of deep fluids has as a consequence, local coastal erosion. The anthropogenic effects are then a part of the causes of the changes in sea level, probably with a greater impact than the natural dynamics of at least one order of magnitude.

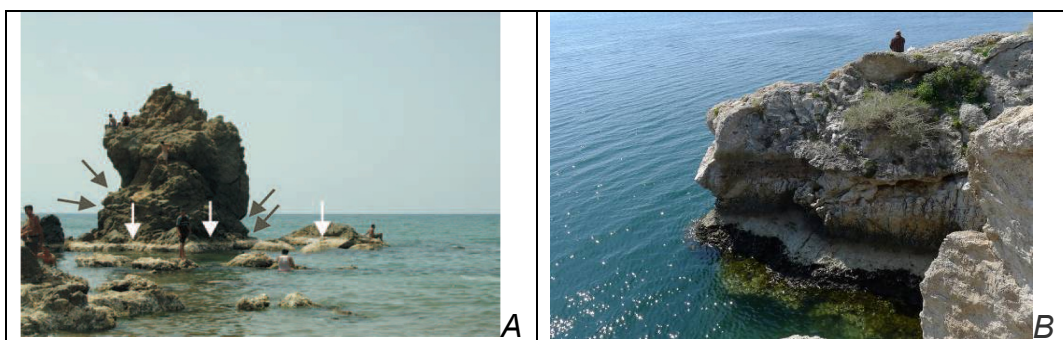


Fig. 21 A) Co-seismic coastal uplift at Le Figurier (Algeria) caused by the Mw= 6.8 Boumerdès Earthquake of May 21, 2003 (from Meghraoui et al., 2004); B) Repeated co-seismic uplifted marine notches in the Gulf of Corinth, at Heraion (Greece),

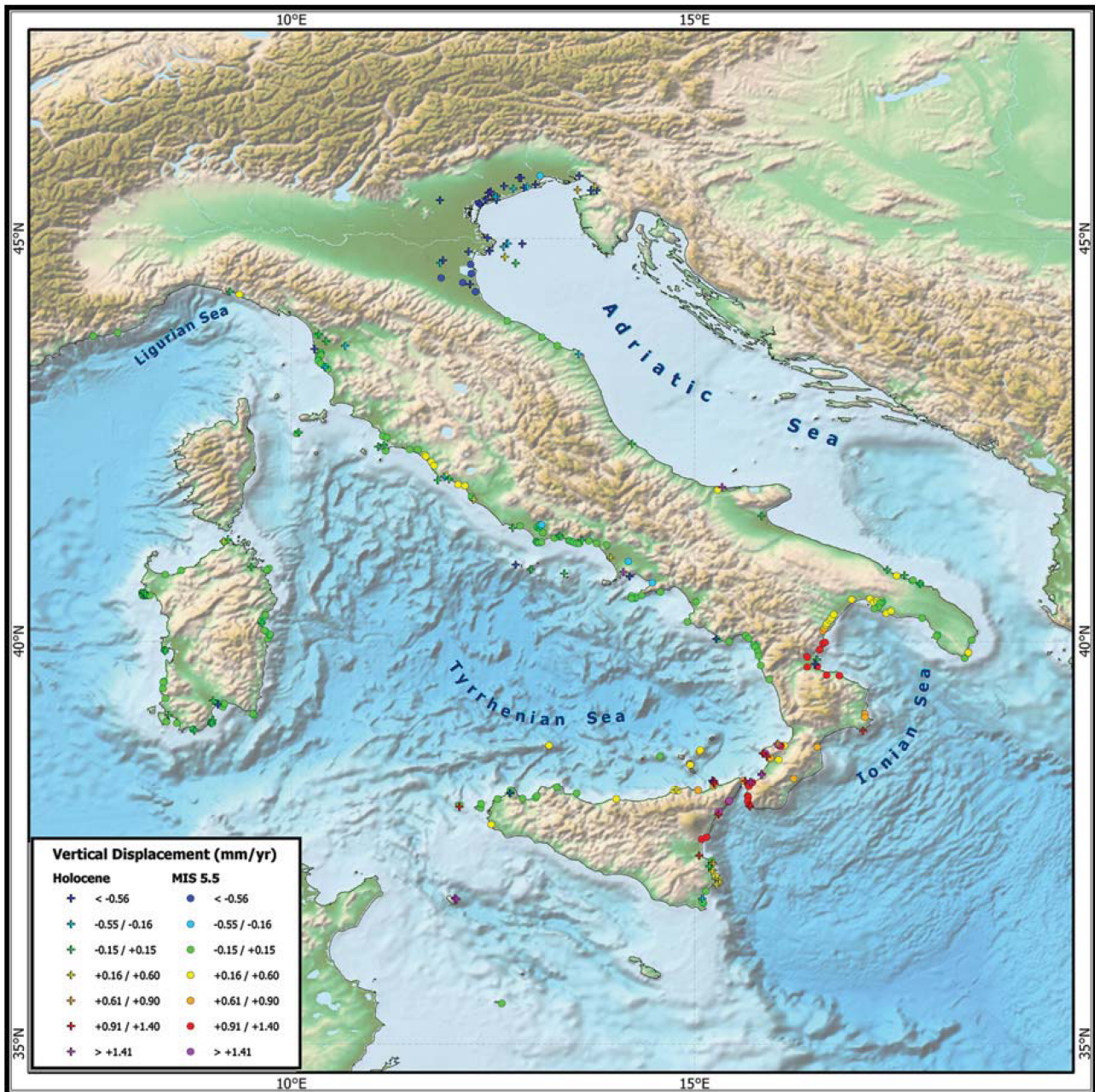


Fig. 22 Rates of vertical movements in Italy (mm/yr) averaged for the Holocene and for the last glacial cycle (From Lambeck et al., 2011) (see annex 2 for details).

7. Recent new findings for the coasts of Calabria

Calabria is one of the most complex geological regions of the Mediterranean basin, which experienced large Earthquakes and land uplift and is still undergoing to active tectonics (Antonioli et al., 2007; Ferranti et al., 2006; 2007; 2010). Its coastlines are displaced at various elevations, thus providing indications on sea level changes and tectonic activity (Pirazzoli, 1976), and shows several archaeological sites of the last ~2.3 ka BP that can be used as powerful indicators of the relative vertical movements between land and sea since their construction. During this Doctorate were investigated part of the Tyrrhenian and Ionian coasts of Calabria, and were found different patterns of the relative sea level change occurring in these two areas. Along the Tyrrhenian coast were studied the

maritime archaeological indicators at Briatico, consisting in an uplifted Roman age fish tank and a submerged breakwater about 320m long. Along the Ionian coast, were observed only submerged constructions, breakwaters and coastal quarries of greek and roman ages, in conjunction with geomorphological indicators, all providing information of a relevant subsidence intervening during the last 2.3 ka BP.

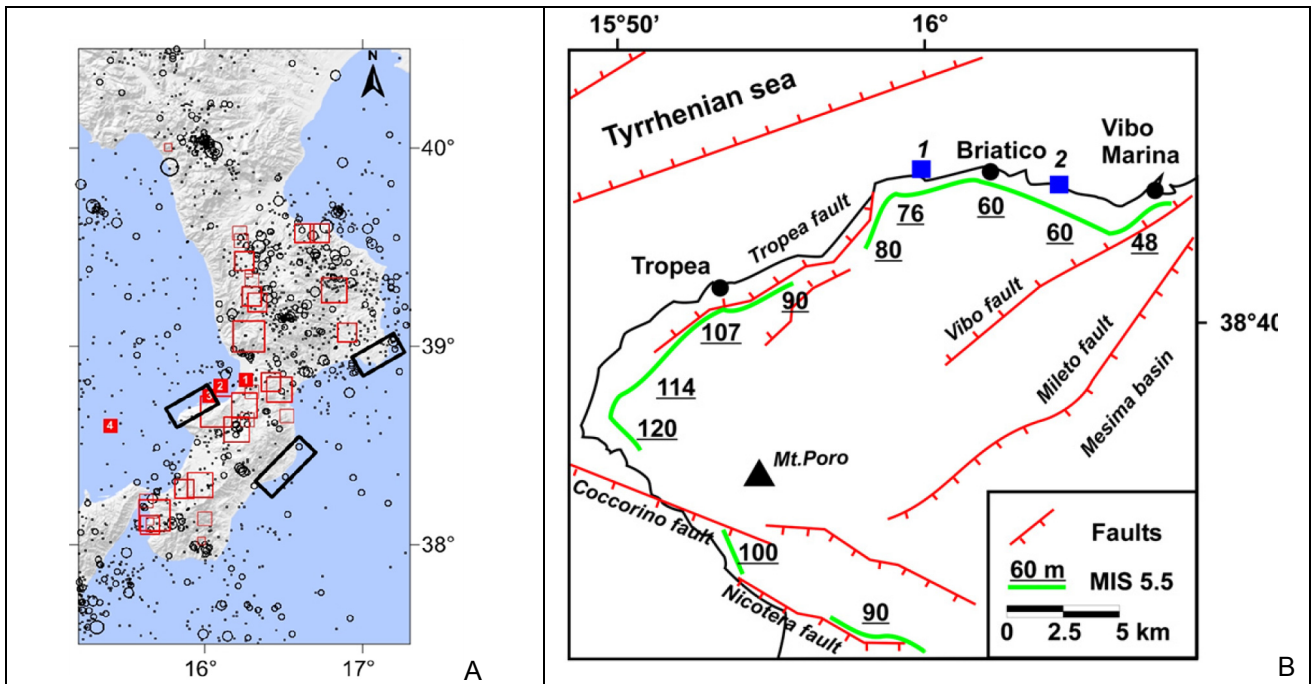


Fig. 23 A) Location of the investigated coastal archaeological areas in Calabria (black rectangles), and seismicity (black dots and red squares are the epicenters of instrumental and historical earthquakes, respectively (size is proportional to Magnitude). The locations of the 1905 earthquake are from: 1=Rizzo (1907), 2=Riuscetti and Schick (1974); 3=Camassi and Stucchi (1997), 4=Michelini et al. (2005) (from Anzidei et al., 2006; Anzidei et al., 2012). B) The MIS 5.5 terrace (green line with elevation in meters) and the main faults at Capo Vaticano promontory (from Miyauchi et al., 1994). Numbered blue squares are 1) the location of the Scoglio Galera fish tank and 2) the pier at the mouth of Trainiti creek. (from Anzidei et al., 2012. See also annex n.6)

7.1 Tyrrhenian coast

Along the Tyrrhenian coast of Calabria, surveys mainly focused in the area between Vibo Valentia marina and the village of Briatico where are located two archaeological structures of Roman age (Fig 23a). The first one is represented by a breakwater built at the mouth of Trainiti creek near Porto Salvo village. The second is a fish tank, excavated on the Scoglio Galera, a small rocky islet near the small village of Santa Irene (Briatico) (see annex 6). The breakwater near Trainiti was excluded from the analysis because in absence of precise constructional and morphological elements in the shallow part of the pier, precise estimation of the intervening relative sea level changes since the time of its construction cannot be determined. In fact there is a lack of precise information on the harbor that today is completely buried under the recent sediments of the coastal plain (Schmiedt, 1966). The second site is the Scoglio Galera, having features particularly valuable as sea level indicator. It is located near the village of Briatico, about 100 m distant from the coast and is ~120 m long and ~40 m wide, extending east-west (Fig 24). This small islet was known

from historical tradition to be used by Arabs to jail the Christians, sinking them in the pools. Recently, marine archaeologists classified this site as a fish tank and a fish processing plant (Mariottini, 2001). The islet was excavated in the bio-marlstone and limestone of Miocene age. The fish tank consists of four nearby pools, E-W aligned, that follow the natural morphology of the islet. The pools have a total length of about 28 m and a constant width of 2.5 m. The two main pools are subdivided into minor ones and are crossed by two main channels, which link the inner basin with the open sea. The latter is protected and suitable for the moorings of ships.

All the channels show the signs of the grooves used to operate the sluice gates, similar to those found in the fish tanks along the Tyrrhenian coasts of central Italy and other localities (Lambeck et al., 2004b; Anzidei et al., 2011b). The inner side of the pools show a present day notch about 40 cm high and 30-60 cm deep. Its bottom part shows an organic platform typical of high hydrodynamics environments, in agreement with the amplitude of the local tides. The northern border displays an abrasion platform up to 6m wide, characterized by *Dendropoma petreum*, a gastropods that usually live in the lower intertidal environment (Antonoli et al., 1999). The platform includes several squared holes excavated in the islet that once supported the wooden poles that made up the reinforcements of high concrete walls, built to protect the islet from the waves.

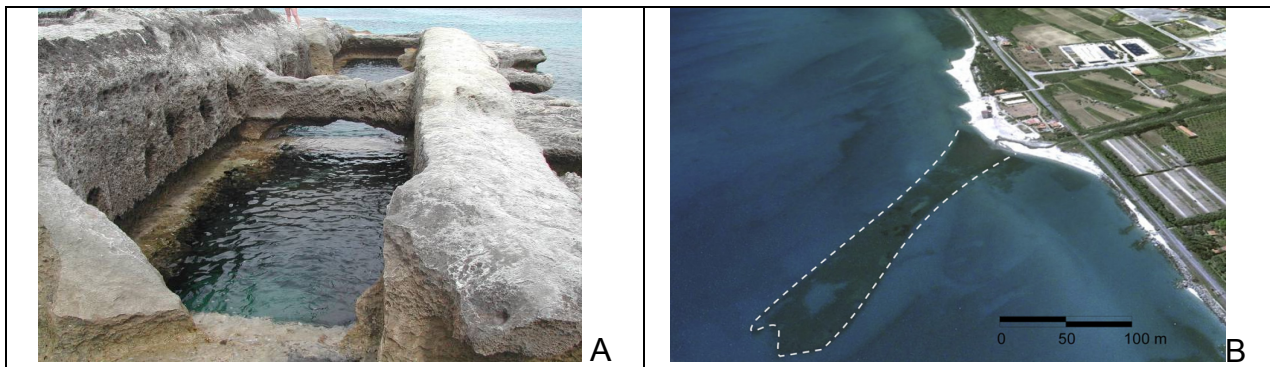


Fig. 24 A) The Scoglio Galera with the pools of the fish tank equipped with channels tidally controlled for water exchange within the basins. Note the tidal notch within the pools, developed only after the fish tank construction; B) Aerial view of the pier at the mouth of Trainini creek (image from Google Earth, <http://www.earth.google.com>).

The sea level curve estimated by Lambeck et al. (2011) predicts a sea level change for this location of ~ 113 cm since the last 1806 ± 50 years, at a mean rate of ~ 0.63 mm/y. Observations have estimated that the relative sea level has changed only ~ 7 cm since the construction of the archaeological site. Therefore, the recent tectonic uplift inferred from the fish tank exceeds by ~ 0.18 mm/y the previous estimates of Miyauchi et al. (1994) obtained from the elevation of the MIS 5.5 marine terrace, which infers an uplift rate of 0.47 mm/y at Briatico. Bianca et al. (2011) found the MIS 5.5 terrace at 216 m of elevation, in contrast to the value of about 60m reported in Miyauchi et al. (1994), thus inferring a long term uplift rate up to 1.74 mm/y. As this value is in large contrast with the previous measurements of Miyauchi et al. (1994). Besides the long term geological data, recent geodetic observations are available in Calabria which show the present day uplift of this region. The tide gauge of Reggio Calabria has recorded a sea level trend of 0.28 mm/y during the time span 1999-2007 (but with higher rates for 2001-2011 as shown in chapter 8 of this thesis). Although the duration of the sea level recordings for this station is still too short to provide a robust estimation, this value can be considered as a preliminary

indication that should correspond to a deficit of ~ 0.8 mm/y in the sea level increase with respect to tectonically stable coastlines of Italy. This result is in agreement with the results from Braitenberg et al. (2011).

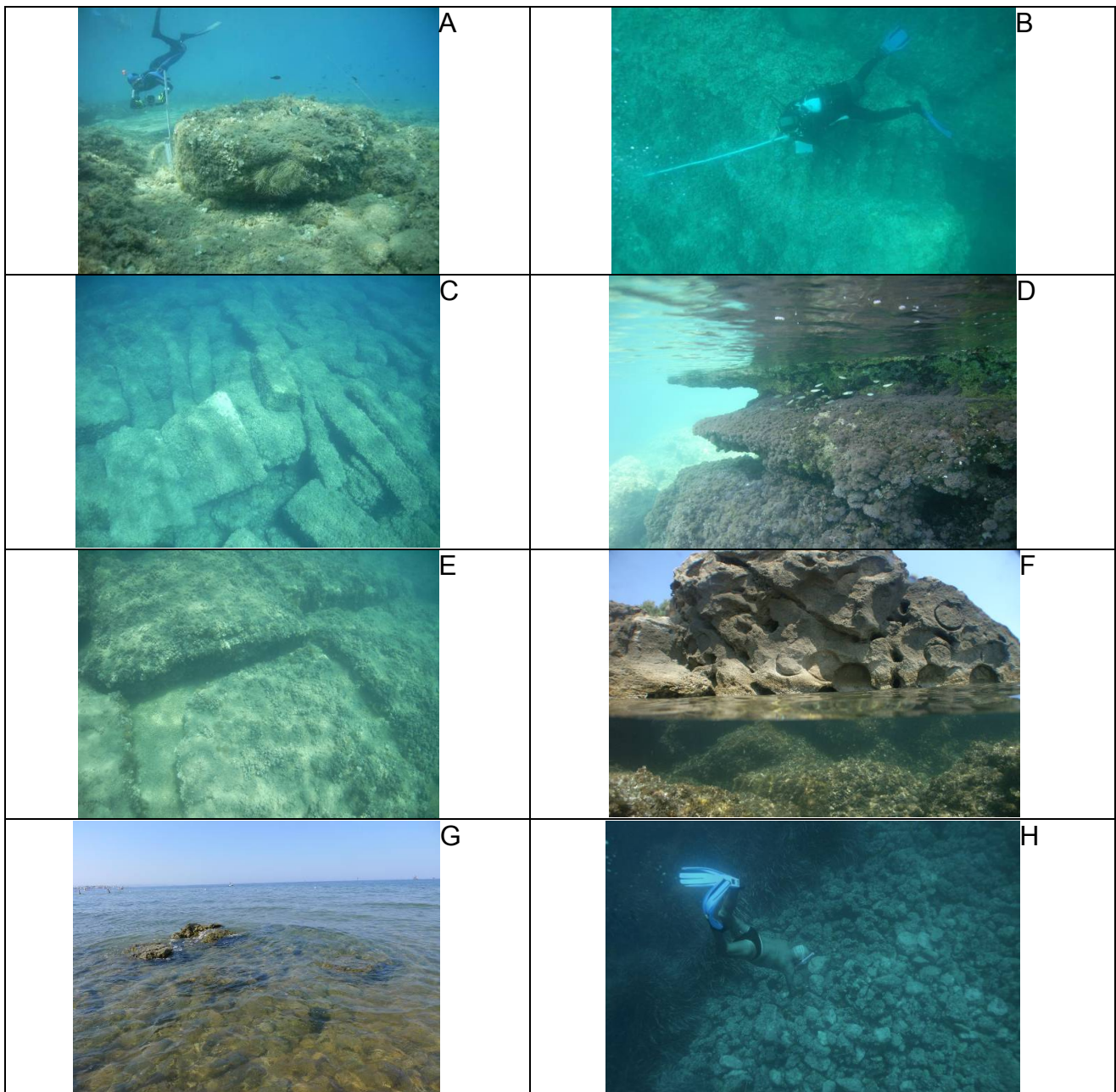


Fig. 25 Archaeological indicators along the Ionian coast of Calabria. A) The millstones of uncertain age at Soverato at -4.5 m (likely carved during the Greek age); B) The stairway of the submerged Greek age quarry at Le Castella at -6.0 ± 0.5 m (2200 yr BP); C) the submerged excavated blocks at Punta Cicala of the nearby quarry; D) The double notch at showing an abrupt rise of still unknown age in relative sea level at Punta Cicala; E) cuttings in the submerged quarry at Punta Cicala; F) the quarry at Punta Cicala showing the remnants of unfinished columns; G) the submerged water well at Capo Donato; H) the breakwater located about 1 nautical mile offshore Le Castella, located in the same area of the historical islets of Ogigia. This site still shows remnants of roman age amphora mixed with the rumbling of cemented stones. A similar structure is present at Capo Rizzuto.

Moreover, the available GPS data show a variable uplifting trend for southern Calabria (Devoti et al., 2010). Therefore, the rate of crustal uplift inferred from the marine archaeological site of Scoglio Galera provides the evidence of a continuous uplift, whose trend is in agreement with the recent instrumental observations. The archaeological data fills a gap between geological and instrumental data, providing new estimations on the tectonic trend of this region during historical times. The vertical uplift rate is based on the elevation of the Quaternary terraces of MIS 5.5 of 124 ka, elevated at 65 m according to Miyauchi et al. (1994) and a uniform uplift since the last 1806±50 yr BP, which is the age of the archaeological site, is assumed. The average value of the relative sea level change inferred from the archaeological site, estimated at ~106 cm for the last 1806±50 yr (radiocarbon age of the wooden pole) while the predicted sea level curve for the last 1806 yr gives a value of ~113 cm. The difference in ~7 cm between predicted and observed data results from the sum of the opposite movements of uplift and subsidence that counterbalance each other. This estimation includes the uncertainties from the model and field observation. This result is in good agreement with the tectonic rate inferred by the elevation of the terraces of MIS 5.5, located at 60 m above sea level, that infer a vertical uplift of 0.47 mm/y (Miyauchi et al., 1994), that caused a displacement of about 85 cm since the last 1806±50 years at the studied site. This estimate, which differs by 21 cm from the present study's results, could result from the measurements of the MIS 5.5 elevation in this region, which shows large spatial variability.

7.2 Ionian coast

Our preliminary results show that this area is undergoing to high rate active subsidence and beach retreat, mainly caused by tectonics. This region requires further investigations through integrated surveys, including aerial photogrammetric analysis and multibeam bathymetry, to estimate timing and extents of these relative vertical deformations that are concentrated in a narrow coastal zone (Fig.25). In this area we have surveyed several archaeological sea level indicators, all in agreement to indicate a relative sea level rise at up to 6.0±0.5 m in the areas between Punta Alice and Crotona. The archaeological sites investigated includes millstones located at -4.1±0.2 m at Soverato, likely carved during the Greek age; the stairway of the submerged Greek age quarry located at Le Castella at -6.0±0.5 m (2200 yr BP); the submerged remnants of unfinished columns, the excavated blocks and cuttings in the bedrock, up to -5.3±0.3 m at Punta Cicala; the submerged water well at Capo Donato at -1.5±0.2 m and finally two breakwaters: one is located at about 1 nautical mile offshore Le Castella at -5.25±1.0 m, in the same area of the historical islets of Ogigia. This site still shows remnants of roman age amphora mixed with the rumbling of cemented stones. The second breakwater investigated is placed in the area of Capo Rizzuto. Its offshore top part is placed up to -3.5±1.0 m. Besides the archaeological sites, we have found traces of a double notch running along the coast near Punta Cicala. The upper notch is of contemporary formation, while the second notch, which formed under the previous one, is submerged at about -1 m and shows an abrupt rise in relative sea level of still unknown age.

7.3 Remarks on the Calabria region

The elevation of the archaeological indicators in Calabria provided new interesting clues of large tectonic activity for this area. Here, the timing of the relative sea level changes can be inferred from the elevation of the Quaternary marine terrace and the coastal archaeological sites of roman age. The only suitable indicator along the Tyrrhenian coast of Calabria is the Scoglio Galera at Briatico dated at 1806±50cal BP. Excluding any

uplifting co-seismic displacement, we hypothesize that this fish tank, underwent to a continuous uplift since the time of its construction, at the same rate of the subsidence signal caused by the glacio-hydro-isostasy. The erosion notches formed in this tectonic environment developed under constant tidal range amplitude, since the relative sea level remained steadily at the same relative level while it was continuously rising together with the Earth's crust (Fig. 26a). The pools do not show any morphological evidence of submerged erosion notches, reinforcing the hypothesis that relative sea level has not changed here since the construction of the fish tank. Assuming a constant rate of uplift since the late Quaternary, including the last 1806 years, then the current elevation of the Scoglio Galera is due to the glacio-hydro-isostatic signal that counterbalances the tectonic signal. Therefore, the uplifting rate for this location can be estimated at ~ 0.65 mm/y for the last 1806 ± 50 BP. The present day biological marker of the *Dendropoma* platform is in agreement with these observations as well as with the tidal notch along the inner side of the pools of the fish tank. These markers developed in an environment characterized by a relative null vertical motion, and consequently are at the same elevation. This balance also includes the recent eustatic increase of ~ 13 cm, as estimated for the Mediterranean by Lambeck et al. (2004b), Anzidei et al. (2011a, 2011b). On the base of these data, the Scoglio Galera did not record co-seismic significant vertical displacements, including the December 8th, 1905 Ms ~ 7 Earthquake, which is the largest in this region occurred in the last centuries, in agreement with the dislocation model proposed by Piatanesi and Tinti (2002). However, co-seismic movements may have occurred before the construction of the fish tank.

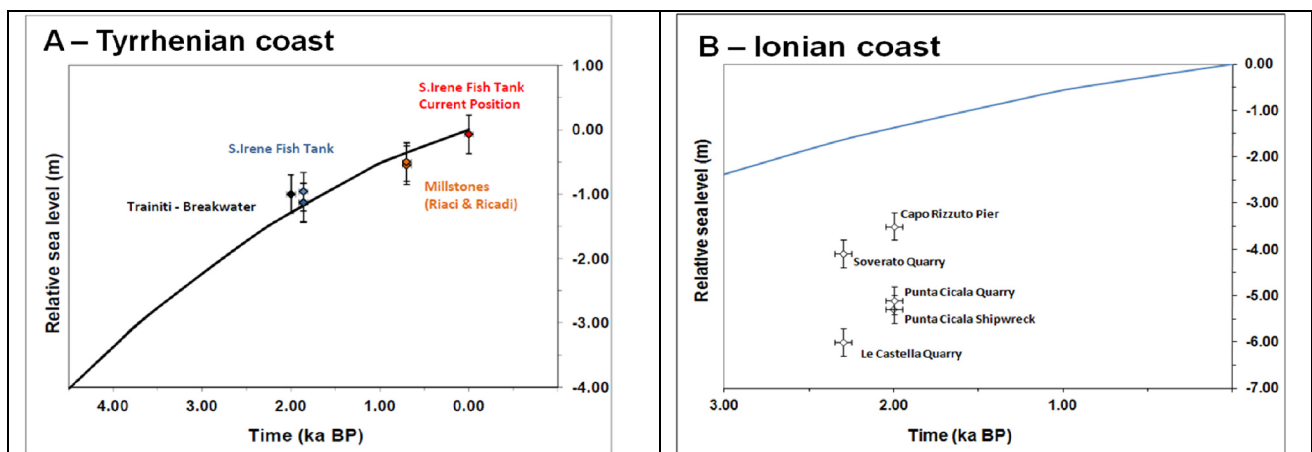


Fig. 26 Plots of the predicted sea level curves (data from Lambeck et al., 2011) compared with the elevation of the archaeological markers (diamonds with error bars for age and elevation). A) the for fish tank of Scoglio Galera (S. Irene, Briatico) along the Tyrrhenian coast; B) for the archaeological indicators found along the Ionian coast of Calabria. Sites located along the Tyrrhenian coast remained at the same elevation with respect to local sea level since 1860 ± 60 ka BP, thus inferring tectonic uplift. Conversely, in the Ionian coast, the archaeological sites fall below the predicted sea level curve, showing a continuous and extensive subsidence since the last 2.3 ka with large rates.

Conversely, in the Ionian coast of Calabria, diffuse coastal submersion is observed at a mean rate of 2.5 mm/yr (Fig.26b). This is in contrast with the marine terraces of MIS 5.5 located on land at elevation up to 30 m that indicate uplift (Ferranti et al., 2006, Bordoni and Valensise, 1998; Padoja et al., 2011), but with rates smaller than in the Tyrrhenian coast. This infers an inversion of the vertical deformation direction that occurs in a narrow belt along the coast. Because the elevations at which are located the archaeological

indicators along the Ionian coast of Calabria in the area comprised between Punta Alice in the North and Kaulonia in the South, is quite homogeneous, (Stanley, 2006), we can hypothesize that the Ionian coast of Calabria is affected by tectonic subsidence besides coastal erosional effects, which is partially caused by the GIA signal.

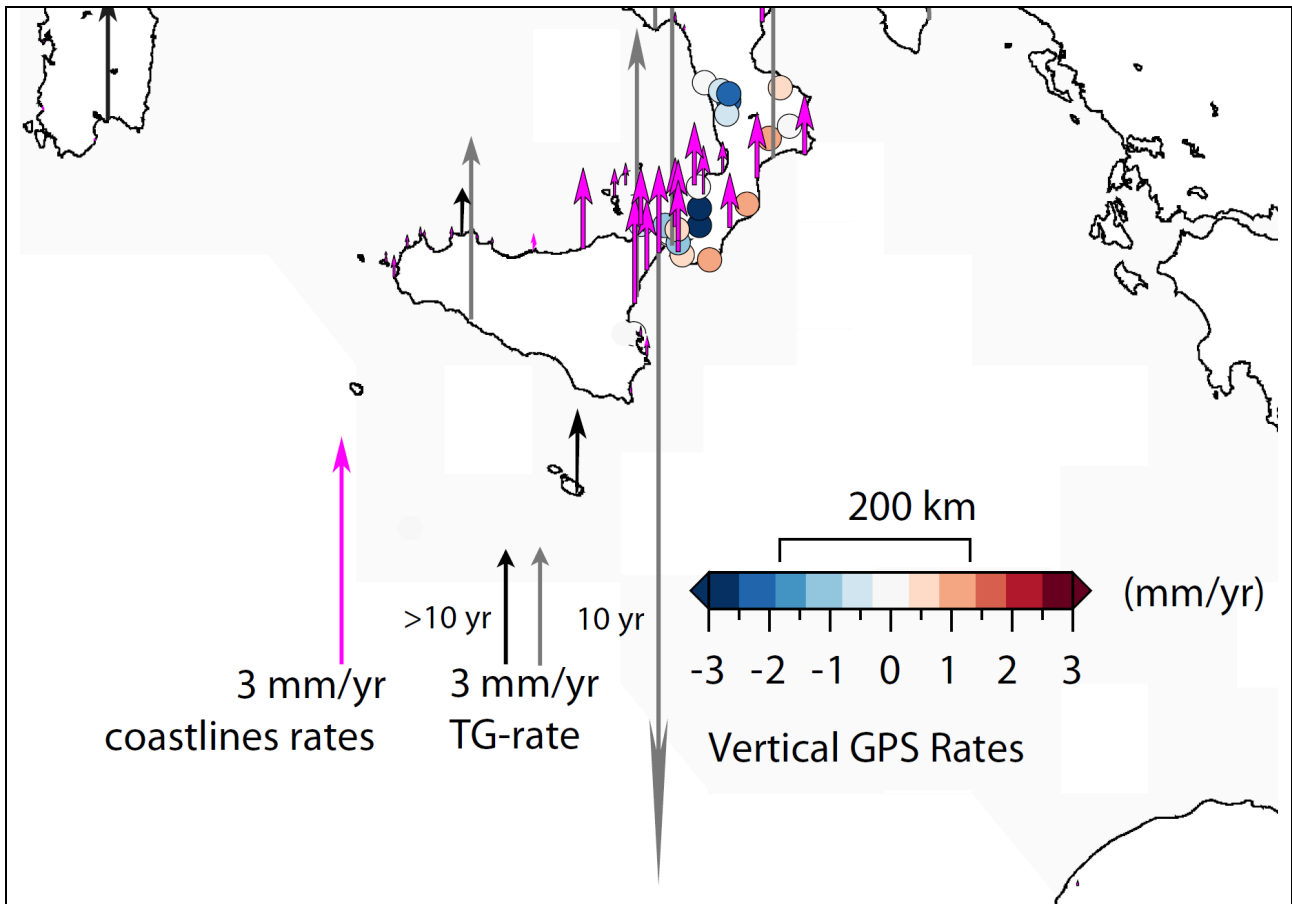


Fig. 27 Current vertical land motion from GPS data along the coast of southern Italy (colored dots show the rate of velocity indicated in the legend (From Serpelloni et al., in preparation). Pink arrows are the uplifting rates of the coastlines based on geological data, from Pedoja et al. (2011). Sea level rates from tidal stations with >20 years (black arrows) and 10 years (grey arrows) of data (see tables 3 and 4 for data), are reported in the map.

The latter has been recently estimated for this region at -0.57 mm/yr (Lambeck et al., 2011). Then the resulting rate of tectonic signal is a subsidence at 1.93 mm/yr. This rate is among the largest that can be observed in the Mediterranean basin. This trend is in agreement with the current beach retreating, which is observed since the last 50 years or more and in agreement with data from the tidal station of Crotona. Although the time series for this station is still too short (2001-2011), it provides a local relative sea level rise at 6.77 ± 2.7 mm/yr that exceeds of 5.0 mm/yr the mean sea level rise estimated for the Mediterranean at 1.77 mm/yr. Reducing this value for GIA and tectonics, we obtain 2.5 mm/yr of residual local sea level change for this location. Vertical GPS data from the nearest stations to the shorelines but often still too far from the coast, show an uplifting trend at <1 mm/yr. GPS position information only provide limited constraints on the vertical motions because the record lengths are near sub-decadal and values are barely significant in view of unresolved questions about the GPS reference frame stability (Altamimi et al.,

2007). Of greater significance are the larger vertical movements occurring in Sicily, with an uplifting signal larger than the uncertainties of the technique (Fig.27). Moreover, the horizontal velocity at the GPS station of KROT, located near Crotona shows local instability or gravity sliding towards the Ionian Sea (D'agostino et al., 2011). This signal is in agreement with the results from seismic lines offshore of Crotona (Minelli and Faccenna, 2010) and with the subsidence shown by the archaeological indicators.

TG rate Crotona mm/yr	Archeo SLC rate mm/yr	GIA rate mm/yr	Tect rate (archo-gia) mm/yr	SLC _{eu} crotona (TG _{Cr} -GIA-tect) mm/yr	SLC _{eu} -mean sl _{med} (res SLC _{diff}) mm/yr
6.77±2.7	2.5	0.57	1.93	4.27	2.5

Table 2 From tidal data to vertical tectonic rate estimated for the Ionian coast of Calabria.

8. Sea level changes at different time scales in the Mediterranean from Tide Gauge data

Tidal measurement is one of the most important branches of oceanography and its history dates back to USA and northern Europe since the eighteenth century. These stations have been used since then for different goals, such as navigation, environment or geodetic applications. During the last decades several countries established networks of sensors devoted to sea level monitoring and therefore is now available a global scale infrastructure, managed by national agencies and single organizations. Additional improvements were performed after the 2004 Indian Ocean tsunami, with the aim to create a Tsunami Early Warning and Mitigation System [Titov et al., 2005]. The global tidal network presently consists in about 200 stations and part of them is located in the Mediterranean. Sea level recordings are distributed often in near real time and can be easily retrieved by internet (www.ioc-sealevelmonitoring.org; www.mareografico.it; and www.pol.ac.uk).

In Italy, the first tide gauges were installed in the mid-nineteenth century in the Oceanographic Institute of Trieste in 1859, at Venice in 1871 (Punta della Salute), at Rimini in 1867 and at Genoa in 1883, at the Navy Hydrographic Institute. Italy was a leading country in this field and since 1896 the network was extended thanks to the Civil Engineer Office, with the stations of Imperia, Livorno, Civitavecchia, Naples, Ancona, Ravenna, Palermo, Catania, Cagliari and La Maddalena. In 1920 were installed two additional tide gauges in Reggio Calabria and Vieste. During the first half on the nineteenth century, several new tidal stations were installed worldwide for navigation applications. In Italy, in 1942 was founded the Tidal Service (Servizio Mareografico) as part of the Ministero dei Lavori Pubblici and in 1989 was established the Tidal National Hydrographic Service under the Presidency of the Council. Finally, in 2002 is established the ISPRA (Istituto Superiore per la Protezione dell'Ambiente), and the Tidal Service became part of the Agency for Environmental Protection and Technical Services. After the 2004 Indonesian destructive tsunami, several countries cooperated for the Tsunami Warning Center and new modern tidal stations and wave-meters were installed in the Oceans. Following this example, in Italy was set up the National Wave-meter Network (Rete Ondametrica Nazionale), and the national tide gauge network was rebuilt. With this scope, were performed geodetic surveys to establish the reference elevations at all the tide gauges of the tidal network. Were measured geodetic benchmarks through high precision leveling surveys tight to the nearest leveling benchmarks of the Istituto

Geografico Militare Italiano (IGM). Since 2001, the Italian tidal network is operational with modern digital tide gauge sensors, suitable for continuous monitoring, equipped with real time data transmission to the ISPRA headquarter in Rome.

8.1. The ISPRA tidal network

The Italian national tide gauge network (Rete Mareografica Nazionale - RMN) is currently managed by ISPRA, and has been designed to measure and monitor the sea level of the Italian seas. Monitoring stations are distributed along the 7375 km of the coastlines, including Sardinia, Sicily and the small islands. Because tsunamis may have large potential impact along the Italian coastlines (i.e. the December, 28, 1908, Mw=7.1 Messina earthquake; Stromboli eruption in 2002, besides large historical events like the 365 AD tsunami originated in western Crete. Shaw et al., 2008), the tidal network was also planned for the detection, characterization and propagation of tsunami waves. Therefore, the ISPRA network represents a powerful tool in the process of building a strategy to improve our knowledge of tsunamis in the Mediterranean, with the aim to attempt the prediction of their effects.

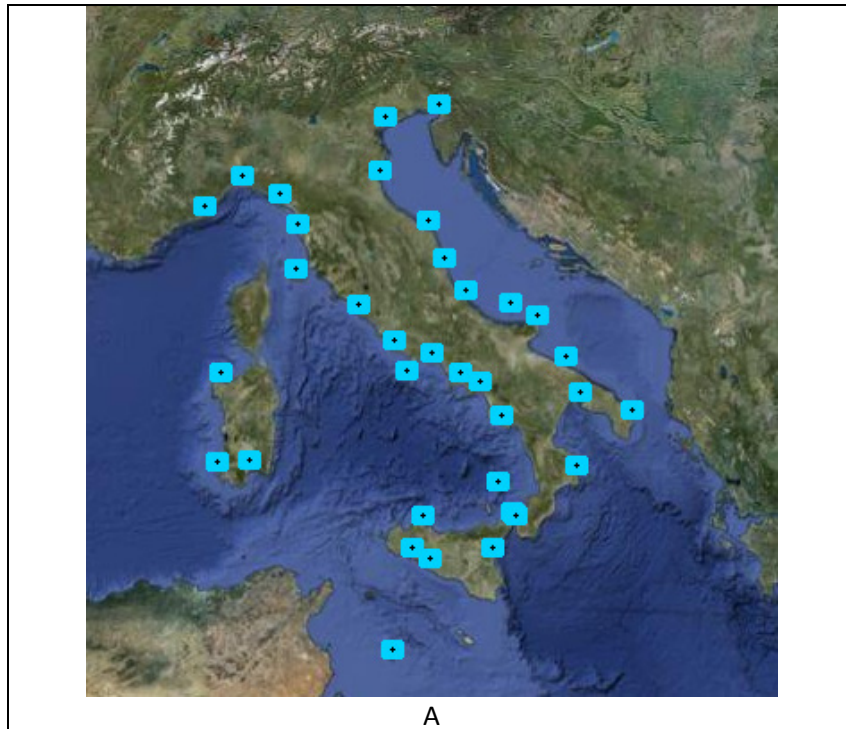
Stations features fit the guidelines of the Intergovernmental Coordination Group for the Tsunami Early Warning and Mitigation System in the Northeast Atlantic area, Mediterranean and connected seas (ICG / NEAMTWS) - Italian Regional Emergency Center - Ministry of Foreign Affairs MFA-DGDC. Presently, the RMN consists in 35 monitoring stations (Fig.28a), mainly located in the principal harbors (Imperia, Genoa, La Spezia, Livorno, Civitavecchia, Cagliari, Carloforte, Porto Torres, Palermo, Porto Empedocles, Catania, Messina, Reggio Calabria, Crotone, Taranto, Otranto, Bari, Vieste, Ortona, Ancona, Ravenna, Venice, Trieste, Naples, Palinuro, Salerno and Lampedusa, San Benedetto del Tronto, Gaeta, Tremiti, Stromboli, Ponza and Elba).

The instrumental equipment includes i) a microwave waveguide and ii) a subsidiary floating device with digital encoding for timely verification of measures. The equipment is suitable for analyzing particular events or phenomena and for data recovery. Recording frequency is at 1 minute, but can be set up to every 10 sec. All stations of the network have remote connection and are equipped with additional sensors consisting in anemometers (placed at 10 m above ground level), barometers, humidity and temperature sensors (FigS.28b, 29).

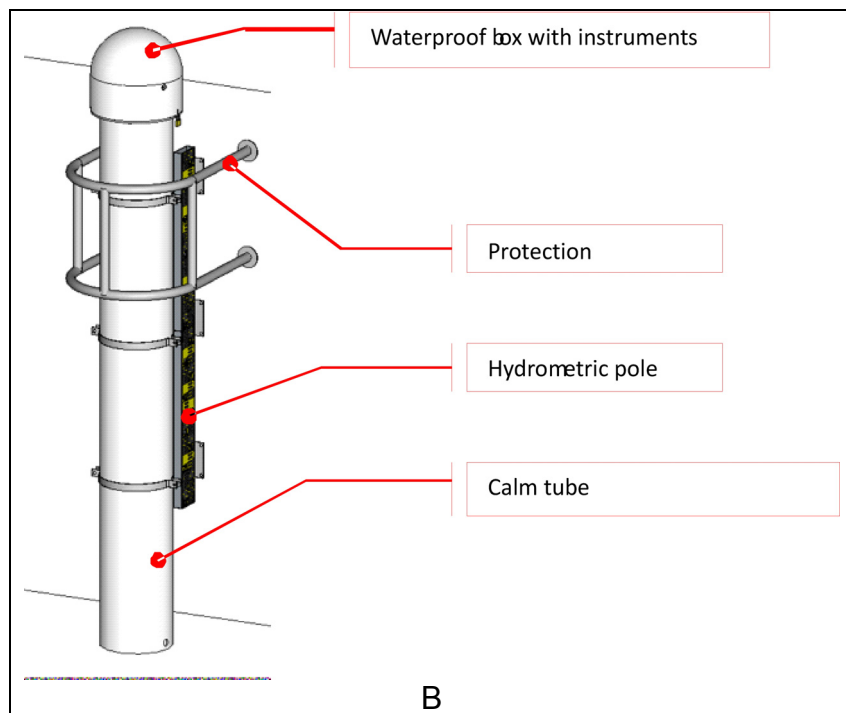
All of these provide real-time measurements of sea and weather conditions at the individual stations. Real time data are transmitted via UMTS IP-S to the ISPRA headquarter in Rome. A spare data transmission system is ensured by IRIDIUM satellite technology that guarantees connection even during eventual black-out of the UMTS system.

To establish the altimetry control, the network is linked to the Italian Leveling Network, managed by the Istituto Geografico Militare Italiano. Topographic surveys ensure a careful control of elevations and horizontal coordinates of the reference benchmarks associated to the tidal stations. Measurements have been performed by DGPS technique.

From the time series of the last 10 years of tidal recordings have been determined at each station the elevation of the tidal references, to obtain the zero level (the elevation reference level).



A



B

Fig.28 A) Location of the current 35 ISPR tidal stations; B) Sketch of a typical tidal installation; B) the tide gauges are attached to the piers of principal harbors and consist in a calm tube that contains the sea level sensor, the hydrometric pole, the protection, the data recording and data transfer system.

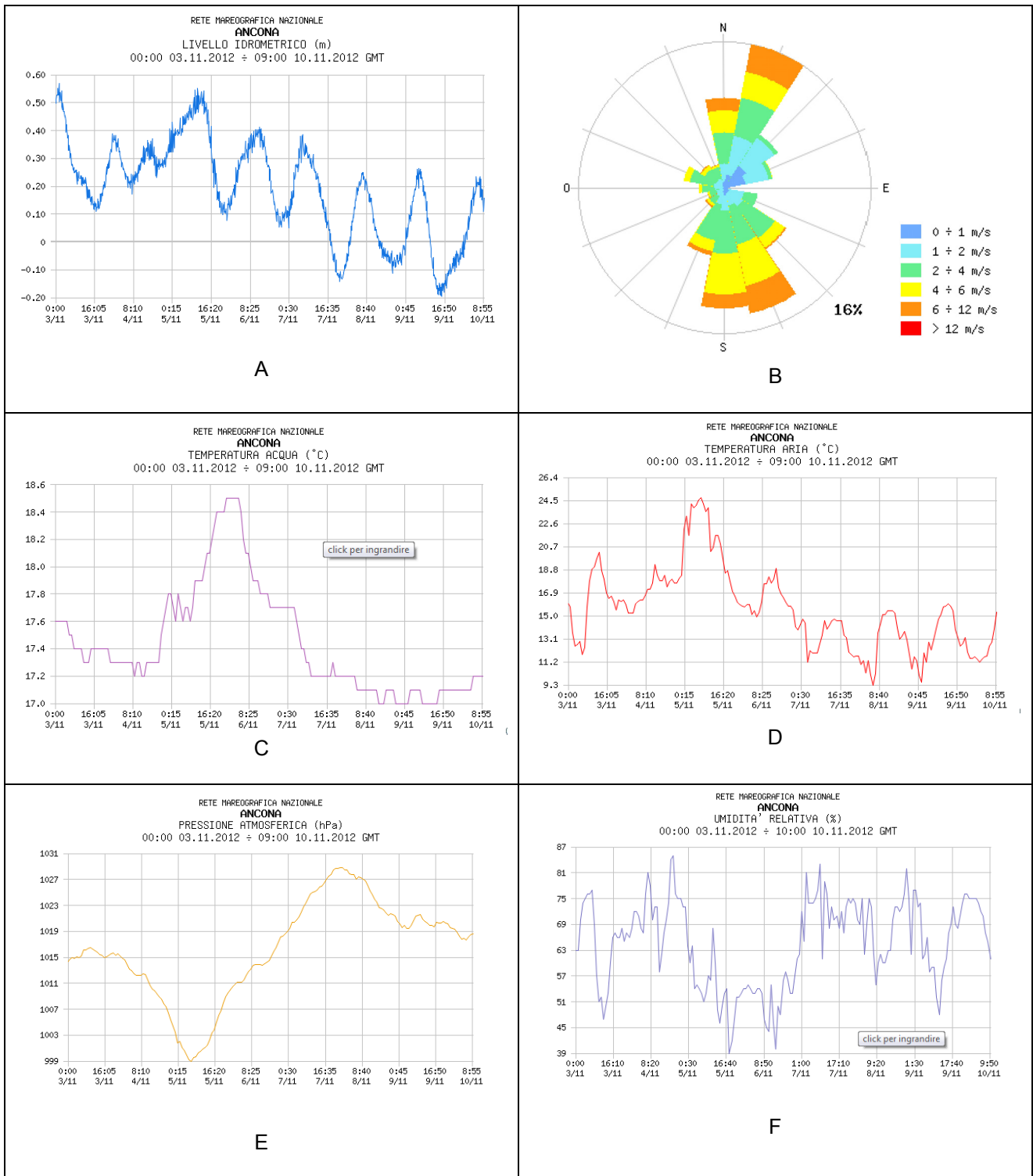


Fig.29 B) example of data products provided for each station of the ISPRA network: A) sea level recording; B) wind plot direction (color scale is wind velocity in m/sec); C) sea water temperature; D) air temperature; E) atmospheric pressure and F) humidity. Data can be retrieved by internet at www.mareografico.it.

Tidal data consist in ASCII files that are stored into a tailor made data base. Observation files, as well as site description, topographic surveys, sensors, data transmitting systems, etc., can be retrieved via internet at www.mareografico.it. Each folder is related to an

individual station and includes tidal data, sea water temperature, atmospheric temperature (ground level), wind intensity and its direction. Available historical tidal data, that go back up to 1986, are also included into the data base.

Since 1998 and until the end of 2009, the database of RMN consisted in tidal data with 10 minutes sampling rate. Since 2010, sampling has been increased and set at 15 seconds, to record rapid oscillation phenomena even related to tsunami type effects. High frequency tidal data represents a fundamental source of information to understand the sea surface dynamics in case of seismic activity. Furthermore, the analysis of tidal signal from a well spatially distributed tidal network allows the studying the timing of propagation of waves and their decay in energy. Summarizing, the availability of time series data of sea level measurements allows estimating:

- low frequency oscillations related to astronomical tides;
- self-fluctuation of basins (natural motion, seiche etc.);
- transient sea level changes due to meteorological phenomena;
- decadal to secular sea level change (thermal expansion, eustatism, glacio-hydro-isostatic signal);
- vertical motion of the land (subsidence and uplift of tectonic, volcanic and anthropogenic nature), that may cause additional local relative sea level changes;
- regional tsunamis and tsunami type signals related to coastal and submarine landslides.

In the following chapters, are shown: i) the analysis of the tidal time series for the time span 2001-2011 of the ISPRA network; ii) the analysis of the tidal time series for longest records from data retrieved at the Permanent Service for Mean Sea Level (www.pol.ac.uk); iii) some examples of tidal recordings of regional tsunamis and the effects induced in the Mediterranean by the Tohoku-Oki giant earthquake of March 11, 2011, as well.

8.3. Tidal time series 2001-2011 - ISPRA network (Italy)

Here are analyzed and discussed the time series of sea level data for a set of 26 tide gauge stations on the ISPRA network, for the period 2001-2011. In particular, the analyses of the annual means, derived from daily data sampled every 10 minutes, previously filtered by ISPRA through the Bloomfield code, to remove eventual raw noise from the recordings, have been performed. Thus, high frequency sea level oscillations caused from tsunami or storms were removed from the data. We clarify that the data set is not affected by eventual vertical land deformations caused by seismic or volcanic events, occurred nearby the tidal stations. In Table 3 are shown the observed sea level rates together with those reduced for the atmospheric pressure acquired at the same locations, by means of a barometric inverse procedure with respect to a reference pressure of 1013 hPa (Wunsch and Stammer, 1997).

Recordings show a very good continuity and consistency. It's worth noting that since the end of 2009 and to the end of 2010, the entire network recorded a sharp rise in sea level that later fell in 2011, returning at value a bit higher than of 2009. The plots shown in Fig.31, evidence that this is a transient signal occurring within the temporal variability of a sea level record. The analysis have shown some stations with trends having unexpected rates, that can be caused by local site instabilities likely related to the installation of the sensors, rather than effects that can be addressed to ground deformation for tectonic origin.

ISPRA tidal network 2001-2011								
A	B	C	D	E	F	G	H	I
<i>Station n.</i>	<i>Station name</i>	<i>Lat</i>	<i>Lon</i>	<i>Observed sea level rate mm/yr</i>	<i>Holosteric sea level rate mm/yr</i>	<i>GIA rate m/yr</i>	<i>Tectonic rate mm/yr</i>	<i>Sea level rate mm/yr</i>
1	Ancona	43.37	13.30	5.42±3.8	5.51±3.4	-0.28	0	5.23
2	Bari	41.08	16.51	9.83±3.6	9.61±3.0	-0.46	0	9.15
3	Cagliari	39.21	9.11	5.97±2.1	5.27±2.3	-0.55	0	4.72
4	Carloforte	39.14	8.30	5.26±2.0	5.35±1.7	-0.55	0	4.8
5	Catania	37.49	15.09	7.94±3.2	7.83±3.0	-0.52	1.3	8.61
6	Civitavecchia	42.00	12.46	12.67±3.4	8.31±4.2	-0.40	0.18	8.09
7	Crotone	39.04	17.08	6.77±2.7	7.30±3.0	-0.53	0.83	7.6
8	Genova	44.41	8.92	6.01±3.2	5.44±2.3	-0.20	0	5.24
9	Imperia	43.87	8.01	4.99±2.6	4.12±1.4	-0.31	0	3.81
10	Lampedusa	35.49	12.60	6.07±2.7	5.90±2.6	-0.50	0	5.40
11	Livorno	43.54	10.29	7.74±3.8	7.82±3.8	-0.35	0	7.47
12	Messina	38.11	15.33	-19.06±4.6	-19.14±4.5	-0.53	0.85	-19.46
13	Napoli	40.83	14.26	6.62±3.0	6.56±2.6	-0.41	-1.5	4.65
14	Ortona	42.21	14.24	8.18±3.4	8.05±3.0	-0.37	0	7.68
15	Otranto	40.14	18.49	4.97±2.8	4.88±2.4	-0.44	0	4.44
16	Palermo	38.07	13.22	5.32±2.8	5.19±2.6	-0.53	0	4.66
17	Palinuro	40.01	15.16	8.64±2.2	8.52±2.2	-0.43	0	8.09
18	Porto Empedocle	37.29	13.52	6.86±2.3	6.61±2.2	-0.50	0	6.11
19	Porto Torres	40.50	08.24	3.88±2.9	3.80±2.6	-0.56	0	3.24
20	Ravenna	44.29	12.16	11.39±4.3	11.24±3.8	-0.18	-3	8.06
21	Reggio Calabria	38.07	15.38	8.92±3.5	8.63±3.4	-0.53	1.1	9.2
22	Salerno	40.40	14.46	4.08±4.0	3.98±3.7	-0.40	0	3.58
23	Taranto	40.28	17.13	13.63±3.7	13.64±3.2	-0.47	0.05	13.22
24	Trieste	45.65	13.75	-7.27±3.5	-7.47±2.8	-0.12	0	-7.35
25	Venezia	45.41	12.42	17.69±3.9	17.47±3.5	-0.12	-0.7	16.65
26	Vieste	41.53	16.10	7.67±3.3	7.74±2.9	-0.42	0	7.32

Table 3 Tidal rates estimated from the mean annual values at 26 stations of the Italian tidal network (ISPRA), observed in the time span 01/01/2001 – 31/12/2012. The column E reports the local sea level rate; the column F the residual sea level rate (holosteric) at individual stations after inverse barometric inversion has been applied. The columns A-G are number, names and positions of the tidal stations. In column G is the GIA rate estimated at the individual stations (from Lambeck et al., 2011). In column H are the tectonic rates estimated at the individual stations (Lambeck et al., 2011 and reference therein). In column I is the residual sea level rate removed from the previous disturbances. Note the negative values of sea level rates (sea level fall) at Messina and Trieste stations due to local instrumental instability. Rates are higher with respect to the long term analysis that give a mean value of the sea level rise at 1.8 mm/yr for the Mediterranean Sea (see Table 2 and Fig.7,8).

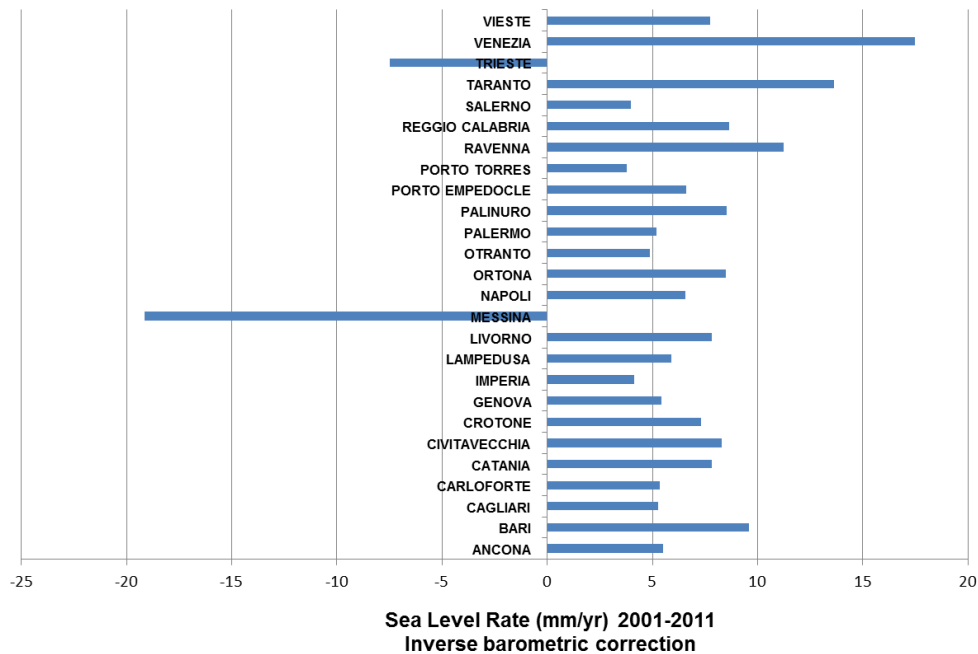
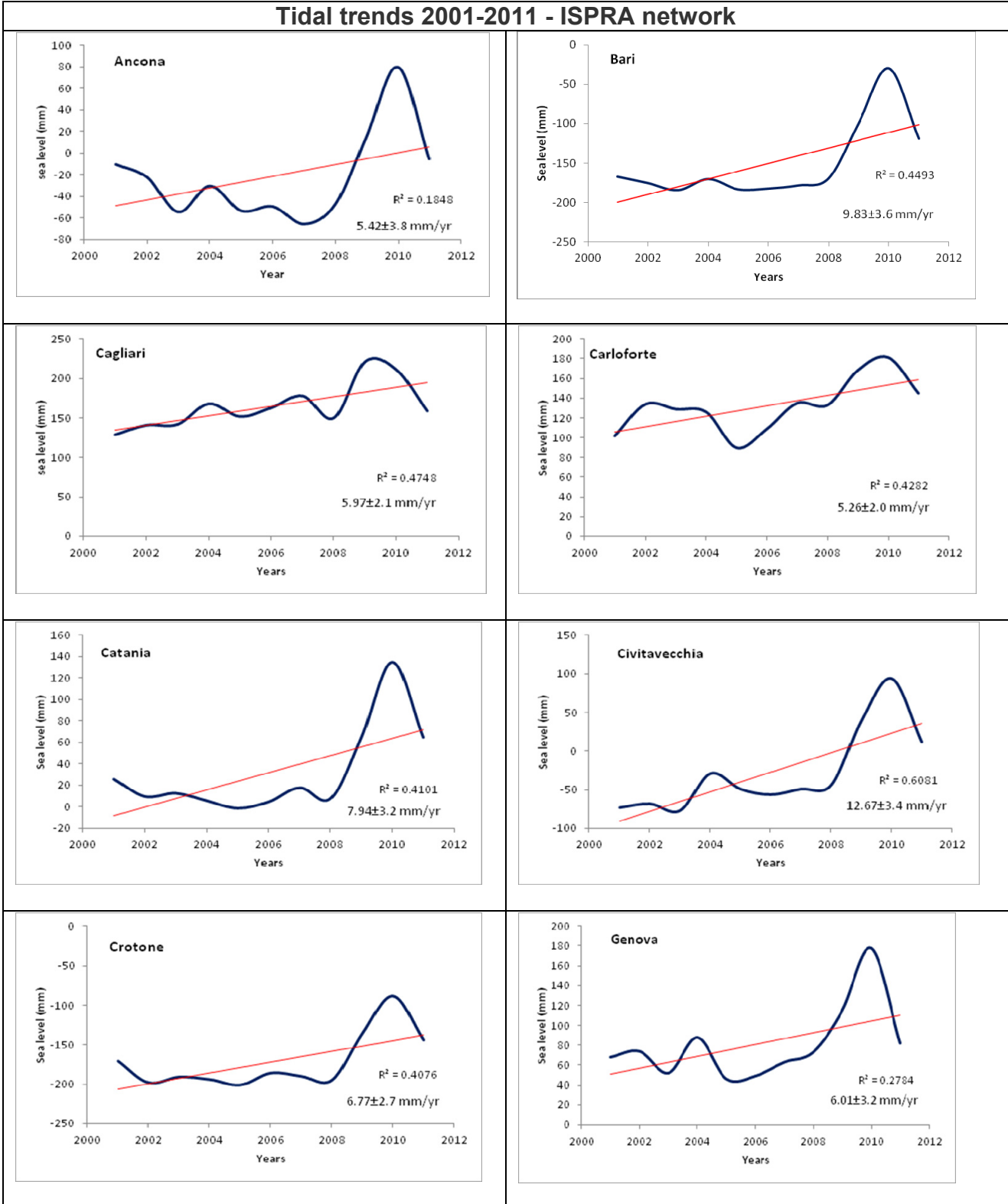


Fig.30 Diagram of the sea level rates at individual stations of the ISPRA tidal stations observed in the time span 01/01/2001 – 31/12/2012. Note the negative values (sea level fall) at Messina and Trieste due to local instrumental instabilities (data correspond to the residual trends values of Fig. 4 and Table 3).

In particular at the stations of Messina and Trieste (Fig.30 and 31). For the period 2001-2011, we found a mean trend of 4.22 ± 1.36 mm/yr, once the inverse barometric correction has been applied. If we consider the observed sea level (without the barometric correction), the mean rate increases at 5.97 ± 1.35 mm/yr (Fig.33). In other words, the latter is the "effective" signal observed along the coast. Finally, local vertical motion of the land, such as subsidence or uplift, in the area where stations are placed, can increase or decrease the relative sea level rate at the individual stations.

In the plots of Figure 30 and 31, are shown the annual mean of sea level values at the individual stations and the corresponding linear trends with related errors (see also Table 3) (straight lines are the linear fit of the data, that represent the optimal set of linear data containing values that increase or decrease in a constant way, according to the equation used to calculate the least squares to a line $y=mx+b$, where m is the slope and b is the intercept. In the plots are also reported the R^2 , or the square of the correlation coefficient, i.e. the ratio of the variance in y attributable to the variance in x).

Tidal trends 2001-2011 - ISPRA network







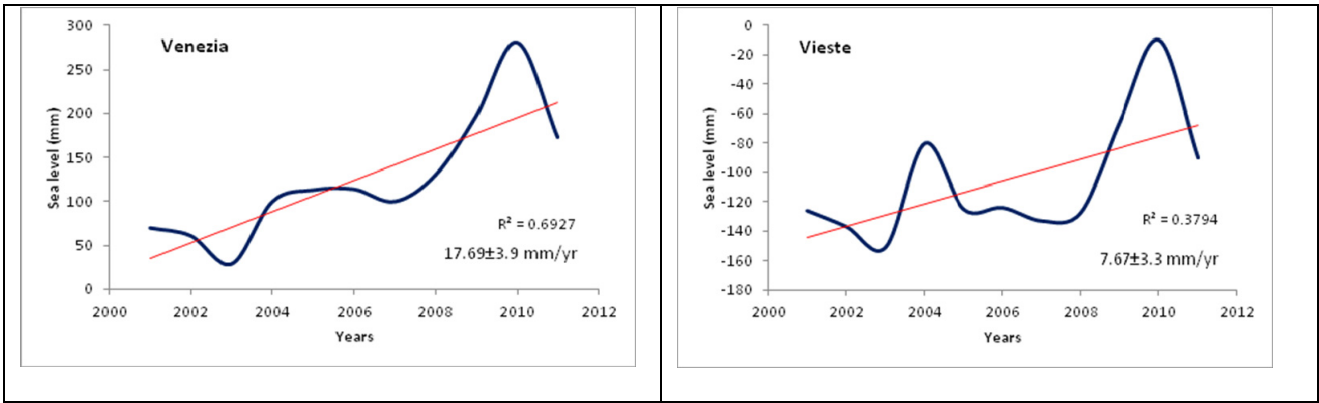


Figure 31 Mean annual values of the tidal trends at 26 stations of the Italian tidal network (ISPRA), observed in the time span 01/01/2001 – 31/12/2011. Plots listed as in Table 3. Data have been reduced for atmospheric pressure. Note the large positive peak at all tidal stations in 2009-2010 and the continuous sea level fall at Messina and Trieste stations likely due to local instrumental instability.

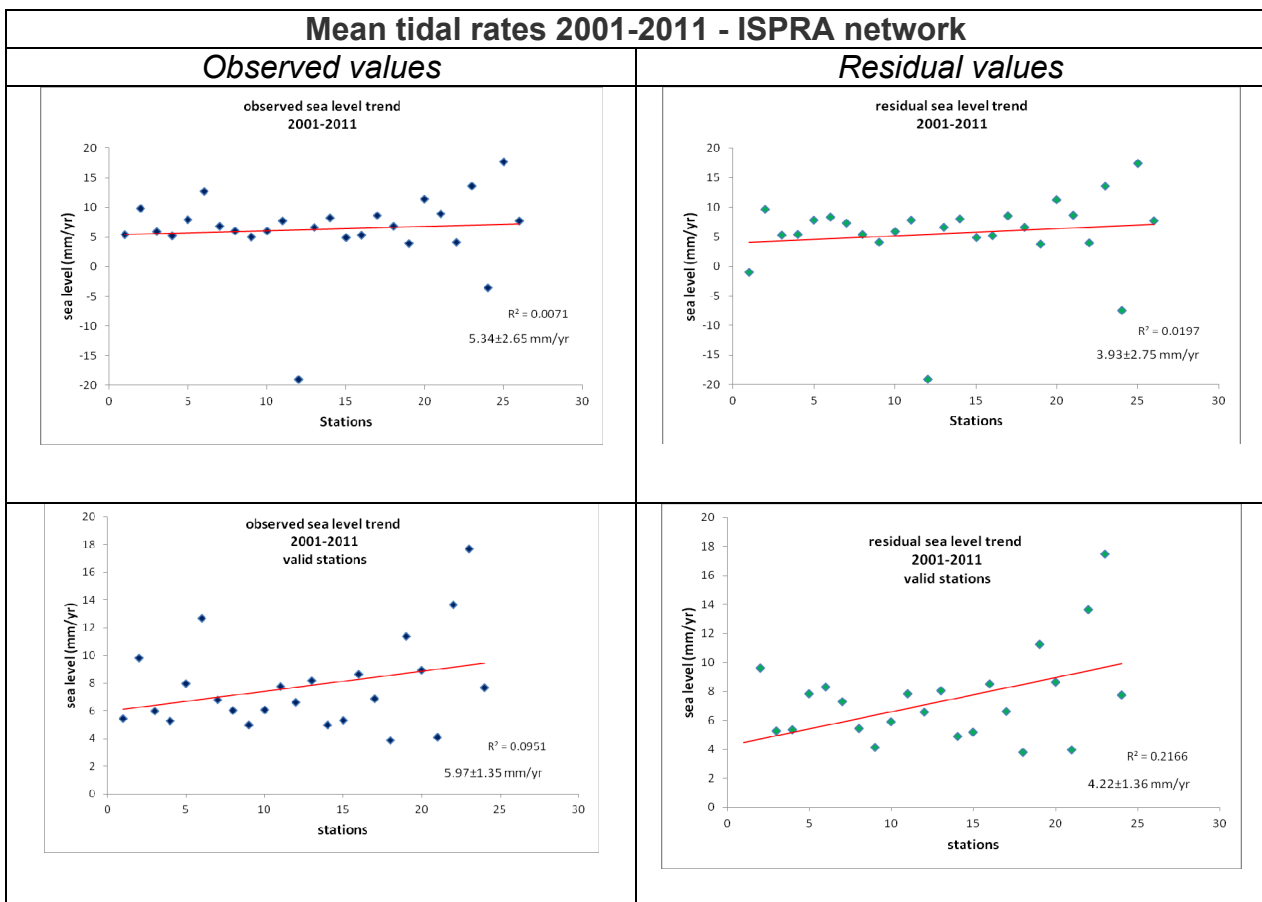


Fig. 32 Plot of the mean sea level rates estimated at the individual tidal stations for the time span 01/01/2001-01/01/2011. In the horizontal axes are the tidal stations, as listed in Table 3. Left: observed mean values of the sea level trend. Right: residual mean values of the sea level trend estimated for valid stations only, after inverse barometric correction has been applied. Top: all data set. Bottom: valid stations only (Messina and Trieste are excluded from the analysis). The linear fit for the whole network, corresponds to a sea level rise at 5.97 ± 1.35 mm/yr (valid stations) and to a value of 4.22 ± 1.36 mm/yr once the barometric effect has been removed. This latter value can be considered within the decadal variability of sea level and is caused by the sum of eustatic, glacio-hydro isostatic and tectonic signal.

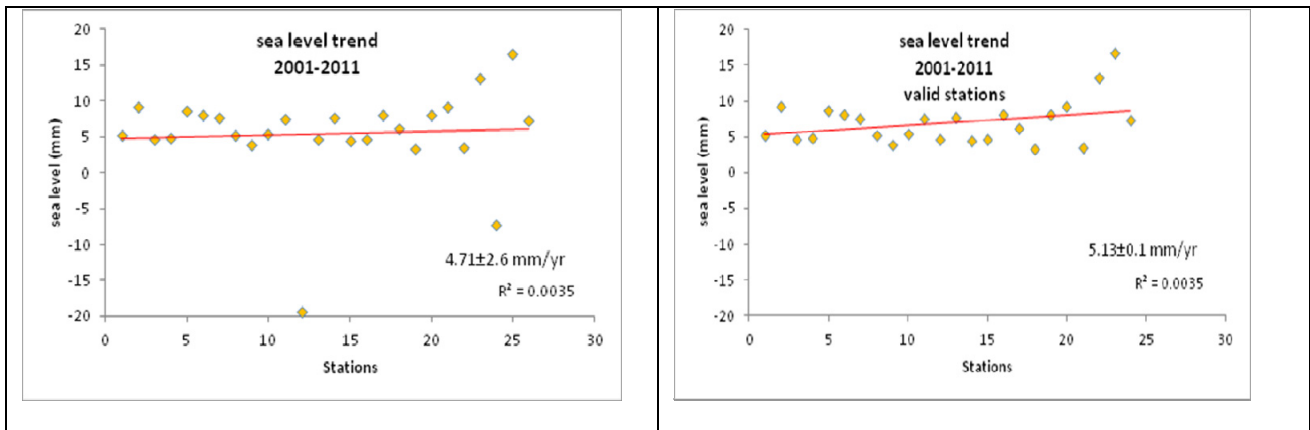


Fig. 33 Plot of the mean sea level rates estimated at the individual tidal stations for the time span 01/01/2001-01/01/2011 after data have been reduced for GIA and tectonics, with values reported in table 3. Horizontal axes are station numbers, as listed in Table 3. Left, all data set: trend is at 4.71 ± 2.6 mm/yr; right plot, valid stations only: trend is at 5.13 ± 0.1 mm/yr (in the latter Messina and Trieste are excluded from the analysis).

8.4. The longest tidal records in the Mediterranean

In this chapter, the sea level trends estimated by the longest tidal time series for a set of available tidal stations located in the Mediterranean are shown (Fig.34). The data set consists in 58 tidal station that collected data in the time span 1884-2011 and at least for more than 13 years (Table 4). Tidal data have been retrieved by the internet at www.pol.ac.uk. In Table 4 are reported for each station the time span of the recordings, the length of the considered records (years), the length of the valid record used in this analysis and the estimated sea level rates. Figure 36, shows the plots of the tidal records for each one of the 56 tidal stations used in this study. Each plot shows the linear trend of the sea level for the time span considered at the tidal stations. The average sea level rate for the entire analyzed data set is 1.78 mm/yr (including the two stations of Bourgas and Varna located in the Black Sea) and 1.79 mm/yr for the Mediterranean region.

Tidal stations that have recorded eventual co-seismic signal have been excluded from the analyses. Exemplary is the case of the tidal station located at Messina, that recorded the land movements caused by the December 28, 1908 Mw=7.1 earthquake. Recordings show ~3.6 cm of pre-seismic sea level fall in the time span 1906-1907, which was followed by an abrupt co-seismic sea level rise of ~50 cm during the main shock and by additional ~27 cm of sea level rise in the time span 1909-1915, caused by the continuous post-seismic relaxation of the earth's crust occurred across the fault (Fig.35).

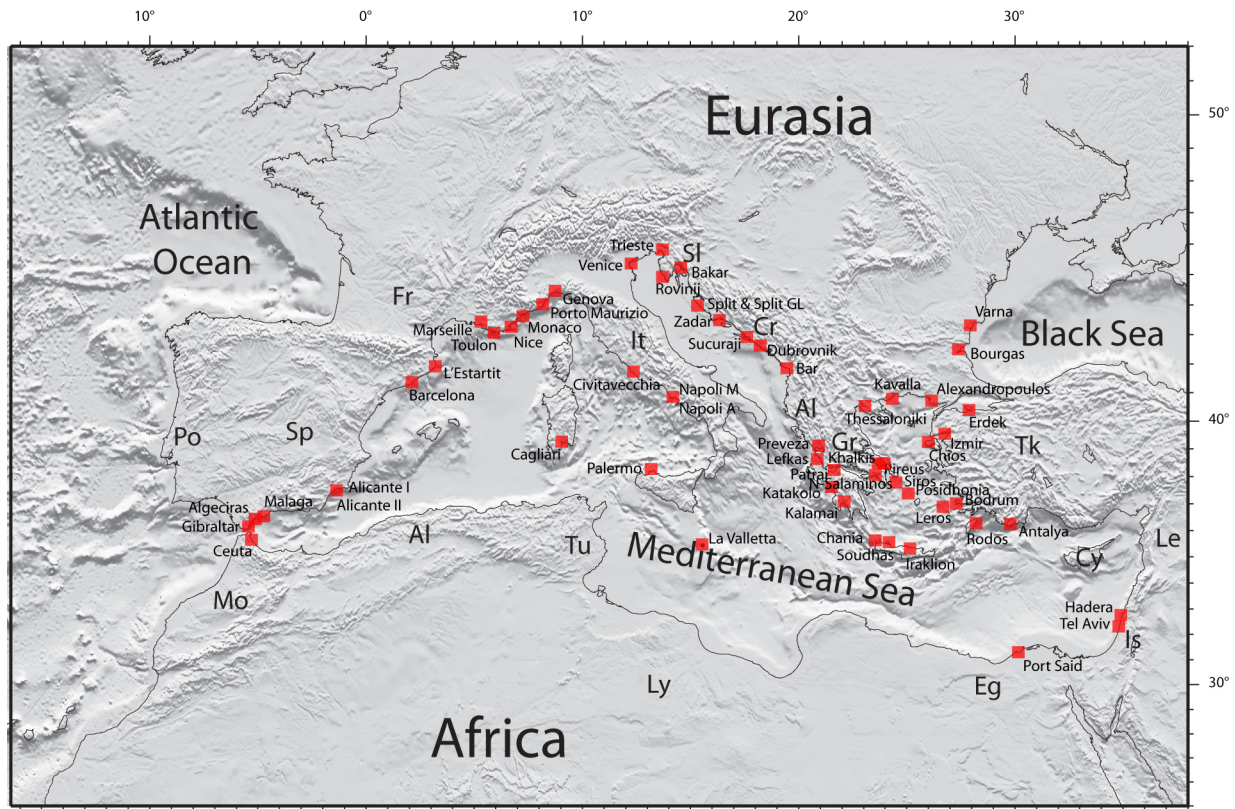


Fig.34 Position of the 57 analyzed tidal stations distributed along the coast of the Mediterranean and 2 in the Black Sea that recorded in the time span 1884-2011, for more than 13 years (see also table 4 for station coordinates, data time span and sea level rates). Note the lack of tidal stations in North Africa.

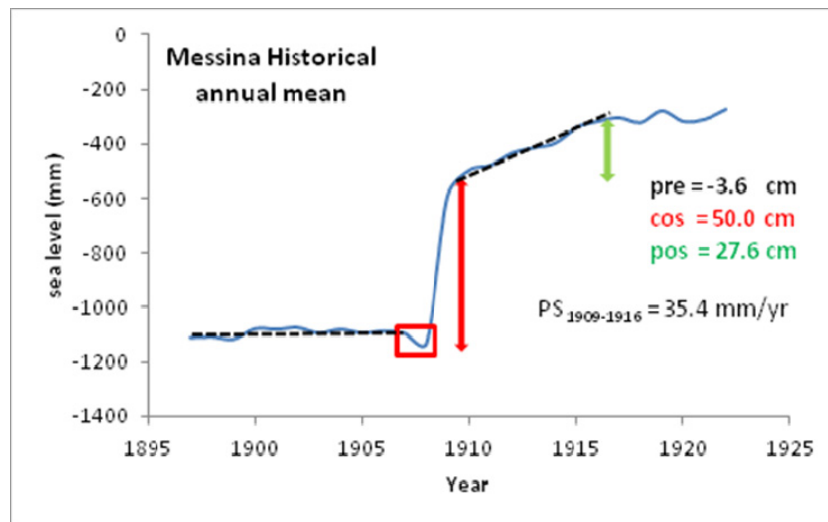
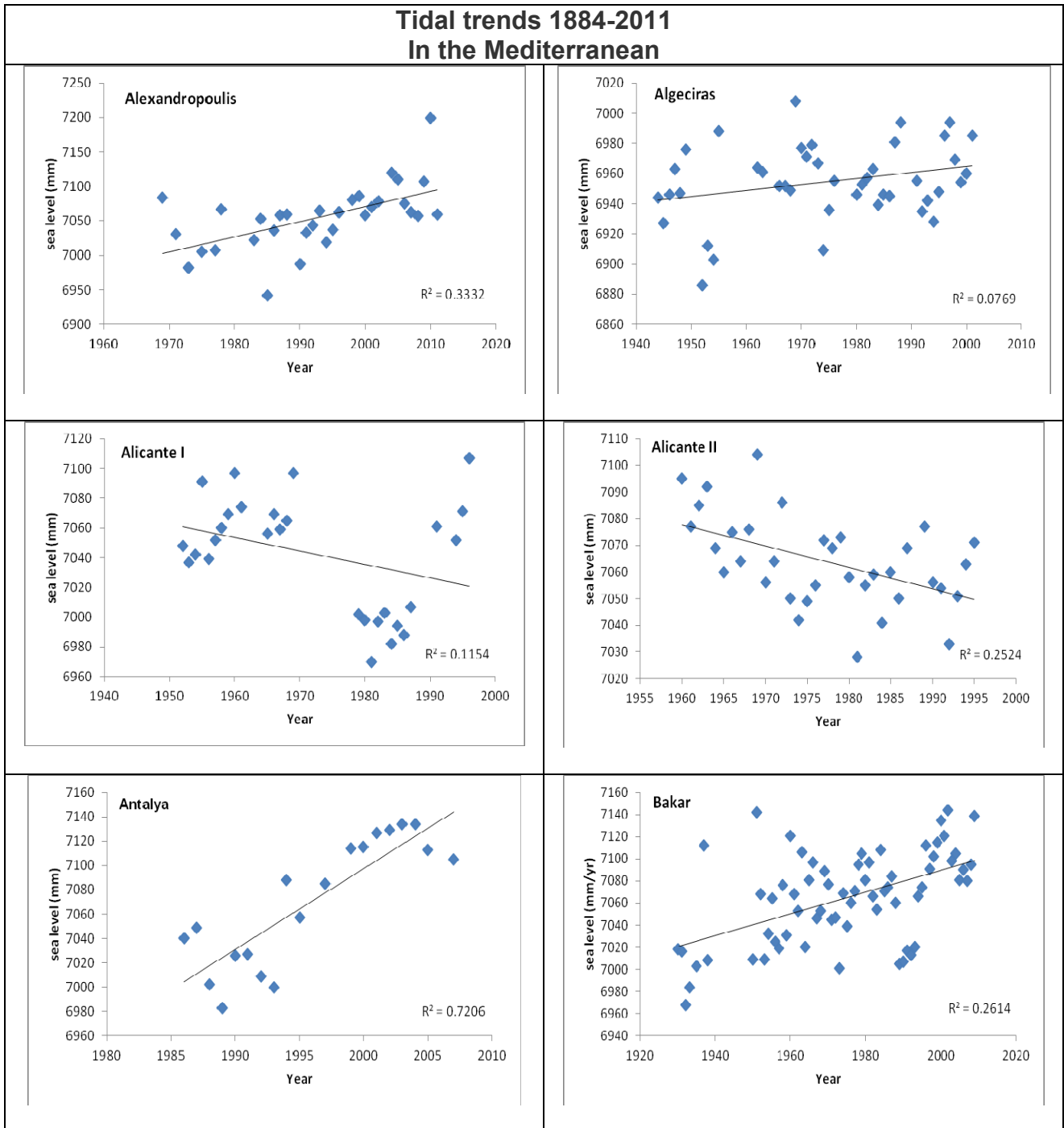


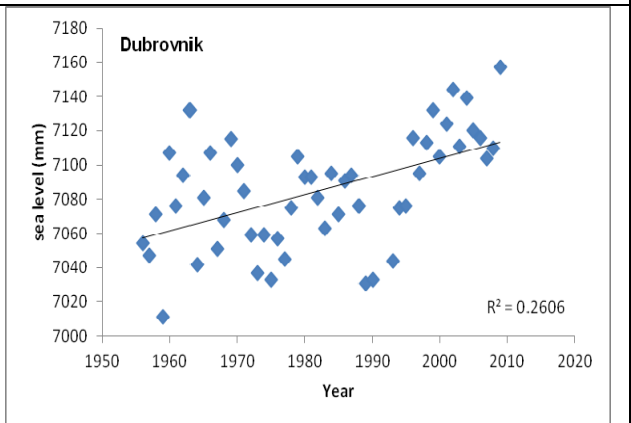
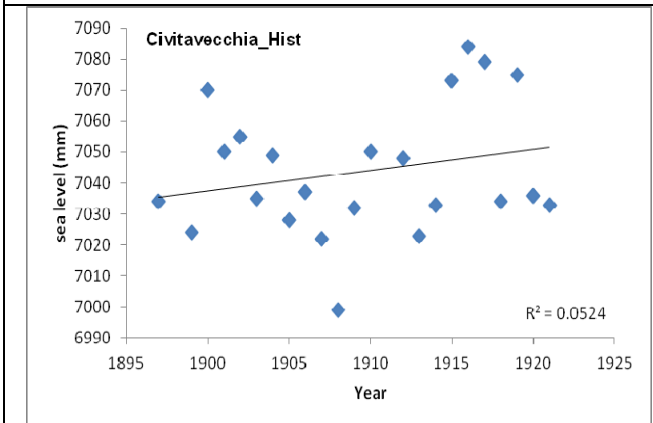
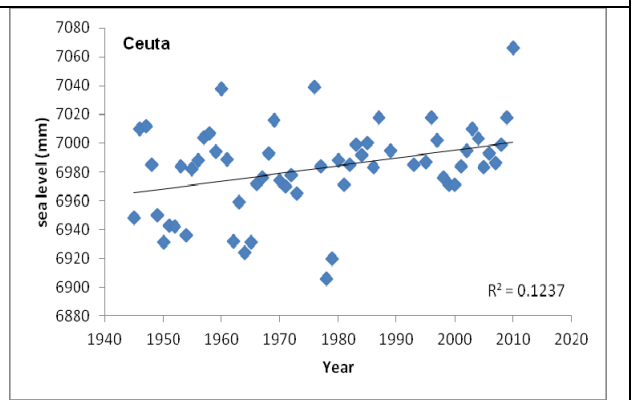
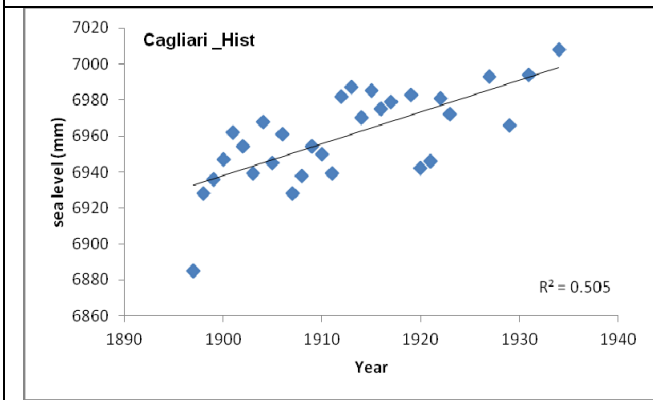
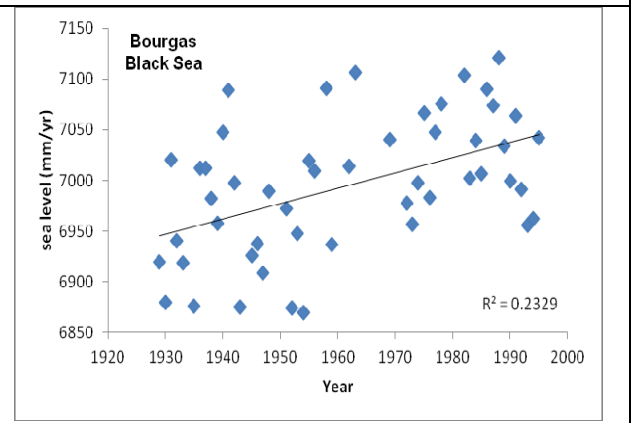
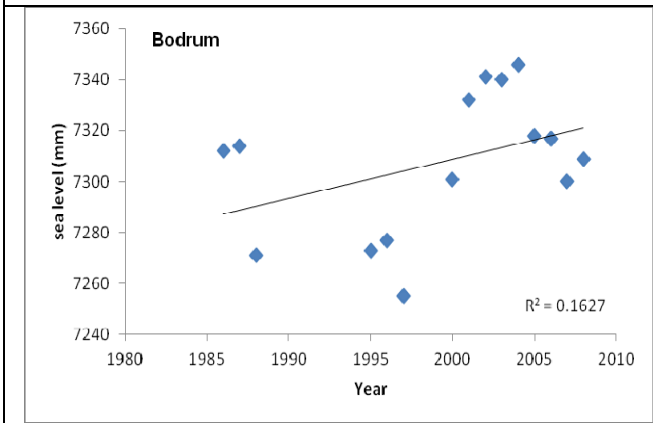
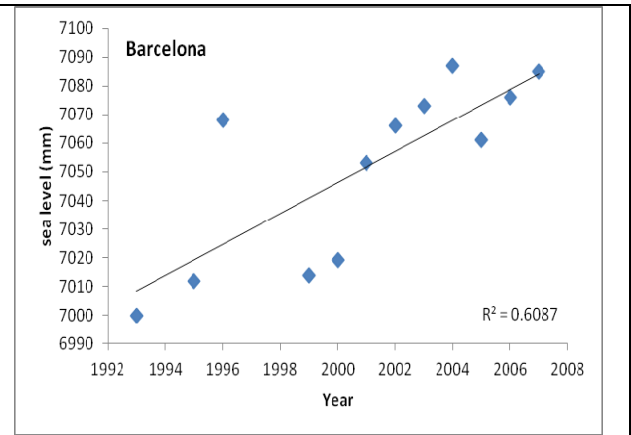
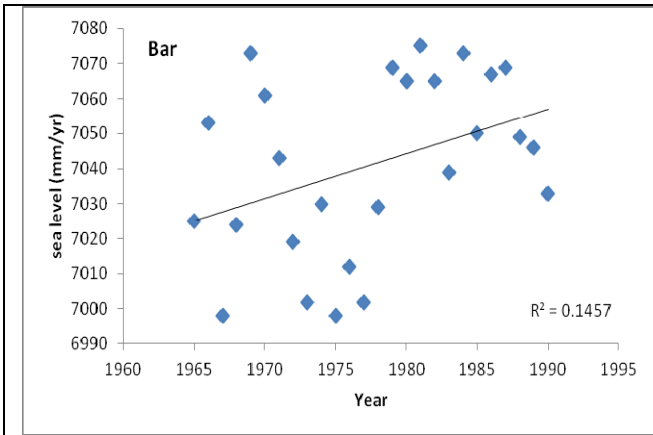
Fig. 35 Historical recording of the Messina tidal station located in the harbor of Messina, for the time span 1897-1922 (data from www.pol.ac.uk). Data show the relative sea level change across the December 28, 1908, Mw=7.1, Messina earthquake, inferred from annual mean values of the tide gauge station. Note the pre- co- and post- seismic signal inferred from the tidal data. Before the earthquake is observed a sea level fall of ~3.6 cm in the time span 1906-1907 (red rectangle). The co-seismic vertical deformation of the land caused a relative sea level rise at ~50.0 cm (double arrow in red) which was followed by ~27.6 cm of continuous post-seismic sea level rise in the time span 1909-1916 (double arrow in green), with a sea level trend at 35.4 mm/yr.

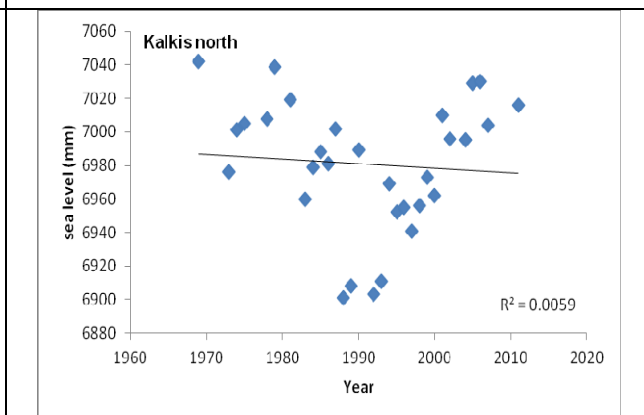
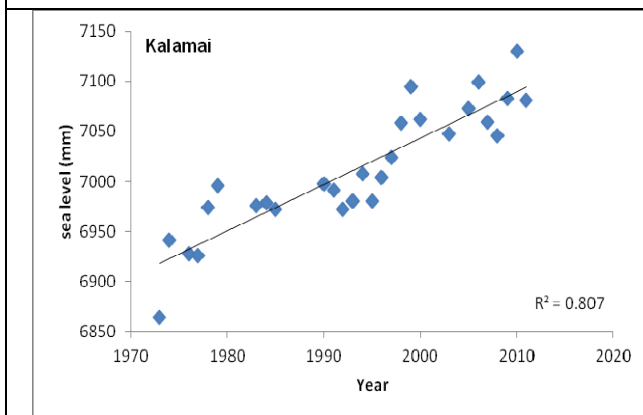
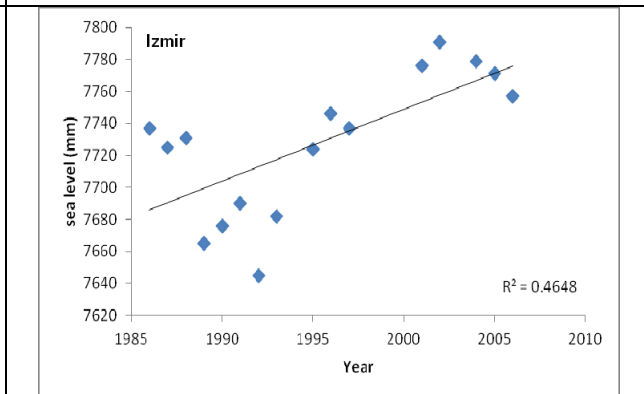
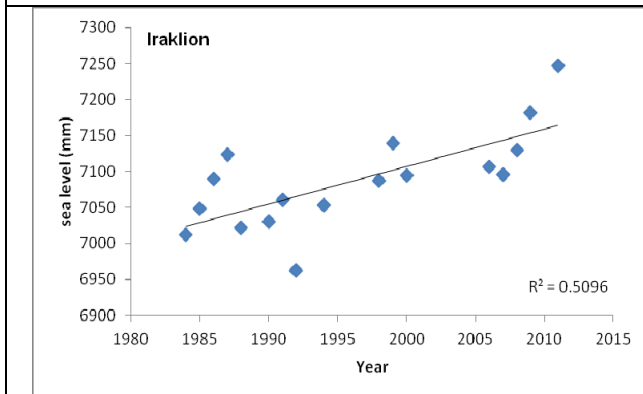
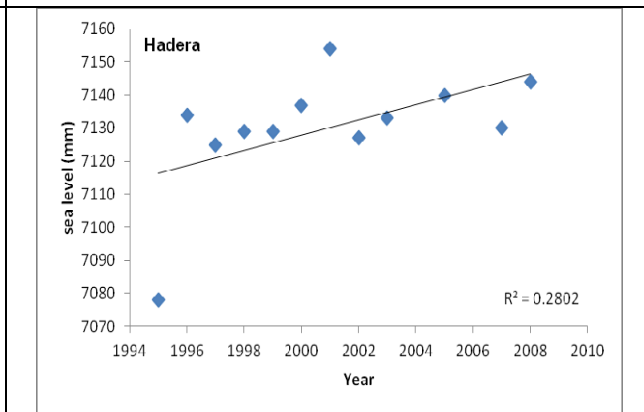
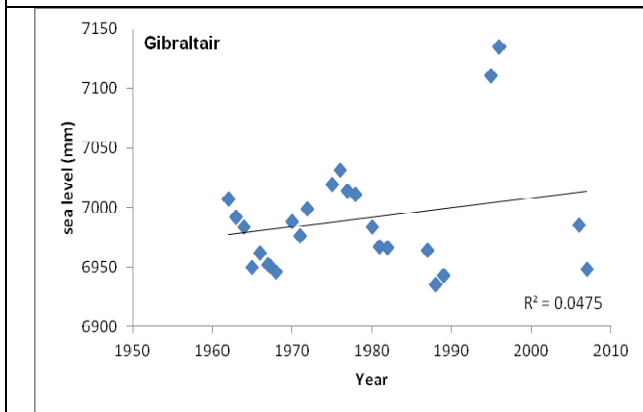
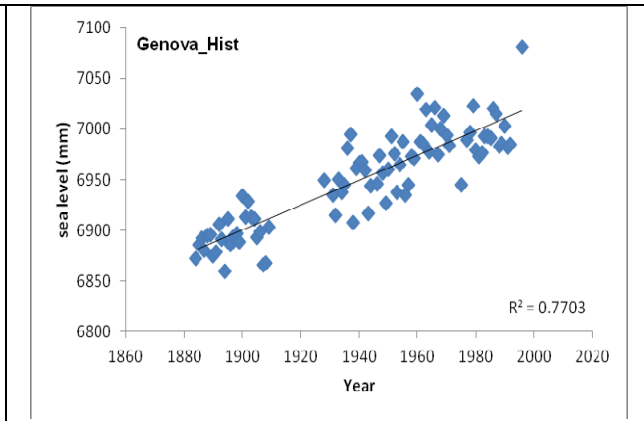
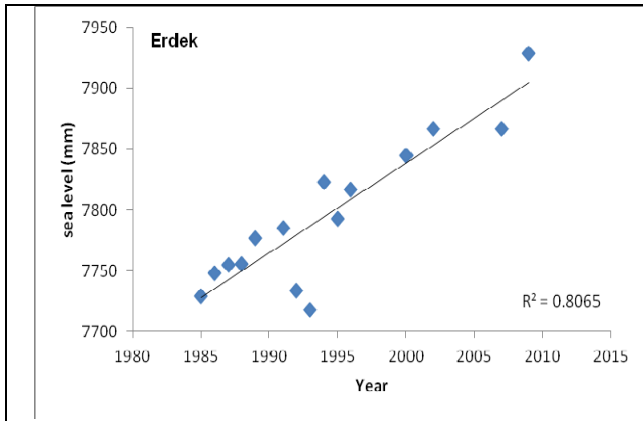
longest tidal records in the Mediterranean									
A	B	C	D	E	F	G	H	I	K
Station n.	Station Name	Country	Lat	Lon	Time span (years)	Valid years	SL rate mm/yr	Tecto mm/yr	GIA
1	Alexandroupolis	GRC	40.844	25.878	1969-2011 (42)	32	2.2±0.6		
2	Algeciras	ESP	36.117	-5.433	1944-2001 (57)	43	0.4±0.2		
3	Alicante I	ESP	38.333	-0.483	1952-1996 (44)	28	-0.9±0.5	0.6	
4	Alicante II	ESP	38.333	-0.483	1960-1997 (37)	35	-0.8±0.2	0.6	
5	Antalya	TUR	36.833	30.617	1986-2007 (21)	19	6.7±1.0	-1.48	
6	Bakar	HRV	45.300	14.533	1930-2009 (79)	67	1.0±0.2	0	0.83
7	Bar	MNE	42.083	19.083	1965-1990 (25)	26	1.3±0.6		1.05
8	Barcelona	ESP	41.350	2.167	1993-2007 (14)	12	5.4±1.4		
9	Bodrum	TUR	37.033	27.417	1986-2008 (22)	15	1.5±1.0		
10	Bourgas	BGR	42.483	27.483	1929-1995 (66)	50	1.5±0.4		
11	Cagliari	ITA	39.200	9.167	1897-1934 (37)	30	1.8±0.3	0	1.2
12	Ceuta	ESP	35.900	-5.317	1945-2010 (65)	59	0.5±1.9	-0.1	
13	Civitavecchia	ITA	42.00	12.46	1897-1921 (24)	23	0.7±0.6	0.18	0.3
14	Dubrovnik	HRV	42.658	18.063	1956-2009 (53)	52	1.1±0.2	0	0.79
15	Erdek	TUR	40.383	27.850	1985-2009 (24)	15	7.4±1.0		
16	Genova	ITA	44.400	8.900	1884-1996 (102)	85	1.2±0.7	0	1
17	Gibraltar	TUR	36.133	-5.350	1962-2007 (45)	24	0.8±0.8	-0.1	
18	Hadera	ISR	32.467	34.883	1995-2008 (13)	12	0.7±0.7	0	
19	Iraklion	GRC	35.348	25.153	1984-2011 (27)	17	5.2±1.3		
20	Izmir	TUR	38.433	26.717	1986-2006 (20)	16	4.5±1.3		
21	Kalamai	GRC	37.024	22.116	1973-2011 (38)	28	4.7±0.4		
22	Khalkis north	GRC	38.472	23.593	1969-2011 (42)	31	-0.3±0.7		
23	Khalkis south	GRC	38.461	23.589	1978-2006 (28)	19	-2.0±1.0		
24	Katakolon	GRC	37.645	21.320	1969-2011 (42)	33	2.0±0.4		
25	Kavalla	GRC	40.935	24.412	1969-2009 (38)	28	-6.0±1.6		
26	Khios	GRC	38.372	26.141	1969-2011 (42)	29	2.9±0.6		
27	La Valletta	MLT	35.900	14.517	1991-2009 (18)	16	0.9±1.6	0	0.26
28	Lefkas	GRC	38.835	20.712	1970-2011 (41)	29	2.6±0.4		2.29
29	Leros	GRC	37.130	26.848	1971-2011 (40)	26	1.0±0.5		
30	L'Estartit	ESP	42.050	3.200	1990-2011 (21)	22	3.8±0.7		
31	Malaga II	ESP	36.717	-4.417	1993-2009 (16)	15	4.4±1.0	0.1	
32	Marseille	FRA	43.300	5.350	1885-2011 (126)	120	1.3±0.1	0	1.2
33	Monaco	MCO	43.733	7.417	1956-2011 (55)	20	0.0±3.5	0	0.37
34	Napoli Arsenale	ITA	40.866	14.267	1899-1922 (24)	24	2.6±0.7	-1.5	2.2
35	Napoli Mandraccio	ITA	40.866	14.267	1896-1922 (27)	27	2.4±0.6	-1.5	2
36	Nice	FRA	43.700	7.267	1978-2011 (33)	28	2.8±0.6	0	2.43
37	North Salaminos	GRC	37.950	23.500	1984-2000 (16)	13	1.0±1.3		
38	Palermo	ITA	38.133	13.333	1897-1921 (24)	20	0.8±0.5	0	0.27
39	Patrai	GRC	38.417	21.729	1969-2006 (37)	29	16.0±0.7		
40	Piraeus	GRC	37.937	23.627	1969-2002 (33)	23	-6.0±1.5		
41	Port Said	EGY	31.250	32.300	1923-1946 (23)	24	4.8±1.0		
42	Porto Maurizio	ITA	43.867	8.017	1897-1921 (24)	24	1.7±0.6	0	1.52
43	Posidhonia	GRC	37.951	22.960	1969-2009 (40)	26	-2.0±1.4		
44	Preveza	GRC	38.959	20.757	1969-2011 (42)	29	0.3±0.7		-0.01
45	Rodos	GRC	36.442	28.236	1972-2011 (39)	18	1.7±0.5		
46	Rovinj	HRV	45.083	13.628	1956-2008 (52)	52	0.4±0.2	0	0.22
47	Siros	GRC	37.440	24.946	1969-2011 (42)	23	4.3±0.8		
48	Soudhas	GRC	35.487	24.082	1969-2001 (32)	28	-2.0±0.8		
49	Split RT	HRV	43.508	16.392	1953-2007 (54)	54	0.6±2.6	0	0.32
50	Split Gradska Luka	HRV	43.507	16.442	1955-2009 (54)	55	0.6±2.6	0	0.32
51	Sucuraji	HRV	43.133	17.200	1987-2005 (18)	17	5.7±1.7	0	5.37
52	Tel Aviv	ISR	32.083	34.767	1996-2009 (13)	12	0.2±1.1	0	
53	Thessaloniki	GRC	40.633	22.935	1969-2009 (40)	33	3.6±0.4		
54	Toulon	FRA	43.117	5.917	1961-2010 (49)	21	0.7±3.8	0	0.6

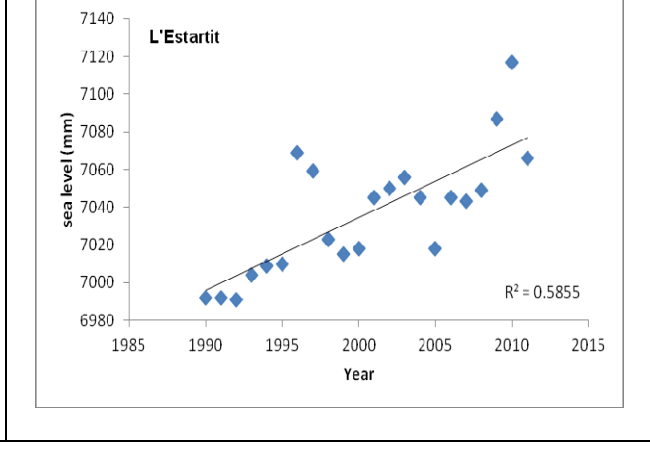
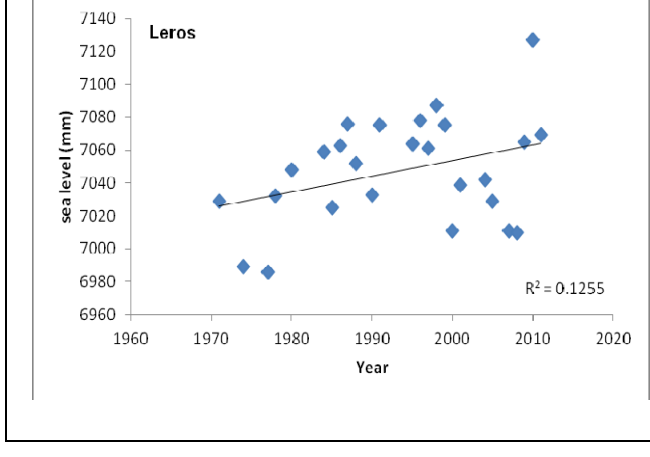
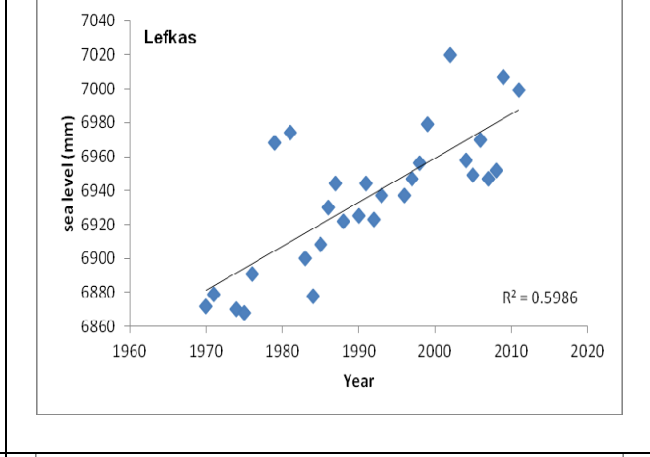
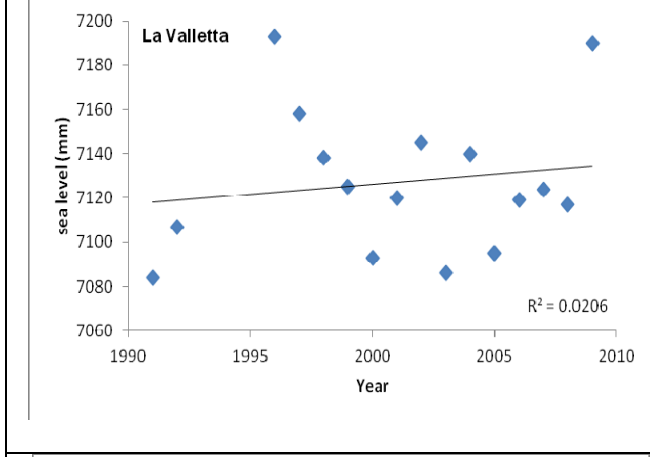
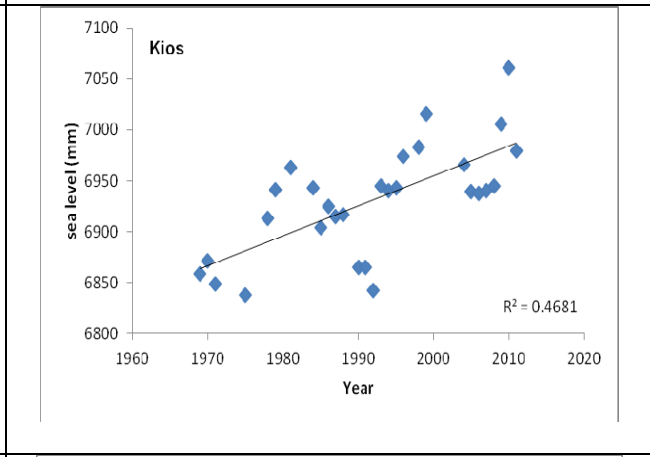
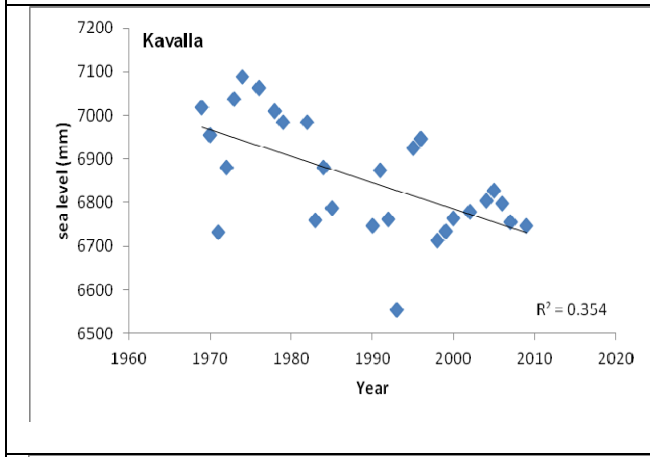
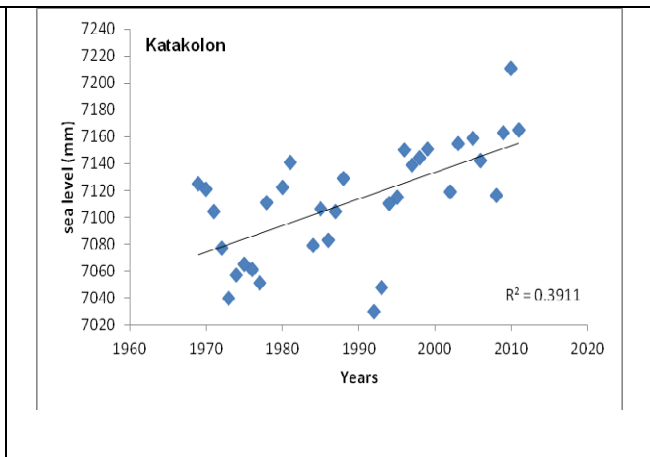
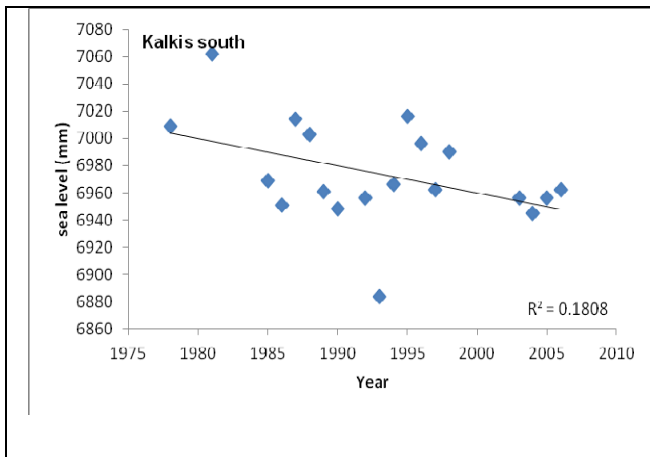
55	Trieste	ITA	45.647	13.758	1905-2011 (106)	101	1.27±0.1	0	1.15
56	Varna	BGR	43.183	27.917	1929-1996 (67)	58	1.5±0.4		
57	Zadar	HRV	44.123	15.235	1995-2008 (13)	14	0.9±1.7	0	0.6

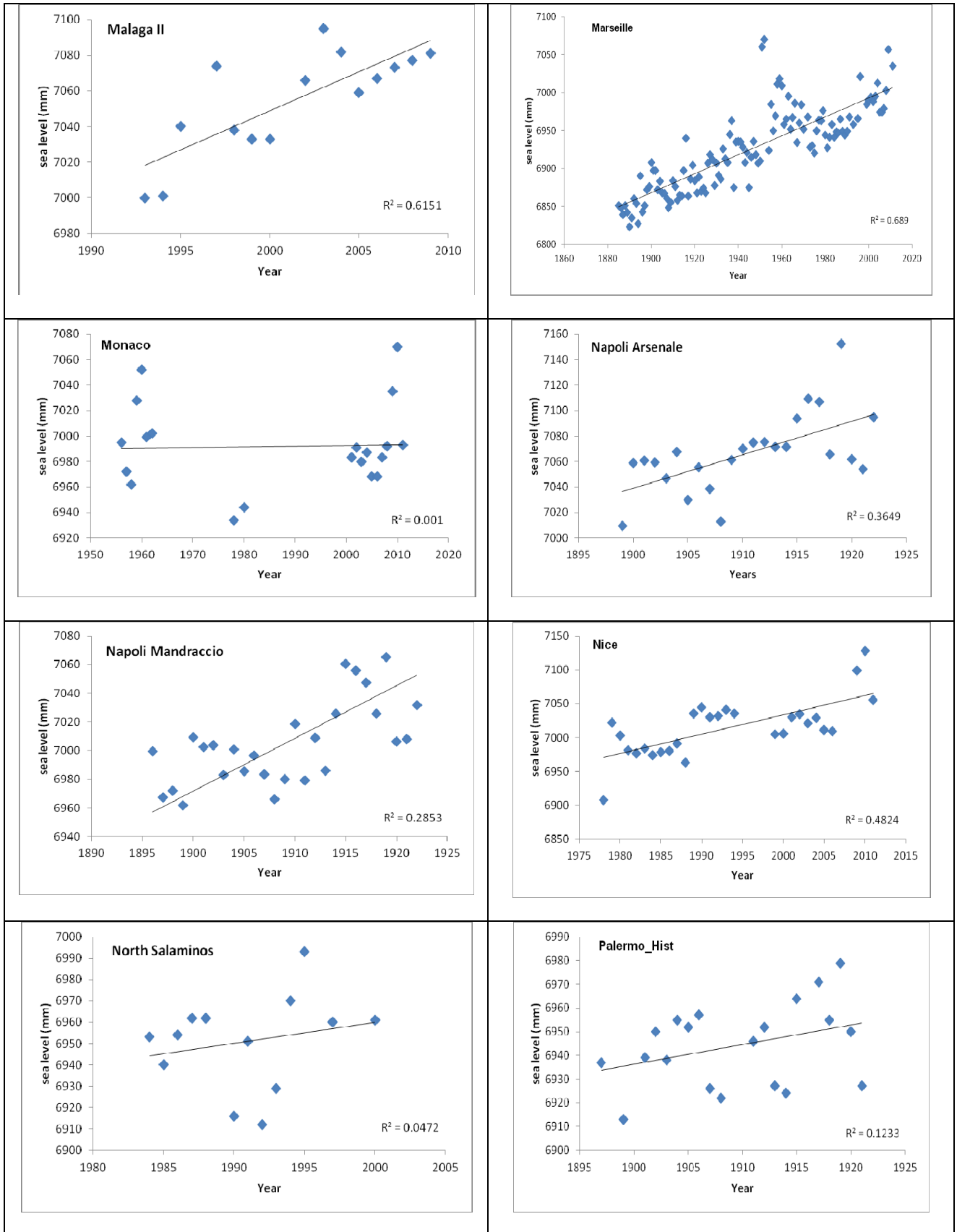
Table 4. Tidal rates estimated from the mean annual values at 55 stations (listed in alphabetical order) of the tidal stations distributed along the coast of the Mediterranean and 2 in the Black Sea (in blue, Bourgas and Varna), that recorded in the time span 1884-2011 (data from www.pol.ac.uk). We analyzed only stations with more than 13 years of recorded data. In the table the station number, the station name, the recording time span, the number of the valid mean annual values data, the sea level rates with their related uncertainties and vertical tectonics estimated at each station, are shown.

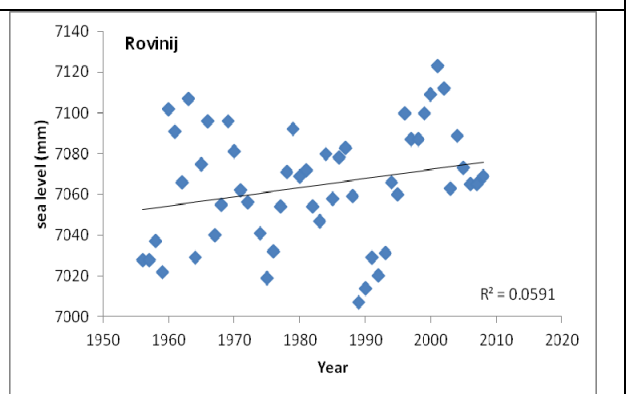
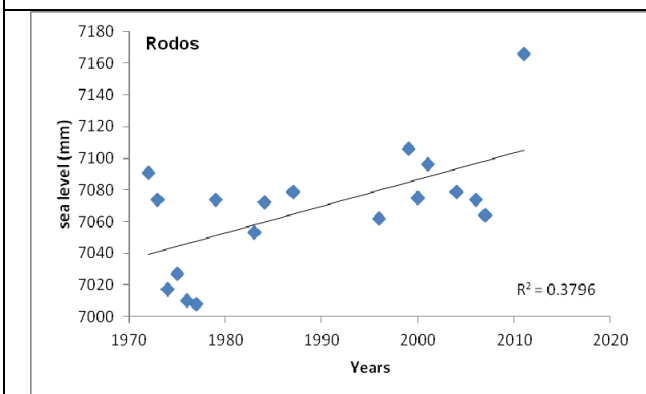
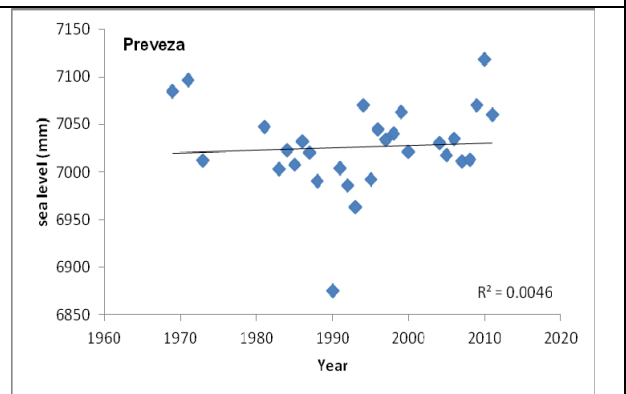
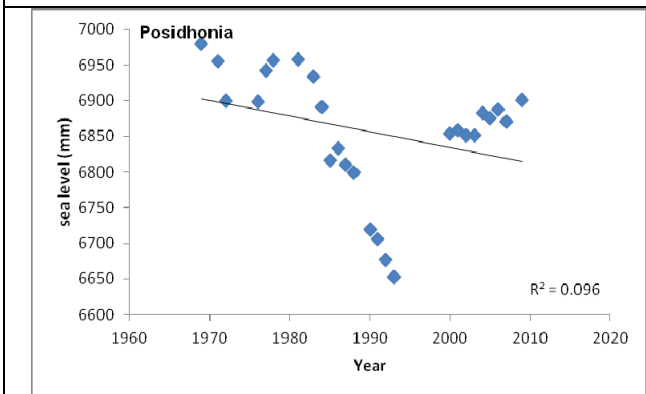
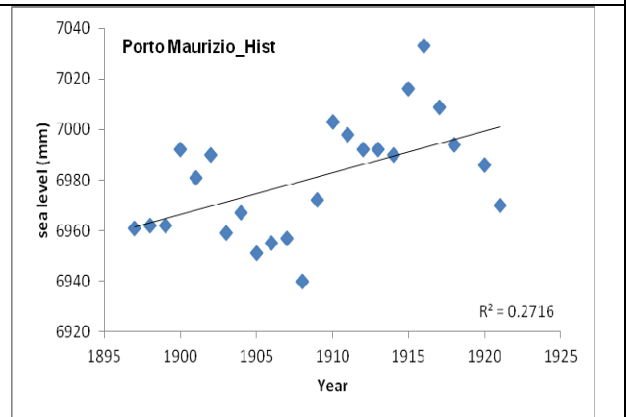
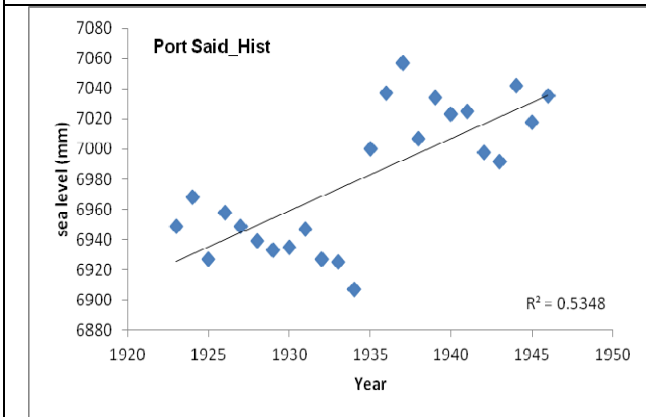
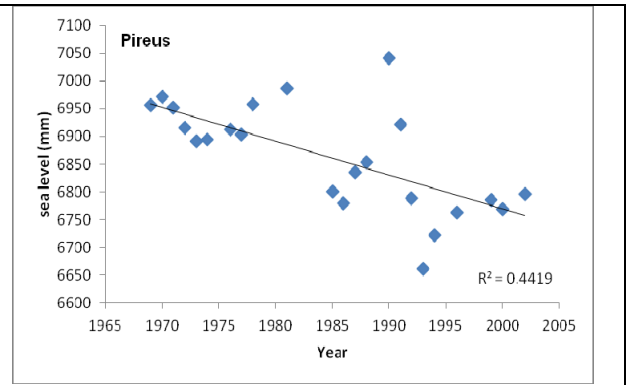
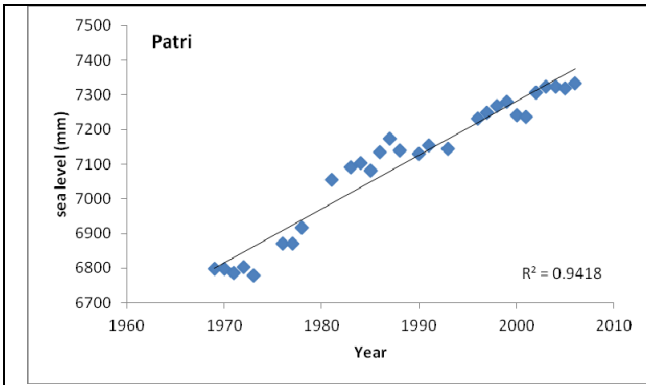


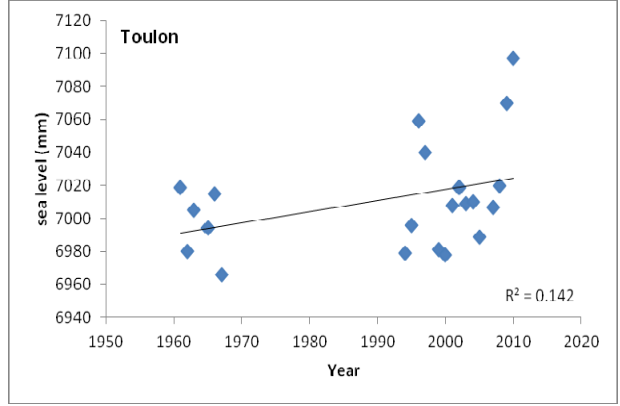
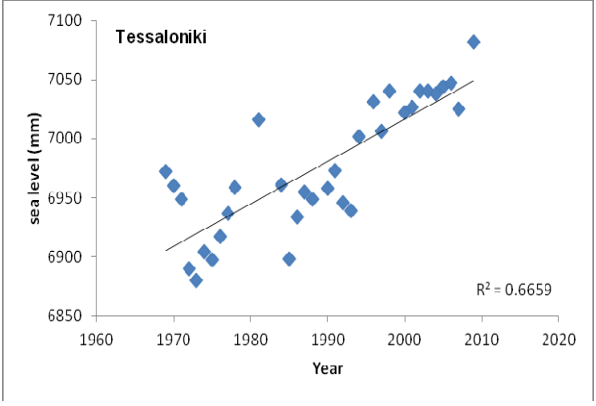
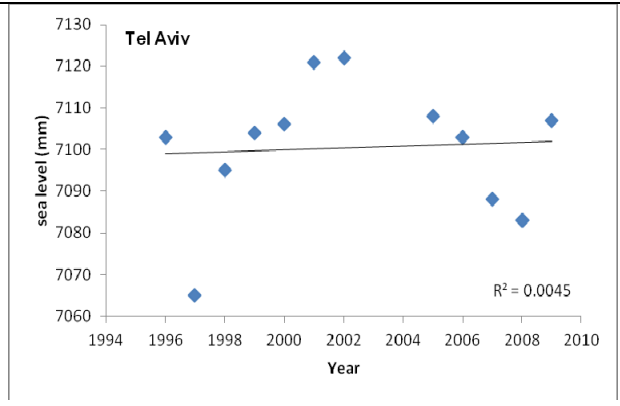
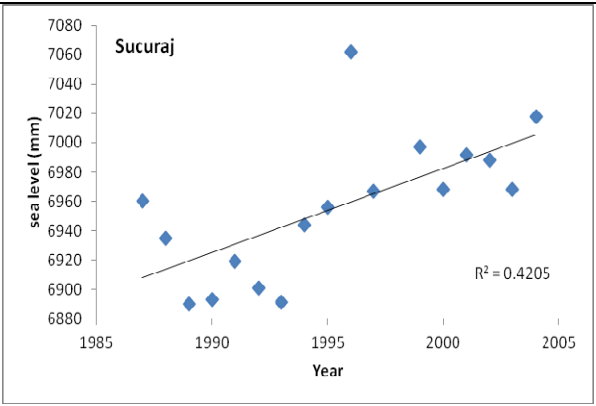
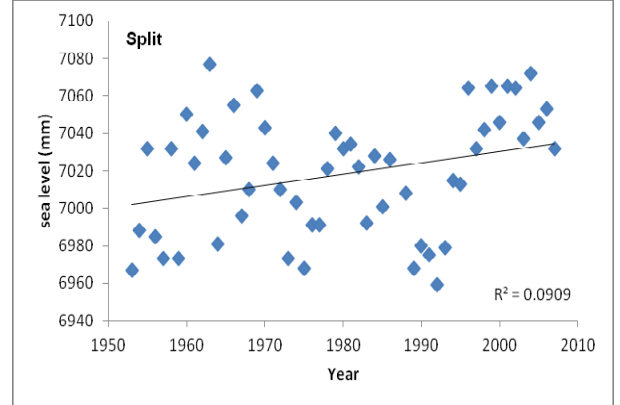
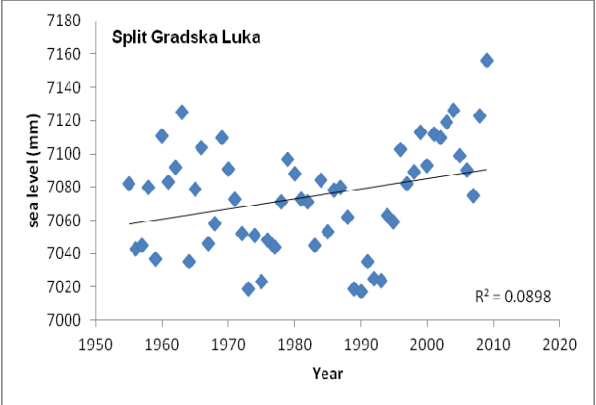
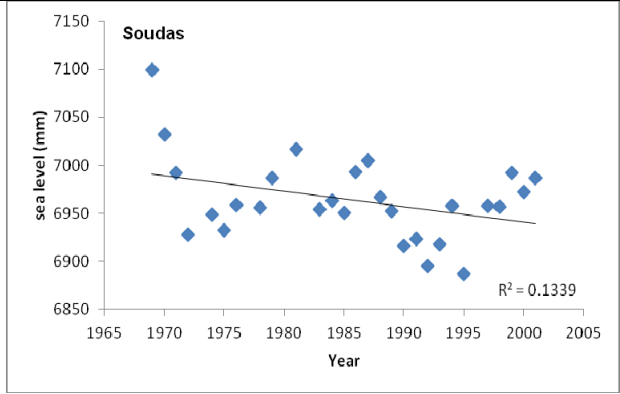
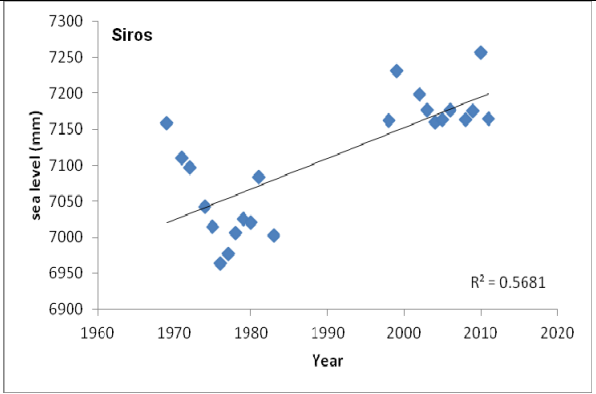


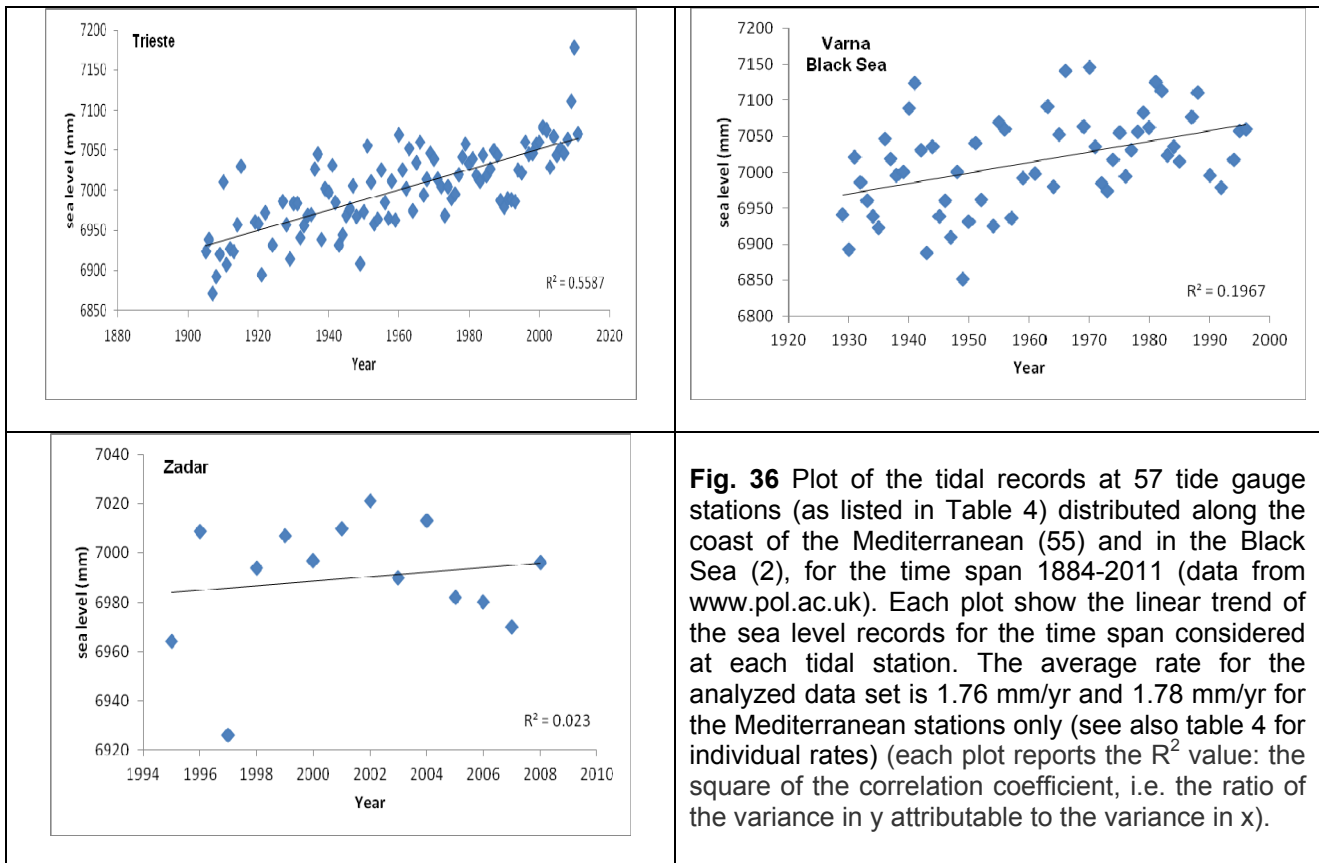












In the following figures are reported some results concerning the relationships between the length of the recordings (years) against the estimated sea level rates and their uncertainties. Figure 37 shows the sea level rates for the stations analyzed in this study. Figure 38 show the estimated sea level rates against valid records and Fig. 39 against all records for 55 analyzed tidal stations in the Mediterranean and 2 in the Black Sea. With valid records are defined the length (years) of the recordings, excluding data interruptions. With all records, we define the age of each station, including periods without data. Therefore, valid records are given by the age of the stations minus the years of missing data recordings.

Stations with valid records improve the analysis and indicate that those with at least 30 years of recordings provide more stable results, with sea level trend values that largely fall within the average value of the whole data set, at ~1-2 mm/yr. Figures 11 and 12, show the uncertainties of the analysis for the estimated sea level rates versus all records (Fig.40) and valid records (Fig.41) for the 55 tidal stations in the Mediterranean and in the Black Sea (2 stations). The uncertainties are decreasing with the increasing duration of the available recordings. Fig. 42 shows the rate of sea level estimated at a set of stations, for which are known the GIA and tectonic rates from independent studies. The analysis provide a sea level rise between 0.72 and 0.97 mm/yr, dependent from the stations used in the analysis (data set includes stations with a mean age of 46 years and a maximum age of 126 years with station numbers corresponding to Table 4).

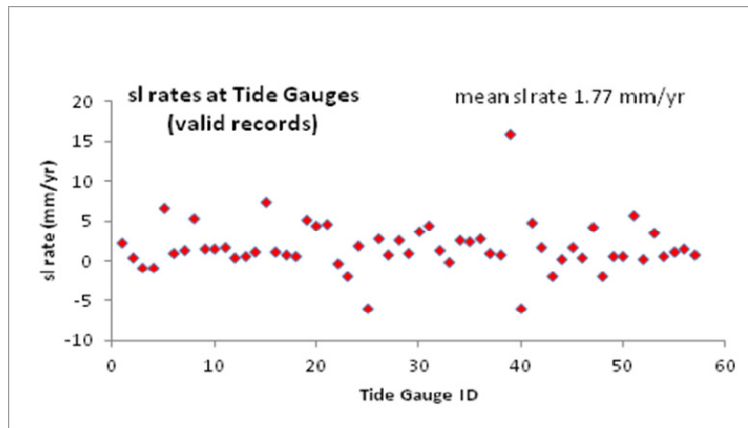


Fig.37 Plot of the estimated sea level rates at the 55 analyzed tide gauge stations in the Mediterranean and in the Black Sea (2 stations). The mean rate estimated in the time span 1884-2011, is 1.78 mm/yr.

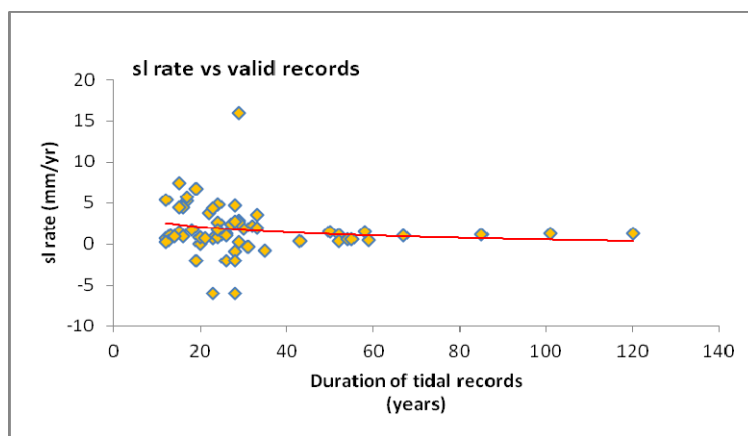


Fig.38 Plot of the estimated sea level rates versus valid records for 55 tidal stations in the Mediterranean and in the Black Sea (2 stations). Note that only after 30-35 years of recordings, the estimated sea level rates are more stable and with values within about 1-2 mm/yr. The red line is the exponential behavior of the trend.

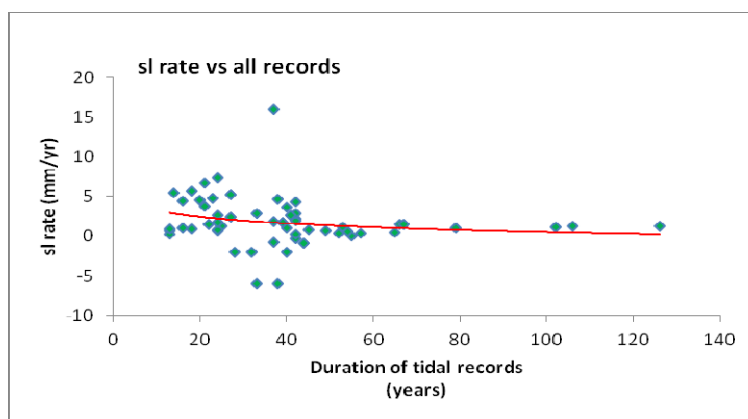


Fig.39 Plot of the estimated sea level rates versus all records for 55 tidal stations in the Mediterranean and in the Black Sea (2 stations). Note that rates are sparser than in the previous figure and only after 40/45 years of recordings, the estimated sea level rates become more stable and with values of about 1-2 mm/yr. The red line shows the exponential behavior of the trend.

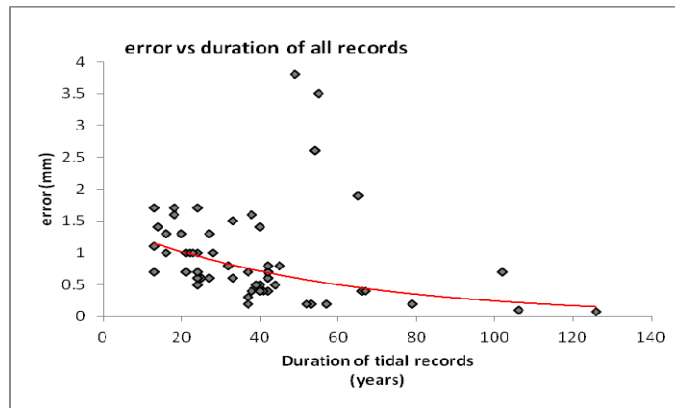


Fig.40 Plot of the uncertainties for the estimated sea level rates versus all records from 55 tidal stations in the Mediterranean and in the Black Sea (2 stations). Uncertainties decrease with the length of the recordings. The red line shows the exponential behavior of the trend.

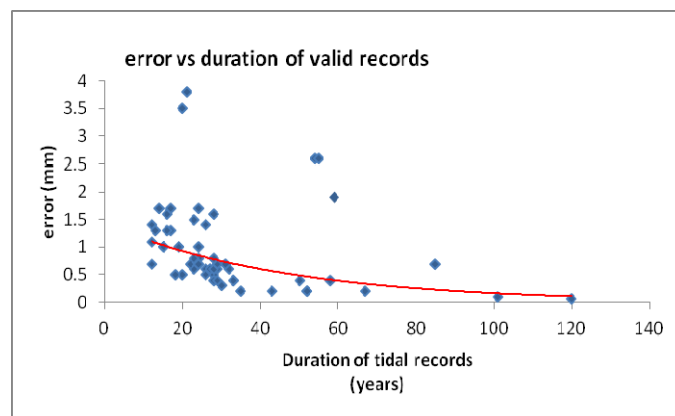


Fig.41 Plot of the uncertainties for the estimated sea level rates versus valid records from 55 tidal stations in the Mediterranean and in the Black Sea (2 stations). Uncertainties decrease with the length of the recordings and become smaller after 35 year of continuous data. The red line shows the exponential behavior of the trend.

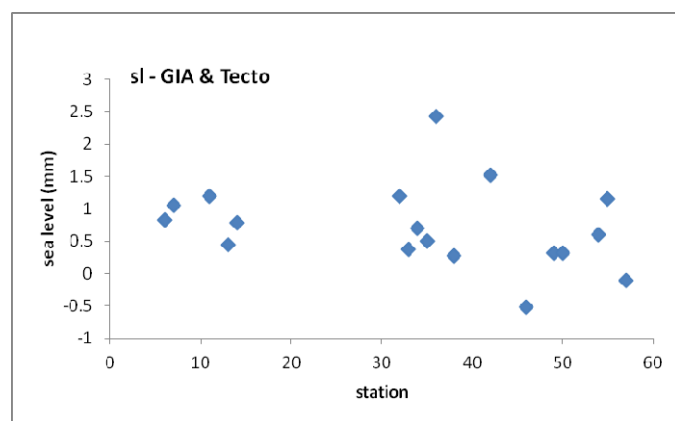


Fig. 42 Plot of the residual sea level for a set of tidal stations for which are known GIA and tectonic rates from independent studies. The analysis provide a sea level rise between 0.72 and 0.97 mm/yr, dependent from the stations used in the analysis (data set includes stations with a mean age of 46 years and a maximum age of 126 years).

9. Tsunami recordings in the Mediterranean from tidal stations: case studies

The modern digital tide gauge stations have now the possibility to provide high frequency data of sea level measurements, with respect to the past analogical instrumentation. Hence, given the available tidal data set, we have the possibility to analyze sea level perturbation related to tsunamis or tsunami-like signals (i.e. not caused by earthquakes, but submarine slides, rapid atmospheric pressure changes at the sea surface, storms). In this chapter we show some examples of transient sea level changes caused by significant earthquakes occurring inside and outside the Mediterranean basin that produced tsunami waves capable to be recorded from regional to global scale tidal networks. Particularly, we focus on two cases: the Boumerdès and Tohoku-Oki earthquakes, of Magnitude 6.8 and 9.0, occurred in 2003 and 2011 in the Mediterranean and in the Pacific Ocean, respectively.

In order to characterize the observed change of dynamical behavior, we used the Empirical Mode Decomposition (EMD) (Huang et al., 1998) to analyze the tidal signal related to both of these events. This technique has been developed to process non stationary data and successfully applied in several different contexts. Through the EMD a time series $L(t)$ of the sea level recording is decomposed into a finite number n of Intrinsic Mode Functions (IMF) $\theta_j(t)$ as:

$$L(t) = \sum_{j=0}^n \theta_j(t) + r_n(t) .$$

The functional form of the (IMF) $\theta_j(t)$ is not given a priori but obtained from the data by following the “sifting” procedure (Huang et al., 1998). This process starts by identifying local minima and maxima of the raw signal $L(t)$. The envelopes of maxima and minima are then obtained through cubic splines and the mean between them, namely $m_1(t)$, is then calculated. The difference between the raw time series and the mean series, $h_1(t) = L(t) - m_1(t)$, represents an IMF only if it satisfies two criteria: i) the number of extrema and zero-crossing does not differ by more than one; ii) at any point the mean value of the envelope defined by the local maxima and the envelope defined by the local minima is zero. If $h_1(t)$ does not support the criteria, the previous steps are repeated by using $h_1(t)$ as raw series and $h_{11}(t) = h_1(t) - m_{11}(t)$, where $m_{11}(t)$ is the mean of the envelopes in this case, is generated. This procedure is repeated k times until $h_{1k}(t)$ satisfies the IMFs properties. Thus $\theta_1(t) = h_{1k}(t)$ represents the first IMF, containing the shortest time scale of the process and having a zero local mean. To guarantee that the IMF components contain enough physical sense with respect to both amplitude and frequency modulations, a criterion to stop the sifting process has been introduced (Huang et al., 1998). A kind of standard deviation, calculated using two consecutive siftings is defined by:

$$\sigma = \sum_{t=0}^N \left[\frac{|h_{1(k-1)}(t)| - |h_{1k}(t)|}{h_{1(k-1)}^2(t)} \right]$$

and the iterative process is stopped when σ is smaller than a threshold value, in our case chosen as 0.3 (as suggested by Huang et al. (1998)). The function $r_1(t) = L(t) - \theta_1(t)$ is called the first residue, and it is analyzed in the same way as just described, thus obtaining a new IMF $\theta_2(t)$ and a second residue $r_2(t)$. The process continues until θ_j or r_j are almost zero everywhere or when the residue $r_j(t)$ becomes a monotonic function from which no more

IMF can be extracted. At the end of the procedure the original time series is decomposed into n empirical modes ordered with increasing characteristic time scale, and a residue $m(t)$ which describes the mean trend if any.

The EMD decomposition is local, namely it preserves information about the local properties of the signal, complete orthogonal: each IMF captures the empirical dynamical behavior of a single independent mode of the system, namely each j -mode describes a single phenomenon within the complex dynamics. The orthogonality property of the IMFs allows filtering and reconstructing the signal through partial sums in equation 1 in order to obtain independent contributions to the signal in different ranges of time scales (Huang et al., 1998; Terradas, Oliver and Ballester, 2004; Vecchio, 2010). Moreover, each IMF has its own timescale and represents a zero mean oscillation experiencing amplitude and frequency modulations, namely the j -th IMF can be expressed as $A_j(t) = A_j(t)\cos[\omega_j(t) \cdot t]$, where $A_j(t)$ and $\omega_j(t)$ represent the amplitude and the frequency of the j -th mode respectively.

The typical IMF timescale τ_j is computed as the average time between local maxima and minima. It cannot be interpreted as the periods of Fourier modes because it provides just an estimate of the timescale characterizing the EMD j -th mode for which it is computed, although many modes with different average periods may contribute to the variability of the actual signal at a particular time scale. The decomposition through IMFs allows defining a meaningful instantaneous frequency for each EMD mode calculated as follows. For each IMF the Hilbert transform is applied, namely:

$$\theta_j^*(t) = \frac{1}{\pi} P \int_{-\infty}^{\infty} \frac{\theta_j(t')}{t-t'} dt'$$

where P indicates the Cauchy principal value. $\theta_j(t)$ and $\theta_j^*(t)$ form the complex conjugate pair so that the instantaneous phase can be calculated as $\Phi_j(t) = \arctan[\theta_j^*(t) / \theta_j(t)]$. It follows that the instantaneous frequency is $\omega_j(t) = d\Phi_j/dt$. This definition of $\omega(t)$ is quite general and in principle some limitations on the data are necessary in order to obtain instantaneous frequency as single value function of time. The latter property is fulfilled by the EMD basis functions which allow obtaining meaningful instantaneous frequency consistent with the physics of the system under study (Huang et al., 1998).

9.1 The May 21, 2003, Mw=6.8, Boumerdès earthquake (Algeria)

The Boumerdès earthquake, of Mw=6.8, occurred on May 21, 2003 along the northern coast of Algeria (Meghragoui et al., 2004). This part of the North African coast is one of the most seismic areas of the Mediterranean that have often released large magnitude earthquakes in the past. The tsunami that followed the Boumerdès earthquake, was recorded by several tidal stations that were active at that time (Fig. 43, 44), and represents one of the very few cases of tsunami recordings in the Mediterranean.

The amplitude of the sea surface oscillation measured at the tidal stations every ten minutes was decreasing with their increasing distance from the epicenter. Also, was observed a temporal shift with the onset of the anomalous fluctuation at the different tidal stations: waves arrived first at the tidal stations located in southern Italy and later in time up to the northern coasts of the Tyrrhenian Sea.

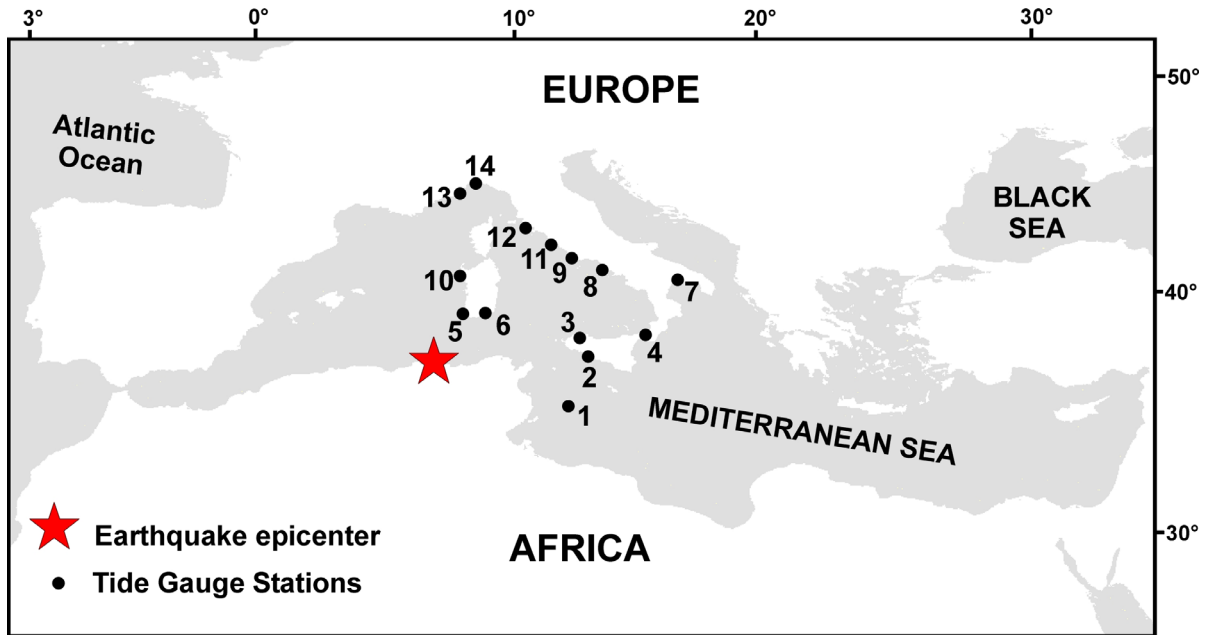


Fig. 43 Map of the tide gauge stations used to study the effects of the Boumerdes earthquake that triggered a tsunami in the central Mediterranean: 1) Lampedusa, 2) Porto Empedocle, 3) Palermo, 4) Reggio Calabria, 5) Carloforte, 6) Cagliari, 7) Taranto, 8) Salerno, 9) Napoli, 10) Porto Torres, 11) Civitavecchia, 12) Livorno, 13) Imperia, 14) Genova. The red star is the location of the earthquake.

Although the detection and analysis of these signals (amplitudes and periods) can be better evaluated using high frequency sampling intervals, in this case we attempted to analyze the data set at ten minutes sampling interval, using the EMD technique.

By applying the EMD to the tide gauge data, a number n of IMFs, depending on the station, is obtained. The highest amplitude IMFs, as expected, are associated to the semidiurnal oscillation representing the main tidal contribution. The orthogonality of the IMF allows to recover four main contributions to $L(t)$, by partial sum in equation (1). The sea level can be written as $L(t) = HF(t) + S D(t) + LF(t) + r n(t)$, where $HF(t)$ is associated with the high-frequency IMFs ($30min \leq t_j \leq 3h$), $S D(t)$ represents the contribution of the semi-diurnal component and $LF(t)$ describes the remaining low-frequency contribution.

The $HF(t)$ contributions, for each station, are reported in Figure 45. In particular a sudden increase of the amplitude is observed for all station but Lampedusa, Napoli, Porto Torres, Reggio Calabria, Salerno, Taranto. By looking at the semidiurnal tidal component, it is split in two or three IMFs, depending to the station. This indicates that one IMF does not suffice to fully account for the temporal behavior of the 12 hour tidal component. This result comes from the high sensitivity of the EMD to local frequency fluctuations, related to the effect of the earthquake, affecting the regularity of the semidiurnal mode of oscillation after the meteorological effects have been removed. As mentioned above, since each IMF is associated to a well defined time scale of the analyzed signal, a regular semidiurnal oscillation should be isolated in a single IMF.

The presence of frequency fluctuations, well localized in time, introduces new time scales in the signal mainly affecting the high amplitude tidal components. When this happens a single IMF is not able to account for the new time scales and the time evolution of the 12 hour oscillation is split into two or more IMFs. Quite obviously, the sum of these EMD modes will describe the full contribution of the semidiurnal oscillation to the sea level. The behavior of $S D(t)$ is not regular, far from stationary and an abrupt change of regime is

observed for $t > 0$. The change of behavior at $t = 0$ is clearly underlined when we look at the instantaneous frequency $\omega(t)$ of the semidiurnal component of the highest-amplitude IMF which is abruptly destabilized in correspondence of the change of the oscillating regime and departs from the constant value of $(2\pi)/12\text{hour}^1$.

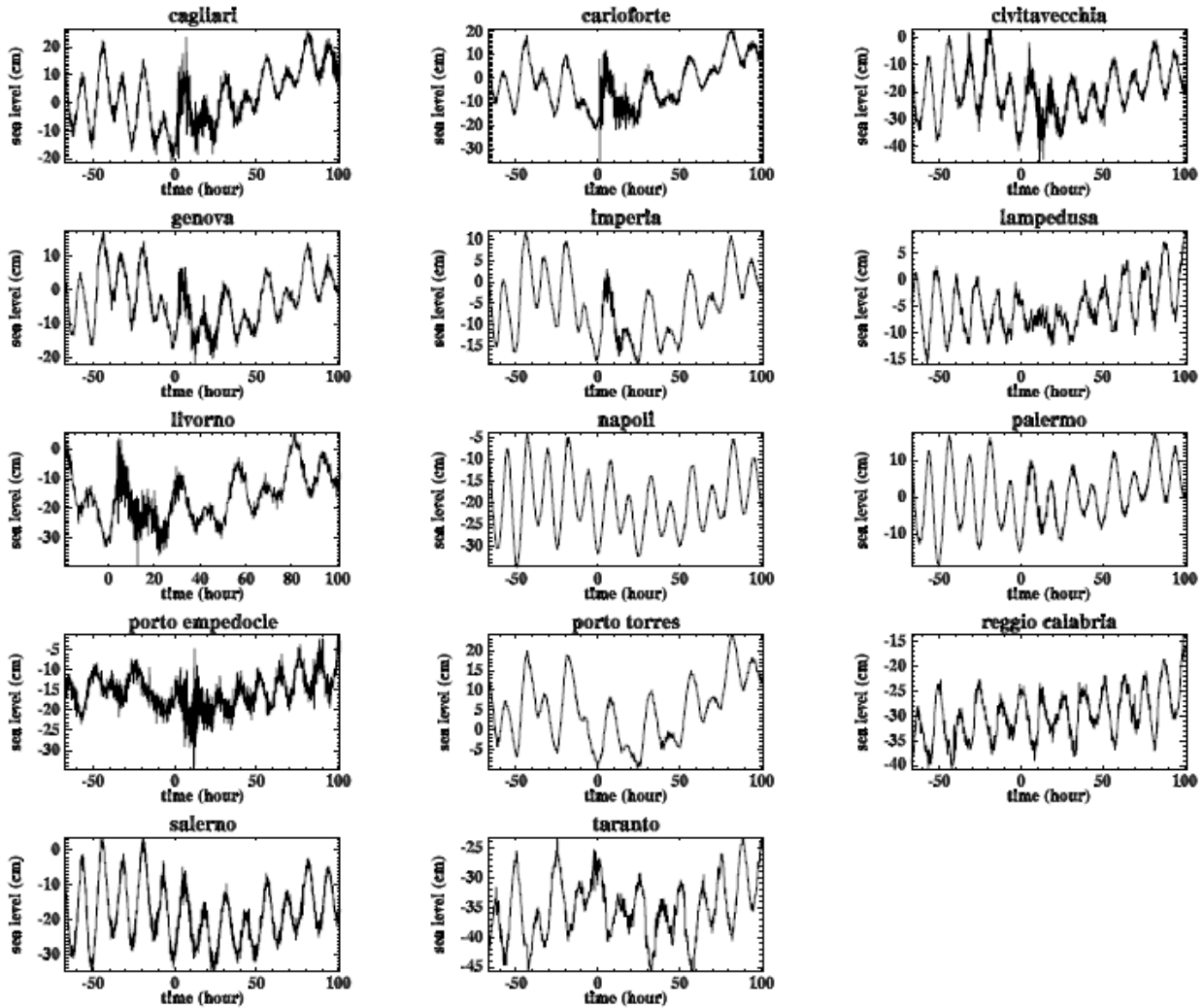


Figure 44 Time evolution of the sea level for each station in the considered period. The time series of the raw tidal data show a change on the tidal oscillation right after the earthquake. The normal tidal oscillations are broken, high frequency fluctuations appear, and the time behavior becomes more complex and highly non stationary. After about 30 hours after the earthquake, the tidal oscillation returns to its usual dynamics.

This effect is observed in all the analyzed stations, including those that do not show the increase of amplitude in $HF(t)$. We remark that for the three nearest stations to the earthquake epicenter, namely Lampedusa, Palermo and Porto Empedocle, the destabilization of the semidiurnal frequency begins slightly before $t = 0$.

This signal, that seems to precede the onset of the earthquake, is still under investigation. EMD modes with longer periods, describe low-frequency phenomena. Figure 16 shows the contour plot of $LF(t)$ for the analyzed stations in the space-time plane, ordered according to the distance from the earthquake's epicenter. The main feature is the presence of a void at around and after $t=0$ occurring in a few hours of duration and depending on the

geographic location. The time at which the void is observe changes, about linearly, with the distance. This result is consistent with a traveling perturbation in the Mediterranean Sea that we address to the sea level perturbation induced by the Boumerdès earthquake (Fig.46).

The occurrence of void in sea level data, mainly presence of tsunami perturbation, has been detected in the past (Joseph et al., 2006; Vecchio et al., 2012), and has been attributed to the local seafloor topography and/or by the different paths taken by the tidal perturbation and reflection effects.

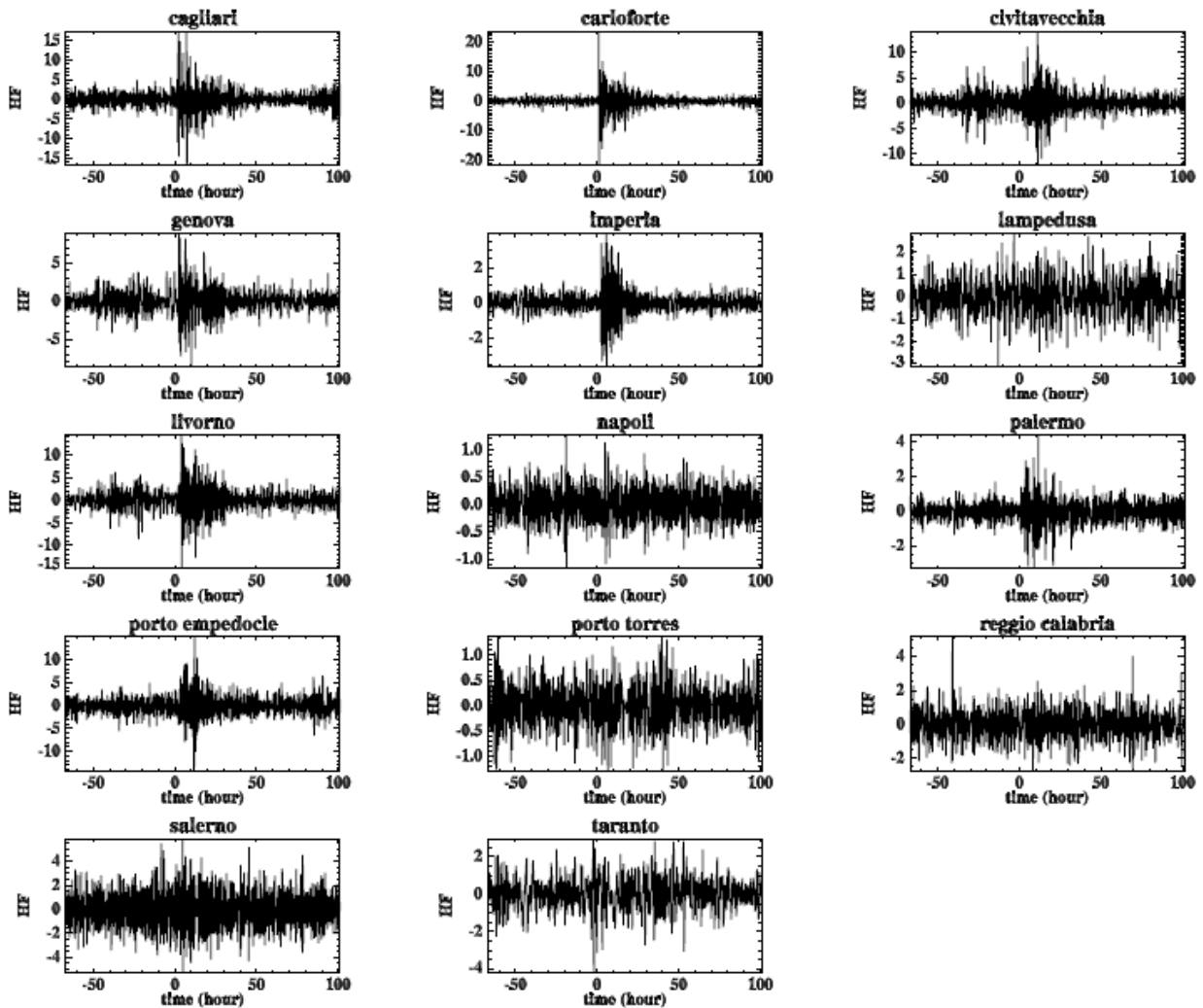


Figure 45 Time evolution of the high frequency contribution $Hf(t)$ for the 14 stations. Time is counted from the origin time of the Boumerdès earthquake.

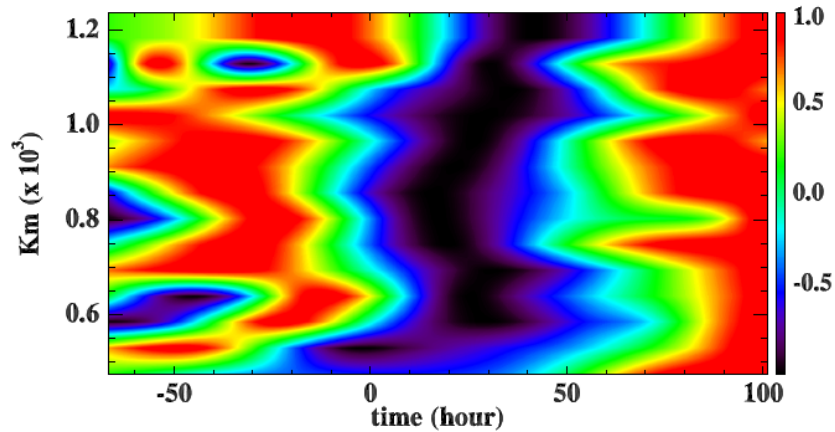


Figure 46 Contours of $S D(t)$ in the space-time plane. The x-axis reports the time counted from the Boumerd'es earthquake, while the y-axis reports the distance in km from the epicenter

9.2 The March 11, 2011, M=9.0, Tohoku-Oki earthquake (Japan)

The second data set analyzed, is related to the Mw 9.0, Tohoku-Oki earthquake of March 11, 2011, at 05:46:23 UTC. This event, occurred along the NE coast of Honshu island (Japan), and triggered a giant tsunami that was felt across the world's Oceans, including the Mediterranean Sea (Fig.47, 48). This event was one of the largest earthquakes ever occurred in the world since historical times (Ito et al., 2011). (see *annex 1 for further details*)

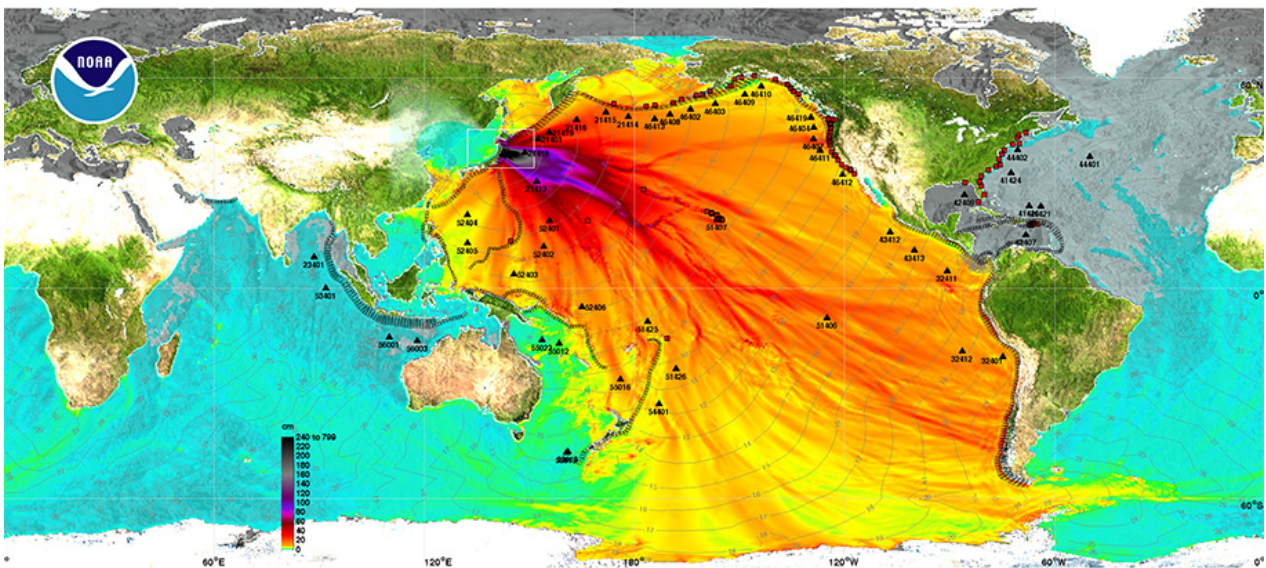


Fig.47 Tsunami propagation as predicted by global propagating models. The estimated arrival time at Gibraltar is ~38 hours after the onset of the Earthquake. (<http://nctr.pmel.noaa.gov/honshu20110311/honshu2011-globalmaxplot.png>).

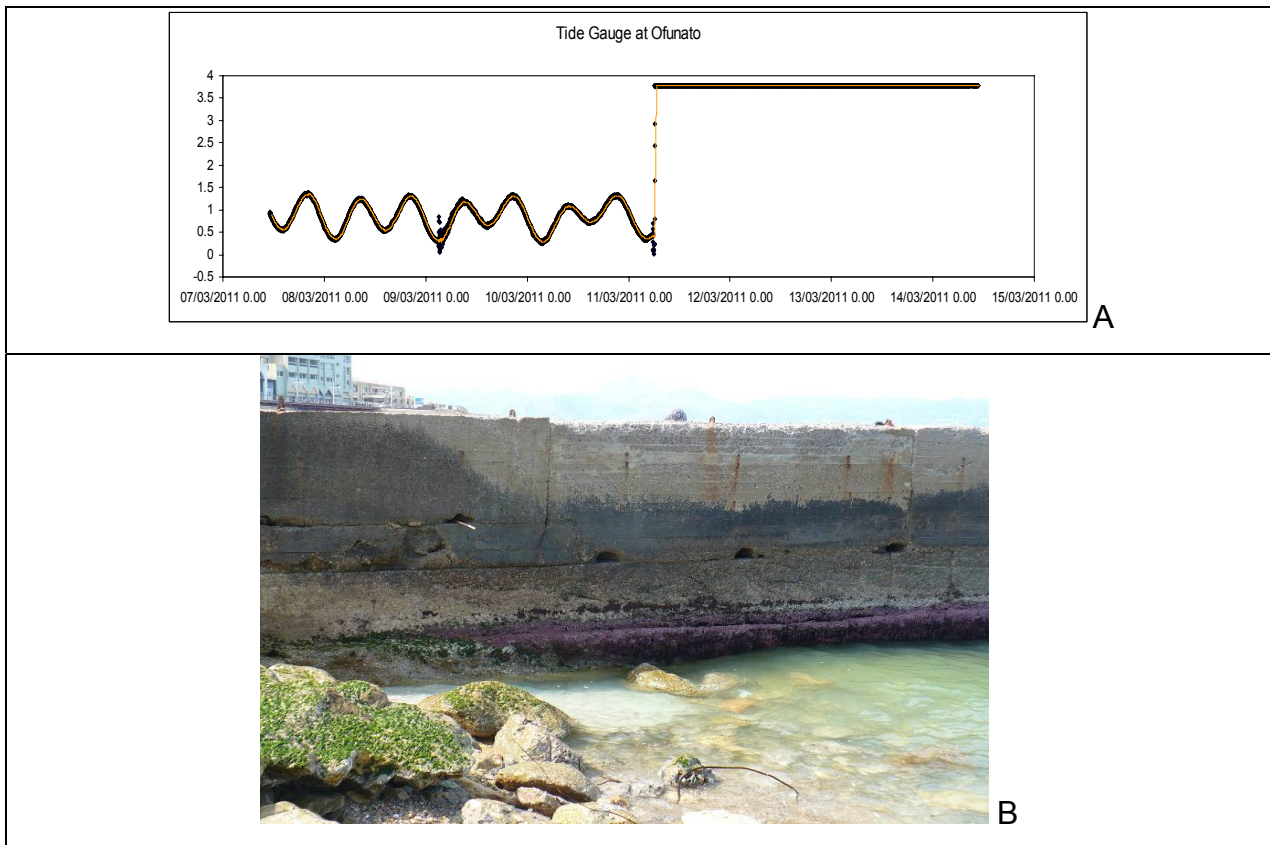


Fig.48 A) Tidal signal at Ofunato (Japan). The onset of the tsunami saturated the recordings (the large step in figure). Later the tide gauge remained flooded (flat signal) (data from <http://www.ioc-sealevelmonitoring.org/>). B) Extreme low tide observed at Iraklion (Crete) on March 13th at 11:53 local time (09:53 UTC). Photo, courtesy of C. (Babbis) Fassoulas.

During the earthquake was released the tectonic stress accumulated over the last 700 years and subsequent tsunami caused an estimated loss of 200–300 billion US dollars and killed more than 10000 people living along the coasts of Japan and elsewhere in the Pacific region. Tsunami crossed the Ocean and perturbed the Mediterranean Sea, across the narrow straits of Gibraltar.

To analyze the tidal signal, we focused on 31 sea level data in the period 9–15 March 2011, collected with a time sampling of 10 minutes and with an accuracy of better than 1 cm. Sea level data have been retrieved by internet from the IOC (www.ioc-sealevelmonitoring.org), ISPRA (www.mareografico.it) and the Permanent Service for Mean Sea Level (PSMSL, www.pol.ac.uk) (Fig. 49). During the considered time window the weather situation around the stations was favorable (calm sea, low wind velocity), thus not inducing critical conditions of the sea surface for the quality of the sea level data set. Moreover, our analysis was restricted to the tidal stations located in sheltered positions (Fig.50A and B).

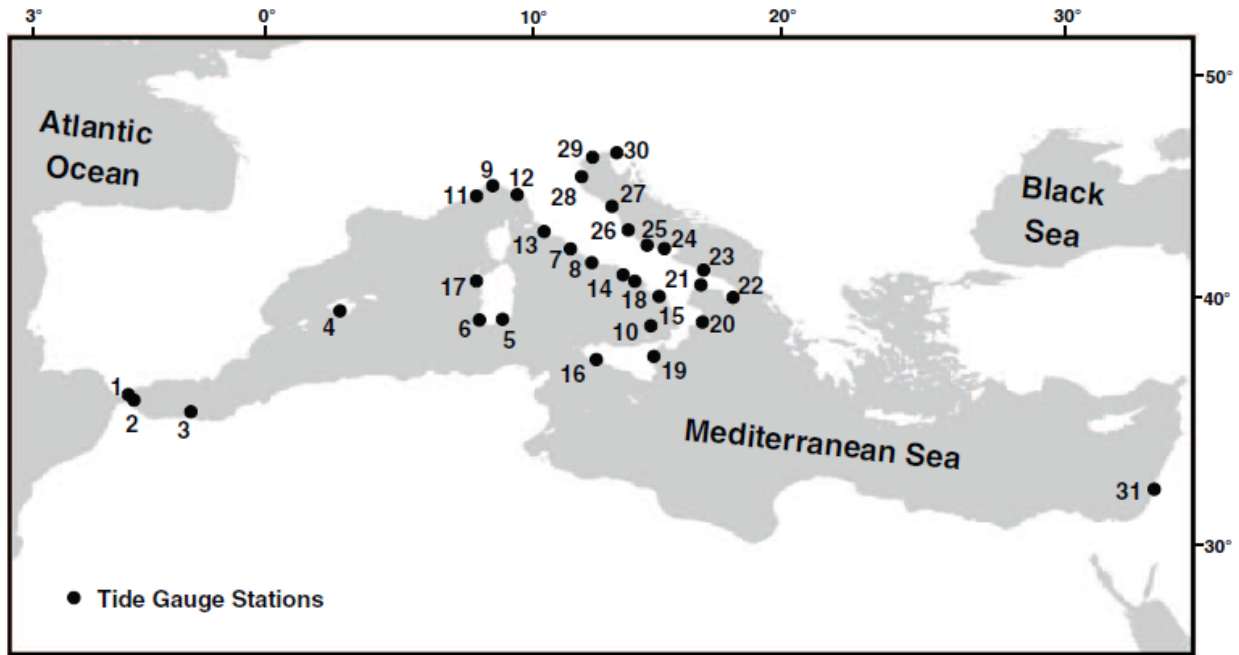


Fig. 49 Map of the tide gauge stations, in the Mediterranean, used to study the effects of the Tohoku-Oki tsunami on the Mediterranean: 1) Gibraltar, 2) Ceuta, 3) Melilla, 4) Palma de Mallorca, 5) Cagliari, 6) Carloforte, 7) Civitavecchia, 8) Gaeta, 9) Genova, 10) Ginostra, 11) Imperia, 12) La Spezia, 13) Livorno, 14) Napoli, 15) Palinuro, 16) Porto Empedocle, 17) Porto Torres, 18) Salerno, 19) Catania, 20) Crotona, 21) Taranto, 22) Otranto, 23) Bari, 24) Vieste, 25) Ortona, 26) San Benedetto, 27) Ancona, 28) Ravenna, 29) Venezia, 30) Trieste, 31) Hadera.

Sea level observations were first reduced for atmospheric pressure variations by applying an inverse barometric correction to the data (Wunsch and Stammer, 1997). Time is measured as the lag from the earthquake occurrence.

A sudden change of regime can be identified in all the signals after the earthquake. In fact, the regular tidal oscillation is broken, more frequencies appear, and the time behavior becomes more complex and highly non stationary. This kind of dynamical behavior is common to all the records we have investigated. In Fig. 51 we report the sea level time series $L(t)$ for the Cagliari station (panel (a)), along with the 12 hours return map $L(t+\Delta)$ vs. $L(t)$, for $\Delta=12$ hours (panel (b)).

The figure roughly provides evidences that after the main-shock the Mediterranean Sea felt a strong phase and amplitude perturbation of the tidal oscillation. In fact, for $t \leq 0$ (blue line), the points of the return map are approximately sorted along a straight line, indicating that the oscillation amplitude and phase remain almost constant. On the contrary for $t > 0$ (red line), the points are distributed on irregular ellipses, indicating that the phase and amplitude are no more constant but change with time.

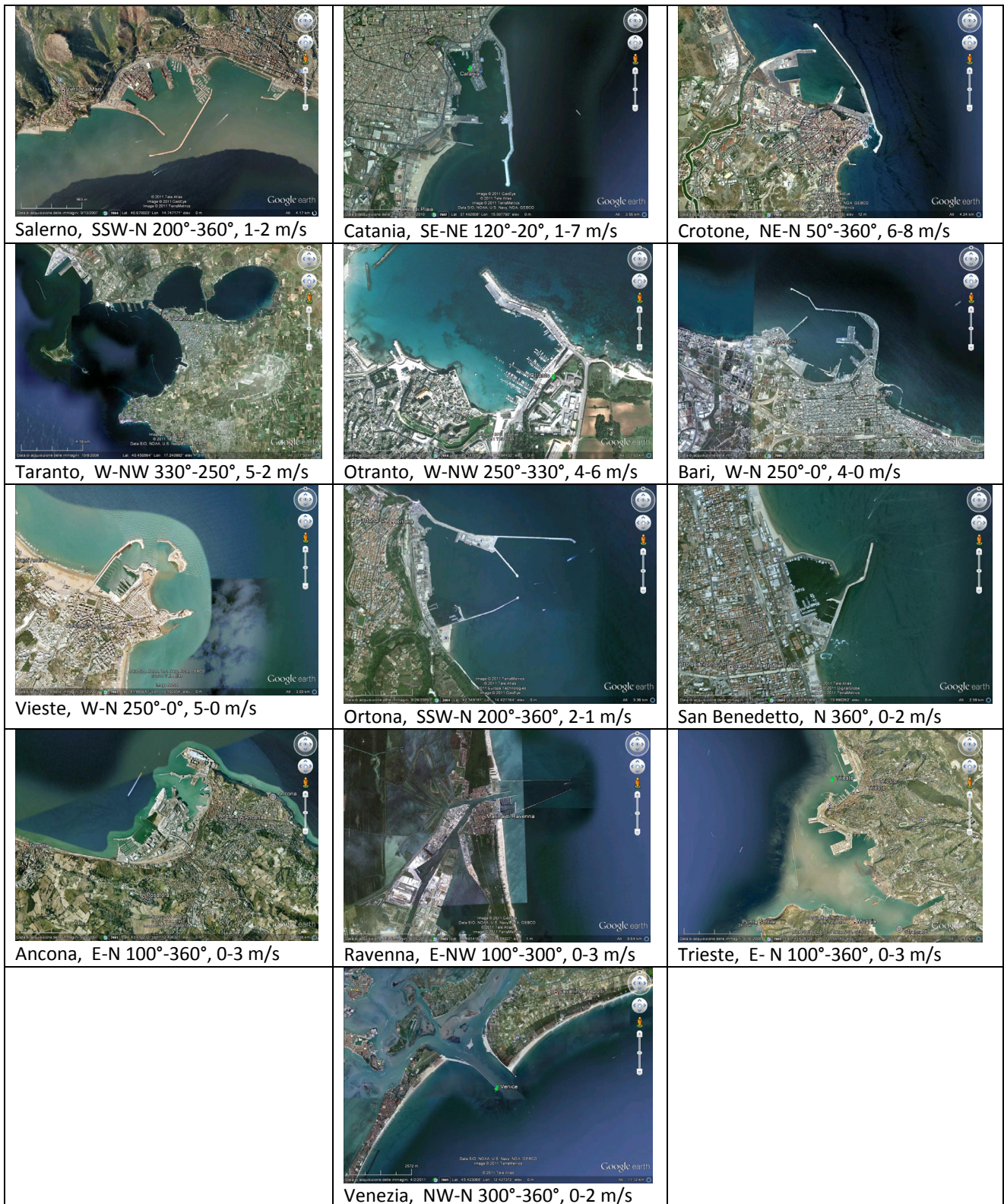


Fig.50 A) Position of the analyzed tidal stations in the Adriatic sea. Below each picture direction and wind angle direction (clockwise from North), wind velocity (min-max m/s), are shown. Values between 30 and 60 hours after the onset of the earthquake (satellite images from Google Earth).



Fig.50 B) Position of the analyzed tidal stations of the ISPRA network in the Tyrrhenian Sea. Below each picture direction and wind angle direction (clockwise from North), wind velocity (min-max m/s), are shown. Values across -30 and +60 hours since the onset of the earthquake (satellite images from Google Earth).

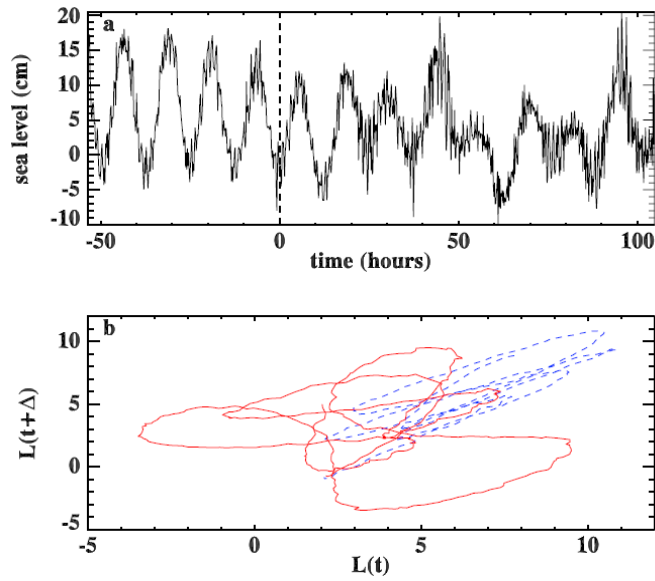


Fig. 51 Time evolution of the sea level $L(t)$ (panel (a)) and the 12 hours return map $L(t+\Delta)$ vs. $L(t)$ (panel (b)) for the Cagliari station ($\Delta=12$ hours). Time is counted from the origin time of the Tohoku-Oki earthquake. The blue dashed line refers to times $t \leq 0$, the red full line refers to times $t > 0$.

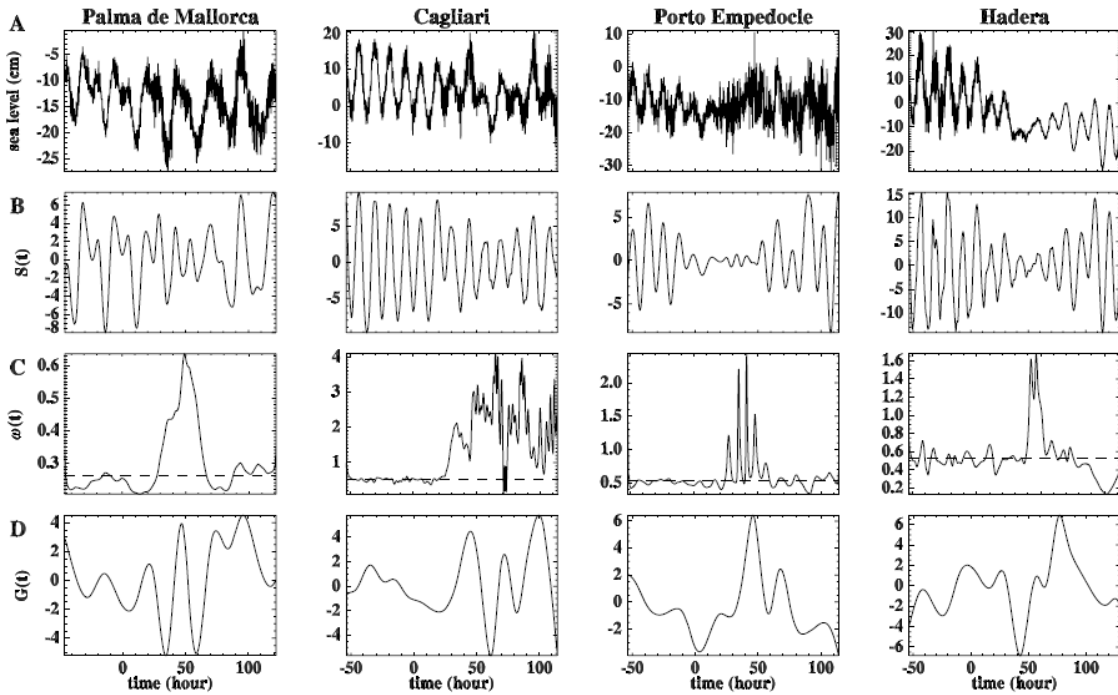


Fig. 52 Time evolution of the sea levels (line A), contribution of the high-amplitude components $S(t)$ (line B), instantaneous frequency of the highest-amplitude IMF (line C), low-frequency contribution $G(t)$ (line D) for the stations of Palma de Mallorca (4), Cagliari (5), Porto Empedocle (16) and Hadera (31). Time is counted from the origin time of the Tohoku-Oki earthquake. The dashed line corresponds to $(2\pi)/12 \text{ hour}^{-1}$ for Cagliari, Porto Empedocle and Hadera and $(2\pi)/24 \text{ hour}^{-1}$ for Palma.

When applied to the Mediterranean tide gauge data, the EMD gives a number n of modes which in general depends on the station under analysis. As obtained from the test of significance for the various IMFs (Wu and Huang, 2004), the first three modes, $j \leq 2$, represent high-frequency noise while higher- j modes are associated with significant oscillations of the sea level at different time scales. For the majority of the stations the IMF with the highest amplitude has a period of $\tau \approx 12$ hours, corresponding to the well-known semidiurnal oscillation. However, in the analyzed data sets, the full semidiurnal component of the tide is split into two or three IMFs, depending on the station. This means that one IMF does not suffice to fully describe the temporal behavior of the 12 hours tidal component. The previous result follows from the high sensitivity of the EMD to local frequency fluctuations. The latter, still persisting when meteorological effects are removed, are strong enough to affect the regularity of the semidiurnal mode of oscillation. As mentioned before, since for the properties of the EMD decomposition each IMF is associated to a well-defined time scale of the signal at hand, a regular semidiurnal oscillation should be isolated in a single IMF. In the presence of localized frequency fluctuations new time scales arise and affect the regular oscillation of the high-energy tidal components.

In this case, a single IMF is not able to account for the new time scales and the time evolution of the 12 hour oscillation is split into two or more IMFs. Of course, the sum of these EMD modes will describe the full contribution of the semidiurnal oscillation to the sea level. For Palma de Mallorca and the stations in the northern sector of the Adriatic Sea (stations 26–30), the simultaneous presence of both diurnal and semidiurnal components, as main tidal constituents, has been detected.

This is a well-known phenomenon and it should depend, in the Adriatic Sea, on the basin characteristics, i.e., the low sea depth and the semi closed shape (Janekovic and Kuzmic, (2005); Capuano et al., 2011). For these cases the previous considerations are also valid for the 24 hours component which is split into two IMF. By exploiting the orthogonality of the EMD decomposition, the signal $L(t)$ has been divided, by partial sum in eq. (1), into four contributions namely $L(t) = \hat{\eta}(t) + S(t) + G(t) + rn(t)$. The function $\hat{\eta}(t)$ is associated with the high frequency noise, $S(t)$, obtained as the sum of the high amplitude components (semidiurnal and for some station also diurnal), represents the basic tidal mode and $G(t)$ describes the remaining low-frequency contribution. An example of the time behavior of $S(t)$ is reported in row B of Fig. 52. Its dynamics is far from being regular and stationary since the waveforms abruptly change after $t=0$. The variation of the main tidal contribution can be better appreciated by looking at the instantaneous frequency of the highest-amplitude IMF (row C of Fig. 52) which is abruptly destabilized in correspondence of the change of the oscillating regime in $S(t)$ and departs from the constant value of $(2\pi)/12$ hour⁻¹. Note that for Palma de Mallorca the reference frequency is $(2\pi)/24$ hour⁻¹ since, in this case, the highest-amplitude mode is associated with the diurnal component. EMD modes with longer periods describe low-frequency phenomena. The function $G(t)$, an example is reported in row D of Fig. 52, is characterized by the increase of amplitude after $t = 0$. Figure 53 shows the contour plot of the functions $G(t)$, ordered according to the distance from Gibraltar. The figure clearly indicates that the time at which the increased amplitude regime is at its maximum absolute value is a function of the distance from the Strait of Gibraltar. This result is consistent with a traveling perturbation in the whole Mediterranean Sea propagating from Gibraltar. The Adriatic stations, for the sake of clarity, have been excluded. For these stations, due to the Adriatic basin geographic characteristics, the time-distance relation is inverted. In fact, the northernmost Adriatic stations are nearer to Gibraltar but the perturbation has to cover a longer path before

reaching them. As shown in Figure 52 the majority of stations shows a peak after $t = 0$, which indicates a positive fluctuation of the sea level. On the other hand, some records, including Hadera and the stations in the Ionian Sea, are characterized by a drop (in blue) followed by the transient increase of the sea level. This behavior can be induced by the local seafloor topography and/or by the different paths taken by the tsunami waves and reflection effects (Joseph A. et al., 2006).

The space-time representation allows estimating the velocity of propagation of the perturbation, in the Mediterranean Sea, to be about $V_p \approx 60$ m/s. Note that, this perturbation is revealed in the whole Mediterranean Sea, being observed up to Hadera, the easternmost station, about 13 hours after Gibraltar. We hypothesize that both the indirect perturbation of the tidal frequency and the direct transfer of small fluctuations beyond the Strait of Gibraltar, are generated from the tsunami triggered by the March 11th 2011, Tohoku-Oki earthquake.

We remark that the timing of both these effects, varying between ~ 45 hours in Gibraltar and ~ 58 hours in Hadera, are in agreement with the results of theoretical models of tsunami propagation for which the perturbation should arrive at Gibraltar in a time of about 38 hours after the earthquake. The obtained results have been tested by looking at the sea level records during the period 9–15 September 2011, in a time window which cannot be related with the Tohoku-Oki earthquake. We assume that, in this period, the possible transient effect of the tsunami is null and the system behaves according to the usual dynamics. As expected, we found that the principal tidal components show a regular behavior and are detected, by the EMD, in a single IMF.

This indicates that the splitting of the principal tidal components into more IMFs along with the instantaneous frequency destabilization could be plausibly in connection with a transient effect, associated with the tsunami.

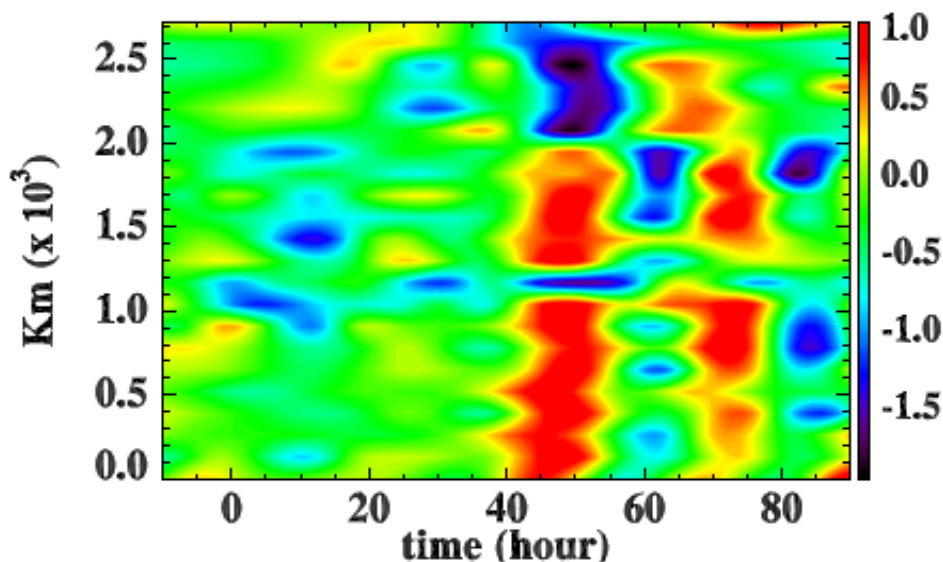


Fig. 53 Contours of $G(t)$ in the space-time plane. The x-axis reports the time counted from the Tohoku-Oki earthquake, while the y-axis reports the distance in km from Gibraltar.

Finally, our analysis shows that this basin felt the effect of the tsunami 40–50 hours after the main-shock, thus indicating that tsunamis generated by giant earthquakes can be global events. The analyses revealed two kinds of transient signatures. Firstly, the

perturbation generates strong frequency fluctuations affecting the regular behavior of the high-amplitude tidal components, usually the semidiurnal and in some cases also the diurnal one.

As a consequence of the perturbation, these components appear highly non stationary and several IMFs are needed to reproduce their full contribution. In addition the instantaneous frequency shows abrupt destabilization after the earthquake occurrence. The physical mechanism causing these manifestations should be related to a resonant response to the tsunami at the strait entrance. Tides in enclosed basins, connected to the open sea by narrow straits, can manifest amplified or damped response to a forcing action outside the basin (Maas, 1987).

Due to nonlinear effects the basin may exhibit chaotic modulation of the tidal amplitude and frequency. Since the Mediterranean Sea is a closed basin with respect to the oceans and is connected to Atlantic Ocean by the narrow strait of Gibraltar, it could be affected by the forcing action of the fluctuations associated with the tsunami and could manifest nonlinear response leading to amplification and frequency destabilization. The second signature consists in a propagating perturbation manifesting itself with a weak increase of amplitude of the low-frequency EMD modes, after the occurrence of the Tohoku-Oki earthquake. This perturbation, significant with respect to the noise level, should be an evidence of the direct transmission of tsunami fluctuations, characterized by long periods, through the Strait of Gibraltar.

The timing of the detected tidal perturbations at the recording stations is in agreement with the prediction of the global models of tsunami propagation, for which the arrival at the Strait of Gibraltar is expected about 38 hours after the onset of the earthquake. Effects on sea levels due to post-seismic deformations (Melini and Piersanti, 2006), capable to cause global sea level raise of the order of a fraction of mm (<http://cires.colorado.edu/bilham/Honshu2011/Honshu2011.html>), and direct propagation of surface seismic waves from the epicenter, arriving at the Mediterranean region 20–30 minutes after the mainshock (www.emsc-csem.org), have been excluded since they are not consistent with the observed sea level variations. Additionally, it is unlikely that free oscillations of the Earth, excited by the high-magnitude Tohoku-Oki earthquake, originated the detected fluctuations since the timing and period of the main mode of oscillation (Aki and Richards, 2002; Kanamori and Anderson, 1975), are not in agreement with the timing and frequency of the sea level perturbations revealed by our observations. However, based on the available seismological and geophysical literature (Aki and Richards, 2002), the effects of free oscillations of the Earth on the sea level have not yet been investigated and the results presented in this paper provide new observational constraints for these studies.

10. Future predictions

In this doctorate thesis, has been illustrated, discussed and analyzed the variability of sea level changes in the time scales of millennia, centuries and up to a few hours. The first can be successfully estimated from geological and archaeological indicators, the latter by tidal data records, including the analysis of transient signals related to tsunami events. The archaeological data fill the gap between the long term geological data and the modern instrumental recordings. The detection and analysis of sea level changes over these different time scales, depends from the length and completeness of the data set. Long term analysis, requires historical time series of data (~100 years), and the use of monthly or annual mean of sea level signal recorded at individual tide gauge stations, provide good information. Conversely, transient signals, such those related to tsunamis, requires high

frequency recordings for a limited time span (days), to cover as much as possible the observed short perturbations.

The analysis of tidal data from tide gauge stations, have shown that the estimated sea level trends is largely dependent from the duration of the available recordings of the analyzed station. Long records, of ~100 years of data, as those available from the tidal stations of Genova, Trieste and Marseille in the Mediterranean, are the most robust data set to estimate secular variations in this enclosed basin and are in agreement to show a mean sea level rate at 1.25 ± 0.3 mm/yr.

Records of ~70-80 years of duration, give similar results, such as at Bakar and Varna (the latter is located in the Black Sea) that measure sea level trends at 1.0 ± 0.2 and 1.5 ± 0.4 mm/yr, respectively. In general, only after ~35 years of continuous recordings, tidal stations can provide affordable data. Short recordings are affected by decadal to inter-decadal variability, preventing us to obtain stable results in the analysis of sea level trends. Thus, the need for time series longer than two-three decades is mandatory to obtain robust and realistic estimates of sea level change rates.

Therefore, the 11 years of sea level recordings from the ISPRA network (see Chapter 8.1), are still too short and their data are not representative for the long term behavior of the sea level. Anyway, they are useful to observe the current variability of the sea level and its impact along the coast. In this way, the observed mean value of ~6 mm/yr of sea level rise recorded by the ISPRA data set along the Italian coasts in the time span 2001-2011, are representative of the temporary acceleration of sea level (particularly for the positive peak occurred in 2009-2010). In addition, data show that sea level trend within a decade, is even more than three times larger than the secular trend estimated for the longest tidal records in the Mediterranean. It is worth noting that previous studies have shown that atmospheric forcing and steric signal, that are included in the recordings, may contribute with amplitudes up to ± 1 mm/yr for short recording periods (Tsimplis et al., 2011). The results shown here are in agreement with Church et al. (2004) who estimated a global rise of about 1-1.5 mm/year while for the last 50 years, this value increased up to 1.8 mm/year. Satellite measurements of the sea surface by radar altimeters determined a global average of raising oceans with a trend of 3.2 mm/yr (Cazenave and Nerem, 2004; Meyssignac and Cazenave, 2012). Results are debated and it is not still clear if this increase (compared to the average of 1.8 mm/yr of tide gauges) is due to a recent acceleration or is associated with decadal cycles (Church et al., 2010 and references therein).

It is worth noting that the rate of sea level estimated at a set of stations, for which are known the GIA and tectonic rates from independent studies, sea level is rising at rates between 0.72 and 0.97 mm/yr (dependent from the stations used in the analysis). For the long recording stations of Genova, Marseille and Trieste, where the tectonic signal is zero, we obtain a sea level at 1.0, 1.2 and 1.1, respectively.

The Intergovernmental Panel on Climate Changes (IPCC) is monitoring the results of sea level trend because sea level rise is a global environmental problem and the estimation of future trend is a crucial topic which is often associated to global warming and climate change. Therefore, the prediction of the future sea level is a debated matter that involves several disciplines of geophysics and Earth sciences.

The recent report of the IPCC in 2007, shows how the average global temperature in 2100 is expected to increase between 1.1°C and 6.4°C (in the previous IPCC 2001 report, the maximum estimates were lower and between 1.4° and 5.8°C). These values have been estimated according to the different emission scenarios that are depending on the adopted models of global socio-economic development. Furthermore, a global sea level rise is

expected in a range between +0.18 and +0.59 m, for the same period (2011 IPCC report predicted values ranging between +0.09 and +0.88 m). The continuous sea level rise is already affecting millions of people living along the worldwide coasts, especially in lowlands and subsiding areas, such as like river deltas or tectonic and volcanic zones. In the Mediterranean, we can recall the critical cases of the Venice lagoon, the Nile delta, south western Turkey and Baia (Phlegrean Fields), all affected by subsidence that dramatically increases the effects of the relative sea level rise. Additionally, many coasts will be soon endangered by marine flooding, like the Versilia plain (see annex 2 for details).

In the Mediterranean, the complex physiography and the specific climatic conditions, as well as the negative hydrogeological balance (evaporates more sea water than it comes from rivers), can help determine a sea level rise between 50% and 100% of the global rates.

Instrumental data and geological and archaeological observations that span over the past centuries are the most valuable data source for the reconstruction of the sea level history. They can be tentatively used to predict the future relative sea level trend at global, regional and local scale. In this way, we have analyzed tidal data from the two longest tidal records of the Italian network, collected in the time span 1905-2011 at the tide gauges of Trieste and Genova (they have both more than 100 years of data), with the aim to understand the secular behavior of long period frequencies of sea level trend.

For the analysis we have applied the EMD technique (see Chapter 9). Our preliminary results, shows a ~45/50 years cycle in the sea level (Fig.54).

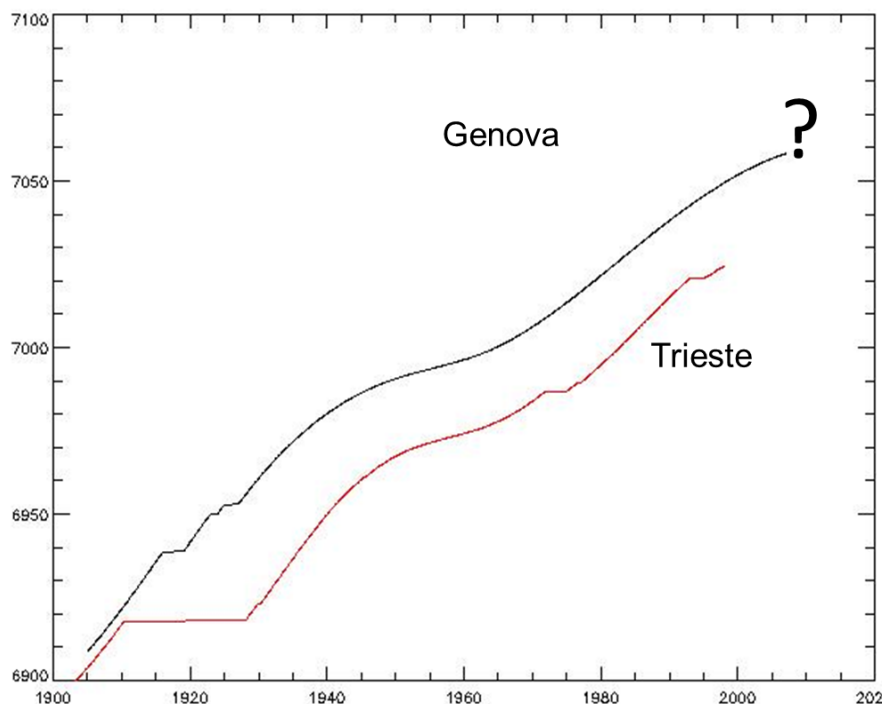


Fig. 54 Tidal analysis from historical records of the tide gauges of Trieste and Genova for the time span 1905-2011. Stations have 85 and 101 years of valid data, respectively. The analysis has shown sea level oscillations with a periodicity of 45/50 years. The sea level trend shown by the two stations, remain always increasing and based on this data an increasing sea level rise for this century can be expected. The question mark indicates the unknown rate of the future sea level trend.

Although further investigations are required, the signal can be roughly addressed to the North Atlantic Oscillation (NAO) (Weng and Neelin, 1998), which is a cyclic climatic perturbation having similar periodical trend. It is worth noting that the sea level shows a trend always positive and with periodical change in velocity. If this trend will continue with this behavior in the next future, an increasing sea level rise can be predicted during this century (the question mark at the top of the plot, aims to indicate the unknown future sea level rise trend).

Although this is just a preliminary interpretation that must be supported by additional climatic data, it is in agreement with the results from Church et al. (2010 and references therein), and the study from Lambeck et al. (2011). They predict by the end of 2100 a sea level rise up to 1 m at global scale and up to 1.53 m for the Italian region, respectively. In addition, Zecca and Chiari (2012), predict even a worst scenario by the end of 2200. When sea level rise is in combination with subsiding vertical land movements, caused by glacio-hydro-isostasy and vertical tectonics, the relative sea levels are increased (see annex 3 for details). This leads to a large uncertainty in an average quantification of the current and future trends, especially in the Mediterranean, being a tectonically active semi-enclosed basin with own hydro-geological features.

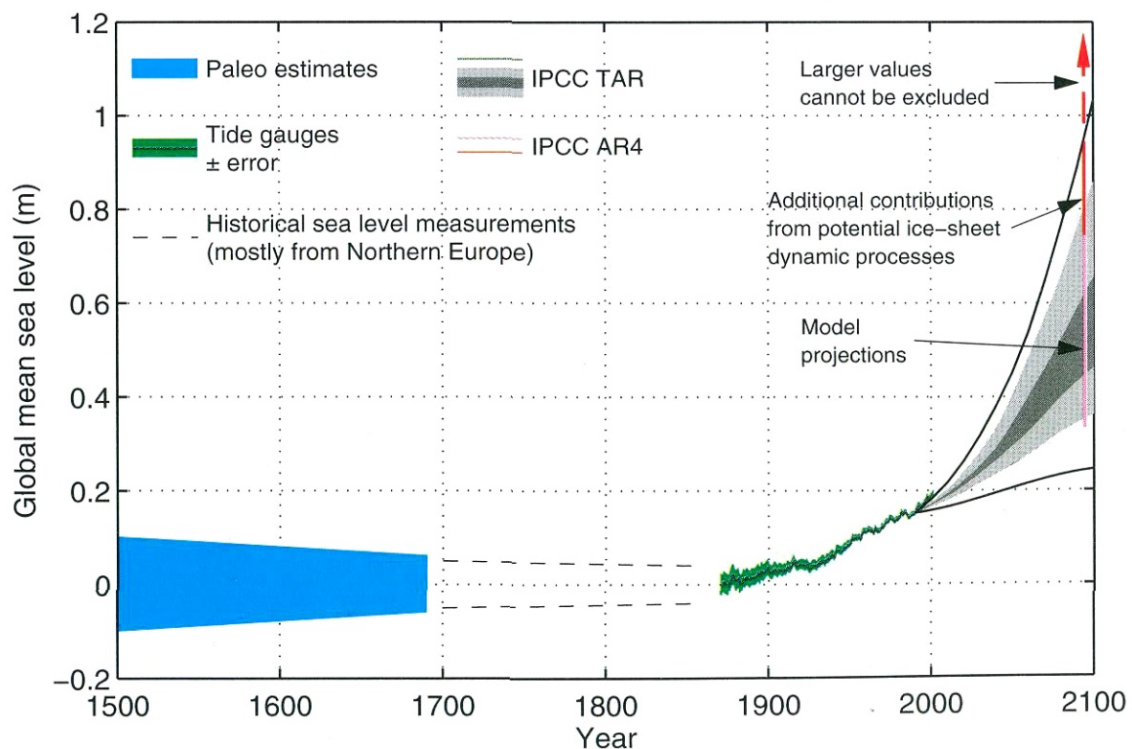


Fig. 55 Reconstruction of the history of sea level from different indicators and prediction for 2100. A global mean sea level rise up to 1 m or more is expected in the worst scenario (From Woodworth et al., 2010).

However, the scientific community, almost unanimously agree that the increase in greenhouse gases in the atmosphere are changing the climate of the planet in such a way as to trigger a rise in sea level on a global scale. We underline, that the scenarios identified by the models for the last decade have even been overtaken by recent global sea level rise at rates higher than those expected only a few years ago (Fig. 55, 56). Based on these type of indicators in combination with tidal analysis and geophysical modeling, Lambeck et al. (2004b) estimated that in the central Mediterranean the onset of the modern sea level rise occurred in recent times, at 100 ± 53 years before present with an

eustatic increase at ~13 cm (see annex 3 and reference therein for further details). Additional studies, found similar results in other parts of the Mediterranean, namely in Northern Africa, Eastern Mediterranean, Malta and northern Tyrrhenian sea (Anzidei et al., 2011a; Anzidei et al., 2011b; Furlani et al., 2012), supporting the validity of the previous results (see annex 4 and 5 for further details). In high tectonically active regions, such as Calabria, the vertical motion of the land can counterbalance the relative sea level change caused by the glacio-hydro-isostasy, even determining an about null relative sea level change along the coast (Ferranti et al., 2010; Anzidei et al., 2012), (see annex 6 for further details).

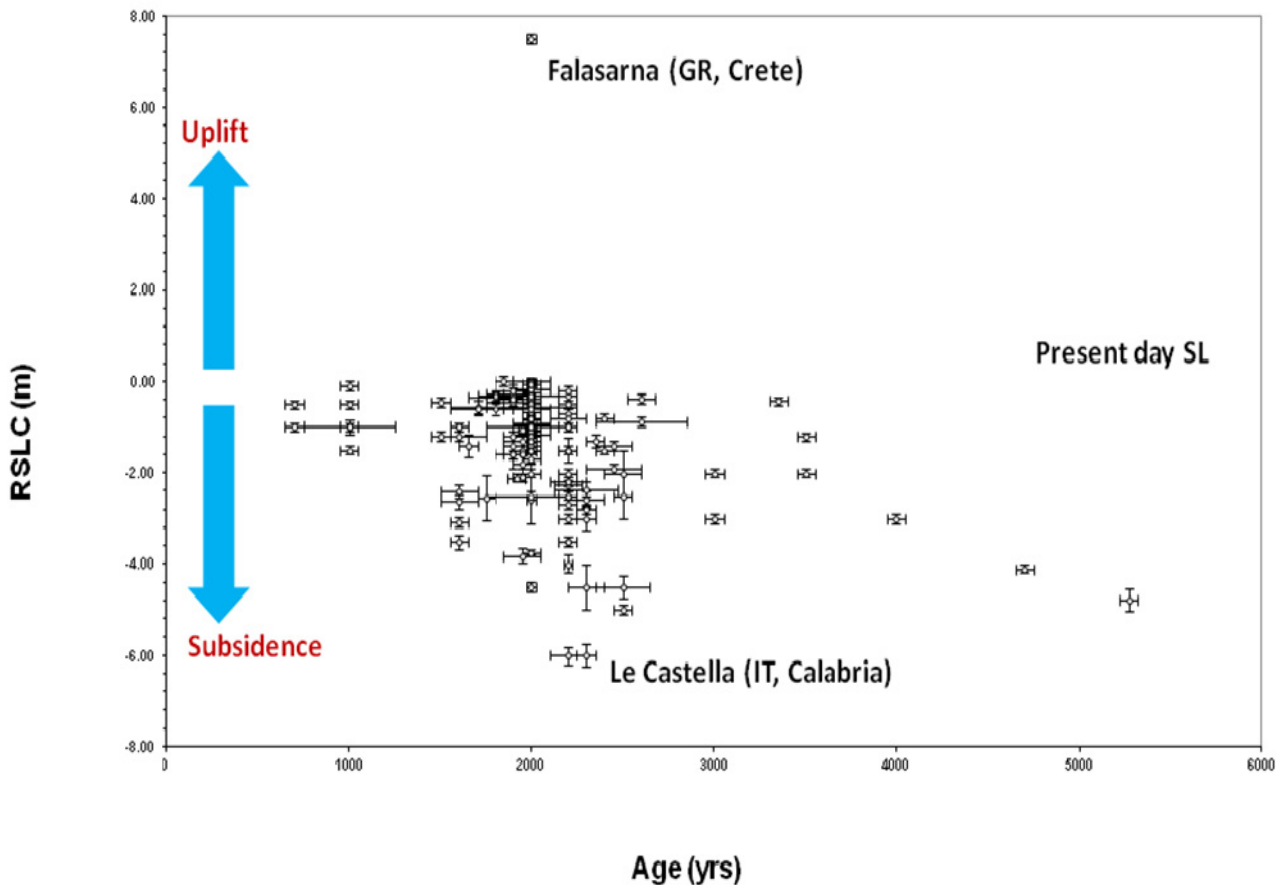


Fig. 56 This plot shows the elevation of about 160 archaeological sites in the Mediterranean. Data have been collected in previous studies and during this Doctorate. A large part of them have been investigated in this doctorate. Note the very low elevation of Le Castella area, in the Ionian sea of Calabria (top site in the plot), and the very high elevation of the roman harbor at Falasarna, displaced at 6.5 m above sea level (Crete Island, Greece) during the 365 A.D. earthquake (estimated magnitude ~8) (Pirazzoli et al., 1992; Shaw et al., 2008). Note also the deeper elevation of the archaeological sites with their increasing age due to the continuing sea level rise since the last LGM.

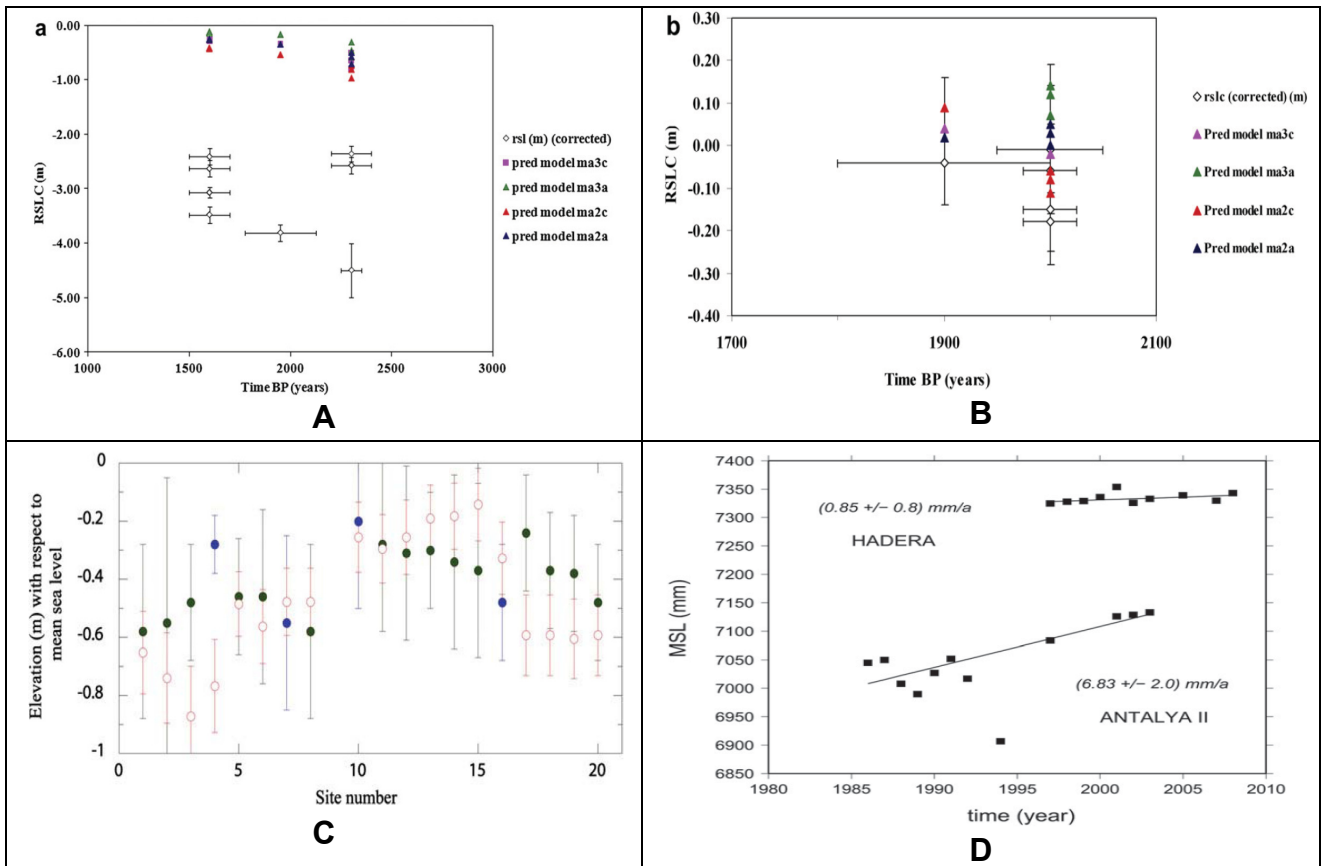


Fig.57. a) Relative sea level change along the coast of SW Turkey observed from archaeological data and from predictions based on different parameters of the glacio-hydro-isostatic model; b) relative sea level change along the coast of Israel from archaeological data and isostatic predictions based on different parameters of the glacio-hydro-isostatic model. C) Elevation (m) of the observed upper (green) and lower (blue) limits to sea level estimates from the archaeological sites compared with the predicted levels for the epoch of construction (open red circles). The predictions include the glacio-hydro isostatic contributions based on the mean of earth models discussed in the text and a contribution of recent increase in ocean volume at an equivalent sea level rate of 1.5 mm/year for the past 100 years; D) Annual mean sea level trends estimated from the tide gauges of Hadera (top) and Antalya (bottom), located along the coast of Israel and SW Turkey, respectively. Although the duration of recordings are too short at both stations (time span 1996-2003 at Hadera and 1985-2005 at Antalya) to provide a reliable secular sea level trend, their data are in agreement with the current elevation of the archaeological sea level indicators and models. Note the anomalous oscillations in Antalya compared with Hadera (valid data from the PMSLS database, www.pol.ac.uk) (from Anzidei et al., 2011a; Anzidei et al., 2011b).

In other regions of the Mediterranean, like in southwest Turkey, or along the Ionian coast of Calabria, tectonic subsidence summed to the glacio-hydro-isostatic signal, is dramatically changing the coastline since the last 2.3 ka BP (Fig. 57, 58) (see annex 4 for details).

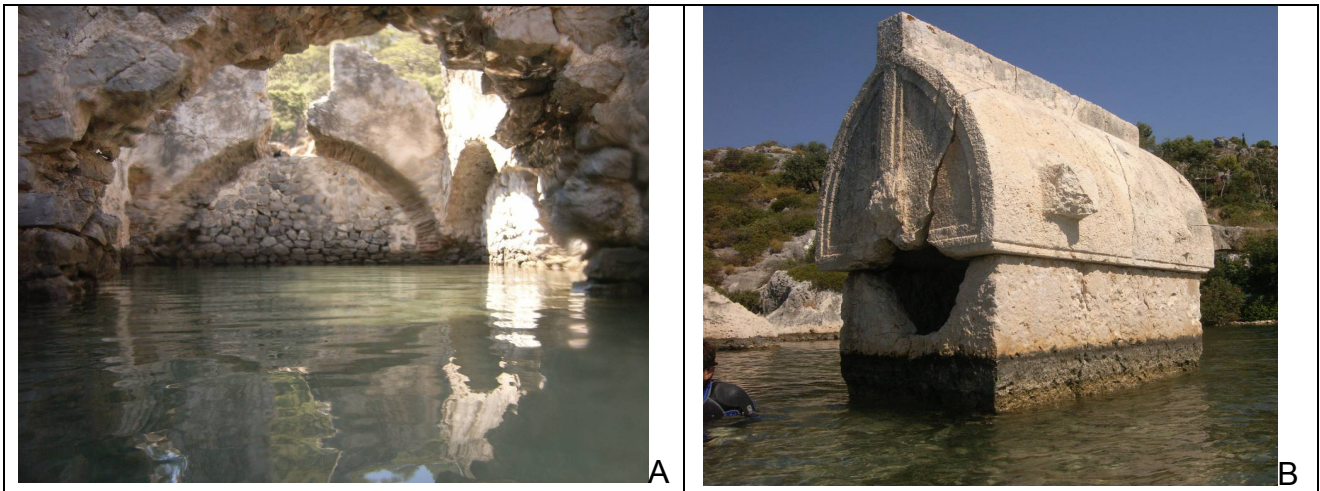


Fig.58 The archaeological evidence of the dramatic relative sea level rise in Turkey. A) Submerged byzantine age building at Domuz Island and (b) Lycian age tombs at Kekova (from Anzidei et al., 2011b).

Researches carried out during recent years, have shown that most of the coastal areas of the world (80% of all existing beaches) is undergoing to erosion (Fig.59). This phenomenon is also a consequence of the ongoing sea level rise, land subsidence and anthropogenic contributions (destruction of dune systems, sand exploitation from rivers, maritime constructions, etc.).



Fig. 59 Example of adaptation to coastal erosion.

The consequences of sea level acceleration on ecosystems and coastal populations are critical: the increase of 1 cm of water roughly correspond to the retreat of the shoreline up to 1 meter, therefore the lower estimate of a sea level rise of 0.5 m will have large social and economic impacts along many coasts of the Earth. To understand the importance of the problem, we recall that in the Mediterranean and particularly along 7500 km of coasts of Italy, 47% of these are steep rocky coasts, while 53% are beaches and ~42% of the latter are currently in erosion (Fig.61).

The IPCC suggests the world governments to undertake appropriate adaptation policies to reduce the impact of future changes in sea level even in relation with the intensification of extreme events, such as those caused by the hurricane Katrina in 2005. The Mediterranean coasts, and particular in Italy are at risk of sea flooding due to: 1) geological features; 2) coastal settlements placed very close to the shorelines; 3) still active isostatic movements; 4) vertical land movements triggered by tectonics and volcanism; 5) natural and anthropogenic subsidence. The sum of these causes will amplify relative sea level changes and subsequent flooding along low elevated coastal areas, particularly those that are already today under the sea level (Gornitz et al., 2002).

Lambeck et al (2011) estimated the projections of the sea level change in Italy for 2100, using published and new sea level data and by adding isostatic and tectonic component to the IPCC and Rahmstorf projections. Comparison of the observations from more than 130 sites (with different geomorphological and archaeological sea level indicators), against the predicted sea level curves, provided estimates of the vertical tectonic contribution to the relative sea level change (see annex 2). The results are based on glacio-hydro-isostatic models developed at the Australian National University. On the basis of the eustatic, tectonic and isostatic components to the sea level change, projections provided the scenarios of marine inundations valid for 33 Italian low elevated coastal plains for the year 2100.

The ice model used for the predictions is described in Lambeck et al. (2006, 2009, 2010) (model K33_j1b_WS9_6). It includes the major ice sheets back to the penultimate interglacial as well as an alpine deglaciation model. No changes in ocean volume occur in this model for the past few centuries. Rheological parameters have been adopted from previous work for the same region (Lambeck et al., 2004a, b) and correspond to the three-layer model with an effective elastic lithospheric thickness of 65 km, an upper mantle viscosity of 3×10^{20} Pa s and a lower mantle viscosity of 3×10^{22} Pa s.

These predictions are for the isostatic-eustatic components from the last glacial cycle only and their variability from site to site reflects both an approximately north-south component from the increasing distance from the former northern ice sheets and a more variable component from the water-loading contribution (Lambeck and Purcell, 2005).

The result of this ongoing response to the past deglaciations causes a variable sea level rise at rates of up to 0.6 mm/year, along the Italian coasts. This is an estimated average for the past 100 years and is representative for future change out to at least 2100 (Fig. 3).

To provide different possible scenarios for the Italian coastal plains in the year 2100, were considered global estimates for the “low-impact” B1 projection of the IPCC (2007) (the lower sea level rise scenario), and the maximum value in Rahmstorf (2007) (higher scenario) (Table 5).

The B1 IPCC (2007) projection includes thermal ocean expansion and glacier and ice sheet melting in a scenario where carbon dioxide will rise to double the pre-industrial concentration by 2100 (Mote et al., 2008). Rahmstorf (2007), by considering that global temperature and sea level rise variations are strongly correlated, applied a linear model for the 21st century that leads to considerably higher projections than those of the IPCC.

The rates for these two different projection scenarios are then combined with local isostatic tectonic values, to delineate zones of the Italian coast that will undergo to marine inundation under the different scenarios by the year 2100. These projections do not include extreme events, or changes in the patterns of such events or in local changes in tidal range. The Digital Elevation Model (DEM) for the near-shore low-lands of Italy, produced by the National Geologic Survey and National Research Council from the Military Geographic Institute's elevation data, was used.

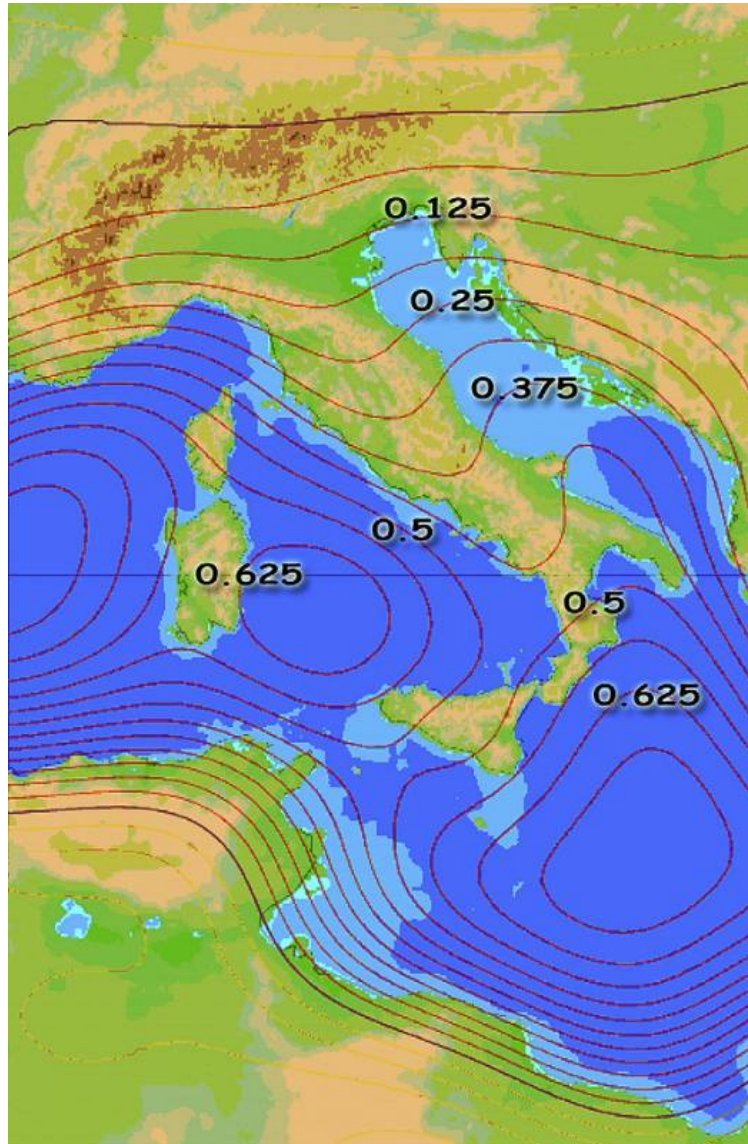


Fig. 60 Predicted present-day isostatic rates for Italy (in mm/yr). This signal corresponds to a relative sea level rise with spatially variable rate, differing by 0.5 mm/yr between the northern Adriatic coast and Sardinia. Red contours denote negative values, orange contours denote positive values, dark red contour correspond to zero change. (From Lambeck et al., 2011).

Scenario	Annual SLR rate (mm/yr)	SLR yr 2100 AD (mm)
IPCC, 2007-B1	1.8-2.8	180-280
Rahmstorf, 2007	5-14	500-1400

Table 5 Expected lower and higher sea level rise scenarios for global effects in the year 2100 (From Lambeck et al., 2011), (see Annex 2 for details).

Because of the relative low resolution (cell size 250 m) this DEM model is useful only for identifying regional trends rather than providing high-resolution detailed projections. In this way have been identified 33 coastal plains that will be susceptible to marine inundation by 2010 under these projections. For some of the most important coastal plains, higher resolution DEM (with cell size 60 m, 40 m, 20 m, 3 m) based on different sources (satellite data, aerial photogrammetric and topographic surveys) were used. Comparison with the

coarser DEM model results confirms the results based on the lower resolution data even if in most cases this leads to an overestimation of the extent of some of the susceptible areas.

This model is calibrated for the central Mediterranean region based on the evidence from sites of long-term tectonic stability, by the elevation of the MIS 5.5 shoreline, and then used to predict sea levels for other locations. Such predictions have been estimated for some 40 representative sites along the Italian coast. Differences between observed and predicted changes can then be interpreted as reflecting vertical tectonic contributions representative of the latter part of the Holocene. Vertical tectonic movements of the Italian coast were estimated at more than 456 sites (211 for the Holocene and 255 from the Last Interglacial. See annex 2 for details). Assuming minimum (180 mm, IPCC, 2007) and maximum (1400 mm, Rahmstorf, 2007) eustatic sea level rise projections, the total projections for sea level by 2100 were calculated, and the coastal zones that are susceptible to marine inundation identified.

The principal result is that for the low-rise IPCC prediction the tectonic and isostatic components produce an important impact with values between 162 and 315 mm whereas for the maximum rise of Rahmstorf, it is the climate change induced signal that dominates (1400 and 1535 mm).

Based on these results, the most prone areas at flooding are located in the north Adriatic Sea, along the coast of Metaponto in the Ionian Sea and several lowlands of the northern Tyrrhenian coast, being placed at low elevations. The amount of coastal land surface that will be likely flooded in the next 100 years is approximately 4500 km². Anyway, these numbers do not consider the unknown effects related to ground subsidence for fluid exploitation that will accelerate flooding.



Fig. 61 Example of accelerated erosion along the Tyrrhenian coast of Latium. Note the buildings too near the shoreline.



Fig. 62 Relative sea level rise (year 2100) for 33 Italian coastal plains. For the Po Delta and Venice Plain, mean values are reported. Data do not include the contribution of local compaction and fluid (gas and water) extraction (From Lambeck et al., 2011). (see annex 2 for details).

Although the values reported in the map of Fig. 62 require further improvements (i.e. new estimates of the current vertical movements from GPS measurements and the extensively use of very high resolution DTMs) (Scicchitano et al., 2012), they are useful to decision makers to plan eventual adaptations and planning new detailed surveys to monitor coastal changes and protect lands against the sea level rise. In addition, the 33 Italian coastal plains are valuable natural areas with locations of important production activities (Aucelli et al., 2006). The expected increase in the frequency and intensity of extreme events (floods, storms, etc..) along these coasts will cause a fast acceleration of sea level rise with subsequent erosion that will lead to loss of land, affecting infrastructures and economic assets.

11. Concluding remarks

On the basis of the current scientific literature and on the result obtained in this doctorate thesis, we can conclude that global sea level has changed continuously in the past and will continue to do so even in the future. Since the last LGM, sea level has risen of ~130 m and the current global estimates give a continuous rising at 3.2 mm/yr. Based on tidal records, in the Mediterranean we obtained an average value of sea level rise at 1.77 mm/yr and 1.2 mm/yr when using a set of very long records that span over three centuries. These rates include the current GIA and the vertical tectonic signals estimated from the MIS 5.5 elevation.

When reduced for local tectonics movements and GIA rates (that varies between 0.12 and 0.62 mm/yr depending of the location), sea level trend shows an average value at 0.84 mm/yr. Anyway, we feel to stress that the tectonic correction based on the long term data, cannot be always representative of the current rates of the vertical motion, thus inducing us to be prudent with the interpretations. In this way, the archaeological observations are extremely useful, particularly for those sites located in tectonically stable areas. They fill a gap between the geological past of the MIS 5.5 and the modern instrumental data and provide data on the vertical tectonic rate of an area. Additionally, from the sea level curve predictions, the current elevation of coastal archaeological structures located in tectonically stable areas and modern tidal data, were identified ~13-15 cm of eustatic change, in agreement with previous studies of Lambeck et al. (2004). This result reinforces the hypothesis of a recent acceleration in sea level in the last 100±50 years. This timing coincides with the beginning of the industrial age, thus supporting the interpretations of the anthropogenic contribution to the observed global change, in agreement with part of the international scientific community.

Besides the long term changes, transient signals caused by regional or global tsunami can be successfully analyzed by EMD technique, when high frequency tidal data are available. In the case of the M=9.0 Tohku-Oki earthquake of March 11, 2011, we estimated an increasing tidal amplitude of about 15 cm in the Mediterranean.

Finally, the future trends projected for 2100 for the Italian region, indicate that sea level will rise up to +1.53 m, in conjunction with increasing global temperatures and tectonic subsidence. This value is larger from the global average of ~1 m, because the Italian region is a tectonically active zone and subsiding processes accelerate the relative sea level rates along the coasts, thus causing coastal erosion and social and economical impacts. Therefore, new coastal structures must be planned taking into account that shorelines will change from place to place in the near future and the decision makers should act on the basis of the future sea level predictions. In this way, we will then turn from emergency to prevention, reducing the impact on productive activities and the environment.

References

- ADEM J. (1989) – *On the effect of the orbital variation on the climates from 4000 yr ago to present*. *Annales geophysicae*, 7, 599-606.
- Altamimi, Z., Collilieux, X., Legrand, J., Garayt, B., Boucher, C., (2007). ITRF2005: a new release of the International Terrestrial Reference Frame based on time series of station positions and earth orientation parameters. *Journal of Geophysical Research* 112, B09401. doi:10.1029/2007JB004949
- AMOROSI A., COLALONGO M.L., FIORINI F., FUSCO F., PASINI G., VAIANI S.C. & SARTI G. (2004) *Palaeogeographic and palaeoclimatic evolution of the Po Plain from 150-ky core records*. *Global and Planetary Change*, 40, 55-78.
- Antonoli, F., Chemello, R., Improta, S., Riggio, S. (1999). The *Dendropoma* (Mollusca Gastropoda, Vermetidae) intertidal reef formations and their paleoclimatological use. *Marine Geology* 161, 155-170
- Antonoli F., Ferranti L. and Lo Schiavo F. (1996) The submerged Neolithic burials of the Grotta Verde at Capo Caccia (Sardinia, Italy) implication for the Holocene sea-level rise. *Memorie Descrittive del Servizio Geologico Nazionale* 52, 329–36.
- ANTONIOLI F., BARONI C., CAMUFFO D., CARRARA C., CREMASCHI M., FRISIA S., GIRAUDI C., IMPROTA S., MAGRI D., MARGOTTINI C., OROMBELLI G., SILENZI S. (2000). *Le fluttuazioni del clima nel corso dell'Olocene*, *Il Quaternario*, Italian Journal of Quaternary Sciences 13, 1, 2000, 95-128.
- ANTONIOLI F., BARD E., SILENZI S., POTTER E. K., IMPROTA S. (2004). *215 KYR history of sea level based on submerged speleothems*. *Global and Planetary Change*, 43, 57-68.
- ANTONIOLI F., ANZIDEI M., AURIEMMA R., GADDI D., FURLANI S., LAMBECK K., ORRÙ P., SOLINAS E., GASPARI, A., KARINJA, S., KOVAČIĆ V., SURACE L. (2007). *Sea level change during Holocene from Sardinia and northeastern Adriatic from archaeological and geomorphological data*. *Quat. Sci. Rev.* 26, 2463-2486.
- ANTONIOLI F, S. SILENZI (2007). *Variazioni relative del livello del mare e vulnerabilità delle pianure costiere italiane*. *Quaderni della società geologica italiana*. 29 pp.
- Anzidei M., Esposito A., Antonoli F., Benini A., Tertulliani A. and Del Grande C. (2006) I movimenti verticali nell'area di Briatico: evidenze da indicatori archeologici marittimi nell'area del terremoto del 1905. In: *8 settembre 1905, terremoto in Calabria* (Guerra I. and Bavaglio A., eds), pp. 301–21. Università della Calabria, Regione Calabria.
- Anzidei M., Antonoli F., Benini A., Gervasi A., I.Guerra (2012). Evidence of vertical tectonic uplift at Briatico (Calabria, Italy) inferred from Roman age maritime archaeological indicators. doi:10.1016/j.quaint.2012.01.019
- Anzidei M., F. Antonoli, K. Lambeck, A. Benini, M. Soussi (2011a). New insights on the relative sea level change during Holocene along the coasts of Tunisia and western Libya from archaeological and geomorphological markers. *Quaternary International*. DOI: 10.1016/j.quaint.2010.03.01
- Anzidei M., F. Antonoli, A. Benini, K. Lambeck, D. Sivan, E. Serpelloni, P. Stocchi (2011b). Sea level change and vertical land movements since the last two millennia along the coasts of southwestern Turkey and Israel. *Quaternary International*. doi:10.1016/j.quaint.2010.05.005
- Aki K. and Richards P. G., (2002). *Quantitative Seismology*, 2nd edition (University Science Books) 2002.
- AUCELLI P.P.C., AMINTI P.L., AMORE C., ARTOM C., BELLOTTI P., BOZZANO A., CAPUTO C., CASTELLINI G., CIPRIANI L.E., COCCO E., CORRADI N., D'ALESSANDRO L., DAMIANI L., DAVOLI L., DE PIPPO T., DEVOTI S., DI GREGORIO F., EVANGELISTA S., FERRARI M., FERRI S., FIERRO G., FONTOLAN G., GINESU S., GIUFFRIDA E., IANNANTUONO E., IULIANO S., LA MONICA G.B., LANDINI B., MASCIOLI F., NESCI O., PALMENTOLA G., PRANZINI E., PUGLIESE F., RANDAZZO G., RAFFI R.,

- ROSSKOPF C.M., SALVATORE M.C., SILENZI S., SIMEONI U., VELTRI P. (2006) - *Lo stato dei litorali italiani*. Gruppo Nazionale per la Ricerca sull'Ambiente Costiero. Studi Costieri, 10, 5-112.
- Auriemma R., Solinas E. (2009). Archaeological remains as sea level change markers: a review. *Quat. Int.* 206, 134-146
- BARD E., HAMELIN B., ARNOLD M., MONTAGGIONI L.F., CABIOCH G., FAURE G., ROUGERIE F. (1996) *Deglacial sea-level record from Tahiti corals and the timing of global meltwater discharge*. *Nature* 382, 241–244.
- BERGER A. (1978) - *Long-term variations of caloric insolation resulting from the Earth's orbital elements*. *Quaternary Research*, 9, 139-167.
- BERGER A. (1988) - *Milankovitch theory and climate*. *Reviews of Geophysics*, 26, 624-657.
- BERGER A., LOUTRE M.F., LASKAR J. (1992) - *Stability of the astronomical frequencies over the Earth's history for paleoclimate studies*. *Science*, 255, 560-566.
- Bianca, M., Catalano, S., De Guidi, G., Gueli, A.M., Monaco, C., Ristuccia, G.M., Stella, G., Tortorici, G., Tortorici, L., Troja, S.O. (2011). Luminescence chronology of Pleistocene marine terraces of Capo Vaticano peninsula (Calabria, southern Italy). *Quaternary International* 232, 114-121.
- Blackman D.J. (1973) Evidence of sea level change in ancient harbours and coastal installations. *Marine Archaeology, Colston Papers* 23, 114–17.
- Blewitt G., Altamimi Z., Davis J., Gross R., Kuo C., Lemoine F.G., Moore A.W., Neilan R.E., Plag H.P., Rotacher M., Shum C.K., Sideris M.G., Schone T., Tregoning P., Zerbini S. (2010). Geodetic observations and global reference frame contributions to understanding sea level rise and variability. In: *Understanding sea level rise and variability*, Eds. P.L. Woodworth, T.Aarup, W.S. Wilson. Blackwell Pub., 256-284
- BONSIGNORE F. & VICARI L. (2000) – *La subsidenza nella Pianura emiliano-romagnola: criticità ed iniziative in atto. Regione Emilia-Romagna, Atti del Convegno “Le Pianure: Conoscenza e Salvaguardia. Il contributo delle scienze della terra”, 8/10 Novembre 1999. pp. 119-121.*
- BORDONI P. & VALENSISE G. (1998) – *Deformation of 125 ka marine terrace in Italy: tectonics implications*. In. Vita-Finzi, eds., *Coastal Tectonic*, Geol. Soc. Spec. Publ., 46: 71-110.
- Braitenberg, C., Mariani, P., Tunini, L., Grillo, B., Nagy, I. (2011). Vertical crustal motions from differential tide gauge observations and satellite altimetry in southern Italy. *Journal of Geodynamics* 51, 233-244.
- Bruckner H., Mullenhoff, M., van der Borg, K., and Vott, A. (2004), Holocene coastal evolution of western Anatolia—the interplay between natural factors and human impact, in *Human Records of Recent Geological Evolution in the Mediterranean Basin—Historical and Archaeological Evidence*. CIESM Workshop Monograph 24: 51–6.
- Bruun, P. (1962) Sea level rise as a cause of shore erosion, *Proc. Am. Soc. Civ. Eng., J. Waterways and Harbors Division*, 88, 117-130.
- Capparelli V. et al. (2011). Long-range persistence of temperature records induced by long-term climatic phenomena. *Phys. Rev. E*, 84, 046103
- Capuano P. et al., *Prog. Oceanogr.*, 91 (2011) 447.
- Caputo M., L. Pieri, Eustatic variation in the last 2000 years in the Mediterranean, *J. Geophys. Res.* 81 (1976) 5787– 5790.
- CARMINATI E., & MARTINELLI G. (2002) - *Subsidence rates in the Po Plain, northern Italy: the relative impact of natural and anthropogenic causation*. *Engineering Geology*, 66, 241–255.

- CARMINATI E., DOGLIONI C., SCROCCA D. (2003) - *Apennines subduction-related subsidence of Venice*. *Geophys. Res. Lett.* 30, 13, 1717, doi:10.1029/2003GL017001.
- CARMINATI E., MARTINELLI G., SEVERI P. (2003) - *Influence of glacial cycles and tectonics on natural subsidence in the Po Plain (Northern Italy): Insights from 14C ages*. *Geochemistry, Geophysics, Geosystem*, 4, Number 101082, doi:10.1029/2002GC000481.
- Carobene, L. and Dai Pra, G. (2003), Middle and Upper Pleistocene sea-level highstands along the Tyrrhenian coast of Basilicata (southern Italy). *Il Quaternario* 4: 173–202.
- CAZENAVE, A. & NEREM R.S. (2004) - *Present-day sea level change: observations and causes*. *Reviews of Geophysics*, 42(3), RG3001, doi:10.1029/2003RG000139.
- Church J.A., Gregory J.M, Huybrechts P., Kuhn M., Lambeck K., Nhuan M.T. et al. (2001) Changes in Sea Level. In: *Climate Change 2001: The Scientific Basis*. Contribution of Working Group 1 to the Third Assessment Report of the Intergovernmental Panel on Climate Change (Houghton J.T., Ding Y., Griggs D.J., Noguer M., van der Linden P.J., Dai X. et al., eds), pp. 639–94. Cambridge University Press, Cambridge.
- CHURCH, J.A. WHITE N.J., COLEMAN R., LAMBECK, K. MITROVICA J.X (2004) - *Estimates of the regional distribution of sea-level rise over the 1950 to 2000 period*. *J. Climate* 17, 2609–2625.
- Church J.A., Woodworth P. L., Aarup T. and Wilson W. S., *Understanding Sea Level Rise and Variability*. (2010). Blackwell Publishing, 428 pages.
- Clauzon, G., Suc, J.-P., Gautier, F., Berger, A., and Loutre, M.- F. (1996), Alternative interpretation of the Messinian salinity crisis: controversy resolved? *Geology* 24: 363–6
- Clottes J., Courtin J., Collina-Girard J., Arnold M. and Valladas H. (1997) News from Cosquer Cave: climatic studies recording, sampling, dates. *Antiquity* 71, 321–6.
- Columella, *De Re Rustica*, XVII
- CROLL J. (1875) - *Climate and Time*. Eds. Appleton and Co., New York.
- CROWLEY T. & KIM K. (1994) - *Milankovitch Forcing of the Last Interglacial Sea Level*. *Science*, 265, 1566–1567
- D'Agostino Nicola, Elisabetta D'Anastasio, Anna Gervasi, Ignazio Guerra, Mladem R. Nedimovic, Leonardo Seeber and Michael Steckler (2011). Forearc extension and slow rollback of the Calabrian Arc from GPS measurements. *Geoph. Res. Lett.*, Vol. 38, L17304, doi:10.1029/2011GL048270
- Daly C., Sea-level exacerbates coastal erosion (2004). *Physics Today*, 57, <http://www.aip.org/pt/iss-2/p24.html>
- De Martini P.M. et al., (2010). A 4000 yrs long record of tsunami deposits along the coast of the Augusta Bay (eastern Sicily, Italy): paleoseismological implications. *Mar. Geol.*, 276, 42-57, doi: 10.1016/j.margeo.2010.07.005
- DOGLIONI C. (1994) - *Foredeeps versus subduction zones*. *Geology*, 22, 3, 271-274.
- Douglas B. C. and W. R. Peltier (2002). The puzzle of global sea-level rise, *Physics Today*, 55, 35, (electronic edition available at <http://www.physicstoday.org/pt/vol-155/iss3/p35.html>)
- Duggen, S., Hoernle, K., van den Bogaard, P., Rupke, L., and Philips Morgan, J. C. (2003), Deep roots for the Messinian salinity crisis. *Nature* 422: 602–6.
- Dumas, B., Gueremy, P., Lhenaff, R., and Raffy, J. (1993), Rapid uplift, stepped marine terraces and raised shorelines on the Calabrian coast of the Messina Straits, Italy. *Earth Surface Processes and Landforms* 18: 241–56.

- Dvorak, J. J. and Mastrolorenzo, G. (1991), The mechanisms of recent vertical crustal movements in Campi Flegrei caldera, southern Italy. *Special Paper of the Geological Society of America* 263: 1–47.
- Emery, K. O., Aubrey, D. G., and Goldsmith, V. (1988), Coastal neo-tectonics of the Mediterranean from tide-gauge records. *Marine Geology* 81: 41–52.
- EMILIANI C. (1954) - *Depth habitat of some species of pelagic foraminifera as indicated by oxygen isotope ratio*. *Am. J. Sci.*, 252, 149-158.
- EMILIANI C. (1977) - *Oxygen isotope analysis of the size fraction between 62 and 250 micrometres in Caribbean cores P6304-8 and P6304-9*. *Science*, 198, 1255-1256
- Farrell W. E. and J. A. Clark (1976). On postglacial sea level, *Geophys. Jour. Royal Astr. Soc.*, 46, 647-667
- FERRANTI L., ANTONIOLI F., MAUZ B., AMOROSI A., DAI PRA G., MASTRONUZZI G., MONACO C., ORRU' P., PAPPALARDO M., RADTKE U., RENDA P., ROMANO P., SANSO' P. & VERRUBBI V. (2005) *Last interglacial sea level high stand markers along the coast of the Italian Peninsula: tectonic implications*. *Journal of Quaternary International*, 145-146, 30-54.
- Ferranti, L., Antonioli, F., Mauz, B., Amorosi, A., Dai Pra, G., Mastronuzzi, G., Monaco, C., Orrù, P., Pappalardo, M., Radtke, U., Renda, P., Romano, P., Sansò, P., Verrubbi, V., 2006. Markers of the last interglacial sea level highstand along the coast of Italy: tectonic implications. *Quaternary International* 145e146, 30-54
- FERRANTI L., MONACO C., ANTONIOLI F., MASCHIO L., KERSHAW S, VERRUBBI V. (2007) – *The contribution of regional uplift and coseismic slip to the vertical crustal motion in the Messina Straits, southern Italy: Evidence from raised Late Holocene shorelines*. *Journal Of Geophysical Research*, 112, B06401, doi:10.1029/2006JB004473.
- Ferranti L., Fabrizio Antonioli , Marco Anzidei, Carmelo Monaco, Paolo Stocchi (2010). The timescale and spatial extent of vertical tectonic motions in Italy: insights from relative sea-level changes studies. *Journal of the Virtual Explorer*, Vol. 36 Paper 30. <http://virtualexplorer.com.au/>
- Firth, C., Stewart, I., McGuire, W. J., Kershaw, S., and Vita-Finzi, C. (1996), Coastal elevation changes in eastern Sicily; implications for volcano instability, in W. J. McGuire, A. P. Jones, and J. Neuberg (eds.), *Volcano Instability on the Earth and Other Planets*. Geological Society, London, Special Publication 110:153–67.
- Flemming N.C. (1969), Archaeological evidence for eustatic changes of sea level and earth movements in the Western Mediterranean in the last 2000 years, *Spec. Pap.-Geol. Soc. Am.* 109 (1969) 1– 125.
- Flemming N. and C. O. Webb (1986). Tectonic and eustatic coastal changes during the last 10,000 years derived from archaeological data, *Z. Geomorph. N.F.*, 62,1-29
- Fornos, J. J., Gelabert, B., Gines, A., Gines, J., Tuccimei, P., and Vesica, P. (2002), Phreatic overgrowths on speleothems: a useful tool in structural geology in littoral karstic landscapes. The example of eastern Mallorca (Balearic Islands). *Geodinamica Acta* 15: 113–25.
- Fouache E., S. Faivre, J.J. Dufaure, V. Kovacic, F. Tassaux (200). New observations on the evolution of the Croatian shoreline between Poreč and Zadar over the past 2000 years, *Z. Geomorphol. N.F.*, Suppl.bd 122, 33– 46.
- Furlani S., Antonioli F., Biolchi S., Gambin T., Gauci R., Lo Presti V., Anzidei M., Devoto S., Palombo M., Sulli A. (2012). Holocene sea level change in Malta. *Quaternary International.*, in press
- Giacobini L., B. Marchesini, L. Rustico (1997) *L'itticoltura nell'antichità*, ENEL eds. Roma,, 275 pp.

- GORNITZ V., COUCH S., HARTIG E. K. (2002) - *Impacts of sea level rise in the New York City metropolitan area*. *Global and Planetary Changes* 32, 61–88.
- Goy, J. L. and Zazo, C. (1988), Sequences of Quaternary marine levels in Elche Basin (eastern Betic Cordillera, Spain). *Palaogeography, Palaeoclimatology, Palaeoecology* 68: 301–10.
- HALLAM A. & J. M. COHEN (1989) - *The Case for Sea-Level Change as a Dominant Causal Factor in Mass Extinction of Marine Invertebrates*. Philosophical Transactions of the Royal Society of London. Series B, Biological Sciences, Vol. 325, No. 1228, Evolution and Extinction, pp. 437-455.
- HAYAS J.D., IMBRIE J., SHACKLETON N.J. (1976) – *Variations in the Earth's orbit: pacemaker of the ice ages*. *Science*, 194, 1121-1131.
- Huang, N. E., et al., (1988). The empirical mode decomposition and the Hilbert spectrum for nonlinear and non-stationary time series analysis. *Royal Soc. London Proc. Series A*, 454, 903.
- Hodell, D. A., Curtis, J. H., Siero, F. J., and Raymo, M. E. (2001), Correlation of late Miocene to early Pliocene sequences between the Mediterranean and North Atlantic. *Palaeoceanography* 16: 164–78.
- Hopley D., Smithers S.G. and Parnell K.E. (2007) *The Geomorphology of the Great Barrier Reef: Development, Diversity and Change*. Cambridge University Press, Cambridge.
- Horton B.P., Edwards R.J. and Lloyd J.M. (1999) UK intertidal foraminiferal distributions: implications for sea-level studies. *Marine Micropalaeontology* 36, 205–23.
- Hsu, K. J., Ryan, W. B. F., and Cita, M. B. (1973). Late Miocene dessication of the Mediterranean. *Nature* 242: 240–4.
- Huang N. E. et al., *Proc. R. Soc. London, Ser. A*, 454 (1998) 903.
- IMBRIE J., HAYS J.D. MARTINSON D.G., MCINTYRE A., MIX A.C., MORLEY J.J., PISIAS N.G., PRELL W.L., SHACKLETON N.J. (1984) - *The orbital theory of pleistocene climate: support from a revised chronology of the marine $\delta^{18}O$ record*. In: A.L. Berger et al. (eds), *Milankovitch and Climate*, Part 1, Reidel Pub. Co, 269-305.
- IMBRIE J., BOYLE E.A., CLEMENS S.C. ET AL. (1992) - *On the structure and origin of major glaciation cycles. 1. Linear responses to Milankovitch forcing*. *Paleoceanography*, 7, 701-738.
- IMBRIE J., BERGER A., SHACKLETON N.J. (1993) - *Role of orbital forcing: a two million year perspective*. In: *Global Changes in the Perspective of the Past*. J.A. Eddy & Oeschger eds. Chichester, Wiley, 263-277.
- IPCC 2001 – *WGI Third Assessment Report. Summary for Policymakers, Climate Change 2001: The Scientific Basis*. Intergovernmental Panel on Climate Change, Geneva.
- IPCC, 2007. Summary for policymakers. Contribution of Working Group I to the Fourth Assessment Report of the Intergovernmental Panel on Climate Change. In: Solomon, S., Qin, D., Manning, M., Chen, Z., Marquis, M., Averyt, K.B., Tignor, M., Miller, H.L. (Eds.), *Climate Change 2007: The Physical Science Basis*. Cambridge University Press, United Kingdom and New York, USA.
- Istituto Idrografico della Marina (2002). Tidal Data Base.
- Ito T. et al. (2011). *Earth Planets Space*, 63, 627
- Janekovic I. and Kuzmic M. (2005). *Ann. Geophys.*, 23, 1.
- Joseph, A., J. T. Odametey, E. K. Nkebi, A. Pereira, R. G. Prabhudesail, P. Mehra, A. B. Rabinovich, V. Kumar, S. Prabhu-Desai and P. L. Woodworth (2006). The 26 December 2004 Sumatra Tsunami recorded on the coast of west Africa. *African Journal of Marine Science*, 28(3-4), 705-712.

- Kanamori H. and Anderson D. L. (1975). *J. Geophys. Res.*, 80 (1975) 8.59001
- Keraudren, B. and Sorel, D. (1987), The terraces of Corinth (Greece)—a detailed record of eustatic sea-level variations during the last 500,000 years. *Marine Geology* 77: 99–107.
- Krijgsman, W. (2002). The Mediterranean: Mare Nostrum of Earth Sciences. *Earth and Planetary Science Letters* 205: 1–12.
- Laborel J., Morhange, C., Lafont, R., Le Campion, J., Laborel-Deguen, F., and Sartoretto, S. (1994). Biological evidence of sea-level rise during the last 4500 years on the rocky coasts of continental southwestern France and Corsica. *Marine Geology* 120: 203–23.
- Lambeck, K., Chappell, J. (2001). Sea level change through the last glacial cycle. *Science* 29, 679-686
- Lambeck K., Esat T.M. and Potter E.K. (2002a). Links between climate and sea levels for the past three million years. *Nature* **419**, 199–206.
- Lambeck K., Purcell A., Jhonston P., Nakada M. and Yokoyama Y. (2003). Water-load definition in the glacio-hydro-isostatic sea-level equation. *Quat. Sci. Rev.* 22, 309-318
- Lambeck, K., Antonioli, F., Purcell, A., Silenzi, S., 2004a. Sea level change along the Italian coast for the past 10,000 yrs. *Quaternary Science Reviews* 23, 1567-1598.
- Lambeck K., C.D. Woodroffe, Antonioli F., Anzidei M., W.R. Geherls, J.Laborel and A.Wright (2010). Paleoenvironmental Records, Geophysical Modeling, and Reconstruction of Sea-Level Trends and Variability on Centennial and Longer Timescales. In *Understanding sea level rise and variability*, Eds. P.L. Woodworth, T.Aarup, W.S. Wilson. Blackwell Pub., 61-121.
- Lambeck, K., Purcell, A. (2005). Sea-level change in the Mediterranean Sea since the LGM: model predictions for tectonically stable areas. *Quaternary Science Reviews* 24, 1969–1988.
- LAMBECK K. and BARD E. (2000). *Sea-level change along the French Mediterranean coast since the time of the Last Glacial Maximum. Earth Planet. Sci. Lett.* 175, 3-4: 202–222.
- LAMBECK K., ANTONIOLI F., PURCELL A. , SILENZI S. (2004a). *Sea level change along the Italian coast for the past 10,000 yrs. Quaternary Science Reviews*, 23, 1567-1598.
- LAMBECK K., ANZIDEI M, ANTONIOLI F., BENINI A, ESPOSITO A. (2004b). Sea level in Roman time in the Central Mediterranean and implications for modern sea level rise. *Earth and Planetary Science Letter*, 224 563-575.
- Lambeck, K., F. Antonioli, M. Anzidei, L. Ferranti, G. Leoni, G. Scicchitano, S. Silenzi. Sea level change along the Italian coast during the Holocene and projections for the future (2011). *Quaternary International*. DOI 10.1016/j.quaint.2010.04.026
- Lambeck K., Fabrizio Antonioli, Marco Anzidei. Sea level change along the Tyrrhenian coast from early Holocene to the present (2010). *Accademia Nazionale dei Lincei, Atti dei convegni Lincei*, 254, IX Giornata mondiale dell'acqua, Il bacino del Tevere, Roma.
- LASKAR J. (1999) - *The limits of Earth orbital calculations for geological time-scale use. Trans. Roy. Soc. Lond.*, 357, 1735-1759
- Lowe J.A., Woodworth P.L., Knutson T., Mc Donald R., McInnes K., Woth K., Von Storch H., Wolf J., Swail V., Bernier N., Gulev S., Horsburg K.J., Unnikrishnan A.S., Hunter J.R., Weisse R. (2010). Past and future changes in extreme sea levels and waves, in *Understanding sea level rise and variability*, Eds. P.L. Woodworth, T.Aarup, W.S. Wilson. Blackwell Pub., 17-51.
- Maas L. R. M. (1987). *J. Fluid Mech.*, 349, 361.

- Melini D. and Piersanti A. (2006). *J. Geophys. Res.*, 111, B03406.
- Mariottini, S., 2001. Volontariato e archeologia subacquea: esperienze di ricerca in Calabria. In: *Lezioni Fabio Faccenna*. Edipuglia, Bari.
- Marriner N., Morhange C., Doumet-Serhal C. and Carbonel P. (2006) Geoscience rediscovers Phoenicia's buried harbors. *Geology* **34**, 1–4.
- Mastronuzzi, G. and Sanso, P. (2000). Boulder transport by catastrophic waves along the Ionian coast of Apulia (southern Italy). *Marine Geology* 170: 93–103.
- Mastronuzzi, G. and Sanso, P (2004). Large boulder accumulations by extreme waves along the Adriatic coast of southern Apulia (Italy). *Quaternary International* 120: 173–84.
- Mc LAREN C. (1842) – *The glacial theory of Professor Agassiz of Neuchatel*. *Am. J. Sci.*, 42: 346-365.
- Meghraoui, M. et al. (2004). Coastal uplift and thrust faulting associated with the Mw = 6.8 Zemmouri (Algeria) Earthquake of 21 May, 2003, *Geophys. Res. Lett.*, doi:10.1029/2004GL020466.)
- Meier M. F. (1984). The contribution of small glaciers to global sea level.. *Science*, 226, 1418-1421.
- Meyssignac B., Cazenave A. (2012). Sea level: A review of present-day and recent-past changes and variability. *Journal of Geodynamics* 58 (2012) 96– 109
- MILANKOVITCH M. (1930). *Mathematische Klimalehre und Astronomische Theorie der Klimaschwankungen*. Handbuch der Klimalogie Band 1 Teil a Borntrager, Berlin.
- MILANKOVITCH M. (1938). *Astronomische Mittel zur Erforschung der erdgeschichtlichen Klimate*. Handb. Geoph., 9: 593-698.
- MILANKOVITCH M. (1941). *Kanon der Erdbestrahlungen und seine Anwendung auf das Eiszeitenproblem*. Beograd: Koniglich Serbische Akademie. (New English Translation, 1998: *Canon of Insolation and the Ice Age Problem*. 636 pp. (Hardbound. Alven Global. ISBN 86-17-06619-9).
- Minelli, L., and C. Faccenna (2010). Evolution of the Calabrian accretionary wedge (central Mediterranean), *Tectonics*, 29, TC4004, doi:10.1029/ 2009TC002562.
- Mitchum G. T. et al. (2010). Modern seal level change estimates. In *Understanding sea level rise and variability*, Eds. P.L. Woodworth, T.Aarup, W.S. Wilson. Blackwell Pub., 17-51.
- Mitrovica J.X. et al. (2010). Surface mass loading on a dynamic Earth: complexity and contamination in the geodetic analysis of global sea-level trends . In *Understanding sea level rise and variability*, Eds. P.L. Woodworth, T.Aarup, W.S. Wilson. Blackwell Pub., 285-325
- Miyauchi, T., Dai Pra, G., Sylos Labini, S., 1994. Geocronology of Pleistocene marine terraces and regional tectonics in the Tyrrhenian coast of southern Calabria, Italy. *Il Quaternario* 7 (1), 17-34.
- Monaco C., Antonioli F., De Guidi G., Lambeck K., Tortorici L. and Verrubbi V. (2004) Holocene tectonic uplift of the Catania Plain (eastern Sicily). *Quaternaria Nova* **8**, 171–85.
- Morhange C., Bourcier M., Laborel J., Giallanella C., Goiran J., Crimaco L. and Vecchi L. (1999) New data on historical relative sea level movements in Pozzuoli, Phlaegrean Fields, southern Italy. *Physics and Chemistry of the Earth* **24**, 349–54.
- Morhange C., Marriner, N., Laborel, L., Todesco, M., and Oberlin, C. (2006). Rapid sea-level movements and non eruptive crustal deformations in the Phlegrean Fields caldera, Italy. *Geology* 34:93–6.

- Morhange C., Laborel J. and Hesnard A. (2001) Changes of relative sea level during the past 5000 years in the ancient harbour of Marseilles, Southern France. *Palaeogeography, Palaeoclimatology, Palaeoecology* **166**, 319–29.
- Mourtzas N.D. (2012). Fish tanks of eastern Crete (Greece) as indicators of the Roman sea level. *Journal of Archaeological Science* **39** (2012) 2392-2408.
- MULLER R.A. & MCDONALD G.J. (1997). *Glacial cycles and astronomical forcing*. *Science*, **277**, 215-218.
- Nakada M. and Lambeck K. (1989) Late Pleistocene and Holocene sea-level change in the Australian region and mantle rheology. *Geophysical Journal of the Royal Astronomical Society* **96**, 497–517.
- Nicholls R.J. Impacts of and responses to sea level rise (2010). In *Understanding sea level rise and variability*, Eds. P.L. Woodworth, T.Aarup, W.S. Wilson. Blackwell Pub., 17-51
- NISI M.F., ANTONIOLI F., DAI PRA G., LEONI G., SILENZI S. (2003a) - *Coastal deformation between the Versilia and the Garigliano Plains (Italy) since the Last Interglacial stage*. *Journal of Quaternary Science*, **18**, 8, 709-721.
- Orrù P.E., Antonioli F., Lambeck K. and Verrubbi V. (2004) Holocene sea-level change in the Cagliari coastal plain (southern Sardinia, Italy). *Quaternaria Nova* **8**, 193–212.
- Pagliarulo R., Fabrizio Antonioli, Marco Anzidei (2012). Sea level changes since Middle Ages along the coast of Adriatic Sea: the case of St. Nicholas Basilica in Bari (Southern Italy). *Quat. Int.* In press.
- Pantosti D. Et al., (2008). Geological evidence of paleotsunamis at Torre degli Inglesi (northeast Sicily), *Geoph. Res. Lett.*, **35**, L05311, doi: 10.1029/2007GL032935
- Pedoja K., L. Husson, V. Regard, P.R. Cobbold, E. Ostancaux, M. E. Johnson, S.Kershaw, M.Saillard, J.Martinod, L. Furgerot, P.Weill, B. Delcaillau (2011). Relative sea-level fall since the last interglacial stage: Are coasts uplifting worldwide? *Earth-Science Reviews* **108** (2011) 1–15
- Peltier W. R. (2000) Global glacial isostatic adjustment, in *Sea level rise: history and consequences*. B. C. Douglas, M. S. Kearney, e S. P. Leatherman, eds., Academic Press, pp. 65-69.
- Pirazzoli P., Stiros, S. C., Arnold, M., Laborel, J., Laborel-Deguen, F., and Papageorgiou, S. (1994a). Episodic uplift deduced from Holocene shorelines in the Perachora Peninsula, Corinth area, Greece. *Tectonophysics* **229**: 201–9.
- PIRAZZOLI P.A. (1991). *World Atlas of Holocene Sea Level Changes*. Elsevier Oceanography Series, 58.
- Pirazzoli P. (1986b), The Early Byzantine Tectonic Paroxysm. *Zeitschrift für Geomorphologie*, NS **62**: 31–49.
- Pirazzoli P.A (1987). Sea level changes in the Mediterranean. In: Tooley and Shennan *Sea level changes*, Basil Blackwell, Oxford, 152-181
- Pirazzoli, P.A. (1976). Sea level variations in the Northwest Mediterranean During Roman Times, *Science*, **194**, 519-521
- Pirazzoli P.A., Ausseil-Badie J., Giresse P., Hadjidaki E. and Arnold M. (1992) Historical environmental changes at Phalasarna harbour, West Crete. *Geoarchaeology* **7**, 371–92.
- Plinius, *Naturalis Historia*, IX.
- Pucci S. et al., (2011). Environment-human relationships in historical times: The balance between urban development and natural forces at Leptis Magna (Libya), *Quat. Int.*, **242**, 171-184, doi: 10.1016/j.quaint.2011.03.050

RAHMSTORF S., CAZENAVE A., CHURCH J. A., HANSEN J. E., KEELING R. F., PARKER D. E., SOMERVILLE R. C. J. (2007a) . *Recent Climate Observations Compared to Projections*. Science, 316, 709.

Rahmstorf, S. (2007b). A semi-empirical approach to projecting future sea-level rise. Science 315, 68-370.

Rodriguez-Vidal, J., Caceres, L. M., Finlayson, J. C., Garcia, F. J., and Martinez-Aguirre, A. (2004), Neotectonics and shoreline history of the Rock of Gibraltar, southern Iberia. *Quaternary Science Reviews* 23: 2017–29.

Schmiedt G., Il livello antico del mar Tirreno, Testimonianze da resti archeologici, E. Olschki, Firenze, 323 pp.

Scicchitano G., Pignatelli C., Spampinato C.R., Piscitelli A., Milella M., Monaco C. and Mastronuzzi G. (2012). Terrestrial Laser Scanner techniques in the assessment of tsunami impact on the Maddalena peninsula (south-eastern Sicily, Italy). *Earth Planets Space*, 64, 889–903.

Serpelloni E., G. Vannucci, S. Pondrelli, A. Argnani, G. Casula, M. Anzidei, P. Baldi and P. Gasperini (2007). Kinematics of the Western Africa-Eurasia plate boundary from focal mechanisms and GPS data. *Geophys. J. Int.* 169, 1180–1200.

SHACKLETON N.J. (1974). *Attainment of isotopic equilibrium between ocean water and the benthonic foraminifera Genus Uvigerina: isotopic changes in the ocean during the last glacial*. In: Les méthodes quantitatives d'étude des variations du climat au cours du Pleistocène, Colloques Internationaux de Centre National de la Recherche Scientifique No. 219. CNRS, Paris, pp. 4-5.

SHACKLETON N.J. (1977). *The oxygen isotope stratigraphic record of the late Pleistocene*. Phil. Trans. Royal Soc. B, 280, 169-179.

SHACKLETON N.J. (1988). *Oxygen isotopes, ice volume and sea level*. Quat. Sci. Rev., 6, 183- 190.

Shaw B., Ambraseys N.N., England P.C., Floyd M.A., Gorman G.J., Higham T.F.G. et al. (2008) Eastern Mediterranean tectonics and tsunami hazard inferred from the AD 365 earthquake. *Nature Geoscience* 1, 268–76.

SILENZI S., DEVOTI S., GABELLINI M., MAGALETTI E., NISI M.F., PISAPIA M., ANGELELLI F., ANTONIOLI F., ZARATTINI A. (2004). *Le variazioni del clima nel Quaternario*. Geo-Archeologia, 1, 15-50.

SIMEONI U., TESSARI U., GABBIANELLI G., SCHIAVI C. (2003a). *Sea storm risk assessment in the Ravenna littoral (Adriatic Sea, Northern Italy)*. In: Ozhan E. (Ed), Proceedings of the Sixth International Conference on the Mediterranean Coastal Environment, 7-11 October 2003, Ravenna, Italy, 1-3, 2223-2234.

SIMEONI U., DEL GRANDE C., GABIANELLI G. (2003b). *Variazioni ed ipotesi evolutive dell'assetto altimetrico del litorale emiliano-romagnolo*. Studi Costieri, 7, 81-93.

Sivan D., Lambeck K., Galili E. and Raban A. (2001) Holocene sea-level changes along the Mediterranean coast of Israel, based on archaeological observations and numerical model. *Palaeogeography, Palaeoclimatology, Palaeoecology* 167, 101–17.

Sivan D., Lambeck K., Toueg R., Raban A., Porath Y. and Shirman B. (2004) Ancient coastal wells of Caesarea Maritima, Israel, an indicator for sea level changes during the last 2000 years. *Earth and Planetary Science Letters* 222, 315–30.

Slim H., Trusset P., Paskoff R. and Oueslati A. (2004) *Le littoral de la Tunisie. Etude Géoarchéologique et Historique*. CNRS Editions, Paris.

Smithers S.G. and Woodroffe C.D. (2000) Microatolls as sea-level indicators on a mid-ocean atoll. *Marine Geology* 168, 61–78.

- Stanley J.D.(2006). Kaulonia, southern Italy: Calabrian Arc tectonics inducing Holocene coastline shifts. *Méditerranée*, n.108, 1-10.
- Steffen K. et al. (2010). Cryospheric contributions to sea level rise and variability. In *Understanding sea level rise and variability*, Eds. P.L. Woodworth, T.Aarup, W.S. Wilson. Blackwell Pub., 17-51
- Stewart, I. (1996), Holocene uplift and palaeoseismicity on the Eliki Fault, western Gulf of Corinth, Greece. *Annali di Geofisica* 39: 575–88.
- Stiros, S. C. (2000), Fault pattern of Nisyros Island volcano (Aegean Sea): structural and archaeological evidence, in W. J. McGuire, D. R. Griffiths, P. L. Hancock, I. S. Stewart, and C. Vita-Finzi (eds.), *The Archaeology of Geological Catastrophes*. Geological Society, London, Special Publication 171:385–97.
- Stocchi, P., and Spada, G. (2009). Influence of glacial isostatic adjustment upon current sea level variations in the Mediterranean, *Tectonoph.*, doi: 10.1016/j.tecto.2009.01.003
- Tallarico A., Dragoni M., Anzidei M., Esposito A. (2003). Modeling Long Term Ground Deformation due to the Cooling of a Magma Chamber: the Case of Basiluzzo Island (Aeolian Islands,Italy), *J. Geophys. Res.*, 108, No. B12, 2568
- Terradas, J., Oliver, R., Ballester, J. L. (2004). Application of Statistical Techniques to the Analysis of Solar Coronal Oscillations. *Astrophys. J.*, 614, 435-447.
- Titov V. et al., *Science*, 23 (2005) 2045.
- Tuccimei, P., Fornos, J. J., Gines, A., Gines, J., Gracia, F.,and Mucedda, M. (2003), Sea level change at Capo Caccia (Sardinia) and Malorca (Balearic Islands) during oxygen isotope substage 5e, based on Th/U datings of phreatic overgrowths on speleothems, in *Puglia 2003—Final Conference Project IGCP 437*.
- Uluğ, A., Duman,M., Ersoy, , S., Ozel, E., and Avci,M. (2005), Late Quaternary sea-level change, sedimentation and neotectonics of the Gulf of Gokova, southeastern Aegean Sea. *Marine Geology* 221: 381–95.
- UREY H.C. (1948). *Oxygen isotopes in nature and in the laboratory*. *Science*, 108, 489-496.
- Varro, *De Re Rustica* III.
- Van Andel, T. H. (1989), Late Quaternary sea-level changes and archaeology. *Antiquity* 63: 733–46.
- VAIL P.R. (1977). *Seismic stratigraphy and global changes of sea level*. In *Payton C.E., Seismic stratigraphy – Application to Hydrocarbon Exploration*, A.A.P.G. Memoir, 26, 49-212.
- VAI G.B., and CANTELLI L. (2004). *Litho-Palaeoenvironmental maps of Italy during the last two climatic extremes two maps 1:1.000.000*. Explanatory notes edited by Antonioli F., and Vai G.B., 32° IGC publications.
- Vecchio, A., Laurenza, M., Carbone, V., Storini, M.(2010). Quasi-biennial Modulation of Solar Neutrino Flux and Solar and Galactic Cosmic Rays by Solar Cyclic Activity. *Astrophys. J. Lett.*, 709, L1-L5.
- Vecchio A., Anzidei M., Capparelli V., Carbone V. and Guerra I. (2012). Has the Mediterranean Sea felt the March 11th, 2011, Mw 9.0 Tohoku-Oki earthquake? *Europhysics Letters*, 98, 59001.
- Vecchio A. and Carbone, V. (2010). Amplitude-frequency fluctuations of the seasonal cycle, temperature anomalies and long-range persistence of climate records. *Phys. Rev. E*, 82, 066101
- Warny, S. A., Bart, P. J., and Suc, J.-P. (2003), Timing and progression of climatic, tectonic and glacioeustatic influences on theMessinian Salinity Crisis. *Palaeogeography, Palaeoclimatology, Palaeoecology* 202: 59–66.

WEFER G. & BERGER W.H. (1991). *Isotope paleontology: growth and composition of extant calcareous species*. Mar. Geol., 100, 207-248.

Weng, W., and J. D. Neelin (1998). On the role of ocean-atmosphere interaction in midlatitude interdecadal variability. *Geophysical Research Letters*, 25, 167-170.

Woodroffe C.D., Samosorn B., Hua Q. and Hart D.E. (2007) Incremental accretion of a sandy reef island over the past 3000 years indicated by componentspecific radiocarbon dating. *Geophysical Research Letters* **34**, L03602.

Wu Z. and Huang N. E., Proc. R. Soc. London, Ser. A,460 (2004) 1597.

Wunsch, C., and Stammer, D., Atmospheric loading and the oceanic inverted barometer effect. *Reviews of Geophys.*, 35(1), 79-107,1997.

Zazo, C., Silva, P. G., Goy, J. L., Hillaire-Marcel, C., Ghaleb, B.,Lario, J., Bardaji, T., and Gonzalez, A. (1999), Coastal uplift in continental collision plate boundaries: data from the Last Interglacial marine terrace of the Gibraltar Straits area (south Spain). *Tectonophysics* 301: 95–109.

Antonio Zecca A. and L.Chiani (2012). Lower bounds to future sea-level rise. *Global and Planetary Change* 98–99, 1–5.

List of papers published during the Doctorate

- 1 - Marco Anzidei, Alessandra Maramai, Paola Montone (2012). The Emilia (northern Italy) seismic sequence of May-June, 2012: preliminary data and results. *ANNALS OF GEOPHYSICS*, 55, 4, 2012. Preface to the volume. Edited by Marco Anzidei, Alessandra Maramai, Paola Montone. doi: 10.4401/ag-6232
- 2 - Anzidei M. and Alessandra Esposito. The lake Albano: bathymetry and level changes. *The Colli Albani Volcano*. Special Publication of IAVCEI, 3. The Geological Society, London, 229-244, 2010.
- 3 - Anzidei M., Federica Riguzzi and Salvatore Stramondo. Current geodetic deformation of the Colli Albani volcano: a review. *The Colli Albani Volcano*. Special Publication of IAVCEI, 3. The Geological Society, London, 299-310, 2010.
- 4 - Anzidei M., F. Antonioli, K. Lambeck, A. Benini, M. Soussi New insights on the relative sea level change during Holocene along the coasts of Tunisia and western Libya from archaeological and geomorphological markers. *Quaternary International*, 2010 DOI: 10.1016/j.quaint.2010.03.01
- 5 - Anzidei M., Fabrizio Antonioli, Alessandra Benini, Anna Gervasi, Ignazio Guerra (2012). Evidence of vertical tectonic uplift at Briatico (Calabria, Italy) inferred from Roman age maritime archaeological indicators. *Quaternary International*, in press (2012), doi:10.1016/j.quaint.2012.01.019
- 6 - Anzidei M., F.Antonioli, A.Benini, K.Lambeck, D.Sivan, E.Serpelloni, P.Stocchi. Sea level change and vertical land movements since the last two millennia along the coasts of southwestern Turkey and Israel. *Quaternary International*, 2010. doi:10.1016/j.quaint.2010.05.005
- 7 - Bennett R. A., E. Serpelloni, S. Hreinsdóttir, M. T. Brandon, G. Buble, T. Basic, G. Casale, A. Cavaliere, M. Anzidei, M. Marjonovic, G. Minelli, G. Molli and A. Montanari (2012). Syn-convergent extension observed using the RETREAT GPS network, northern Apennines, Italy. *Jou. of Geoph. Res.*, Vol. 117, B04408, doi:10.1029/2011JB008744.
- 8 - Devoti R., L. Anderlini, M. Anzidei, A. Esposito, A.Galvani, G.Pietrantonio, A.Pisani, F.Riguzzi, V.Sepe & E.Serpelloni (2012). The coseismic and postseismic deformation of the L'Aquila, 2009 earthquake from repeated GPS measurements. *Ital. J. Geosci.* (Boll. Soc. Geol. It.), Vol. 131, No. 3 (2012), pp. 348-358, 5 figs., 3 tabs. (doi: 10.3301/IJG.2012.15) © *Società Geologica Italiana, Roma 2012*
- 9 - Esposito A., Marco Anzidei, Simone Atzori, Roberto Devoti, Guido Giordano, Grazia Pietrantonio. Modeling ground deformations of Panarea volcano hydrothermal/geothermal system (Aeolian Islands, Italy) from GPS data. *Bullettin of Volcanology*, DOI 10.1007/s00445-010-0346-y.
- 10 - Fabris M., Paolo Baldi, Marco Anzidei, Arianna Pesci, Giovanni Bortoluzzi, Stefano Aliani. High resolution topographic model of Panarea Island by fusion of photogrammetric,

Lidar and bathymetric digital terrain models. *The Photogrammetric Record* 25(132): 382–401, 2010.

11 - Ferranti L., Fabrizio Antonioli, Marco Anzidei, Carmelo Monaco, Paolo Stocchi. The timescale and spatial extent of vertical tectonic motions in Italy: insights from relative sea-level changes studies. *Jour. of the Virtual Explorer*, 2010 Volume 36 Paper 30. <http://virtualexplorer.com.au/>

12 - Furlani S., Fabrizio Antonioli, Sara Biolchi, Timothy Gambin, Ritienne Gauci, Valeria Lo Presti, Marco Anzidei, Stefano Devoto, Mariarita Palombo, Attilio Sulli. Holocene sea level change in Malta. *Quat. Int.*, 2012.

13 - Guglielmino F., Marco Anzidei, Pierre Briole, Panagiotis Elias and Giuseppe Puglisi. 3D displacement maps of the 2009 L'Aquila earthquake (Italy) by applying the SISTEM method to GPS and DInSAR data. *Terra Nova*, 2012. doi: 10.1111/ter.12008

14 - Lambeck K., F. Antonioli, M. Anzidei, L. Ferranti, G. Leoni, G. Scicchitano, S. Silenzi. Sea level change along the Italian coast during the Holocene and projections for the future. *Quaternary International*, 2010a. DOI 10.1016/j.quaint.2010.04.026

15 - Lambeck K., Fabrizio Antonioli, Marco Anzidei. Sea level change along the Tyrrhenian coast from early Holocene to the present. *Accademia Nazionale dei Lincei, Atti dei convegni Lincei*, 254, IX Giornata mondiale dell'acqua, Il bacino del Tevere, Roma, 2010a.

16 - Lambeck K., Colin D. Woodroffe, Fabrizio Antonioli, Marco Anzidei, W. Roland Gehrels, Jacques Laborel, and Alex J. Wright. Paleoenvironmental Records, Geophysical Modeling, and Reconstruction of Sea-Level Trends and Variability on Centennial and Longer Timescales. In: *Understanding sea level rise and variability*, Eds. Philip L. Woodworth, Thorkild Aarup, and W. Stanley Wilson. Blackwell Publishing, 61-121, 2010b.

17 - Pagliarulo R., Fabrizio Antonioli, Marco Anzidei. Sea level changes since Middle Ages along the coast of Adriatic sea: the case of St. Nicholas Basilica in Bari (Southern Italy). *Quat. Int.*, 2012 in press.

18 - Serpelloni E., R. Bürgmann, M. Anzidei, P. Baldi, B. Mastrolembo Ventura, E. Boschi (2010). Strain accumulation across the Messina Straits and kinematics of Sicily and Calabria from GPS data and dislocation modeling. *EPSL*, 298 347–360. doi:10.1016/j.epsl.2010.08.005

19 - Enrico Serpelloni, Letizia Anderlini, Antonio Avallone, Valentina Cannelli, Adriano Cavaliere, Daniele Cheloni, Ciriaco D'Ambrosio, Elisabetta D'Anastasio, Alessandra Esposito, Grazia Pietrantonio, Anna Rita Pisani, Marco Anzidei, Gianpaolo Cecere, Nicola D'Agostino, Sergio Del Mese, Roberto Devoti, Alessandro Galvani, Angelo Massucci, Daniele Melini, Federica Riguzzi, Giulio Selvaggi, Vincenzo Sepe (2012). GPS observations of coseismic deformation following the May 20 and 29, 2012, Emilia seismic events (northern Italy): data, analysis and preliminary models. The Emilia (northern Italy) seismic sequence of May-June, 2012: preliminary data and results. *ANNALS OF*

GEOPHYSICS, 55, 4, 2012. Edited by Marco Anzidei, Alessandra Maramai, Paola Montone. doi: 10.4401/ag-6168

20 - Vecchio A., M. Anzidei, V. Capparelli, V. Carbone and I. Guerra. Has the Mediterranean Sea felt the March 11th, 2011, Mw 9.0 Tohoku-Oki earthquake?. EPL, 98 (2012) 59001. doi: 10.1209/0295-5075/98/59001

Annexes

Annex 1

(6 pages)

Abstract – The possibility that the tsunami, generated as a consequence of the large Mw 9.0 Tohoku-Oki earthquake of March 11th 2011, could be recorded by the tide gauge stations located in the Mediterranean Sea has been investigated. We find two kinds of transient signatures which should be attributed to the far-field destabilizing effect of the tsunami on the usual tidal components: 1) the excitation of a broad spectrum of frequency fluctuations, superimposed to the diurnal and semidiurnal tidal components, 2) the change of amplitude of the low-frequency tidal components in the Mediterranean, related to the sea surface fluctuation perhaps caused by the direct transmission of the tsunami across Gibraltar.

A. Vecchio, M. Anzidei, V. Capparelli, V. Carbone and I. Guerra. Has the Mediterranean Sea felt the March 11th, 2011, Mw 9.0 Tohoku-Oki earthquake?. EPL, 98 (2012) 59001. doi: 10.1209/0295-5075/98/59001

Has the Mediterranean Sea felt the March 11th, 2011, Mw 9.0 Tohoku-Oki earthquake?

A. VECCHIO^{1(a)}, M. ANZIDEI^{1,2}, V. CAPPARELLI^{1,3}, V. CARBONE^{1,4} and I. GUERRA¹

¹ *Dipartimento di Fisica, Università della Calabria - Ponte P. Bucci Cubo 31C, 87036 Rende (CS), Italy, EU*

² *Istituto Nazionale di Geofisica e Vulcanologia - Roma, Italy, EU*

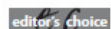
³ *British Antarctic Survey, Natural Environment Research Council - Cambridge, UK, EU*

⁴ *IPCF/CNR, Università della Calabria - Rende (CS), Italy, EU*

received 1 February 2012; accepted in final form 10 May 2012
published online 12 June 2012

PACS 91.30.Nw – Tsunamis
PACS 91.10.Tq – Earth tides
PACS 92.05.-x – General aspects of oceanography

Abstract – The possibility that the tsunamis, generated as a consequence of the large Mw 9.0 Tohoku-Oki earthquake of March 11th 2011, could be recorded by the tide gauge stations located in the Mediterranean Sea has been investigated. We find two kinds of transient signatures which should be attributed to the far-field destabilizing effect of the tsunami on the usual tidal components: 1) the excitation of a broad spectrum of frequency fluctuations, superimposed to the diurnal and semidiurnal tidal components, 2) the change of amplitude of the low-frequency tidal components in the Mediterranean, related to the sea surface fluctuation perhaps caused by the direct transmission of the tsunami across Gibraltar.

 Copyright © EPLA, 2012

Introduction. – On March 11, 2011 at 05:46:23 UTC the NE coast of Honshu island (Japan) was struck by one of the largest earthquakes ever occurred in the world since historical times. The Mw 9.0 event released the tectonic stress accumulated over the last 700 years [1] and triggered a giant tsunami that caused an estimated loss of 200–300 billion US dollars and killed more than 10000 people living along the coasts of Japan and elsewhere in the Pacific region [1–3]. The period of a tsunami wave ranges from few minutes to several tens of minutes and generally it depends on the geographic location. At the same time, its amplitude is large enough to be identified within the normal tidal and nontidal spectrum of the sea level variability processes [4–6]. Recent studies showed that large tsunamis can propagate through the oceans up to very distant regions [7–11]. Small-amplitude sea level oscillations, superimposed to the normal tides, were recorded in connection with the eastern Indian ocean tsunami of December 26 2004, even along the coasts of the British Isles, thousand of km away from the Mw 9.3 earthquake epicenter, and up to the West coast of Africa. These results could explain the finding of the overall

tendency of giant earthquakes to produce a global relative sea level variation [12].

The propagation of tsunamis in oceans is a topic largely investigated by means of fluid numerical simulations in shallow-water approximation (see, *e.g.*, [8,13] and references therein). This approach allowed to understand many properties of the propagation, such as the role of the orientation and intensity of the offshore seismic line source and the trapping effect of mid-ocean ridge topographic waveguides that influences wave amplitude, directionality, and global propagation patterns (see, *e.g.*, ref. [8]). On the other hand, the possibility that a tsunami wave, produced by a far seismic event, could affect in some way the Mediterranean Sea, has received less attention. This is mainly attributable to the irregular bathymetry of the Strait of Gibraltar, that is believed to produce a strong damping and multiple reflections of the wave thus decreasing the probability of penetration in the Mediterranean basin. After the large 2004 Indian Ocean tsunami, additional improvements to global tide gauge systems were performed for the monitoring of both tsunamis [8] and variations in sea level [11]. This allowed to achieve, also in the Mediterranean, real-time data with a quite homogeneous spatial coverage and high time resolutions, needed

^(a)E-mail: antonio.vecchio@fis.unical.it

to reveal possible low-amplitude fluctuations due to the far-field destabilizing effect of tsunamis in this basin.

The present paper aims to investigate the occurrence of possible signatures in sea level data at high-quality tide gauge stations, after the megathrust Japan earthquake of March 2011, in the Mediterranean, a remote sea far from the earthquake epicenter. This investigation will support new insights on the physics of tsunami propagation across narrow straits, such as the one of Gibraltar, the transient effect on sea level, in remote basins in relationships with the Earth's free oscillations induced by high-magnitude earthquakes, and finally investigate the resonance effects in enclosed sea basins, such as the Mediterranean, in response to tsunami events.

Data analysis. – We focused on 31 sea level data in the period 9–15 March 2011. The sea level signals, having a time sampling of 10 minutes and an accuracy of better than 1 cm, have been retrieved from the IOC sea level station monitoring¹, from the Institute for Environmental Protection and Research (ISPRA)² and from the Permanent Service for Mean Sea Level (PSMSL)³. The geographic distribution of the tide gauge stations is reported in fig. 1. During the considered time window the weather situation around the stations was favorable (mainly calm sea, low and constant wind velocity), thus not inducing critical conditions of the sea surface for the quality of the sea level data set. Moreover, our analysis was restricted to the tidal stations located in sheltered positions; namely, the effects of both intensity and direction of the wind on the sea level recordings, based on the length of the fetch and the subsurface topography for the location⁴, were negligible [5]. Sea level observations were first reduced for atmospheric pressure variations by applying an inverse barometric correction to the data [14]. As an example of raw data, in fig. 2 (row A) we show the sea level time series $L(t)$ at four stations. Time is measured as the lag from the earthquake occurrence. A sudden change of regime can be identified in all the signals after the earthquake. In fact, the regular tidal oscillation is broken, more frequencies appear, and the time behavior becomes more complex and highly nonstationary. This kind of dynamical behavior is common to all the records we investigated. In fig. 3 we report the sea level time series $L(t)$ for the Cagliari station (panel (a)), along with the 12 hours return map $L(t + \Delta)$ vs. $L(t)$, for $\Delta = 12$ hours (panel (b)). The figure roughly provides evidences that after the mainshock the Mediterranean Sea felt a strong phase and amplitude perturbation of the tidal oscillation. In fact, for $t \leq 0$ (blue line), the points of the return map are approximately sorted along a straight line, indicating that the oscillation amplitude and phase remain almost constant. On the

¹www.ioc-sealevelmonitoring.org.

²www.mareografico.it.

³www.pol.ac.uk.

⁴Cf. the Fetch- and Depth-Limited Wave Calculations facilities at <http://woodshole.er.usgs.gov/staffpages/csherwood/sedrx-equations/RunSPMWave.html>.

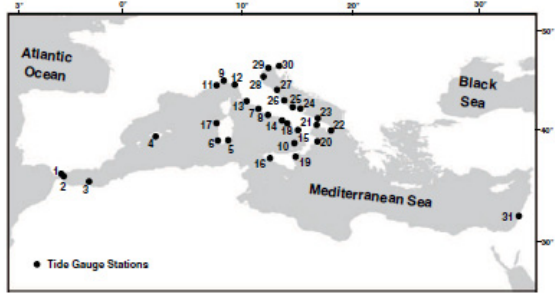


Fig. 1: Map of the tide gauge stations, in the Mediterranean, used in this study. Numbers refer to the following stations: 1) Gibraltar, 2) Ceuta, 3) Melilla, 4) Palma de Mallorca, 5) Cagliari, 6) Carloforte, 7) Civitavecchia, 8) Gaeta, 9) Genova, 10) Ginostra, 11) Imperia, 12) La Spezia, 13) Livorno, 14) Napoli, 15) Palinuro, 16) Porto Empedocle, 17) Porto Torres, 18) Salerno, 19) Catania, 20) Crotona, 21) Taranto, 22) Otranto, 23) Bari, 24) Vieste, 25) Ortona, 26) San Benedetto, 27) Ancona, 28) Ravenna, 29) Venezia, 30) Trieste, 31) Hadera.

contrary for $t > 0$ (red line), the points are distributed on irregular ellipses, indicating that the phase and amplitude are no more constant but change with time.

In order to characterize the observed change of dynamical behavior, we use the Empirical Mode Decomposition (EMD) [15], a technique developed to analyze nonstationary time series and used in various contexts [16–18], including geophysical systems [19–22]. Each sea level time series $L(t)$ is decomposed into a finite number n of Intrinsic Mode Functions (IMF) $\theta_j(t)$ as

$$L(t) = \sum_{j=0}^n \theta_j(t) + r_n(t). \quad (1)$$

The IMFs, containing information about the local properties of the signal, are empirical, *i.e.* not given *a priori* but obtained from the data by following the “sifting” method [15]. This procedure starts by identifying local extrema of $L(t)$. The envelopes of maxima and minima are then obtained through cubic splines and the mean between them, $m_1(t)$, is calculated. The difference quantity $h_1(t) = L(t) - m_1(t)$ represents an IMF only if it satisfies two criteria: i) the number of extrema and zero-crossing does not differ by more than one; ii) at any point the mean value of the two envelopes is zero. If i) and ii) are not satisfied, the previous steps are repeated by using $h_1(t)$ as raw series and $h_{11}(t) = h_1(t) - m_{11}(t)$, where $m_{11}(t)$ is the mean of the envelopes in this case, is generated. This procedure is repeated k times until $h_{1k}(t)$ satisfies the IMF's properties. Thus $\theta_1(t) = h_{1k}(t)$ represents the first IMF, associated with the shortest time scale of the process. To guarantee that the IMF components have enough physical sense with respect to both amplitude and frequency modulations, a criterion to stop the sifting

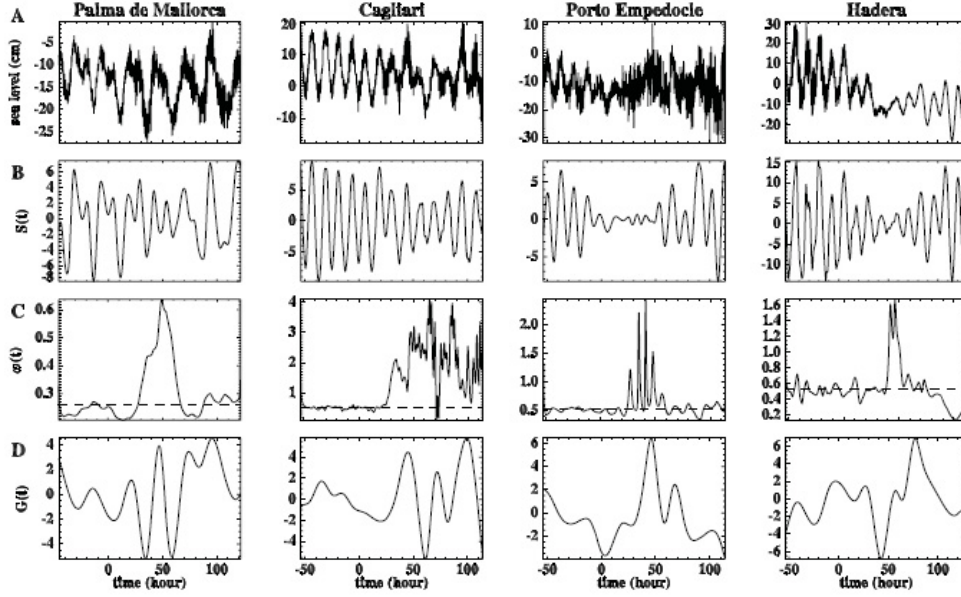


Fig. 2: Time evolution of the sea levels (line A), contribution of the high-amplitude components $S(t)$ (line B), instantaneous frequency of the highest-amplitude IMF (line C), low-frequency contribution $G(t)$ (line D) for the stations of Palma de Mallorca (4), Cagliari (5), Porto Empedocle (16) and Hadera (31). Time is counted from the origin time of the Tohoku-Oki earthquake. The dashed line corresponds to $(2\pi)/12 \text{ hour}^{-1}$ for Cagliari, Porto Empedocle and Hadera and $(2\pi)/24 \text{ hour}^{-1}$ for Palma.

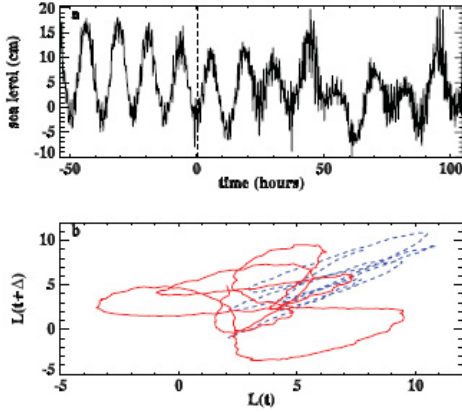


Fig. 3: (Colour on-line) Time evolution of the sea level $L(t)$ (panel (a)) and the 12 hours return map $L(t+\Delta)$ vs. $L(t)$ (panel (b)) for the Cagliari station ($\Delta = 12$ hours). Time is counted from the origin time of the Tohoku-Oki earthquake. The blue dashed line refers to times $t \leq 0$, the red full line refers to times $t > 0$.

process has been introduced [15]. A kind of standard deviation, calculated using two consecutive siftings, is defined $\sigma = \sum_{t=0}^N [(|h_{1(k-1)}(t)| - |h_{1k}(t)|) / h_{1(k-1)}^2(t)]$ and the iterative process is stopped when σ is smaller than a threshold

value, in our case chosen as 0.3 [15]. The function $r_1(t) = L(t) - \theta_1(t)$, the first residue, is analyzed in the same way as just described, thus obtaining a new IMF $\theta_2(t)$ and a second residue $r_2(t)$. The process continues until θ_j or r_j are almost zero everywhere or when the residue $r_j(t)$ becomes a monotonic function from which no more IMF can be extracted. At the end of the procedure n empirical modes, ordered with increasing characteristic time scale, and a residue $r_n(t)$, which describes the mean trend if any, are obtained. Each IMF has its own time scale, τ_j , and represents a zero mean oscillation experiencing amplitude and frequency modulations; namely the j -th IMF can be written as $\theta_j(t) = A_j(t) \cos[\omega_j(t) \cdot t]$, where $A_j(t)$ and $\omega_j(t)$ are the time-dependent amplitude and frequency of the j -th mode, respectively. The IMF time scale is computed as the average time between local maxima and minima. The EMD allows to define, for each IMF, a meaningful instantaneous frequency calculated as follows. The Hilbert transform is applied on each IMFs, namely

$$\theta_j^*(t) = \frac{1}{\pi} P \int_{-\infty}^{\infty} \frac{\theta_j(t')}{t-t'} dt', \quad (2)$$

where P indicates the Cauchy principal value. $\theta_j(t)$ and $\theta_j^*(t)$ form the complex conjugate pair so that the instantaneous phase can be calculated as $\phi_j(t) = \arctan[\theta_j^*(t)/\theta_j(t)]$. The instantaneous frequency follows as $\omega_j(t) = d\phi_j/dt$. This definition of $\omega(t)$ is quite general

and in principle some limitations on the data are necessary in order to obtain instantaneous frequency as a single-value function of time. The latter property is fulfilled by the EMD basis functions which allow to obtain a meaningful instantaneous frequency consistent with the physics of the system under study [15].

The EMD represents a powerful tool for the time-frequency analysis of nonlinear and nonstationary data. Being based on an adaptive basis, it allows to overcome some disadvantages of the Fourier spectral analysis when applied to real nonperiodic and nonstationary data, such as the *a priori* definition of the Fourier modes, that are often far from being proper eigenfunctions of the phenomenon at hand. Moreover, when dealing with nonperiodic data, Fourier modes are mixed together in order to build up a solution corresponding to the fictitious periodic boundary conditions imposed by the analysis. On the other hand, the EMD does not introduce spurious harmonics, as in the case of Fourier analysis, in reproducing nonstationary data and nonlinear waveform deformations. The EMD frequency is derived by differentiation rather than convolution, as in the case of Fourier, and, therefore, there is not an uncertainty principle limitation on time or frequency resolution. The EMD decomposition is complete and orthogonal. The latter property, even if not theoretically guaranteed, is practically fulfilled [15] and should be checked numerically *a posteriori*. In our case, we verified that the obtained IMFs can be considered at a good approximation as orthogonal. The orthogonality ensures that each IMF captures the empirical dynamical behavior of a single independent mode of the system, namely each j -mode describes a single phenomenon within the complex dynamics. This allows to filter and reconstruct the signal through partial sums in eq. (1) in order to obtain independent contributions to the signal in different ranges of time scales [15,17,18].

Results. – When applied to the Mediterranean tide gauge data the EMD gives a number n of modes which in general depends on the station under analysis. As obtained from the test of significance for the various IMFs [23], the first three modes, $j \leq 2$, represent high-frequency noise while higher- j modes are associated with significant oscillations of the sea level at different time scales. For the majority of the stations the IMF with the highest amplitude has a period of $\tau \approx 12$ hours, corresponding to the well-known semidiurnal oscillation. However, in the analyzed data sets, the full semidiurnal component of the tide is split into two or three IMFs, depending on the station. This means that one IMF does not suffice to fully describe the temporal behavior of the 12 hours tidal component. The previous result follows from the high sensitivity of the EMD to local frequency fluctuations. The latter, still persisting when meteorological effects are removed, are strong enough to affect the regularity of the semidiurnal mode of oscillation. As mentioned before, since for the properties of the EMD decomposition each

IMF is associated to a well-defined time scale of the signal at hand, a regular semidiurnal oscillation should be isolated in a single IMF. In the presence of localized frequency fluctuations new time scales arise and affect the regular oscillation of the high-energy tidal components. In this case, a single IMF is not able to account for the new time scales and the time evolution of the 12 hour oscillation is split into two or more IMFs. Of course, the sum of these EMD modes will describe the full contribution of the semidiurnal oscillation to the sea level. For Palma de Mallorca and the stations in the northern sector of the Adriatic Sea (stations 26–30), the simultaneous presence of both diurnal and semidiurnal components, as main tidal constituents, has been detected. This is a well-known phenomenon and it should depend, in the Adriatic Sea, on the basin characteristics, *i.e.*, the low sea depth and the semiclosed shape [24,25]. For these cases the previous considerations are also valid for the 24 hours component which is split into two IMF. By exploiting the orthogonality of the EMD decomposition, the signal $L(t)$ has been divided, by partial sum in eq. (1), into four contributions namely $L(t) = \eta(t) + S(t) + G(t) + r_n(t)$. The function $\eta(t)$ is associated with the high-frequency noise, $S(t)$, obtained as the sum of the high-amplitude components (semidiurnal and for some station also diurnal), represents the basic tidal mode and $G(t)$ describes the remaining low-frequency contribution. An example of the time behavior of $S(t)$ is reported in row B of fig. 2. Its dynamics is far from being regular and stationary since the waveforms abruptly change after $t = 0$. The variation of the main tidal contribution can be better appreciated by looking at the instantaneous frequency of the highest-amplitude IMF (row C of fig. 2) which is abruptly destabilized in correspondence of the change of the oscillating regime in $S(t)$ and departs from the constant value of $(2\pi)/12 \text{ hour}^{-1}$. Note that for Palma de Mallorca the reference frequency is $(2\pi)/24 \text{ hour}^{-1}$ since, in this case, the highest-amplitude mode is associated with the diurnal component.

EMD modes with longer periods describe low-frequency phenomena. The function $G(t)$, an example is reported in row D of fig. 2, is characterized by the increase of amplitude after $t = 0$. Figure 4 shows the contour plot of the functions $G(t)$, ordered according to the distance from Gibraltar. The figure clearly indicates that the time at which the increased amplitude regime is at its maximum absolute value is a function of the distance from the Strait of Gibraltar. This result is consistent with a traveling perturbation in the whole Mediterranean Sea propagating from Gibraltar. The Adriatic stations, for the sake of clarity, have been excluded from fig. 4. For these stations, due to the Adriatic basin geographic characteristics, the time-distance relation is inverted. In fact, the northernmost Adriatic stations are nearer to Gibraltar but the perturbation has to cover a longer path before reaching them. As shown in fig. 4 the majority of stations shows a peak (in red) after $t = 0$, which indicates

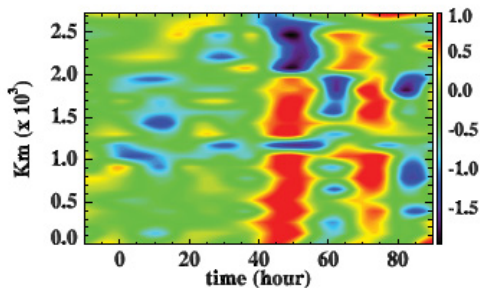


Fig. 4: (Colour on-line) Contours of $G(t)$ in the space-time plane. The x -axis reports the time counted from the Tohoku-Oki earthquake, while the y -axis reports the distance in km from Gibraltar.

a positive fluctuation of the sea level. On the other hand, some records, including Hadera and the stations in the Ionian Sea, are characterized by a drop (in blue) followed by the transient increase of the sea level. This behavior can be induced by the local seafloor topography and/or by the different paths taken by the tsunami waves and reflection effects [9]. The space-time representation allows to estimate the velocity of propagation of the perturbation, in the Mediterranean Sea, to be about $V_p \simeq 60$ m/s. Note that, this perturbation is revealed in the whole Mediterranean Sea, being observed up to Hadera, the easternmost station, about 13 hours after Gibraltar.

We hypothesize that both the indirect perturbation of the tidal frequency and the direct transfer of small fluctuations beyond the Strait of Gibraltar, are generated from the tsunami triggered by the March 11th 2011, Tohoku-Oki earthquake. We remark that the timing of both these effects, varying between ~ 45 hours in Gibraltar and ~ 58 hours in Hadera, are in agreement with the results of theoretical models of tsunami propagation for which the perturbation should arrive at Gibraltar in a time of about 38 hours after the earthquake⁵. The obtained results have been tested by looking at the sea level records during the period 9–15 September 2011, in a time window which cannot be related with the Tohoku-Oki earthquake. We assume that, in this period, the possible transient effect of the tsunami is null and the system behaves according to the usual dynamics. As expected, we found that the principal tidal components show a regular behavior and are detected, by the EMD, in a single IMF. This indicates that the splitting of the principal tidal components into more IMFs along with the instantaneous frequency destabilization could be plausibly in connection with a transient effect, associated with the tsunami. As an example, the results for the Cagliari station are reported in fig. 5. The raw data are shown in panel (a), and panel (b) shows the regular semidiurnal component associated with the largest-amplitude IMF, whose characteristic time

⁵<http://nctr.pmel.noaa.gov/honshu20110311/honshu2011-globalmaxplot.png>.

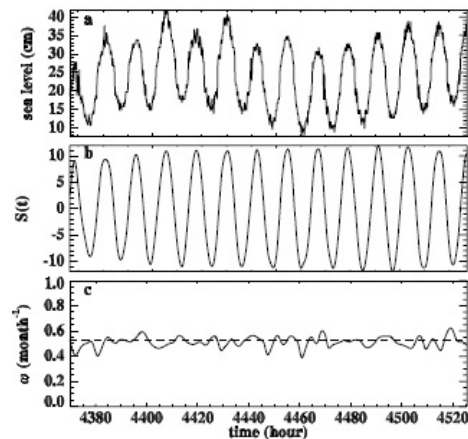


Fig. 5: Time evolution of the sea levels (a), semidiurnal IMF (b) and instantaneous frequency (c) for the Cagliari station. Time is counted from the origin time of the Tohoku-Oki earthquake.

scale is 12.27 hours. Panel (c) shows the instantaneous frequency of the IMF reported in panel (b). The striking difference with fig. 2 is evident. As expected, the frequency is centered around the value $2\pi/12 \text{ hour}^{-1}$ with low-amplitude superimposed stochastic fluctuations.

Conclusions. – In this paper we investigated the anomalous sea level changes for 31 stations in the Mediterranean basin, due to a transient perturbation in the period 9–15 March 2011. Once the atmospheric pressure effects have been removed and the wind intensity and direction have been accounted for, with respect to the position of the individual tidal stations, we hypothesize that the perturbation is a consequence of the tsunami generated by the March 11th, 2011, Mw 9.0 Tohoku-Oki earthquake. Our analysis shows that the Mediterranean felt the effect of the tsunami 40–50 hours after the mainshock thus indicating that tsunamis generated by strong earthquakes are truly global events. In particular, we revealed two kinds of transient signatures. Firstly, the perturbation generates strong frequency fluctuations affecting the regular behavior of the high-amplitude tidal components, usually the semidiurnal and in some cases also the diurnal one. As a consequence of the perturbation, these components appear highly nonstationary and several IMFs are needed to reproduce their full contribution. In addition the instantaneous frequency shows abrupt destabilization after the earthquake occurrence. The physical mechanism causing these manifestations should be related to a resonant response to the tsunami at the strait entrance. Tides in enclosed basins, connected to the open sea by a narrow strait, can manifest amplified or damped response to a forcing action outside the basin [26]. Due to nonlinear effects the basin may exhibit chaotic modulation of the tidal amplitude and frequency. Since the Mediterranean

Sea is similar to a closed basin with respect to the oceans and is connected to Atlantic Ocean by a narrow strait, it could be affected by the forcing action of the fluctuations associated with the tsunami and could manifest nonlinear response leading to amplification and frequency destabilization. The second signature consists in a propagating perturbation manifesting itself with a weak increase of amplitude of the low-frequency EMD modes, after the occurrence of the Tohoku-Oki earthquake. This perturbation, significant with respect to the noise level, should be an evidence of the direct transmission of tsunami fluctuations, characterized by long periods, through the Strait of Gibraltar.

The timing of the detected tidal perturbations at the recording stations are in agreement with the prediction of the global models of tsunami propagation, for which the arrival at the Strait of Gibraltar is expected about 38 hours after the onset of the earthquake. Effects on sea levels due to post-seismic deformations [12], capable to cause global sea level raise of the order of a fraction of mm (<http://cires.colorado.edu/~bilham/Honshu2011/Honshu2011.html>) and direct propagation of surface seismic waves from the epicenter, arriving at the Mediterranean region 20–30 minutes after the mainshock (www.emsc-csem.org), have been excluded since they are not consistent with the observed sea level variations. Additionally, it is unlikely that free oscillations of the Earth, excited by the high-magnitude Tohoku-Oki earthquake, originated the detected fluctuations since the timing and period of the main mode of oscillation [27,28] are not in agreement with the timing and frequency of the sea level perturbations revealed by our observations. However, based on the available seismological and geophysical literature [27] the effects of free oscillations of the Earth on the sea level have not yet been investigated and the results presented in this paper provide new observational constraints for these studies. The physical mechanisms, briefly described above, need deeper investigations and will be tackled in a future paper.

We thank an anonymous referee for very useful comments. We are grateful to GIOVANNI ARENA of ISPRA and PHILIP WOODWORTH of PSMSL who provided tidal data.

REFERENCES

- [1] ITO T. *et al.*, *Earth Planets Space*, **63** (2011) 627.
- [2] HAYES G. P., *Earth Planets Space*, **63** (2011) 529.
- [3] HIROSE F. *et al.*, *Earth Planets Space*, **63** (2011) 513.
- [4] CARTWRIGHT D. E., *Tides, A Scientific History* (Cambridge University Press) 1999.
- [5] GILL A. E., *Atmosphere-Ocean Dynamics* (Academic Press, New York) 1982.
- [6] LAMBECK K., *Geophysical Geodesy The Slow Deformations of the Earth* (Oxford Science Publications) 1988.
- [7] MERRIFIELD M. A. *et al.*, *Geophys. Res. Lett.*, **32** (2005) L09603, doi:10.1029/2005GL022610.
- [8] TITOV V. *et al.*, *Science*, **23** (2005) 2045.
- [9] JOSEPH A. *et al.*, *Afr. J. Mar. Sci.*, **28** (2006) 705.
- [10] WOODWORTH P. L. *et al.*, *Weather*, **60** (2005) 263.
- [11] WOODWORTH P. L., AARUP T. and WILSON W. S., *Understanding Sea Level Rise and Variability*, Vol. 456 (Blackwell Publishing) 2010.
- [12] MELINI D. and PIERSANTI A., *J. Geophys. Res.*, **111** (2006) B03406.
- [13] GEIST E. L., *Adv. Geophys.*, **51** (2009) 107, doi:10.1016/S0065-2687(09)05108-5.
- [14] WUNSCH C. and STAMMER D., *Rev. Geophys.*, **35** (1997) 79.
- [15] HUANG N. E. *et al.*, *Proc. R. Soc. London, Ser. A*, **454** (1998) 903.
- [16] CUMMINGS D. A. T. *et al.*, *Nature*, **427** (2004) 344.
- [17] TERRADAS J., OLIVER R. and BALLESTER J. L., *Astrophys. J.*, **614** (2004) 435.
- [18] VECCHIO A. *et al.*, *Astrophys. J. Lett.*, **709** (2010) L1.
- [19] JÁNOSI I. M. and MÜLLER R., *Phys. Rev. E*, **71** (2005) 056126.
- [20] SALISBURY J. I. and WIMBUSH M., *Nonlinear Proc. Geophys.*, **9** (2002) 341.
- [21] ZHEN-SHAN L. and XIAN S., *Meteorol. Atmos. Phys.*, **95** (2007) 115.
- [22] VECCHIO A., CAPPARELLI V. and CARBONE V., *Atmos. Chem. Phys.*, **10** (2010) 9657.
- [23] WU Z. and HUANG N. E., *Proc. R. Soc. London, Ser. A*, **460** (2004) 1597.
- [24] JANEKOVIĆ I. and KUZMIĆ M., *Ann. Geophys.*, **23** (2005) 1.
- [25] CAPUANO P. *et al.*, *Prog. Oceanogr.*, **91** (2011) 447.
- [26] MAAS L. R. M., *J. Fluid Mech.*, **349** (1987) 361.
- [27] AKI K. and RICHARDS P. G., *Quantitative Seismology*, 2nd edition (University Science Books) 2002.
- [28] KANAMORI H. and ANDERSON D. L., *J. Geophys. Res.*, **80** (1975) 8.

Annex 2
(8 pages)

Abstract - Published and new sea level data are used to provide projections of sea level change in Italy for the year 2100 by adding new isostatic and tectonic component to the IPCC and Rahmstorf projections. Comparison of the observations from more than 130 sites (with different geomorphological and archaeological sea level markers) with the predicted sea level curves provides estimates of the vertical tectonic contribution to the relative sea level change. The results are based on the most recent ANU model for the ice sheets of both hemispheres, including an alpine deglaciation model. On the basis of the eustatic, tectonic and isostatic components to the sea level change, projections are provided for marine inundation scenarios for the Italian coastal plains for the year 2100, that today are at elevations close to current sea level.

K. Lambeck, F. Antonioli, M. Anzidei, L. Ferranti, G. Leoni, G. Scicchitano, S. Silenzi. Sea level change along the Italian coast during the Holocene and projections for the future. *Quaternary International*, 2010. DOI 10.1016/j.quaint.2010.04.026



Contents lists available at ScienceDirect

Quaternary International

journal homepage: www.elsevier.com/locate/quaint

Sea level change along the Italian coast during the Holocene and projections for the future

K. Lambeck^{a,b}, F. Antonioli^{c,*}, M. Anzidei^d, L. Ferranti^e, G. Leoni^c, G. Scicchitano^f, S. Silenzi^g

^a Research School of Earth Sciences, Australian National University, 0200 Canberra, Australia

^b Antarctic Climate & Ecosystems Cooperative Research Centre, Hobart, Australia

^c ENEA – National Agency for New Technologies, Energy and Environment, Rome Italy

^d INGV, Rome, Italy

^e Earth Science Department, Naples, Italy

^f Earth Science Department, Catania, Italy

^g ISPRA – Institute for Environmental Protection and Research, Rome, Italy

ARTICLE INFO

Article history:

Available online 8 May 2010

ABSTRACT

Published and new sea level data are used to provide projections of sea level change in Italy for the year 2100 by adding new isostatic and tectonic component to the IPCC and Rahmstorf projections. Comparison of the observations from more than 130 sites (with different geomorphological and archaeological sea level markers) with the predicted sea level curves provides estimates of the vertical tectonic contribution to the relative sea level change. The results are based on the most recent ANU model for the ice sheets of both hemispheres, including an alpine deglaciation model. On the basis of the eustatic, tectonic and isostatic components to the sea level change, projections are provided for marine inundation scenarios for the Italian coastal plains for the year 2100, that today are at elevations close to current sea level.

© 2010 Elsevier Ltd and INQUA. All rights reserved.

1. Introduction

The aim of this paper is: (i) to upgrade the observational data set of sea level indicators on a consistent and calibrated time scale with tide and atmospheric pressure applied; (ii) to provide predicted sea level curves since the Last Glacial Maximum at 40 reference sites that are representative of the Italian coast (see Appendix 1 on additional material, only in the on-line version, and Fig. 1); (iii) from the comparison of observed and isostatic predictions to calculate the vertical tectonic displacement for each site; (iv), to provide projections for sea level rise by 2100 that include the isostatic and tectonic components and the contributions from different climate scenarios.

The observational database includes geomorphological markers of palaeo-sea level, coastal archaeological data, and sedimentary core analysis. Their age and elevation uncertainties are discussed and consistent calibration programs for the time scale and for the reductions of elevation measurements to mean sea level have been used. Using the same methodology of Lambeck et al. (2004a) and Antonioli et al. (2007, 2009a, b), the current elevations of these

observed data points are compared with the glacio-hydro-isostatic predicted sea level elevations at each location both to test the model and the choice of model parameters and to estimate the tectonic contributions.

The three principal contributions to sea level change, measured with respect to land, along the Italian coast, are (i) the sea level response to the past glacial cycle, including the response to the most recent glacial unloading of the major ice sheets and the European Alps and the response to the ocean floor loading by the melt water – the glacio-hydro-isostatic and eustatic contributions, (ii) changes in ocean volume in more recent times from thermal expansion, recent glacier melting etc., and (iii) vertical land movements, including uplift as in Calabria and Sicily and subsidence as in the northern Adriatic. The isostatic response requires models for the past ice sheets, and these have been estimated from inversions of rebound data from the formerly glaciated regions. The recent ANU ice models described in Lambeck et al. (2010) were used. The isostatic response also requires rheological parameters that may be regionally variable and these are estimated from the sea level data for sites that are believed to be tectonically stable. For the Italian coast, tectonic stability is assumed when the Last Interglacial (Llg) shorelines occur at about 6 m above present sea level. Where the Llg markers occur above or below this level, it is assumed that the area has been subjected to uplift or subsidence

* Corresponding author.

E-mail address: fabrizio.antonioli@enea.it (F. Antonioli).

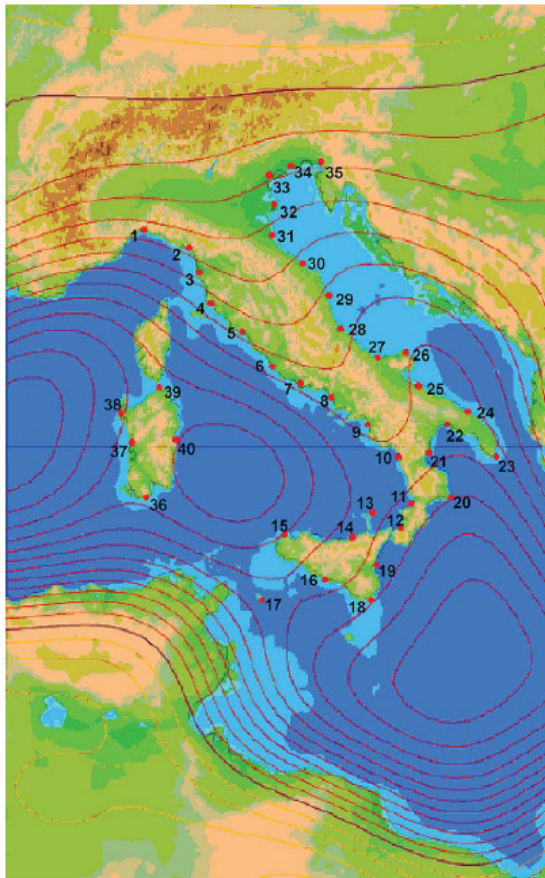


Fig. 1. Map of Italian coast with location of the sites with predicted sea level curves in Appendix 1.

(see Nisi et al., 2003; Ferranti et al., 2006, for discussion about tectonic stability along the Italian coast). Thus the solutions are based on an iterative process in which the rheological parameters are tested against the tectonically stable sites and these parameters are then used across the region to estimate the departures from stability.

The isostatic signal in sea level is the result of an ongoing process and can be predicted once the ice and Earth parameters have been established. Thus predictions of this component can be made with some confidence. The tectonic contribution is also an ongoing process but it is often of an episodic nature and any projections are based on the assumption that the average contributions established from the geological/archaeological record are representative of future change as well. Any climate-driven changes to sea level are of necessity based on projections of the climate change itself, and two scenarios here that reflect the lower and upper ranges that have been variously proposed are considered here. The former is the IPCC (2007) lower limit estimate of a global sea level rise of 180 mm by 2100; the latter uses the Rahmstorf (2007) estimate of 1400 mm.

As was palaeo-sea level, future sea level change will not be spatially uniform. The spatial variability of the future isostatic and

tectonic contributions can be extrapolated from the analysis of the present data but the climate models are not yet adequate to represent the spatial variability from the climate signals with any confidence. Hence the projections presented here will be based of necessity on the global averages of this latter contribution. It is emphasized that the resulting sea level projections are not predictions, but estimates of what may happen under certain scenarios and assumptions. As model and observational capabilities improve the projections will need to be correspondingly updated.

2. Material and methods

2.1. Glacio-hydro-isostatic model

The ice model used throughout the subsequent predictions is described in Lambeck et al. (2006, 2009, 2010) and includes the most recent developments for the ice sheets in both hemispheres (its complete identification number is K33_j1b_WS9_6). It includes the major ice sheets back to the penultimate interglacial as well as an alpine deglaciation model. No changes in ocean volume occur in this model for the past few centuries. Rheological parameters have been adopted from previous work for the same region (Lambeck et al., 2004a, b) and correspond to the three-layer model with an effective elastic lithospheric thickness of 65 km, an upper mantle viscosity of 3×10^{20} Pa s and a lower mantle viscosity of 3×10^{22} Pa s.

Figs. 1 and 2 illustrate predictions for selected sites for the past 20,000 years. These predictions are for the isostatic–eustatic components from the last glacial cycle only and their variability from site to site reflects both an approximately north–south component from the increasing distance from the former northern ice sheets and a more variable component from the water-loading contribution (c.f. Figs. 1 and 2 in Lambeck and Purcell, 2005). This spatial variability continues up to the present as is illustrated in Fig. 3. Along the entire Italian coast, sea level is rising as a result of

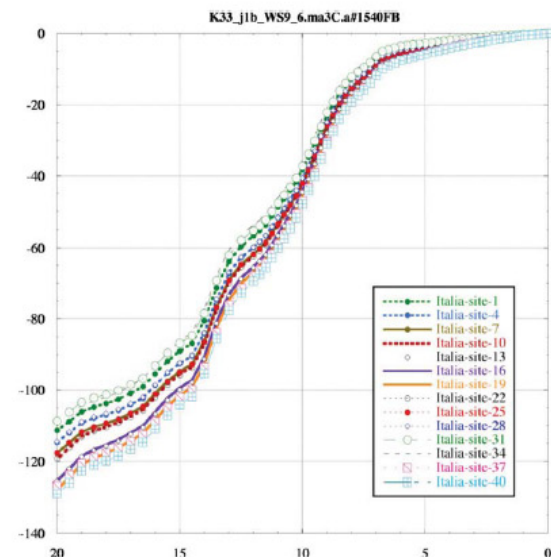


Fig. 2. Eustatic and glacio-hydro-isostatic predictions for selected Italian sites for the past 20,000 years Site locations in Fig. 1.

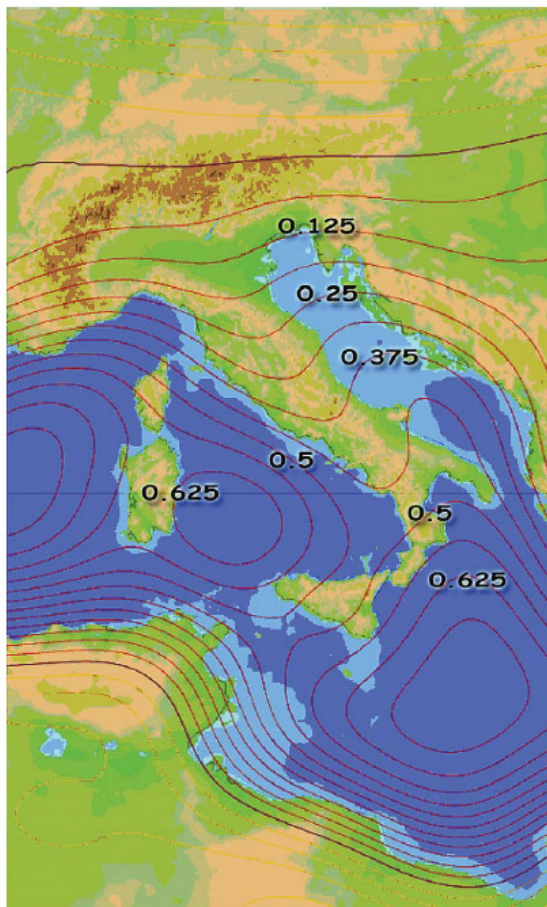


Fig. 3. Predicted present-day isostatic rates for Italy (in mm/yr). For the entire Italian coast this contribution is one of a relative sea level rise but the rate is spatially variable across the region, differing by 0.5 mm/yr between the northern Adriatic coast and Sardinia. Red contours denote negative values, orange contours denote positive values, dark red contour correspond to zero change. (For interpretation of the references to colour in this figure legend, the reader is referred to the web version of this article).

this ongoing response to the past deglaciations at rates of up to 0.6 mm/year.

The sea level rise illustrated in Fig. 3 represents the average for the past 100 years and is also representative for future change out to at least 2100. Changes in ocean volume during the past century have occurred, from both ongoing mountain deglaciation and thermal warming but the isostatic response to the former have been ignored for this region since these contributions from the European Alps are small (Estermann et al., 2010). Whether they remain small in the future will depend on the fate of the remaining alpine glaciers.

2.2. Observational sea level database

The data used are from Lambeck et al. (2004), Silenzi et al. (2004), Ferranti et al. (2006), Antonioli et al. (2009), Simeoni and Masucci (2009) and from Scicchitano et al. (2011), Antonioli et al. (this issue), Rovere et al. (this issue), Parlagreco et al. (this issue), Ferranti et al. (this issue), Spampinato et al. (this issue), and Orrù et al. (this issue). The complete observational data set, along with the isostatic predictions, are given in Appendix 2 and 3, online version. Appendix 2 gives the Holocene observational data set and Appendix 3 summarizes the elevations of the Llg shoreline. For details on the markers used (Fig. 4), error bars, calibration program and other specifications, please refer to the quoted papers.

Fig. 5 illustrates some representative results of comparisons between observations and the glacio-eustatic predictions. The Versilia Plain is an area of mostly tectonic stability and the agreement is generally within observational uncertainties back to about 9000 years. In particular, the precise estimates based on the *Cerastoderma* sp. lagoonal fossils (the red data points in Fig. 5a) agree well with the predictions. The North Adriatic coast observations, from Venice to Ravenna, lie below the predicted values (Fig. 5c) and are indicative of subsidence, consistent with the Llg occurring well below present sea level. The result for SW Calabria and NE Sicily in Fig. 5b is representative of uplifting areas, with the observed values occurring above the model predictions.

2.3. Italian sea level scenarios for 2100

To provide a range of possible scenarios for the Italian coastal plains in the year 2100, recently published global estimates that span the lower and higher ranges were considered, namely the global estimates for the “low-impact” B1 projection of the IPCC (2007) (the lower sea level rise (SLR) scenario), and the maximum value in Rahmstorf (2007) (higher scenario, see Table 1). As noted before, spatial variability resulting from the non-uniform



Fig. 4. A representative collection of relative sea level markers used. (a) measuring the Roman age fish tanks at Torre Astura La Banca. (b) A Present tidal notch at Lampedusa island Sicily channel. (c) A submerged tidal notch near Trieste, Adriatic sea. (d) Measuring the late-Roman age Basilica of Nora, Sardinia, Tyrrhenian sea. (e) The fish tank of Punta della Vipera, Civitavecchia, Tyrrhenian sea. (f) An uplifted fossil beach at Scilla, Tyrrhenian sea. (g) The MIS 5.5 tidal notch on the Orosei gulf at the altitude of 8 m, Sardinia, Tyrrhenian sea. (h) A Roman age dock, punta Sottile Trieste, Adriatic sea. (i) An uplifted MIS 5.5 terrace, inner margin at 126 m, Scilla, Tyrrhenian sea. (j) A Phoenician age breakwater at Malfatano cape, in Southern Sardinia, Tyrrhenian sea. (k) A Vermetid reef, S. Vito lo Capo, Sicily, Tyrrhenian sea. (l) Uplifted barnacle at Palmi, Calabria, Tyrrhenian Sea. (m) A submerged speleothem, Argentarola island, Tyrrhenian sea.

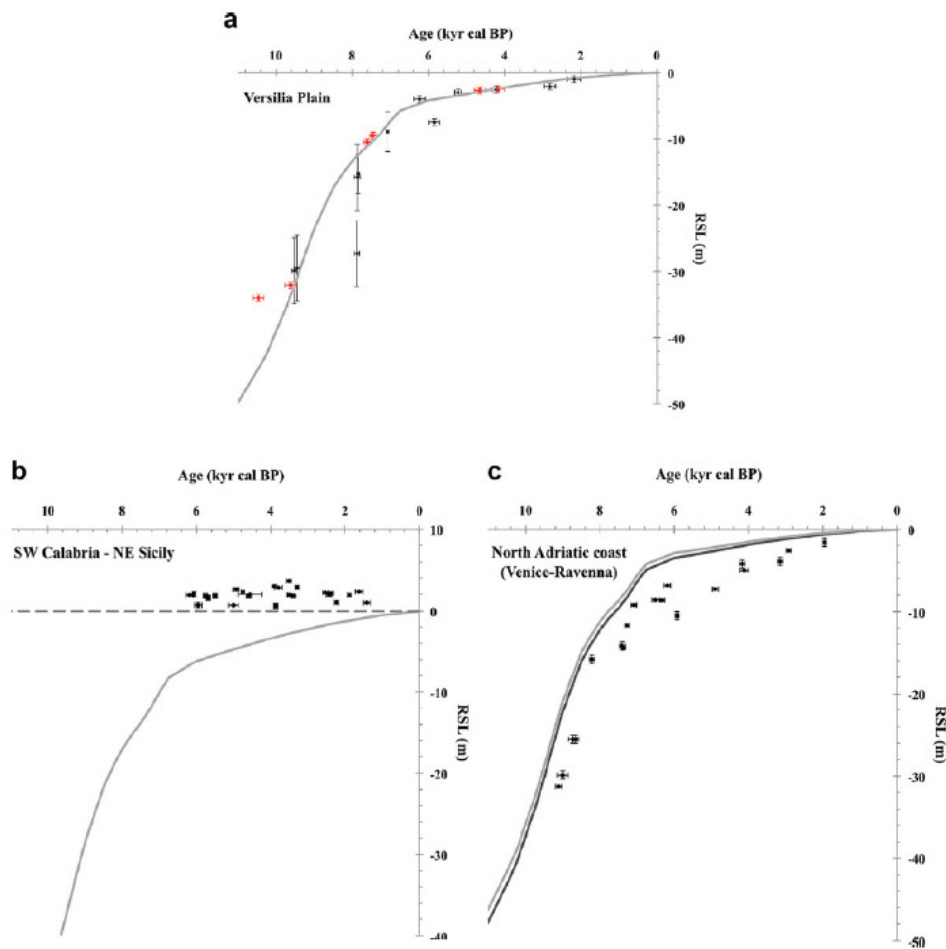


Fig. 5. Representative results of comparisons between observations and the glacio-eustatic predictions. (a) The Versilia Plain as an area of mostly tectonic stability, (b) SW Calabria and NE Sicily which is representative of uplifting areas, (c) the North Adriatic coast from Venice to Ravenna which is affected by strong subsidence.

response of sea level to heat climate change is ignored, simply because current models are inadequate to predict this with confidence.

The B1 IPCC (2007) projection includes thermal ocean expansion and glacier and ice sheet melting in a scenario where carbon dioxide will rise to double the pre-industrial concentration by 2100 (see Mote et al., 2008 for additional considerations). Rahmstorf (2007), by considering that global temperature and SLR variations are strongly correlated, applied a linear model for the 21st century that leads to considerably higher projections than those of the IPCC. This result is used only to be indicative of some of the maximum rates that have been suggested.

The rates for these two different projection scenarios are combined with local isostatic tectonic values, to delineate zones of the Italian coast that will be impacted by marine inundation under one or the other scenario by the year 2100. The Digital Elevation Model (DEM) for the near-shore low-lands of Italy, produced by the National Geologic Survey and National Research Council from the Military Geographic Institute's elevation data, was used. These

projections do not include extreme events, nor changes in the patterns of such events or in local changes in tidal range.

Because of the relative low resolution (cell size 250 m) this DEM model is useful only for identifying regional trends rather than providing high-resolution detailed projections. Nationally, some 33 coastal plains of significant areas are identified that will be susceptible to marine inundation by 2010 under these projections. For some of the most important coastal plains, higher resolution DEM (with cell size 60 m, 40 m, 20 m, 3 m) based on different sources (satellite data, aerial photogrammetry and topographic surveys) were used. Comparison with the coarser DEM model

Table 1
Expected lower and higher sea level rise scenarios for global effects in the year 2100.

Scenario	Annual SLR rate (mm/yr)	SLR yr 2100 AD (mm)
IPCC, 2007-B1	1.8–2.8	180–280
Rahmstorf, 2007	5–14	500–1400

results confirms the results based on the lower resolution data even if in most cases this leads to an overestimation of the extent of some of the susceptible areas.

3. Discussion

3.1. Tectonic rates (MIS 5.5 versus Holocene)

Long-term coastal displacement rates are inferred from the present elevation of markers of the Last Interglacial highstand (MIS 5.5), with a nominal age of 124 ka (Ferranti et al., 2006; Antonioli et al., 2009a, b). This marker is well developed along the coast of the central Mediterranean Sea and offers an excellent opportunity to discern broad patterns of differential displacement within adjacent tectonic sectors of Italy (Fig. 6). At a regional and sub-regional scale, the tectonic implications of the irregular distribution of the MIS 5.5 markers present elevation has been discussed in previous papers (Ferranti et al., 2006; a few additional observations have also been reported in Antonioli et al., 2009a, b). Of interest in the context of the present paper is whether the long-term rates established at the 100 ka scale are confirmed by the compilation of Holocene markers or whether the rates averaged over a few thousand years only are not representative of these longer time scales.

As mentioned above, the Llg position has been used to identify areas of significant vertical tectonic displacement in the past 120,000 years and such areas have not been used in solutions for the earth rheological parameters appropriate for the region. Thus, the observational data can be 'corrected' for the isostatic–eustatic

signals and their comparison with the observed values provides an estimate of tectonic displacement. For locations where there is both Holocene and Llg sea level information it is possible to check whether the long-term average rates from the Llg data are representative of shorter, Holocene, time scales. Holocene uplift rates are calculated for all sites (see Table 2, Fig. 5). In parts of southern Italy the Holocene uplift rates are greater with respect to these long-term uplift rates inferred from the MIS 5.5 highstand (e.g. Lambeck et al., 2004a, b; Antonioli et al., 2006; Ferranti et al., 2008), primarily in southern Calabria and north-eastern Sicily with rates greater than 2 mm/yr (Fig. 5, 6). The pattern of Holocene uplift shows a tail in southern Sicily, in a manner similar to the MIS 5.5 marker (Fig. 6). No Holocene marker indicates the opposite tail along the Ionian Sea coast of southern Italy seen in the MIS 5.5 marker as a progressive decrease in elevation from the Apulia region to the NE (Fig. 6).

Unlike southern Italy, sites in north-eastern Italy are subsiding at rates of 0.5–1 mm/yr. The tectonic subsidence rates estimated from the younger sediments (0–4 ka cal BP) result in higher rates than the average based on the older Holocene (6–11 ka cal BP) which are consistent with the rates inferred from the MIS 5.5 markers (see Fig. 5, 6). This is attributed to compaction of the younger sediments rather than to changes in tectonic subsidence.

Many sites in central Italy, Sardinia and NW Sicily indicate stability or slow subsidence due to glacio-hydro-isostatic movements. A similar pattern is found on the Southern Adriatic coast in Apulia. In these areas, the Holocene and Tyrrhenian vertical displacement rates are strikingly similar. A few anomalies in this general pattern of stability occur. One is in the active volcanic area

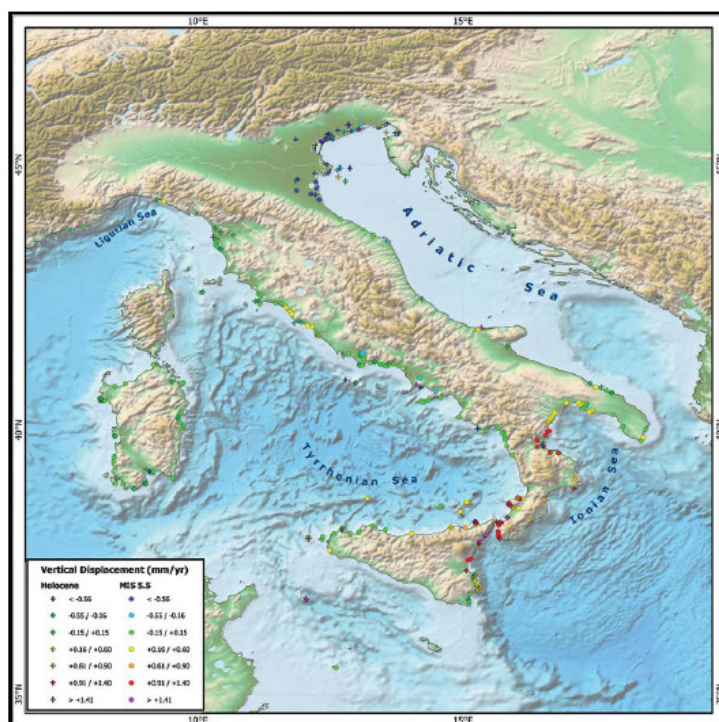


Fig. 6. Rates of vertical movements in Italy (mm/yr) averaged for the Holocene and for the last glacial cycle.

Table 2

Sea level rise (cm) scenario for the year 2100 AD in coastal zones that are susceptible to marine inundation.

Coastal plain	Vertical displacement rate	Vertical displacement for 2100 (isostasy + tectonics mm)	Relative sea level rise for the year 2100 calculated on 2010	
	(isostasy + tectonics mm/yr)		Lower impact scenario IPCC 2007 B1 (+180 mm)	Higher impact scenario Rahmstorf 2007 (+1400 mm)
Albinia	-0.33	-29.7	210	1430
Alento	-0.5	-45	225	1445
Cagliari	-0.6	-54	234	1454
Catania	0	0	180	1400
Cecina	-0.3	-27	207	1427
Coglians	-0.63	-56.7	237	1457
Colostrai-Flumendosa-Murtas	-0.63	-56.7	237	1457
Crati	0.2	18	162	1382
Fondi	-0.4	-36	216	1436
Garigliano	-0.4	-36	216	1436
Gioia Tauro	0	0	180	1400
Grosseto	-0.33	-29.7	210	1430
Burano Lagoon	-0.37	-33.3	213	1433
Lesina	-0.42	-37.8	218	1438
Manfredonia	-0.44	-39.6	220	1440
Metaponto	0.2	18	162	1382
Noto	-0.58	-52.2	232	1452
Oristano	-0.62	-55.8	236	1456
Orsei	-0.63	-56.7	237	1457
Pantani Cuba and Longarini	-0.58	-52.2	232	1452
Pilo	-0.63	-56.7	237	1457
Piombino e Follonica	-0.32	-28.8	209	1429
Po and Veneto-Friuli	-1.5	-135	315	1535
Pontina	-0.44	-39.6	220	1440
Pontina coastal lakes	-0.44	-39.6	220	1440
Porto Pino-Palmas	-0.6	-54	234	1454
Tiber (Rome Plain)	-0.39	-35.1	215	1435
S. Eufemia	0	0	180	1400
Trapani Saltponds	-0.57	-51.3	231	1451
Sele	-0.44	-39.6	220	1440
Tortoli	-0.63	-56.7	237	1457
Versilia	-0.3	-27	207	1427
Volturno	-0.44	-39.6	220	1440

Vertical land movement and sea level rise at year 2100. Columns 2 and 3 give the present rate of vertical land movement and the total land displacements at 2100, respectively, due to isostatic and tectonic contributions.

Columns 4 and 5 give the total relative sea level change due to these contributions and two different climate scenarios.

Assumed are minimum value of eustatic/steric sea level rise of 180 mm, "low-impact" (B1 projections) over the period 2090–2099 (IPCC 2007) and a maximum of 1400 mm (Rahmstorf 2007). In the first case, the tectonic and isostatic contribution are strongly significant on the final results (relative sea level in 2100). In the second case, their contribution are less significant. Tectonic movements are those reported in the figure. For the Po Plain, a maximum value is reported. All these values do not include the contribution of recent soil compaction and fluid (gas and water) withdrawal.

near Naples, with strong subsidence at rates slightly higher than the long-term rates. Another, of isolated uplift, occurs on the Northern shore of Gargano in Apulia that is not seen in the long-term record.

3.2. Future scenarios for the Italian coastal plains in the year 2100

By considering that local sea level change is the sum of global effects, such as thermal expansion and ocean volume increase by glacier and ice sheet melting, and regional or factors such as tectonics, isostatic rebound and local subsidence, low and high estimates for future sea level scenarios along 33 Italian coastal plains in the year 2100 are provided (Table 2, Fig. 7) for both the B1 emission scenario of the IPCC (2007) (180 mm in 2100 AD) and the linear model of Rahmstorf (2007) (1400 mm in 2100 AD). For the B1 scenario, the tectonic and isostatic contributions form a major part of the total projection of the relative sea level rise whereas in the second case of the Rahmstorf model, the projection is dominated by the climate change signal (see Table 2 for results of these projections for the year 2100).

For much of the Italian coast, adding local factors (tectonic and isostasy) to the global climate signal projections for future sea level rise results in an increasing vulnerability of the littoral zones and

coastal plains, with the only exception occurring in south-west Calabria and north-eastern Sicily where the strong positive vertical tectonic movements dominate. Such local effects will play a decisive role on the assessment of coastal vulnerability, particularly for the more probable B1 emission scenario of the IPCC (2007).

Along the northern Tyrrhenian and Ligurian coast of the Italian Peninsula, the sectors potentially vulnerable to the sea level rise in the year 2100 are the Versilia area, the Ombrone River Delta and the Orbetello Lagoon. In the central Tyrrhenian Sea, the sea level rise will impact mainly on the coast near Rome, the southern Latium with its many coastal lakes, the Volturno littoral and the Sele River area. Along the Adriatic coast, in the northern sector Venice, Grado and Marano Lagoons are particularly vulnerable to future sea level rise, even in the absence of additional effects of fluid extraction from the near surface and sediment compaction. For the Central Adriatic coast, wide portions of the inland areas of the Emilia-Romagna sector are potentially vulnerable, including the Marche and Abruzzi coasts where respectively more than 50% and 60% of the beaches are presently subject to erosion, as well as the Lesina and Varano Lakes in Apulia Region. In Sardinia, the most vulnerable areas are the wetland of Cagliari and Oristano. In Sicily, where erosion occurs along more than 400 km of coast, the Trapani and Catania plains are the most vulnerable areas for the next century (Fig. 7).



Fig. 7. Relative sea level rise (year 2100) for 33 Italian coastal plains. For the Po Delta and Venice Plain, mean values are reported. Data do not include the contribution of local compaction and fluid (gas and water) extraction.

4. Conclusion

With the improved glacio-hydro-isostatic rebound model parameters, the predictive model for sea level change that is valid for future centuries provided that no additional processes occur such as, for example, a rapid collapse of Antarctic or Greenland ice. Based on the evidence from sites of long-term tectonic stability, as measured by the elevation of the MIS 5.5 shoreline, this model can be calibrated for the central Mediterranean region and then used to predict sea levels for other locations. Such predictions have been presented here for some 40 representative sites along the Italian coast. Differences between observed and predicted changes can then be interpreted as reflecting vertical tectonic contributions representative of the latter part of the Holocene. Vertical tectonic movements of the Italian coast were estimated at more than 456 sites (211 for the Holocene and 255 from the Last Interglacial, Appendix 1 and 2.

Assuming minimum (180 mm, IPCC, 2007) and maximum (1400 mm, Rahmstorf, 2007) eustatic sea level rise projections, the total projections for sea level by 2100 were calculated, and the coastal zones that are susceptible to marine inundation identified. The principal result is that for the low-rise IPCC prediction the tectonic and isostatic components produce an important impact with values between 162 and 315 mm whereas for the maximum rise of Rahmstorf, it is the climate change induced signal that dominates (1400 and 1535 mm).

Acknowledgements

We thank Mark Siddall and Tiziano Vittori for the useful reviews. This work was supported by the VECTOR project funded by the Italian Ministry of Education, University and Research.

Appendix. Supplementary data

Supplementary data associated with this article can be found in the online version, at doi:10.1016/j.quaint.2010.04.026.

References

- Antonioli, F., D'Orefice, M., Ducci, S., Firmati, M., Foresi, L., Graciotti, R., Perazzi, P., Pantaloni, M. Paolaeogeographic Reconstruction of northern Tyrrhenian coast using archaeological and geomorphological markers at Pianosa Island (Italy). *Quaternary International*, in this issue.
- Antonioli, F., Ferranti, L., Lambeck, K., Kershaw, S., Verrubbi, V., Dai Pra, G., 2006. Late Pleistocene to Holocene record of changing uplift rates in southern Calabria and northeastern Sicily (southern Italy, Central Mediterranean Sea). *Tectonophysics* 422, 23–40.
- Antonioli, F., Anzidei, M., Auriemma, R., Gaddi, D., Furlani, S., Lambeck, K., Orrù, P., Solinas, E., Gaspari, A., Karinja, S., Kovačić, V., Surace, L., 2007. Sea level change during Holocene from Sardinia and northeastern Adriatic (Central Mediterranean sea) from archaeological and geomorphological data. *Quaternary Science Reviews* 26, 2463–2486.
- Antonioli, F., Ferranti, L., Fontana, A., Amorosi, A.M., Bondesan, A., Braitenberg, C., Dutton, A., Fontolan, G., Furlani, S., Lambeck, K., Mastronuzzi, G., Monaco, C., Spada, G., Stocchi, P., 2009a. Holocene relative sea-level changes and vertical movements along the Italian coastline. *Journal of Quaternary International* 221, 37–51.
- Antonioli, F., Amorosi, A., Correggiari, A., Doglioni, C., Fontana, A., Fontolan, G., Furlani, S., Ruggieri Spada, G., 2009b. Relative sea-level rise and asymmetric subsidence in the northern Adriatic. *Rendiconti Online Soc. Geol.*, 34–36.
- Estermann, G., Lambeck, K., McQueen, H.W.S., 2010. Ice-volume changes in mountain glaciers: recent past and future. *Global and Planetary Change*.
- Ferranti, L., Antonioli, F., Amorosi, A., Dai Prà, G., Mastronuzzi, G., Mauz, B., Monaco, C., Orrù, P., Pappalardo, M., Radtke, U., Renda, P., Romano, P., Sansò, P., Verrubbi, V., 2006. Elevation of the last interglacial highstand in Sicily (Italy): a benchmark of coastal tectonics. *Quaternary International* 145, 146, 30–54.
- Ferranti, L., Monaco, C., Antonioli, F., Maschio, L., Kershaw, S., Verrubbi, V., 2008. Alternating steady and stick-slip uplift in the Messina straits, southern Italy: evidence from raised late Holocene shorelines. *JGR* 112, B06401. doi:10.1029/2006JB004473.
- Ferranti, L., Pagliarulo, R., Antonioli, F., Randisi, A. Relative Sea level changes and differential Tectonic motion at the ancient Sybaris (Calabria, southern Italy). *Quaternary International*, in this issue.
- IPCC, 2007. Summary for policymakers. Contribution of Working Group I to the Fourth Assessment Report of the Intergovernmental Panel on Climate Change. In: Solomon, S., Qin, D., Manning, M., Chen, Z., Marquis, M., Averyt, K.B., Tignor, M., Miller, H.L. (Eds.), *Climate Change 2007: The Physical Science Basis*. Cambridge University Press, Cambridge, United Kingdom and New York, NY, USA.
- Lambeck, K., Antonioli, F., Purcell, A., Silenzi, S., 2004a. Sea level change along the Italian coast for the past 10,000 yrs. *Quaternary Science Reviews* 23, 1567–1598.
- Lambeck, K., Anzidei, M., Antonioli, F., Benini, A., Esposito, E., 2004b. Sea level in Roman time in the Central Mediterranean and implications for modern sea level rise. *Earth and Planetary Science Letters* 224, 563–575.
- Lambeck, K., Purcell, A., 2005. Sea-level change in the Mediterranean Sea since the LGM: model predictions for tectonically stable areas. *Quaternary Science Reviews* 24, 1969–1988.
- Lambeck, K., 29 May 2009. A study of the variation of sea level along the Italian coasts. Vector Project Final Report.
- Lambeck, K., Purcell, A., Funder, S., Kjær, K., Larsen, E., Möller, P., 2006. Constraints on the Late Saalian to early Middle Weichselian ice sheet of Eurasia from field data and rebound modelling. *Boreas* 35 (3), 539–575.
- Lambeck, K., Purcell, A., Zhao, J., Svensson, N.-O., 2010. The Scandinavian ice sheet: from MIS 4 to the end of the Last Glacial Maximum. *Boreas* 39 (2), 410–435.
- Mote, P., Petersen, A., Reeder, S., Shipman, H., Whitely Binder, L., 2008. Sea level rise in the coastal waters of Washington State. A report by The University of Washington Climate Impacts Group and the Washington Department of Ecology, pp. 11.
- Nisi, M.F., Antonioli, F., Dai Pra, G., Leoni, G., Silenzi, S., 2003. Coastal deformation between the Versilia and the Garigliano Plains (Italy) since the Last Interglacial stage. *Journal of Quaternary Science* 18 (8), 709–721.
- Orrù, P., Puliga, G., Deiana, G., Solinas, E. Palaeoshorelines of the historic period, Sant'Antioco Island, south-western Sardinia (Italy). *Quaternary International*, in this issue.
- Parflegreco, L., Mascioli, F., Miccadei, E., Antonioli, F., Gianolla, D., Devoti, S., Leoni, G. Holocene Relative Sea Level Rise along the Abruzzo coast (western central Adriatic). *Quaternary International*, in this issue.
- Rahmstorf, S., 2007. A semi-empirical approach to projecting future sea-level rise. *Science* 315, 68–370.
- Rovere, A., Antonioli, F., Enei, F., Giorgi, S., 2011. Relative sea level change at the archaeological site of Pyrgi (Santa Severa, Rome) during the last seven millennia. *Quaternary International* 232, 82–91.
- Scicchitano, G., LoPresti, V., Spampinato, C.R., Morticelli, M.G., Antonioli, F., Auriemma, R., Ferranti, L., Monaco, C. Millstones as indicators of relative sea level changes in northern Sicily and southern Calabria coastlines. *Quaternary International*, in this issue.
- Silenzi, S., Molinaro, A., Devoti, S., Nisi, M.F., Zarattini, A., 2004. Underwater geomorphological survey of Palmarola Island (Tyrrhenian Sea, Southern Latium): Holocene coastal evolution and neotectonic evidences. *Quaternaria Nova* 8, 229–246.
- Simeone, M., Masucci, P., 2009. Analisi geoarcheologiche nell'Area Marina Protetta Parco 522 Sommerso di Gaiola (Golfo di Napoli). *Il Quaternario. Ital. J. Quat. Sci.* 22 (1), 25–32.
- Spampinato, C.R., Monaco, C., Costa, B., DeGuidi, G., DiStefano, A., Scicchitano, G. The contribution of tectonics to relative sea-level change during the Holocene in south-eastern Sicily coastal area: new data from bore-holes. *Quaternary International*, in this issue.

Annex 3
(18 pages)

Abstract - In any discussion of the evolution of a river basin, the history of sea level change is important since river gradients and delta developments are strongly influenced by local sea level. Also, sea level provides a reference for inferring past vertical tectonic stability from the geological record. Hence it is appropriate that the discussion on the Tiber basin starts with sea level change along the Tyrrhenian coast during the Holocene.

Kurt Lambeck, Fabrizio Antonioli, Marco Anzidei. Sea level change along the Tyrrhenian coast from early Holocene to the present. Accademia Nazionale dei Lincei, Atti dei convegni Lincei, 254, IX Giornata mondiale dell'acqua, Il bacino del Tevere, Roma, 2010.

ACCADEMIA NAZIONALE DEI LINCEI

ATTI DEI CONVEGNI LINCEI

254

IX GIORNATA MONDIALE DELL'ACQUA

IL BACINO DEL TEVERE

(Roma, 23 marzo 2009)



ROMA 2010
SCIENZE E LETTERE
EDITORE COMMERCIALE

© by Accademia Nazionale dei Lincei

*Si ringrazia la «Associazione Amici dell'Accademia dei Lincei»
per la collaborazione offerta alla edizione del presente volume*

ISSN: 0391-805X
ISBN: 978-88-218-1020-6

FINITO DI STAMPARE NEL MESE DI OTTOBRE 2010

Antica Tipografia dal 1876 S.r.l. – 00186 Roma, Piazza delle Cinque Lune, 113

Azienda con Sistema Qualità certificata ISO 9001 – 14001

KURT LAMBECK^(a), FABRIZIO ANTONIOLI^(b), MARCO ANZIDEI^(c)

SEA LEVEL CHANGE ALONG THE TYRRHENIAN COAST FROM
EARLY HOLOCENE TO THE PRESENT

INTRODUCTION

In any discussion of the evolution of a river basin, the history of sea-level change is important since river gradients and delta developments are strongly influenced by local sea level. Also, sea level provides a reference for inferring past vertical tectonic stability from the geological record. Hence it is appropriate that the discussion on the Tiber basin starts with sea level change along the Tyrrhenian coast during the Holocene.

The past evidence for sea level comes from inferences of the position of the sea surface with respect to the present. Hence it is a relative measure; a function of both the changing position of the ocean surface and of the land surface or an integrated measure of changes in ocean volume, land movement and redistribution of water within the ocean basins. The observation therefore contains information on all the processes that change these surfaces: on geophysical, glaciological and oceanographic processes.

A consequence is that sea levels have a memory of the past. One process is the changing ice volume on the continents during glacial cycles. Because of the mantle viscosity the planet continues to deform long after deglaciation has ended and the 'glacial isostatic' signal is still very much in evidence today – not only in the formerly glaciated regions but also in areas far from the past ice sheets. The present-day tectonic movements of the land surface have their origins in the past evolution of the planet's interior and

^(a) Research School of Earth Sciences – Australian National University – CANBERRA, ACT 0200, Australia.

^(b) ENEA – Special Project Global Change – Via Anguillarese, 301 – 00060 S. MARIA DI GALERIA (Rome).

^(c) Istituto Nazionale di Geofisica e Vulcanologia – Via di Vigna Murata, 605 – 00143 ROME.

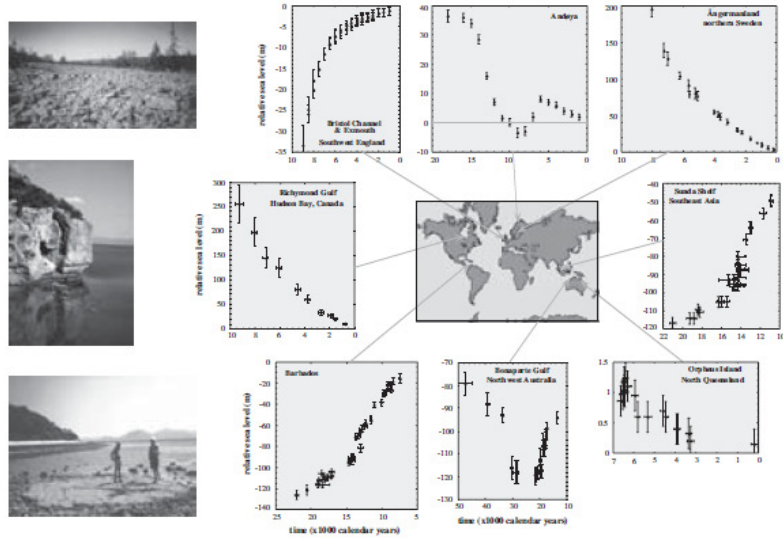


Fig. 1 – Observations of sea level change in different parts of the world from what are believed to be tectonically stable areas. The time scale is in 1000 years and is not the same for all sites. The vertical scale is the relative sea-level change in meters. This scale is not the same for all sites. The three illustrations on the left indicate some of the geological evidence on which the sea level curves have been constructed. Top: A boulder beach in northern Sweden which is now at ~200 m above sea level but which formed about 10000 years ago. Middle: Uplifted erosion notches in the Gulf of Corinth. The highest notch is about 3 m above sea level and dates from ~ 5000 years ago. This example indicates rapid uplift as a consequence of seismic activity. Bottom: A fossil coral colony that is now above its growth limits by about 1.5 m and which dates at ~ 6000 years before present. This example is from Orpheus Island on the Great Barrier Reef of Australia. Other ‘micro-atolls’ from the same area indicate that here sea level has been falling slowly for the past 60000 years.

what we see today was pre-ordained millions of years back in time, in the Italian case, largely by the convergence of the African and European continents. On a shorter time scale, the sea surface response to thermal pulses is not instantaneous, reflecting the convective time constants of the oceans.

Another important general point is that the sea level change is not spatially uniform. On the short term there are dynamic ocean effects from winds and currents. On the longer term the ocean is an equipotential surface and changes as the gravity field is modified by any redistribution of mass within the planet and on its surface. Also, land movements are spatially variable. Together, this results in a complex spatial pattern of sea-level

change, as well as the time-dependent pattern, and this is well documented in the geological record even in the absence of vertical tectonic movements (Fig. 1) (Lambeck and Chappell, 2001). If this is true for the past, then it will also be true for present and future change and a description of the change by a single number is of limited value.

To reiterate, sea level has changed relative to the land for as long as there have been oceans due to geological processes that change the ocean-basin configurations and cause land movements; to the glaciological cycles of more recent geological time, that cause changes in ocean volume, in the gravity field and in the shape of the 'solid' surface; and to oceanographic and climate forcing. These changes at any time are not uniform over the surface and they are on-going. Thus the old truism, that we must learn from the past to understand the future is valid for sea level studies because part of what we measure today has its origins in the past and provide the 'natural' background signals upon which any 'climate change' signals will be superimposed.

The consequences of this change have been felt on the human time scale from the time man started the journey out of Africa. At periods of low sea level landbridges formed or waterways were much restricted in width such that most of the major land masses could be reached without losing sight of land. At times of rapidly rising sea levels coastal communities in middle and low latitudes were systematically threatened by the encroaching sea and ultimately inundated, giving rise to the various flood legends (Lambeck, 1996) and to the separation of groups of people from their ancestors by water bodies too wide to be crossed as, for example the separation of Tasmania from mainland Australia (Lambeck and Chappell, 2001). In some regions the rising sea supplied the sediments for accretion of the coastal zone, particularly with human assistance such as in the Netherlands. In other regions, the sea reached above its present level, such as in the Pacific at ~ 6000-4000 years ago, creating the atoll islands that today are under renewed threat from sea-level rise.

SEA LEVEL CHANGE DURING GLACIAL CYCLES

In the absence of tectonics the principal driver of sea level change during quaternary time has been climate with the growth and decay of the land-based ice sheets following the planetary rhythms. This description is provided by the glacio-hydro isostatic theory for the deformation of the earth and of its gravity field under time-dependent and spatially realistic surface loads of ice and water.

This theory includes the following components (Cathles, 1975; Peltier, 1998; Lambeck and Johnston, 1998):

- As an ice sheet grows it takes water out of the ocean by an amount, if distributed uniformly over the ocean, referred to as the ice-volume equivalent sea level change. In the absence of any other processes affecting ocean volume it equates to eustatic sea level change. When the ice sheet melts, the melt water is added into the oceans. The ice sheets growth and decay is constrained by geological evidence for ice margin location through time and by ice thickness estimates based on geological evidence (rarely) or on glaciological models (more often).
- As the ice sheet grows or decays the gravitational attraction between ice and water is modified and the sea surface follows the new equipotential surface. This modifies the water distribution within the ocean basin. This changed water load in turn modifies the mass distribution and the gravitational potential. The meltwater is distributed into realistic descriptions of the ocean basins.
- Under the changing ice load the load stresses are transmitted via the lithosphere to the mantle which induces mantle flow away from the stressed areas and subsidence of the crust beneath and in the immediate vicinity of the ice. Hence the gravity field is further modified and there is an additional feedback to sea-level change.
- The water added or removed from the oceans modifies the ocean-load stress and hence the mantle stress field. This induces further mantle flow, surface deformation, gravity change and sea level modification.
- During the rise and fall of sea level the ocean basins deform and the basin margins migrate adding further complexity to the feedback process.
- Finally, with the mass redistribution the planet's inertia tensor is modified, changing thereby its rotation and centrifugal force and hence the equipotential surface.

To quantify the theory, the Earth's response functions must be known - its elasticity and viscosity structure - as must the history of the ice movements. Neither is particularly well known and will be partly constrained by observations of the sea level itself. Thus sea level change data from within the former ice margins are sensitive primarily to the ice thickness and mantle rheology, whereas sea-level observations far from the former ice margins are particularly sensitive to the total amount of ice added or removed from the oceans at any time. By a selective analysis of sea level data from different locations around the globe it becomes possible to develop an internally consistent description of the rheology and ice parameters that are consistent with the patterns of sea level, as recorded in Fig. 1, for example.

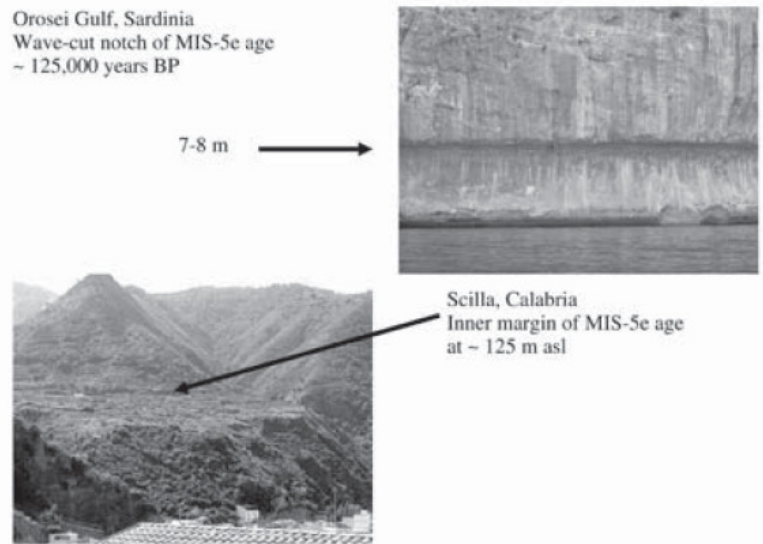


Fig. 2 – Two examples of the Last Interglacial (~125,000 years ago) shoreline location.

SEA LEVEL CHANGE ALONG THE ITALIAN COAST

For Italy, the past sea levels are the result of two main processes: the tectonic evolution of the Mediterranean region as a whole, and the response of the sea and the land to the glacial cycles. The tectonic influence is significant in some localities, as illustrated in Fig. 2. The erosion notch seen in the Gulf of Orosei in Sardinia formed during the Last Interglacial, at ~ 125,000 years ago, when sea levels globally were only a few meters above their present value and this area is believed to be tectonically stable to a high degree (Antonioli *et al.*, 2007). The elevated inner margin of the Last Interglacial sea in Calabria, in contrast, is at ~ 170 m above sea level and this is clearly a region of turmoil (Ferranti *et al.*, 2006). Sea level data from Sardinia will provide information on the glacial signal and data from Calabria will provide information on this and the tectonic signal. With the proviso that we can extrapolate the glacial signal from Sardinia to Calabria then the tectonic movements at this latter site can be established. This requires the quantitative theory for how the ocean and land surfaces respond to the glacial cycle and the parameters that define the ice history and the earth rheology.

For Italy, the main components of the glacial-cycle signature since the time of the last glaciation, are (Lambeck *et al.*, 2004a):

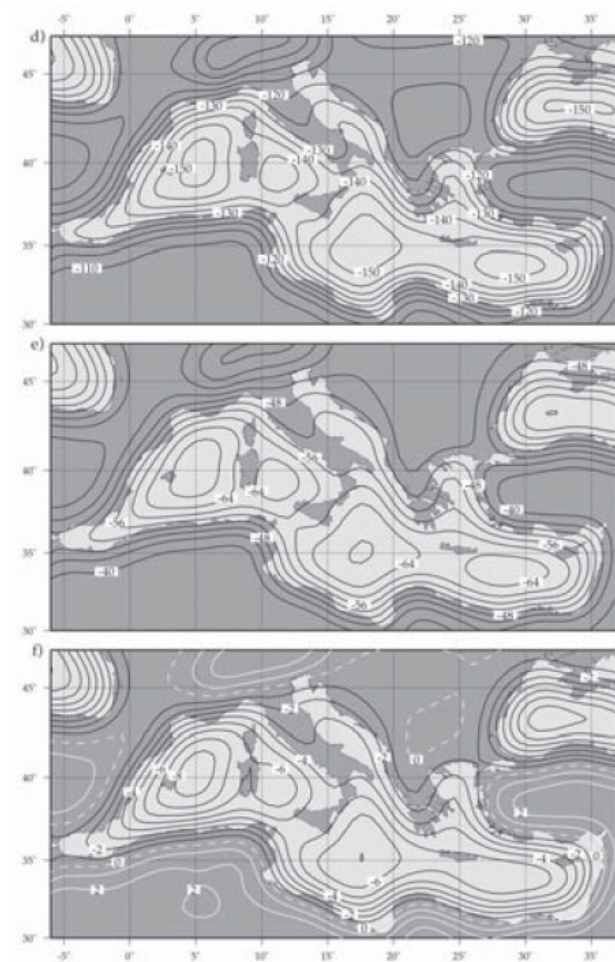


Fig. 3 – Predicted sea levels for the Mediterranean at three epochs. Top: 20,000 years before present (BP); Middle, 12,000 years BP; Bottom (6000 years BP).

- The ice-volume equivalent sea level signal, the globally average and spatially independent measure of ice-volume change.
- The mantle response to the deglaciation of the northern ice sheets (Eurasia, North America, Greenland) which in these cases is manifested by a slow subsidence of the crust of a broad uplifted zone that developed around the ice sheets during the ice sheet growth.

- The sea-floor response to the influx of meltwater into the Mediterranean basin.
- A contribution in the north from Alpine deglaciation.

Secondary effects include the contributions from Antarctic melting and from the glaciation-induced changes in planetary rotation. Nominal predictions of the total change are illustrated in Fig. 3 (Lambeck and Purcell, 2005). They show the spatial variability largely due to the water loading effect (120 m of meltwater added into the oceans if regionally isostatically compensated by the lithosphere would result in a sea floor subsidence of about 35m in the middle of a large basin and about half that amount at the basin margin). Visually this pattern largely masks the regional northerly to southerly trend from the mantle response to the ice sheet deglaciation but it can be seen in the asymmetry in the zero contour at 6000 years BP at the north and south margins of the Mediterranean, for example. Patterns such as these are substantiated by comparison with observational data across the region as well as for other parts of the world and the theory provides a good framework for discussing sea level along the Italian coast line.

The process for testing the model is then as follows:

- Schematically we define the relative sea level as

$$\Delta\zeta_{\text{rsl}} = \Delta\zeta_{\text{esl}} + \Delta\zeta_{\text{e}} + \Delta\zeta_{\text{T}}$$

where $\Delta\zeta_{\text{rsl}}$ is the (observed) sea level change, $\Delta\zeta_{\text{esl}}$ is the ice-volume equivalent sea level change, $\Delta\zeta_{\text{esl}}$ is the total isostatic signal (ice and water load, deformation and gravitation, and rotational changes), and $\Delta\zeta_{\text{T}}$ is the tectonic component.

- We adopt the null hypothesis that there are areas of vertical tectonic stability, even within Italy, based on the evidence of the elevation of the Last-Interglacial shoreline and on the historical record of seismicity, or absence of seismicity.
- We use sea level data from these areas to test the models and infer model Earth-model parameters (E) that describe best the agreement between observations and predictions.
- We calculate the isostatic corrections $\Delta\zeta_{\text{I}}$ and the $\Delta\zeta_{\text{esl}} = \Delta\zeta_{\text{rsl}} - \Delta\zeta_{\text{I}}$ for the observation sites and epochs where we believe tectonic stability is plausible.
- If the $\Delta\zeta_{\text{rsl}}$ agree with expected values from analyses outside of the Mediterranean where we have greater confidence in the stability assumption, or where we can correct for it, then we accept the null hypothesis. Otherwise we calculate the tectonic component $\Delta\zeta_{\text{T}} = \Delta\zeta_{\text{rsl}}(\text{obs}) - (\Delta\zeta_{\text{I}} + \Delta\zeta_{\text{esl}})$.

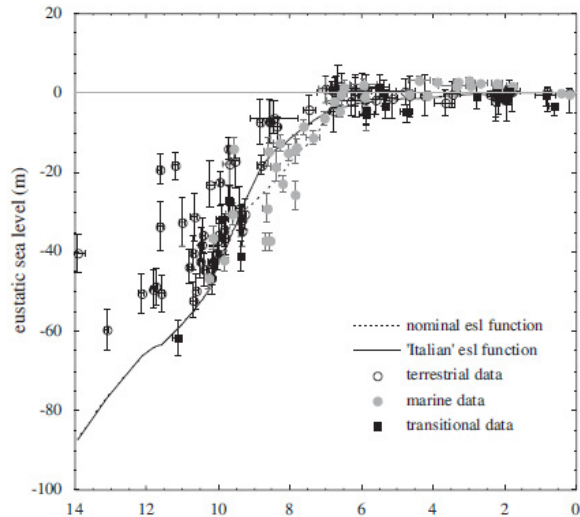


Fig. 4 – Comparison of the ‘reduced’ observational data, the $\Delta\zeta_{\text{esl}}$ estimates with the global $\Delta\zeta_{\text{esl}}$ function (the dashed line). The open circle markers correspond to terrestrial data points and should lie above the $\Delta\zeta_{\text{esl}}$ function. The grey markers refer to material formed below sea level and should lie below this function. The solid black square points are believed to have been formed in the intertidal zone and should, therefore, lie on the red-dashed line. The error bars include both the observational uncertainties and the uncertainties of the model predictions.

The observational evidence for sea level change is from both archaeological and geological sources. The latter are mainly from sediments that were deposited in shallow marine waters or in a terrestrial or supra-tidal environment. As such they form limiting values: terrestrial sediments found at -10 m indicate that sea levels were below this level at the time of deposition. The ages of deposition are determined from radiocarbon dating with the ages calibrated to a uniform time scale.

By way of illustration, Fig. 4 is a preliminary result based on a 2004 compilation of Italian sea level data (Lambeck *et al.*, 2004a). The areas of assumed tectonic stability are the Tyrrhenian coast with the exception of the Naples area, Puglia, western and southeastern Sicily, Sardinia and the Gulf of Genoa (Ferranti *et al.*, 2006). Agreement between observations and predictions for data within these localities is generally satisfactory when the uncertainties of both the observations and the predictions are taken into consideration. Around 8000 years ago there is however, some systematic discrepancy between the observed and predicted with marine data points

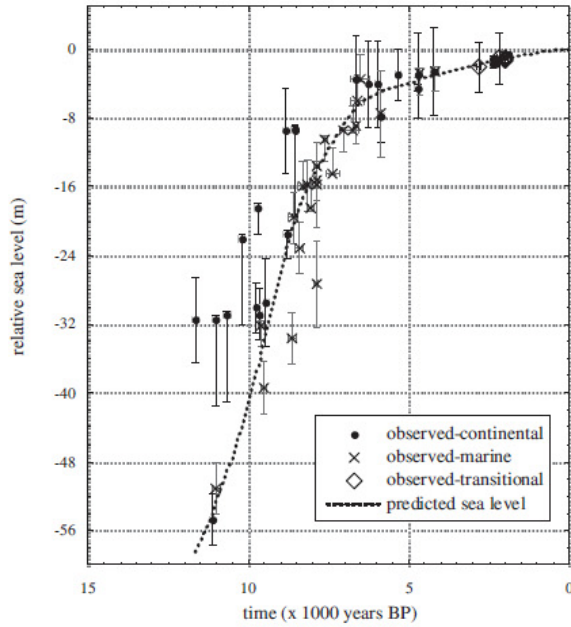


Fig. 5 – Predicted (dotted line) and observed sea level reduced to Roma-Tiber, from continental, marine and transitional data.

lying above their expected limits, and that leads us to conclude that the ice volume equivalent sea-level function $\Delta\zeta_{\text{esl}}$ may need some refinement. The nominal function used in this analysis is not in fact well constrained for this time, the emphasis of the original solution being on the earlier period, and from more recent evaluations, as yet unpublished, we conclude that the 'Italian' $\Delta\zeta_{\text{esl}}$ gives a better representation for this interval. We conclude that within the observational and model uncertainties that the assumption of tectonic stability for the selected sites is valid.

For the coastline at the mouth of the Tiber we are interested in obtaining a 'best' sea level curve that is representative of this area. This zone is affected by continuous sedimentation that has caused the coastline to advance up to modern times (Bencivenga *et al.*, 1995; Bellotti *et al.*, 1994). There are some observations from core sites near Roma airport but generally there is insufficient data to observationally construct a sea-level function. Instead we use observational data from a number of regional sites (at locations ϕ and epochs t) to calculate the differential isostatic corrections



Fig. 6 – Roman epoch indicators of sea level. *Top-left*: Remains of fish tank at La Banca. The outer wall foundations that protected the tanks from wave action are clearly visible. The inner walls arising above sea level represent the highest level of the footwalks that now surround the submerged tanks. *Top-right*: The Roman epoch harbour at Ventotene where the footwalks are now submerged. *Lower-left*: The insitu sluice gate at La Banca. *Lower-right*: Detail of the submerged sluicegate within the pool complex at Ventotene. By establishing sea level for the Roman epoch from this sluicegate the original elevation of the footwalks at Ventotene can be established.

$$\varepsilon_{\zeta_1}^{\zeta} = \Delta\zeta_1(\phi, t) - \Delta\zeta_1(\text{ref}, t)$$

between these sites and a reference location (*ref*, *t*) within the Tiber plain, and then calculate the ‘reduced’ observational value for the reference site – the value that would have been observed if site *f* coincided with the reference site. That is

$$\Delta\zeta_{\text{obs}}(\text{ref}, t) = \Delta\zeta_{\text{obs}}(\phi, t) - \varepsilon_{\zeta_1}(\phi, t)$$

The advantage of this approach is that the isostatic corrections change only gradually along the Tyrrhenian coast such that the differential corrections are more accurate than their absolute values. The result is shown in Fig. 5 and this represents our best estimate of the sea level rise along the coast of Latium for the past 12,000 years, this limit in time being the result of an absence of older observations in the region.

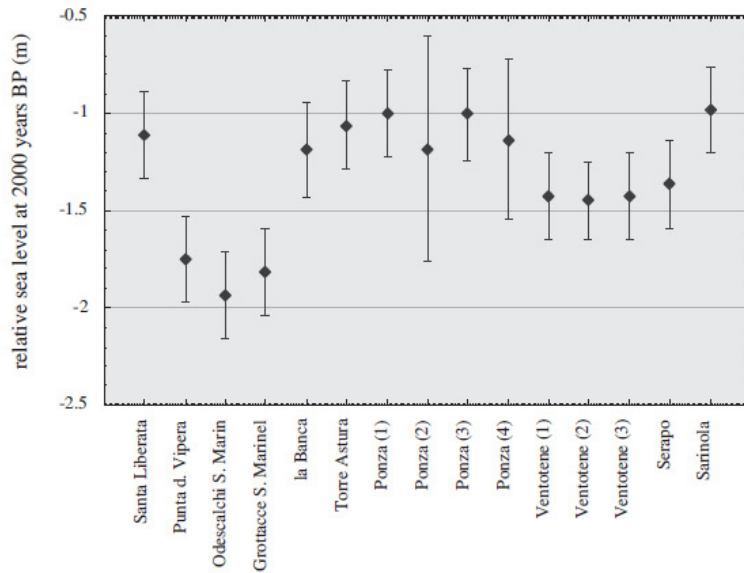


Fig. 7 – The Roman epoch sea level estimates from 15 fish tanks, corrected for tectonics and differential isostasy to reduce all estimates to Torre Astura. Their mean value is an estimate of sea level at this reference site in the absence of vertical tectonics.

SEA-LEVEL CHANGE FOR THE PAST 2000 YEARS

The geological evidence for sea level change for the past 2000-3000 years is generally of relatively low accuracy for this part of the coast but instead we have some high-quality archaeological data within this interval, notably the fish tank information from the Roman epoch of ~2000 years BP. These structures and their functioning have been fully described in the classic literature such that there is not the usual uncertainty associated with archaeological data of having to guess the functionality of the structures. For them to be functional the inlet and outlet channels and sluice gates must lie within the tidal oscillations and because the tidal range is small along much of the Italian coast where these structures are found, the present locations of these features relative to present sea level provide a precise estimate of change (Fig. 7).

The significance of the Roman epoch fish tanks for sea level studies was first recognised by M. Caputo who commissioned the authoritative surveys of Roman epoch fish tanks by Schmiedt (1972) and who made the first attempt to quantify the change in sea level since Roman times (Caputo and

Pieri, 1976). It was noted that for most locations the tanks were no longer functional, sea level having risen to a level where the channels and sluice gates are below sea level. This is an important observation because it should be possible to compare this change with the modern instrumental records to establish whether the latter are representative of a period longer than their actual record. The issue is that these records started mostly in the early twentieth century, so that it is not possible to assess whether the observed signal is part of the natural background signal or related to a human-induced climate change signal whose first impacts can be expected within that century.

Recently we revisited the question of whether we could obtain improved estimates of sea-level change from this archaeological data set, using our improved understanding of the isostatic and tectonic movements to correct the data for isostatic and tectonic contributions. Fig. 7 illustrates the results from 15 fish tanks in which it was possible to identify the channels, the positions of the sluice gates and their posts and sliding grooves, and the levels of the crepidenes (footwalks). They are distributed from near Argentario to Gaeta. Vertical tectonics along this section of the coast, as measured by the elevations of the last interglacial shorelines (formed ~ 125,000 years ago) and as indicated by a relatively low level of seismic activity, are believed to be small (Boschi et al. 1995). Also, the isostatic change over the past 2000 years is nearly constant for these localities so that it becomes possible to predict the differences in isostatic displacements for the sites to considerable accuracy and to reduce the measurements for all sites to a common location, in the same way as done for the geological data.

For the results in Fig. 7, all measurements have been reduced to Torre Astura, have been corrected for tidal differences and the ocean response to atmospheric pressure between the time of observation and the annual mean tide, for tectonics and for differential isostasy. The three anomalous results from Punta della Vipera and Santa Marinella may be the result of tectonics because here the last interglacial shoreline is higher (at ~ 30 m) than for the other sites where it is found at between 4 and 10 m. We have assumed that the uplift has been uniform over the past 125,000 years, whereas these results indicate that this may not have been appropriate. We have kept these numbers, however, with an appropriately large uncertainty to calculate the mean sea level change at Torre Astura over the past 2000 years as a rise of 1.35 ± 0.07 m.

We also analysed the tide gauge records for this section of the coast. There does not appear to be a single continuous record from the late 19th century to the present but we have been able to construct a composite record from overlaps between individual records and by correcting for differential isostasy to reference it to Torre Astura (Fig. 8). From this we conclude that sea level here has been rising at an average rate of 1.56 ± 0.20 mm/year.

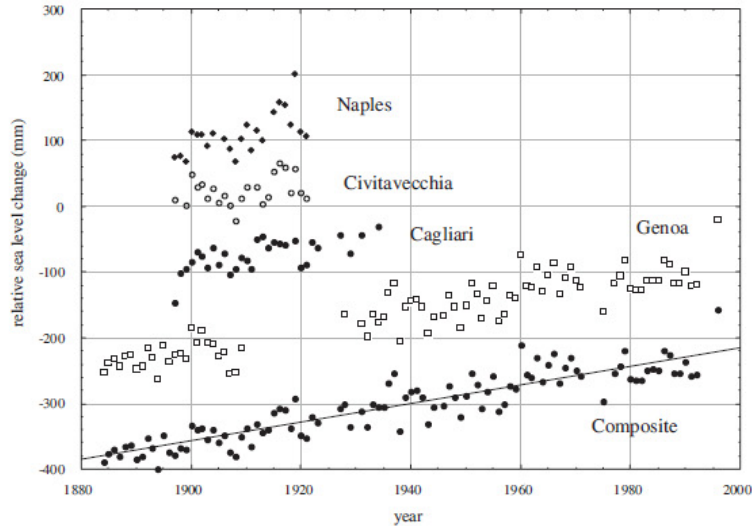


Fig. 8 – Tide gauge (annual mean values) records from four sites. Tectonic corrections have been applied where appropriate. Differential isostatic corrections have been applied to reduce the individual records to the Torre Astura site. The composite record is also shown. This includes the isostatic contribution for this site as well as any eustatic change.

Both the sea-level at 2000 BP and the present rate of change are affected by the isostatic signal from the past deglaciation and over the past 2000 years this signal has not been linear. When corrected for this, the ‘eustatic’ sea level at Torre Astura is 0.13 ± 0.09 m below present and the corrected present day eustatic rate is 1.02 ± 0.21 mm/year⁽¹⁾. Extrapolating this back in time means that the Roman epoch sea level is reached about 100 years ago (Lambeck *et al.*, 2004b). Uncertainties remain large, but the results indicate that the non-isostatic part of the modern observed sea level rise started about 100 years ago.

We are currently revising this work, using improved geological data sets, improvements in the resolution of the numerical modelling, and searching for additional archaeological records but we anticipate that the essential conclusions remain unchanged, that sea levels along the Tyrrhenian coast are - in the absence of tectonics - rising from both the ‘natural’ background signal and from a ‘modern’ signal that may be attributable to climate change.

⁽¹⁾ Strictly this contribution measures the local effect of recent increases in ocean volume due mainly to recent melting of glaciers and ocean warming. This contribution may vary regionally (see below).

FUTURE CHANGE

What the past record has shown is that there are natural background signals in sea level against which any ‘human-induced’ signals must be measured. A principal part of this background signal is the glacio-hydro-isostatic contribution that for Italy is not insignificant and that results in a rising future sea level even if there is no further climate-signal contribution. This rise is predictable with a high degree of confidence that can be improved by examining the past geological and archaeological records and by understanding the deglaciation history of the now-gone ice sheets and ice caps. For northern Italy, the influence from the Alpine deglaciation is not unimportant (Lambeck and Purcell, 2005). The other component of the natural signal is the tectonic one (we include subsidence by sediment compaction and sediment loading). This is less predictable and some analyses of sea-level change on different geological time scales indicate that the rates of vertical movement have not been constant. Forward prediction of these tectonic effects are no better than the prediction of earthquake activity. But the geological record does reveal which areas are particularly prone to vertical movement. The spatial scale of the tectonic movements is generally much shorter than that of the isostatic change and a greater density of field data is desirable in order to develop an improved understanding of these contributions to the land stability and to the relative sea-level change. (In some areas the tectonic contribution may be dominated by the consequences of sediment discharge from river systems and predictive models for this can be developed with some confidence.)

Two contributions to the ‘human-induced’ sea level signals must be recognised. One is land movements caused by extraction of fluids from the near-surface crust and this is essentially a local problem for local resolution. The other is the signal introduced by global warming, through thermal expansion of the oceans, melting of mountain glaciers and polar ice caps, and changes in the surface and ground water storage (Church *et al.*, 2001; Church *et al.*, in press). Estimates for these contributions are all still of low accuracy and are not yet at a point where they can unequivocally explain what is occurring today. We do not therefore address this contribution here but we do make one observation. Just as in the past, sea level has varied spatially so will it do so in the future. This is because of the earth’s response to changes in the surface loads as water is added to or removed from the oceans and because of the ocean’s response to the changing heat content within it. Both are capable of realistic evaluation under different climate scenarios provided that quality observations systems exist for calibrating and fine-tuning these evaluations through the time ahead.

ACKNOWLEDGEMENTS – This work has been supported by the VECTOR project funded by the Italian Ministry of Education, University and Research, by ENEA and INGV, and by the Australian Research Council and the ANU.

REFERENCES

- ANTONIOLI F., ANZIDEI M., LAMBECK K., AURIEMMA R., GADDI D., FURLANI S., ORRÙ P., SOLINAS E., GASPARI A., KARINJA S., KOVAČIĆ V., SURACE L., 2007. *Sea-level change during the Holocene in Sardinia and in the northeastern Adriatic (central Mediterranean Sea) from archaeological and geomorphological data*. *Quaternary Science Reviews*, 26, 19-21: 2463-2486.
- BELLOTTI P., CHIOCCI F.L., MILLI S., TORTORA P., VALERI P., 1994. *Sequence stratigraphy and depositional setting of the Tiber delta: integration of high-resolution seismics, well logs and archeological data*. *Journal of Sedimentary Research*, 64: 416-432.
- BENCIVENGA M., DI LORETO E., LIPERI L., 1995. *Il regime idrologico del Tevere, con particolare riguardo alle piene nella città di Roma*, *Memorie Descrittive della Carta Geologica d'Italia*, 50: 125-172.
- BOSCHI E., FERRARI G., GASPERINI P., GUIDOBONI E., SMIRIGLIO G., VALENISE G., (eds.) 1995. *Catalogo dei Forti Terremoti in Italia dal 461 a.C. al 1980*. 973 pp., ING, Roma – SGA, Bologna.
- CAPUTO M., PIERI L., 1976. *Eustatic variation in the last 2000 years in the Mediterranean*. *Journal of Geophysical Research*, 81: 5787-5790.
- CATHLES L.M., 1975. *The Viscosity of the Earth's Mantle*. 386 pp. Princeton University Press, Princeton.
- CHURCH J.A., GREGORY J.M., HUYBRECHTS P., KUHN M., LAMBECK K., NHUAN M.T., QIN D., WOODWORTH P.L., 2001. Changes in Sea Level. In: J.T. HOUGHTON, Y. DING, D.J. GRIGGS, M. NOGUER, P.J., VAN DER LINDEN, X. DAI, K. MASKELL, C.A. JOHNSON (eds.), *Climate Change 2001: The Scientific Basis. Contribution of Working Group 1 to the Third Assessment Report of the Intergovernmental Panel on Climate Change*. Cambridge University Press, Cambridge: 641-693.
- FERRANTI L., ANTONIOLI F., MAUZ B., AMOROSI A., DAI PRA G., MASTRONUZZI G., MONACO C., ORRÙ P., PAPPALARDO M., RADTKE U., RENDA P., ROMANO P., SANSÒ P., VERRUBBI V., 2006. *Markers of the last interglacial sea-level high stand along the coast of Italy: Tectonic implications*. *Quaternary International*, 145-146: 30-54.
- LAMBECK K., 1996. *Shoreline reconstructions for the Persian Gulf since the last glacial Maximum*. *Earth and Planetary Science Letters*, 142: 43-57.
- LAMBECK K., ANTONIOLI F., PURCELL A., SILENZI S., 2004a. *Sea-level change along the Italian coast for the past 10,000 yr*. *Quaternary Science Reviews*, 23: 1567-1598.
- LAMBECK K., ANZIDEI M., ANTONIOLI F., BENINI A., ESPOSITO A., 2004b. *Sea level in Roman time in the Central Mediterranean and implications for recent change*. *Earth and Planetary Science Letters*, 224: 563-575.
- LAMBECK K., CHAPPELL J., 2001. *Sea Level Change through the last Glacial Cycle*. *Science*, 292: 679-686.
- LAMBECK K., JOHNSTON P., 1998. *The viscosity of the mantle: Evidence from analyses of glacial rebound phenomena*. In: I. JACKSON (ed.), *The Earth's mantle: Composition, structure, and evolution*. Cambridge University Press, Cambridge: 461-502.

- LAMBECK K., PURCELL A., 2005. *Sea-level change in the Mediterranean Sea since the LGM: model predictions for tectonically stable areas*. *Quaternary Science Reviews*, 24: 1969-1988.
- PELTIER W.R., 1998. *Postglacial variations in the level of the sea: implications for climate dynamics and solid-earth geophysics*. *Reviews of Geophysics*, 36, 4: 603-689.
- SCHMIEDT G., 1972. *Il livello antico del mar Tirreno, Testimonianze da resti archeologici*. 323 pp. E. Olschki, Firenze.
- World Climate Research Project to be published. CHURCH J., WOODWORTH P., WILSON S., AARUP T. (eds.), *Sea-level Rise and Variability*. Blackwell Publishing. (in press).

Annex 4

(8 pages)

Abstract - along the Turkish coasts of the Gulf of Fethye (8 sites), and Israel, between Akziv and Caesarea (5 sites). The structures selected are those that, for effective functioning, can be accurately related to sea level at the time of their construction. Thus their positions with respect to present sea level provide a measure of the relative sea level change since their time of construction. Useful information was obtained from the investigated sites spanning an age range of ~2.3 ~1.6 ka BP. The inferred changes in relative sea level for the two areas are distinctly different, from a rise of 2.41 to 4.50 m in Turkey and from 0 to 0.18 m in Israel. Sea level change is the combination of several processes, including vertical tectonics, glaciohydro-isostatic signals associated with the last glacial cycle, and changes in ocean volume. For the Israel section, the present elevations of the MIS-5.5 Tyrrhenian terraces occur at a few meters above present sea level and vertical tectonic displacements are small. Data from GPS and tide gauge measurements also indicate that any recent vertical movements are small. The MIS-5.5 shorelines are absent from the investigated section of the Turkish coast, consistent with crustal subsidence associated with the Hellenic Arc. The isostatic signals for the Israel section of the coast are also small (ranging from 0.11 mm/yr to 0.14 mm/yr, depending on site and earth model) and the observed (eustatic) average sea level change, corrected for this contribution, is a rise of 13.5 ± 2.6 cm during the past e2 ka. This is attributed to the time-integrated contribution to sea level from a combination of thermal expansion and other increases in ocean volume. The observed sea levels from the Turkish sites, in contrast, indicate a much greater rise of up to 2.2 mm/yr since 2.3 ka BP occurring in a wide area between Knidos and Kekova. The isostatic signal here is also one of a rising sea level (of up to ~1 mm/yr and site and earth model dependent) and the corrected tectonic rate of land subsidence is ~1.48 mm/yr. This is the primary cause of dramatic relative sea level rise for this part of the coast.

M. Anzidei, F. Antonioli, A. Benini, K. Lambeck, D. Sivan, E. Serpelloni, P. Stocchi. Sea level change and vertical land movements since the last two millennia along the coasts of southwestern Turkey and Israel. *Quaternary International*, 2010.
doi:10.1016/j.quaint.2010.05.005



Contents lists available at ScienceDirect

Quaternary International

journal homepage: www.elsevier.com/locate/quaint

Sea level change and vertical land movements since the last two millennia along the coasts of southwestern Turkey and Israel

M. Anzidei^{a,b,*}, F. Antonioli^c, A. Benini^d, K. Lambeck^e, D. Sivan^f, E. Serpelloni^a, P. Stocchi^g

^a Istituto Nazionale di Geofisica e Vulcanologia, via di Vigna Murata 605, 00143 Roma, Italy

^b Università della Calabria, Dipartimento di Fisica, Cosenza, Italy

^c ENEA, Italy

^d Università della Calabria, Dipartimento di Archeologia e Storia delle Arti, Cosenza, Italy

^e Research School of Earth Sciences, The Australian National University, Canberra 0200, Australia

^f Department of Maritime Civilizations and the Leon Recanati Institute for Maritime Studies, School of Marine Studies, University of Haifa, Israel

^g DEOS, Faculty of Aerospace Engineering, TU Delft, Delft, The Netherlands

ARTICLE INFO

Article history:

Available online 19 May 2010

ABSTRACT

This paper provides new relative sea level data inferred from coastal archaeological sites located along the Turkish coasts of the Gulf of Fethye (8 sites), and Israel, between Akziv and Caesarea (5 sites). The structures selected are those that, for effective functioning, can be accurately related to sea level at the time of their construction. Thus their positions with respect to present sea level provide a measure of the relative sea level change since their time of construction. Useful information was obtained from the investigated sites spanning an age range of 2.3–1.6 ka BP. The inferred changes in relative sea level for the two areas are distinctly different, from a rise of 2.41 to 4.50 m in Turkey and from 0 to 0.18 m in Israel. Sea level change is the combination of several processes, including vertical tectonics, glacio–hydro–isostatic signals associated with the last glacial cycle, and changes in ocean volume. For the Israel section, the present elevations of the MIS-5.5 Tyrrhenian terraces occur at a few meters above present sea level and vertical tectonic displacements are small. Data from GPS and tide gauge measurements also indicate that any recent vertical movements are small. The MIS-5.5 shorelines are absent from the investigated section of the Turkish coast, consistent with crustal subsidence associated with the Hellenic Arc. The isostatic signals for the Israel section of the coast are also small (ranging from –0.11 mm/yr to 0.14 mm/yr, depending on site and earth model) and the observed (eustatic) average sea level change, corrected for this contribution, is a rise of 13.5 ± 2.6 cm during the past 2 ka. This is attributed to the time-integrated contribution to sea level from a combination of thermal expansion and other increases in ocean volume. The observed sea levels from the Turkish sites, in contrast, indicate a much greater rise of up to 2.2 mm/yr since 2.3 ka BP occurring in a wide area between Knidos and Kekova. The isostatic signal here is also one of a rising sea level (of up to 1 mm/yr and site and earth-model dependent) and the corrected tectonic rate of land subsidence is 1.48 mm/yr. This is the primary cause of dramatic relative sea level rise for this part of the coast.

© 2010 Elsevier Ltd and INQUA. All rights reserved.

1. Introduction

During past decades, sea level change within the Mediterranean has been estimated from instrumental measurements, as well as from archaeological, geological, and biological indicators (Pirazzoli, 1976; Flemming and Webb, 1986). This paper examines mainly archaeological and geological evidence for the late Holocene

relative sea level change along the coastline of Turkey and Israel (Fig. 1). Geological indicators are a powerful source of information from which the relative sea level change can be estimated for selective periods back to the last interglacial (Ferranti et al., 2008), while the archaeological and instrumental data fill a gap between geological and present time. A particularly good estimate of relative sea level change can be obtained for the last 2 ka from archaeological coastal installations (Lambeck et al., 2004b; Antonioli et al., 2007). The Mediterranean, with its small tidal range and continuous human settlement throughout historical times, has the most complete archaeological record relevant for sea level studies, with a large number of coastal archaeological sites that are often well

* Corresponding author. Istituto Nazionale di Geofisica e Vulcanologia, via di Vigna Murata 605, 00143 Roma, Italy.

E-mail address: marco.anzidei@ingv.it (M. Anzidei).

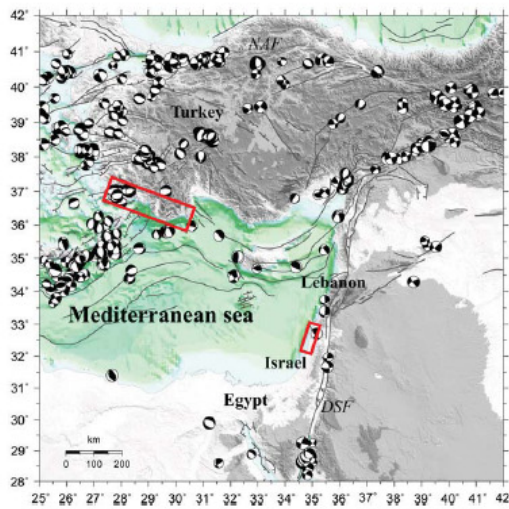


Fig. 1. Current seismicity and focal mechanisms of the studied region (CMT catalogues from: www.globalcmt.org; www.bo.ingv.it/RCMT; www.seismo.ethz.ch/mt). Main faults, the North Anatolian Fault (NAF) and the Dead Sea Fault (DSF) are shown on the map. The detailed maps of Fig. 2 are identified by the red rectangles.

dated and well preserved with functional features that can be precisely related to sea level at the time of their construction. Hence, they can be successfully used to constraint past local sea levels. Fish tanks, piers, docks, pools, quarries, harbors and slipways constructions, generally built around 2 ± 0.3 ka BP are reliable indicators and provide a valuable insight of the regional variation in sea level during the last two millennia (Flemming, 1969; Schmiedt, 1974; Caputo and Pieri, 1976; Pirazzoli, 1976; Flemming and Webb, 1986; Lambeck et al., 2004a,b; Antonioli et al., 2007; Lambeck et al., in press, and references therein).

Local sea level change is a combination of various factors, including changes in ocean volume from the addition or subtraction of water. This includes contributions from temperature changes in the water column and contributions from changes in ice sheets and glaciers. The response of the ocean and the earth to changing ice and water loads, usually referred to as glacio-hydroisostasy, is important, as are vertical tectonic movements of the land surface, local compaction of sediments or changes in meteorological forcing of the ocean surface. Of these, through the nature of the observational data used, subsidence arising from compaction of sediments or from the extraction of ground water is unlikely to be important and the dominant contributions considered here are tectonics and the isostatic factors. The latter have been previously evaluated for Mediterranean sites and the same models and parameters are used here as have previously been found satisfactory (Lambeck, 1995; Sivan et al., 2001; Lambeck et al., 2004a,b; Antonioli et al., 2007; Anzidei et al., 2011). Geological evidence, in the form of the present elevation of the MIS-5e shoreline, along with instrumental data from GPS and tide gauge recordings, has been used to examine tectonic stability of the sites, relevant elements for the understanding of the recent geodynamic evolution of these areas of the Mediterranean basin. These isostatic and tectonic components are then compared with the observed sea levels to establish whether there have been additional changes in local and regional levels.

This paper examines archaeological evidence from the eastern Mediterranean coast of southeastern Turkey and Israel (Figs. 1 and

2a,b), where the development of maritime constructions reached its greatest concentration in Hellenistic and Lycian times (2.3 ka BP) and continued during the Roman and Byzantine ages (2 ka and 1.6 ka respectively). Particularly, the coasts of Israel contains many still very well preserved remains. The best preserved sites provide new information on constructional levels that can be accurately related to mean local sea levels between 2300 and 1600 BP.

2. Geodynamic setting of Eastern Mediterranean

The geological and geodynamic features of Israel and Turkey reflect those of the eastern Mediterranean region, which is subjected to the long-lasting plate convergence between Africa/Arabia and Eurasia (Dewey et al., 1973; Le Pichon et al., 1988; Dewey et al., 1989), active since the Late Cretaceous (DeMets et al., 1994; Calais et al., 2003). The current dynamics of the Africa-Eurasia plate boundary, as delineated by earthquake distribution, runs roughly east-west across the basin and is characterized by narrow to broad seismic belts of seismicity and deformation that result in a complex pattern of crustal stress and strain fields (Jackson and McKenzie, 1988; Rebai et al., 1992; Jiménez-Munt et al., 2003; Vannucci and Gasperini, 2004). The several lithospheric blocks move according to their different structural and kinematic features including subduction, back-arc spreading, rifting, thrusting, normal and strike

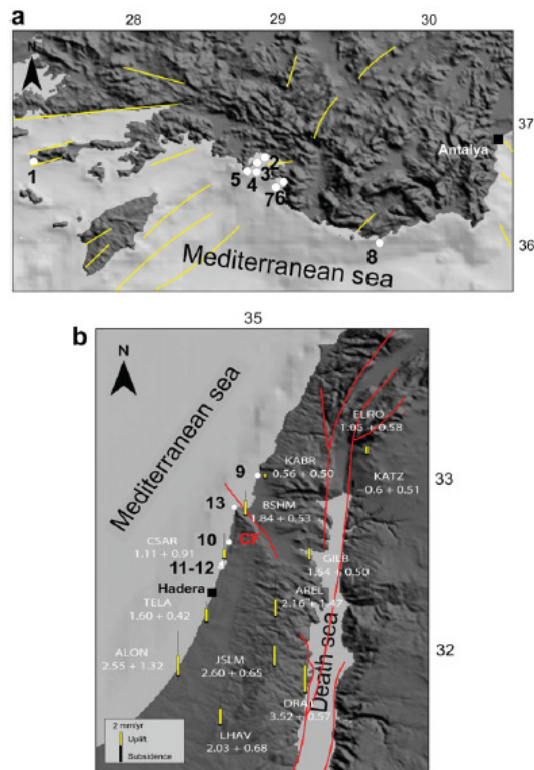


Fig. 2. Investigated sites (white dots with numbers as in Table 1) along the coast of a) Turkey and b) Israel. Yellow lines identify the principal faults. CF is the Carmel Fault. In b) the locations of the tide gauge of Hadera and the GPS network are also shown. Vertical GPS velocities (in mm/y) are estimated for the time span 1998–2008. See also Table 1 for site data.

slip faulting (Jolivet and Faccenna, 2000; Faccenna et al., 2001; Mantovani et al., 2001). In this geodynamic framework, the Anatolia and the Levantine areas are both dominated by the northward motion of the Arabian plate that produces the westward extrusion of the Anatolia peninsula and the two important and still active strike slip fault systems of the Dead Sea in Israel and the North Anatolia in Turkey along which large earthquakes have occurred throughout historical times (Guidoboni et al., 1994; Boschi et al., 1995; www.globalcmt.org; www.bo.ingv.it/RCMT; www.seismo.ethz.ch/mt) (Fig. 1). In addition, the Gulf of Fethye will also be affected by the convergence along the Hellenic arc (McKenzie, 1970; Kalafat et al., 2004; Serpelloni et al., 2007 and references therein), as also reflected in previous estimates of the uplift of Rhodes and Karpathos and further to the north and with subsidence of the eastern part of the Gulf (see Fig. 17b of Lambeck, 1995).

Of importance for the current investigation is the vertical land movement and one indicator of vertical stability is provided by the elevation of the Last Interglacial shoreline. From areas believed to be tectonically stable elsewhere within the Mediterranean, this shoreline usually occurs at 5–7 m above mean sea level and its actual position can therefore be indicative of vertical movements on a time scale of 10^5 years. This shoreline feature, readily identified by sediments containing *Strombus bubonius* and other Senegalese fauna, has not been identified within the Fethye area, and its absence is consistent with a continuous broad subsidence of this region, in agreement with independent observations which estimate subsidence trends in the Gulf of Gökova (Uluğ et al., 2005) and at Gemile Island (Lambeck, 1995).

Previous research along the Israel coast has identified Last Interglacial fossil deposits at between 12 and 2 m above present sea level (Sivan et al., 1999; Galili et al., 2007), and this has been used to argue for a tectonically stable coast (Sneh, 2000; Galili et al., 2007). The stratigraphic relationship of these particular deposits to coeval sea level is not well known, and tectonic stability can only be assumed to within ± 5 m over the past 120,000 years, yielding a vertical tectonic rate of ± 0.04 mm/yr. Inland from the coast, the vertical tectonics are likely to become increasingly dominated by deformation along the Dead Sea Fault.

3. Instrumental data

There are 6 tide gauge stations along the Mediterranean coast of Turkey but only the station of Antalya (Fig. 2a) is located near the investigated archaeological sites. For Israel, there is the Hadera tide gauge station, south of Caesarea (Fig. 2b). The data used from these sites are from the Permanent Service for Mean Sea Level (PSMSL) (Woodworth and Player, 2003; www.pol.ac.uk/psmsl/). The time series records for both Antalya and Hadera (Fig. 3), are too short (<20 years, with missing years for the former, and 11 years with two missing years for the latter) to provide significant estimates for long-term trends, although the record for Antalya points to a rising sea level, consistent with the subsidence noted for the Gulf of Fethye. The record from Hadera is consistent with the inference from the LIG elevations for vertical stability to within ± 0.04 mm/yr.

GPS position information also only provide limited constraints on the vertical motions because the record lengths are sub-decadal, and then only for the Israel coast (Fig. 2b). The Israel network has been analysed together with about 500 stations belonging to several CGPS networks in the Euro-Mediterranean and African area, using GAMIT software (Herring, 2004) as well as regional and global solutions from SOPAC (<http://sopac.ucsd.edu>) using the ST_FILTER software (<http://gipsy.jpl.nasa.gov/qoca>). The final position time series were computed in the IGS05 reference frame. Velocities were estimated from the time series after removing jumps due to stations' equipment changes (or co-seismic offsets)

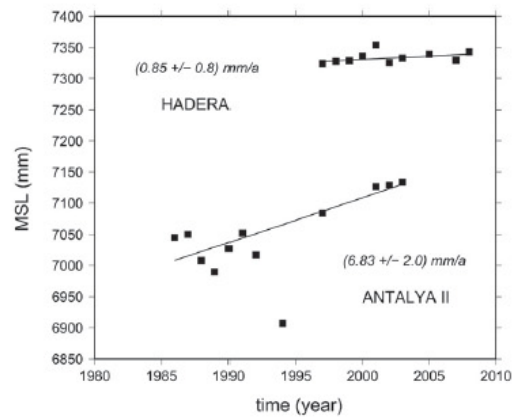


Fig. 3. Annual mean sea level trends estimated from the tide gauges of Hadera (top) and Antalya (bottom), located along the coast of Israel and SW Turkey, respectively. Although the duration of recordings are too short at both stations (time span 1996–2003 at Hadera and 1985–2005 at Antalya) to provide a reliable secular sea level trend, their data are in agreement with archaeological sea level indicators and models. Note the anomalous oscillations in Antalya compared with Hadera (valid data from the PSMSL database, www.pol.ac.uk).

and the seasonal signals (with annual and semi-annual period). Uncertainties were computed adopting a white + colored error noise model (Williams et al., 2004), to produce a self-consistent and homogeneous three-dimensional velocity field and estimates of vertical land movements. The results are consistent with earlier inferences that this region is undergoing horizontal northwestern motion with an average velocity of 1 cm/yr (McClusky et al., 2000). The vertical displacements present a less systematic pattern (Fig. 2b). All coastal sites indicate an upwards displacement with a weighted average value that is barely significant in view of unresolved questions about the GPS reference frame stability (Altamimi et al., 2007). If the reference frame correction to the vertical rate of $1.8\sin(\text{latitude})$ mm/yr proposed by these authors is applied, then the weighted mean vertical rate is 0.6 ± 0.7 mm/yr and consistent with tectonic stability for the coastal sites. Of greater significance is that larger vertical movements occur only in the inland regions, approaching the tectonic area dominated by the Dead Sea Fault zone (Fig. 2b) and consistent with higher elevations of LIG sediments at these more inland sites.

4. Materials and methods

Thirteen archaeological sites were surveyed along the coasts of Turkey and Israel (Fig. 1). Eight are located in Turkey (Fig. 2a) and five in Israel (Fig. 2b), all of different ages and with multiple sea level indicators (Table 1). Analysis follows the procedures already applied in other areas of the Mediterranean (Lambeck et al., 2004b; Antonioli et al., 2007), and consisted of four sequential steps: 1) the measurements of the elevation of the significant archaeological markers of maritime structures with respect to the present sea level by simple optical or mechanical methods and during favorable meteorological conditions (calm sea, absence of wind); 2) correction of the elevation measurements for tide and atmospheric pressure affecting the level of the sea surface at the time of surveys, using the data and algorithms adopted by the Permanent Service for Mean Sea Level (www.pol.ac.uk, as well as Woodworth, 1991; Woodworth and Player, 2003) for the Mediterranean Sea (atmospheric corrections are based on the inverted barometer

Table 1

Elevation of archaeological data versus sea level prediction models. (A) Site numbers (number in brackets according to database list); (B) names as indicated in Figs 2a,b, 4a,b and 5a,b; (C) country; (D) type of archaeological remain; (E) and (F) are the WGS84 coordinates of the sites; (G) age estimates based on historical documentation and archaeological data; (H) observed relative sea level change (corrected for tide and pressure values at the time of measurements) estimated from the functional elevation of the significant markers; (I) elevation error estimates; (J) limiting value of survey data; UL = upper limit, LL = lower limit of the archeological markers; (K–N) are the predicted sea levels at 2 ka according to different parameters used in the model; (O) estimate of average rate of vertical tectonic movement. Architectural features used to define sea level: B = buildings, BR = breakwater, CH = channels, D = docks, H = harbor; FT = fish tank, P = pools, PV = pavement, SW = slipways, T = tombs. For pools and fish tanks we considered a minimum functional elevation corresponding to at least 0.3 m above the maximum local high tide. Elevation data are the average values of multiple measurements collected at the best preserved parts of the investigated structures. All elevation data are corrected for tides and atmospheric pressure. The maximum tidal range in this part of the Mediterranean is ~0.40 m. Tidal corrections have been performed using the algorithms of the PSMSL (www.pol.ac.uk). The atmospheric pressure correction is for the difference in pressure at the time of observation and the mean annual pressure for the site and is based on the inverted barometer assumption using nearby station data from www.metoffice.com. The tectonic rates assume uniform uplift since the time of construction of the archaeological markers. The uncertainty estimates include observational and model uncertainties.

A	B	C	D	E	F	G	H	I	J	K	L	M	N	O
Site No	Site name	Country	Marker	Latitude	Longitude	Age (ka)	Obs rslc. (m)	σ obs (m)	Limit	ma3C (m)	ma3A (m)	ma2C (m)	ma2A (m)	Up tectonic rate (mm/yr)
1 (8)	Cnidos	Turkey	BR,H	36.685	27.373	2.3±100	-2.57	0.3	UL	-0.8	-0.58	-0.97	-0.71	-0.73±0.23
2 (6)	Scopea_Bay	Turkey	D	36.675	28.915	1.95±175	-3.81	0.3	UL	-0.34	-0.17	-0.54	-0.35	-1.71±0.25
3 (4)	Domuz_Is.	Turkey	B	36.667	28.905	1.6±100	-2.41	0.3	UL	-0.26	-0.12	-0.42	-0.26	-1.26±0.26
4 (5)	Kala_Kapi	Turkey	B	36.643	28.893	1.6±100	-2.63	0.3	UL	-0.27	-0.13	-0.42	-0.26	-1.40±0.26
5 (3)	Cleophras_bath	Turkey	B, PV	36.640	28.855	1.6±100	-3.52	0.3	UL	-0.27	-0.14	-0.42	-0.27	-1.95±0.26
6 (1)	Gemile_Is.	Turkey	D	36.555	29.064	1.6±100	-3.07	0.2	LL	-0.29	-0.15	-0.43	-0.27	-1.66±0.19
7 (2)	Tersane_bay	Turkey	SW	36.541	29.051	2.3±100	-4.50	1	LL	-0.5	-0.31	-0.73	-0.5	-1.68±0.67
8 (7)	Kekova	Turkey	T,D,B,PV	36.189	29.860	2.3±100	-2.36	0.3	UL	-0.65	-0.46	-0.81	-0.58	-0.70±0.23
9 (13)	Alziv	Israel	FT	33.049	35.100	2±25	-0.06	0.2	UL,LL	-0.02	0.07	-0.11	0.00	0.06±0.14
10 (12)	Dor	Israel	CH,P	32.620	34.917	2±50	-0.01	0.2	UL	0.03	0.12	-0.08	0.03	0.09±0.14
11 (9)	Caesarea_1	Israel	D	32.503	34.889	2±25	-0.15	0.2	UL	0.05	0.14	-0.06	0.05	0.02±0.14
12 (10)	Caesarea_2	Israel	P	32.497	34.889	2±25	-0.18	0.2	UL,LL	0.05	0.14	-0.06	0.05	0.01±0.14
13 (206)	Shiqmona	Israel	P	32.825	34.955	2±100	-0.04	0.2	UL	0.04	0.09	0.09	0.02	0.07±0.14

assumption using the closest available meteorological data obtained at www.metoffice.com); 3) error estimation for ages and elevation measurements of the archaeological markers, after their functional heights were evaluated on the basis of accurate archaeological interpretations (age errors are estimated from the architectural features; elevation errors derived from the measurements, corrections and estimates of the functional heights; and 4) examination of the predicted and observed sea levels, by comparing the current elevations of the markers (i.e. the relative sea level change at each location) with the sea level elevation predicted by the geophysical model for each location. In the areas where the elevations of the markers are in agreement with the predicted sea-level curve, tectonic stability is hypothesized. Conversely, when the elevations of the markers are below or above that of the predicted sea-level curve, the area has experienced tectonic subsidence or uplift.

As the investigated archaeological structures were originally used year round, it is assumed that the defining levels correspond to the annual mean conditions at the time of construction. Functional heights of the archaeological benchmarks were used to estimate relative sea level change in each location. This parameter is defined as the elevation of specific architectural parts of an archaeological structure with respect to an estimated mean sea level at the time of their construction. It depends on the type of structure, on its use and on the local tide amplitude (Lambeck et al., 2004b; Auriemma and Solinas, 2009). Functional heights also define the minimum elevation of the structure above the local highest tides (Lambeck et al., 2004b). This information can also be deduced from previous publications (Schmiedt, 1965, 1974; Flemming, 1969; Flemming and Webb, 1986), from historical documents (Hesnard, 2004), from the remnants of the Roman Age shipwrecks (Charlin et al., 1978; Steffy, 1990; Pomey, 2003; Medas, 2003), and through rigorous estimation of the functional heights of the piers, by using and interpreting different type of markers on the same location (Lambeck et al., 2004b). The use of these structures (which is dependent on their conservation), the accuracy of the survey and the estimation of the functional heights were all used in considering the observational uncertainties at each site.

The theory used here for describing the glacio–hydro–isostatic process has been previously discussed in Lambeck et al. (2003) and its applications to the Mediterranean region have been most recently re-discussed in Lambeck et al. (2004a,b), Lambeck and Purcell (2005), and Antonioli et al. (2007). The input parameters into these models are the ice models from the time of the Last Interglacial to the present and the earth rheology parameters. These are established by calibrating the model against sea-level data from tectonically stable regions and from regions that are sensitive to particular subsets of the sought parameters (Lambeck, 1995; Lambeck et al., 1998; Lambeck, 2002; Lambeck et al., 2006; Antonioli et al., 2006). This paper uses the same iteration results for the ice and earth models as in Anzidei et al. (2011). The isostatic signals will generally be earth-model dependent, as is illustrated in Table 1 for a number of Earth models that differ in their upper mantle viscosity ($2 = 2 \times 10^{20}$ Pa s; $3 = 3 \times 10^{20}$ Pa s) and lower mantle viscosity ($A = 10^{22}$ Pa s, $C = 3 \times 10^{22}$ Pa s) for lithosphere with an effective elastic thickness of 65 km. Models with other values for this last parameter between 50 and 80 km give very similar results. With this observational data set alone, particularly with the unknown tectonic contributions to the Turkey rates of sea-level change, it is not possible to establish optimum values from this analysis alone, although analyses from elsewhere in the Mediterranean indicate that this range of parameters provides a consistent description of the sea-level data for the region.

5. Archaeological data along the coast of Turkey

The Mediterranean coasts of Southeastern Turkey contain a number of archaeological sites, such as urban structures and harbors installations (Flemming et al., 1973) that are useful for sea level studies. Approximately 150 km of the Turkish coast along the Gulf of Fethye, from the northwestern site of the ancient harbor of Cnidus, located on the Datça peninsula, up to the southeastern site of Kekova was examined (Fig. 2a). In this region, coastal installations such as buildings, docks, tombs, slipways and breakwaters built during the last 1.6–2.3 ka, can still be found. It is remarkable

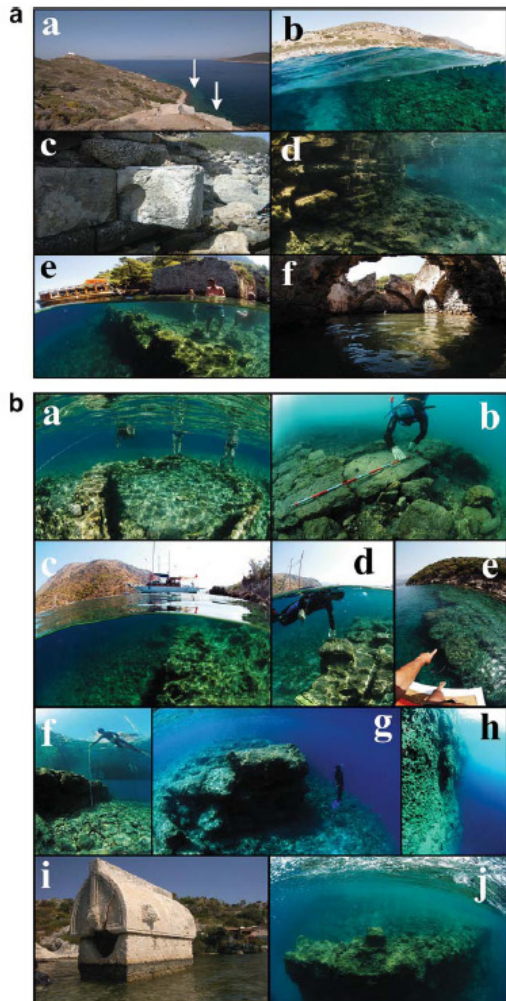


Fig. 4. a The archaeological evidence of the relative sea live rise in Turkey. Cnidos: a) the coastline out of the northern harbor with a Greek age pier (marked by the white arrows), b) the Hellenic age submerged pier in the southern harbor, c) the Roman age bollard in the southern harbor, d) submerged Byzantine age buildings at Cala Kapi, e–f) Byzantine age buildings of Cleopatra's bath at Twelve Islands, (Gulf of Fethye). b The archaeological and geomorphological evidence of the relative sea live rise in Turkey: a) Byzantine age building at Domuz Island, (b) the Hellenic age pier of Tersane island, c–g) the Byzantine age pier of Gemile Island with bollards; h) a submerged stalactite (unknown age) along the coast of Fethye; i) Lycian age tombs and j) harbor installations at Kekova. See Figs 1 and 2a for site location and Table 1 for data.

that all these sites are largely submerged, providing the dramatic evidence of the relative sea level change in this region during the last 2.3 ka (Figs. 4a,b and 6a; Table 1). The harbor of Cnidos and the settlement of Kekova are the most important archaeological settlements in this area, and they display different types of sea level markers that include well preserved piers with bollards. The harbor of Cnidos was surveyed for the first time in 1968 by Flemming, who published the elevations of bollards, from which he estimated a minor sea level rise with respect to the other archaeological sites located south of this site followed by a possible tectonic uplift occurred during the last 2 ka. Other significant indicators include

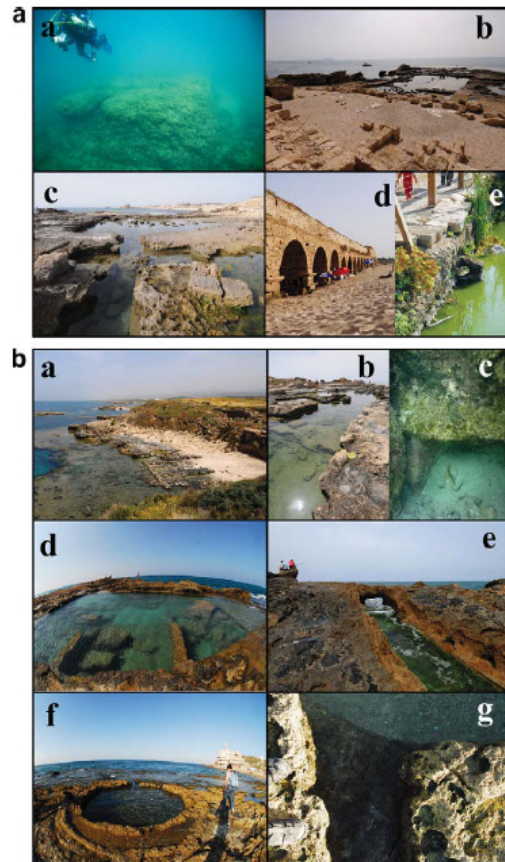


Fig. 5. a The archaeological evidence of relative sea level rise in Israel: a) the submerged remnants of the collapsed Herod's harbor of Caesarea; b) the roman age pool of Caesarea, equipped with c) channels tidally controlled for the exchange of water in the basin; d) the aqueduct of Caesarea. This structure is still in situ and indicates that major seismic disturbances since its construction are unlikely, e) the bollard in the inner harbor of Caesarea. See Figs 1 and 2b for site location and Table 1 for data. b The archaeological evidence of relative sea level rise in Israel: a) the Roman age dock and b) the pools connected with sea level at Dor; c) the sluice gate raised in its original position in the Roman age fish tank of Alziv (d), equipped with tidally channels controlled for water exchange in the basin (e); f) the small round pool of Shiqmona, near Haifa with channels equipped with grooves for the sluice gates (g). See Figs 1 and 2b for site location and Table 1 for data.

the stairs of a submerged harbor at Skopea Island (placed at -3.81 m), foundations of building walls at Cleopatra's bath (at -3.52 m), Domuz Island (at -2.41 m) and Kala Kapi (at -2.63 m), slipways at Tersane (at -3.52 m) and finally tombs, docks, slipways and other buildings at Kekova. All the markers are consistent with a relative sea level rise of 2.3 m, since the last 2.3 ka (Figs. 4a,b and 6a; Table 1). This inference of subsidence is consistent with the absence of coastal sediments that contain the characteristic Senegalese fauna that is indicative of MIS 5.5 highstands elsewhere in the Mediterranean.

6. Archaeological data along the coast of Israel

Abundant archaeological installations, whose ages may go back to the Bronze age, characterize the 100 km of the coast of Israel between Caesarea and Akziv, below the Lebanese border (Sivan et al.,

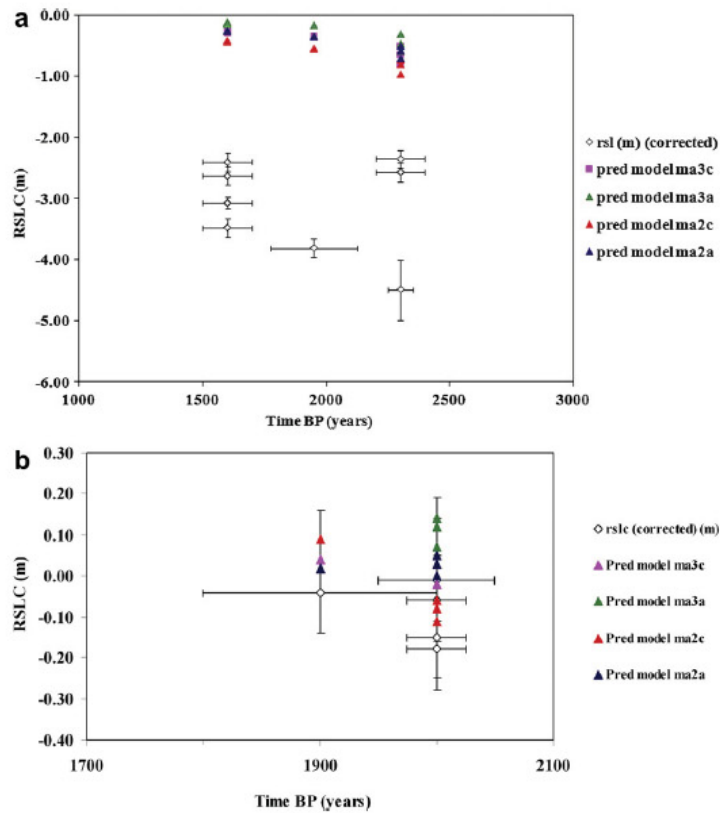


Fig. 6. a) Relative sea level change along the coast of SW Turkey observed from archaeological data and from predictions based on different parameters of the glacio-hydro-isostatic model (see text); b) relative sea level change along the coast of Israel from archaeological data and isostatic predictions based on different parameters of the glacio-hydro-isostatic model (see text).

2004 and references therein) (Fig. 2b). The most precise archaeological sea level indicators are the coastal installations of Roman age that span a period of a few centuries around 2 ka BP. Previous research from the elevation of fish tanks, harbors, quarries and slipways indicates nearly no sea level change since Roman time. Some sites, such as the pool at Caesarea, provide an excellent example of almost unchanged relative sea level since its construction (Figs. 5a,b and 6b; Table 1). This rock-cut pool, located on the headland west of the Roman Theater at Caesarea, has also been also known as "Cleopatra's Bath". The architecture and technology of *piscina* was popular in Italy during the period of the late Republic and the Early Empire and were usually integrated with the maritime villas. They were designed to ensure a constant flow of sea-water during a tidal cycle by a series of channels leading to and from the sea with intermediate sluice gates, and sometimes with tunnels, providing very precise sea level indicators (Lambeck et al., 2004b).

Other significant sites are the pool and the docks of Dor, the fish tank of Akziv with its in situ sluice gate which dates the site to the Early Roman period (based on the technology similarity to the fish tanks in Italy), and the small round pool of Shiqmona, near Haifa (this latter site, although it is of uncertain age, can be roughly attributed to the Roman age, as similar structures are present along the coasts of Italy and are dated at 2 ± 0.1 ka). All these sites show values of local relative sea level rise within 0.01 ± 0.2 and 0.18 ± 0.2 m, since the last 2 ka (Fig. 6b; Table 1).

Data from the most submerged part of the harbor of Caesarea has not been used as it is presently collapsed (Fig. 5a). The authors support the hypothesis, based on these investigations and previous studies (Raban, 1990 and references therein), that this installation was not destroyed during an earthquake, but that it collapsed due to the poor mechanical quality of the geological units beneath its foundations (Reinhardt, 1999).

7. Discussion

For the Israel sites, the isostatic contributions to the observed relative sea level change are small and not critically dependent on earth-model parameters (Table 1, columns K–N). This is a consequence of a near canceling out of the water-loading or hydro-isostatic component and the ice-loading or glacio-isostatic component of the deglaciation effect of the Late Pleistocene high-latitude ice sheets. These predicted corrections to sea level observations are also of very comparable amplitude to the observed values, and this indicates that any vertical tectonic displacements have been small at all the Israel sites during the past 2000 years. Thus, for the past two millennia relative sea levels here provide a quite direct estimate of the eustatic component of sea level: the changes due to ocean volume increases that have not been included in the ice models. The nominal ice model that has been used in these isostatic models has constant grounded ice volume for the

past 2000 years and the difference between the observed and predicted sea levels provide a measure of any change in ice volume in this interval, including changes in mountain glaciers, and any other contributions such as thermal expansion of the oceans. The former contribution will be associated with its own loading and gravitational terms, but since the locations are far from any significant ice loads this additional contribution will be small.

While the data set is limited, an estimate of the eustatic correction and the optimum earth-model parameters within a restricted range of $(2-4) \times 10^{20}$ Pa s for the upper mantle and $(1-3)$ for the lower mantle can be attempted. This yields values of 2.5×10^{20} and 2×10^{22} Pa s for the two layers respectively and an eustatic rise in sea level during the past 2000 years of only 13.5 ± 2.6 cm. For a present-day eustatic sea level rise of 1.2–1.5 mm/yr, this implies that if the present-day rise is extrapolated back in time the Roman epoch levels were reached only about 100 years ago, confirming the earlier result of Lambeck et al. (2004b) and consistent with the similar results from Roman sites in Tunisia and Libya (Anzidei et al., 2011).

Archaeological data from other periods, mainly from archaeological indicators such as coastal quarries, water wells and Roman and Byzantine installations (Fig. 4a) (Nir and Eldar, 1987; Mart and Perecman, 1996; Nir, 1997; Galili and Sharvit, 1998; Sivan and Galili, 1999; Sivan et al., 2004; Galili et al., 2007) have confirmed the generally good agreement between the observed and isostatic predicted values consistent with an absence of vertical tectonic deformation (within the observational limits) as far back as 10,000 BP (Sivan et al., 2001), that the sea-level curve here reflects primarily the eustatic component, and that it can be used as a first-order reference for other eastern Mediterranean coasts to establish rates of tectonic uplift or subsidence. This can be effectively illustrated with the information discussed above for the section of the Turkish coast between Cnidos and Kekova that is dominated by diffuse tectonics (strike slip and normal faulting) at the eastern end of the Hellenic arc tectonic system (Jackson and McKenzie, 1988; Altunel et al., 2003). The archaeological sites provide evidence of major submergence of this region, of between 2.4 and 4.5 m, depending on site, over the past 2300 years (Fig. 5).

The isostatic corrections for these sites are larger than for the Israel sites and also show a greater dependence on the Earth model (Table 1) although the range of the corrections lie within the uncertainties of the observations and the tectonic subsidence signal clearly dominates the other contributions. Using the optimum earth and eustatic parameters established from the Israel data, the average tectonic rates of uplift for the past 1.6–2.3 ka can be calculated (column O in Table 1). The uncertainties of these estimated rates are 0.2 mm/yr and are dominated by the observational uncertainties. Within uncertainties, the sites within the Gulf of Fethye yield consistent rates of subsidence of 1.48 ± 0.3 mm/yr.

The absence of elevated Last Interglacial shorelines is consistent with these rates of subsidence. If the above rates are representative of longer time intervals, then these shorelines can be expected at depths of up to 200 m below present sea level. The subsidence recorded at the Antalya tide gauge, albeit of limited quality but independently confirmed by Burkay et al. (2007), indicate that the present rate may be higher than the longer-term average, but a longer record will be required before significance can be attached to this observation.

8. Conclusion

The evidence from archaeological data shows that the coasts of SW Turkey underwent a maximum relative sea level rise between 2.4 and 4.5 ± 0.3 m over the last 2.3 ka. During about the same period, the coast of Israel shows a near constancy of sea level. The observed changes can be attributed to the glacio–hydro–isostatic

signal, eustasy and vertical tectonics. The glacio–hydro–isostatic contribution to the observed changes plays approximately a null role along the coasts of Israel and has a minor contribution in Turkey. The estimated eustatic change since 2 ka BP of 13.5 ± 2.6 cm is in agreement with previous results for central Mediterranean and North Africa. If the present-day rise of 1.2–1.5 mm/yr shown by tide gauge data is extrapolated back in time to the Roman epoch, levels were reached 100 years ago establishing that the onset of the modern sea level rise occurred in the late nineteenth or early twentieth century. The sea level prediction model fits the archaeological observation in Israel. In Turkey, which is one of the highest seismic regions of the Mediterranean, all the archaeological markers largely fall below the predictions due to intervening vertical tectonics. Recent sea level and crustal deformation trends inferred from the available geodetic data, although of short duration, are consistent with tectonic stability for the coast of Israel and a still active subsidence of SW Turkey.

Finally, this analysis shows that the coast of Israel is tectonically stable since the last 2.0 ka while a broad tectonic subsidence has affected the SW coast of Turkey between Cnidos and Kekova, at an average rate of 1.48 ± 0.3 mm/yr since the last 2.3 ka. Estimates are in agreement with the elevation of the MIS-5.5 shorelines which are at normal elevation along the coast of Israel and absent along the Turkish coasts, consistent with the long-term crustal subsidence associated with tectonics of the eastern ending of the Hellenic Arc which is the primary cause of dramatic relative sea level rise for this region.

Acknowledgments

We are thankful to Eng. Paolo Gaburro and Cap. Mustafâ Yiltir for their skilled assistance during marine surveys in Turkey. The anonymous reviewers and Norm Catto and Sanja Faivre improved this paper with their suggestions. This study has been partially funded by INGV, ENEA, Leon Recanati Institute, Australian National University and MIUR – Prin 2006, Grant Project “Il ruolo del riaggiustamento isostatico post-glaciale nelle variazioni del livello marino globale e Mediterraneo: nuovi vincoli geofisici, geologici ed archeologici”, coordinator Prof. Giorgio Spada.

References

- Altamimi, Z., Collilieux, X., Legrand, J., Garayt, B., Boucher, C., 2007. ITRF2005: a new release of the International Terrestrial Reference Frame based on time series of station positions and earth orientation parameters. *Journal of Geophysical Research* 112, B09401. doi:10.1029/2007JB004949.
- Altunel, E., Stewart, I.S., Barka, A., Piccardi, L., 2003. Earthquake faulting at ancient Cnidos, SW Turkey. *Turkish Journal of Earth Sciences* 12, 137–151.
- Antonoli, F., Ferranti, L., Lambeck, K., Kershaw, S., Verrubbi, V., Dai Pra, G., 2006. Late Pleistocene to Holocene record of changing uplift rates in southern Calabria and eastern Sicily (southern Italy, Central Mediterranean Sea). *Tectonophysics* 422, 23–40.
- Antonoli, F., Anzidei, M., Auriemma, R., Gaddi, D., Furlani, S., Lambeck, K., Orrù, P., Solinas, E., Gaspari, A., Karinja, S., Kovačić, V., Surace, L., 2007. Sea level change during Holocene from Sardinia and northeastern Adriatic (Central Mediterranean sea) from archaeological and geomorphological data. *Quaternary Science Reviews* 26, 2463–2486.
- Anzidei, M., Antonoli, F., Lambeck, K., Benini, A., Soussi, M., 2011. New insights on the relative sea level change during Holocene along the coasts of Tunisia and western Libya from archaeological and geomorphological markers. *Quaternary International* 232, 5–12.
- Auriemma, R., Solinas, E., 2009. Archaeological remains as sea level change markers: a review. *Quaternary International* 206, 134–146.
- Boschi, E., Guidoboni, E., Ferrari, G., Valensise, G., Gasperini, P., 1995. *Catálogo dei forti terremoti in Italia dal 461 a.C. al 1980*. ING SGA, Bologna.
- Burkay, S., Ebru, E., Ercan, K., 2007. Trend analysis of sea levels along Turkish coasts. *Hydrology Days* 2007, 152–160.
- Calais, E., DeMets, C., Nocquet, J.M., 2003. Evidence for a post-3.16-Ma change in Nubia-Eurasia-North America plate motions? *Earth and Planetary Sciences Letters* 216, 8–92.
- Caputo, M., Pieri, L., 1976. Eustatic variation in the last 2000 years in the Mediterranean. *Journal of Geophysical Research* 81, 5787–5790.

- Charlin, G., Gassend, J.M., Lequémont, R., 1978. L'èpave antique de la baie de cavalière – Le Levandou, Var. *Archeonautica* 2.
- DeMets, C., Gordon, R.G., Argus, D.F., Stein, S., 1994. Effect of recent revisions to the geomagnetic reversal time scale on estimates of current plate motions. *Geophysical Research Letters* 21, 2191–2194.
- Dewey, J.F., Pitman, W.C., Ryan, W.B.F., Bonnin, J., 1973. Plate tectonics and the evolution of the Alpine system. *Geological Society of America Bulletin* 84, 3137–3180.
- Dewey, J.F., Helman, M.L., Turco, E., Hutton, D.H.W., Knott, S.D., 1989. Kinematics of the Western Mediterranean. Special Publication. In: Coward, M.P., Dietrich, D., Park, R.G. (Eds.), *Alpine Tectonics*, vol. 45. Geological Society, pp. 265–283.
- Faccenna, C., Thorsten, W., Becker, L., Lucente, F., Jolivet, L., Rossetti, F., 2001. History of subduction and back-arc extension in the Central Mediterranean. *Geophysical Journal International* 145, 809–820.
- Ferranti, L., Monaco, C., Antonioli, F., Maschio, L., Kershaw, S., Verrubbi, V., 2008. Alternating steady and stick-slip uplift in the Messina straits, southern Italy: evidence from raised late Holocene shorelines. *Journal of Geophysical Research* 112, B06401. doi:10.1029/2006JB004473.
- Flemming, N.C., Webb, C.O., 1986. Tectonic and eustatic coastal changes during the last 10,000 years derived from archaeological data. *Zeitschrift für Geomorphologie NF* 62, 1–29.
- Flemming, N.C., Czartoryska, N.M.G., Hunter, P.M., 1973. Archaeological evidence for eustatic and tectonic components of relative sea level change in the South Aegean. In: Blackman, D.J. (Ed.), *Marine Archaeology*. Butterworths, London, pp. 1–16.
- Flemming, N.C., 1969. Archaeological Evidence for Eustatic Changes of Sea Level and Earth Movements in the Western Mediterranean in the Last 2000 Years. Geological Society of America, Special Paper 109.
- Galili, E., Sharvit, J., 1998. Ancient coastal installations and the tectonic stability of the Israeli coast in historical times. Special Publications. In: Stewart, I.S., Vita-Finzi, C. (Eds.), *Coastal Tectonics*, vol. 146. Geological Society, London, pp. 147–163.
- Galili, E., Zviely, D., Ronen, A., Mienis, H.K., 2007. Beach deposits of MIS 5e high sea stand as indicators for tectonic stability of the Carmel coastal plain, Israel. *Quaternary Science Reviews* 26, 2544–2557.
- Guidoboni, E., Comastri, A., Traina, G., 1994. Catalogue of ancient earthquakes in the Mediterranean area up to the 10th century. In: Istituto Nazionale di Geofisica Roma. *Società Geofisica e Ambiente*, Bologna, 504 pp.
- Herring, T.H., 2004. GLOBK: Global Kalman Filter VLBI and GPS Analysis Program Version 10.0. Massachusetts Institute of Technology, Cambridge.
- Hesnard, A., 2004. Vitruve, De architectura, V 12, et le port romain de Marseille. In: *Le strutture dei porti e degli approdi antichi*. ANSER, pp. 175–204.
- Jackson, J., McKenzie, D., 1988. The relationship between plate motions and seismic moment tensors, and the rates of active deformation in the Mediterranean and Middle East. *Geophysical Journal International* 93, 45–73.
- Jiménez-Munt, I., Sabadini, R., Gardi, A., 2003. Active deformation in the Mediterranean from Gibraltar to Anatolia inferred from numerical modeling and geodetic and seismological data. *Journal of Geophysical Research* 108 (B1). doi:10.1029/2001JB001544 2006.
- Jolivet, L., Faccenna, C., 2000. Mediterranean extension and the Africa-Eurasia collision. *Tectonics* 19, 1095–1106.
- Kalafat, D., Günes, Y., Kekovali, K., Berberoglu, M., 2004. Earthquake Activity of the Gulf of Gökova. Report Kandilli Observatory & ERI, National Earthquake Monitoring Center. Cengelköy/Istanbul, Turkey. http://www.emsc-csem.org/Doc/Gokova_0804.pdf.
- Lambeck, K., Purcell, A., 2005. Sea-level change in the Mediterranean Sea since the LGM: model predictions for tectonically stable areas. *Quaternary Science Reviews* 24, 1969–1988.
- Lambeck, K., Smither, C., Johnston, P., 1998. Sea-level change, glacial rebound and mantle viscosity for northern Europe. *Geophysical Journal International* 134, 102–144.
- Lambeck, K., Purcell, A., Johnston, P., Nakada, M., Yokoyama, Y., 2003. Water-load definition in the glacio-hydro-isostatic sea-level equation. *Quaternary Science Reviews* 22, 309–318.
- Lambeck, K., Antonioli, F., Purcell, A., Silenzi, S., 2004a. Sea level change along the Italian coast for the past 10,000 yrs. *Quaternary Science Reviews* 23, 1567–1598.
- Lambeck, K., Anzidei, M., Antonioli, F., Benini, A., Esposito, E., 2004b. Sea level in Roman time in the central Mediterranean and implications for modern sea level rise. *Earth and Planetary Science Letters* 224, 563–575.
- Lambeck, K., Purcell, A., Funder, S., Kjaer, K., Larsen, E., Möller, P., 2006. Constraints on the Late Saalian to early Middle Weichselian ice sheet of Eurasia from field data and rebound modelling. *Boreas* 35, 539–575.
- Lambeck, K., Woodroffe, C.D., Anzidei, M., Antonioli, F., Gehrels, W.R., Plassche, O. van de., Wright, A.J. Palaeoenvironmental records, geophysical modelling and reconstruction of sea-level trends and variability on centennial and longer time scales. In: Church, J.A., Woodworth, P.L., Aarup, T., Wilson, W.S., (Eds.), *Understanding Sea-level Rise and Variability*. Blackwell Publishing, London, in press.
- Lambeck, K., 1995. Late Pleistocene and Holocene sea-level change in Greece and south-western Turkey: a separation of eustatic, isostatic and tectonic contributions. *Geophysical Journal International* 122, 1022–1044.
- Lambeck, K., 2002. Sea-level change from mid-Holocene to recent time: an Australian example with global implications. In: Mitrovica, J.X., Vermeersen, B. (Eds.), *Glacial Isostatic Adjustment and the Earth System*. American Geophysical Union, Washington, DC, pp. 33–50.
- Le Pichon, X., Bergerat, F., Roulet, M.J., 1988. Plate Kinematics and Tectonics Leading to the Alpine Belt Formation: a New Analysis. Geological Society of America, Special Paper 218111–131.
- Mantovani, E., Cenni, N., Albarello, D., Viti, M., Babbucci, D., Tamburelli, C., D'Onza, F., 2001. Numerical simulation of the observed strain field in the central-eastern Mediterranean region. *Journal of Geodynamics* 31 (5), 519–556.
- Mart, Y., Perelman, I., 1996. Neotectonic activity in Caesarea, the Mediterranean coast of central Israel. *Tectonophysics* 254, 139–153.
- McClusky, S., Balassanian, S., Barka, A., Demir, C., Ergintav, S., Georgiev, I., Gurkan, O., Hamburger, M., Hurst, K., Kahle, H., Kastens, K., Kekelidze, G., King, R., Kotzev, V., Lenk, O., Mahmoud, S., Mishin, A., Nadariya, M., Ouzounis, A., Paradissis, D., Peter, Y., Prilepin, M., Reilinger, R., Sanli, I., Seeger, H., Tealeb, A., Toksoz, M.N., Veis, G., 2000. Global Positioning System constraints on plate kinematics and dynamics in the eastern Mediterranean and Caucasus. *Journal of Geophysical Research* 105 (B3), 5695–5719.
- McKenzie, D.P., 1970. Plate tectonics of the Mediterranean region. *Nature* 226, 239–243.
- Medas, S., 2003. The Late-Roman Parco di Teodorico Wreck, Ravenna, Italy: preliminary remarks on the hull and the shipbuilding. In: Beltrame, C. (Ed.), *Boats, Ships and Shipyards*. Proceedings of the Ninth International Symposium on Boat and Ship Archaeology, Venice 2000, pp. 42–48. Oxford.
- Nir, Y., Eldar, I., 1987. Ancient wells and their geoarchaeological significance in detecting tectonics of the Israel Mediterranean coastline region. *Geology* 15, 3–6.
- Nir, Y., 1997. Middle and late Holocene sea-levels along the Israel Mediterranean coast – evidence from ancient water wells. *Journal of Quaternary Science* 12 (2), 143–151.
- Pirazzoli, P.A., 1976. Sea level variations in the northwest Mediterranean during Roman times. *Science* 194, 519–521.
- Pomey, P., 2003. Reconstruction of Marseilles 6th century BC Greek ships. In: Beltrame, C. (Ed.), *Boats, Ships and Shipyards*. Proceedings of the Ninth International Symposium on Boat and Ship Archaeology, Venice 2000, pp. 57–65. Oxford.
- Raban, A., 1990. Oceanographic understanding of ancient harbour engineers of the Levant. In: Proc. 4th International Congress on the History of Oceanography. *Deutsch Hydrographie Zeitschrift* vol. 22, pp. 257–271.
- Rebai, S., Philip, H., Taboada, A., 1992. Modern tectonic stress field in the Mediterranean region: evidence for variation in stress directions at different scale. *Geophysical Journal International* 110, 106–140.
- Reinhardt, E., 1999. Destruction of Herod the Great's harbour at Caesarea Maritima, Israel. *Geoarchaeological evidence*. *Geology* 27, 811–814.
- Schmiedt, G., 1965. *Antichi porti d'Italia*, vol. 45. L'Universo, 234–238.
- Schmiedt, G., 1974. *Il livello antico del mar Tirreno*. In: Olschki, E. (Ed.), *Testimonianze da resti archeologici*, Firenze, 323 pp.
- Serpelloni, E., Vannucci, G., Pondrelli, S., Argnani, A., Casula, G., Anzidei, M., Baldi, P., Gasperini, P., 2007. Kinematics of the Western Africa-Eurasia plate boundary from focal mechanisms and GPS data. *Geophysical Journal International*. doi:10.1111/j.1365-246X.2007.03367.x
- Sivan, D., Galili, E., 1999. Holocene tectonic activity in the Galilee coast and shallow shelf, Israel, a geological and archaeological study. *Israel Journal of Earth Science* 48, 47–61.
- Sivan, D., Gvirtzman, G., Sass, E., 1999. Quaternary stratigraphy and paleogeography of the Galilee Coastal Plain, Israel. *Quaternary Research* 51, 280–294.
- Sivan, D., Wdowinski, S., Lambeck, K., Galili, E., Raban, A., 2001. Holocene sea-level changes along the Mediterranean coast of Israel, based on archaeological observations and numerical model. *Palaeogeography, Palaeoclimatology, Palaeoecology* 167, 101–117.
- Sivan, D., Lambeck, K., Toueg, R., Raban, A., Porat, Y., Shirman, B., 2004. Ancient coastal wells of Caesarea Maritima, Israel, an indicator for sea level changes during the last 2000 years. *Earth and Planetary Science Letters* 222, 315–330.
- Sneh, A., 2000. Faulting in the coastal plain of Israel during the Late Quaternary, re-examined. *Israel Journal of Earth Sciences* 49 (1), 21–29.
- Steffy, J.R., 1990. The boat: A preliminary study of its construction. In: Wachsmann, S., et al. (Eds.), *The Excavation of an Ancient Boat in the Sea of Galilee (Lake Kinneret)*. Israel Antiquities Authority, Jerusalem, pp. 29–47.
- Uluğ, A., Duman, M., Ersoy, X., Özel, E., Avci, M., 2005. Late quaternary sea-level change, sedimentation and neotectonics of the Gulf of Gökova: Southeastern Aegean Sea. *Marine Geology* 221, 381–395.
- Vannucci, G., Gasperini, P., 2004. The new release of the database of earthquake mechanisms of the Mediterranean Area (EMMA Version 2). *Annals of Geophysics* 47 (1), 307–334.
- Williams, S.D.P., Bock, Y., Fang, P., Jamason, P., Nikolaidis, R.M., Prawirodirdjo, L., Miller, M., Johnson, D.J., 2004. Error analysis of continuous GPS position time series. *Journal of Geophysical Research* 109, B03412. doi:10.1029/2003JB002741.
- Woodworth, P.L., Player, R., 2003. The permanent service for mean sea-level: an update to the 21st century. *Journal of Coastal Research* 19, 287–295. <http://www.pol.ac.uk/PSMSL/>.
- Woodworth, P.L., 1991. The permanent service for mean sea-level and global sea-level observing system. *Journal of Coastal Research* 7, 699–710.

Annex 5
(8 pages)

Abstract - New data of sea level changes for the Mediterranean region along the coasts of northern Africa are presented. Data are inferred from archaeological sites of Punic-Roman age located along the coast of Tunisia, between Tunis and Jerba island and along the western coast of Libya, between Sabratha and Leptis Magna. Data are based on precise measures of presently submerged archaeological markers that are good indicators of past sea-level elevation. Nineteen selected archaeological sites were studied in Tunisia and four in Libya, all aged between w2.0 and w1.5 ka BP. The functional elevations of significant archaeological markers were measured with respect to the sea level at the time of measurements, applying corrections for tide and atmospheric pressure values. The functional elevations of specific architectural parts of the sites were interpreted, related to sea level at the time of their construction providing data on the relative changes between land and sea. Observations were compared against sea level change predictions derived from the glacio-hydro-isostatic model associated with the Last Glacial cycle. The results indicate that local relative sea level change along the coast of Tunisia and Libya, has increased 0.2 O 0.5 m since the last w2 ka. Besides minor vertical tectonic movements of the land, the observed changes are produced by eustatic and glacio-hydro-isostatic variations acting in the Mediterranean basin since the end of the last glacial maximum.

M. Anzidei, F. Antonioli, K. Lambeck, A. Benini, M. Soussi New insights on the relative sea level change during Holocene along the coasts of Tunisia and western Libya from archaeological and geomorphological markers. *Quaternary International*, 2010 DOI: 10.1016/j.quaint.2010.03.01



Contents lists available at ScienceDirect

Quaternary International

journal homepage: www.elsevier.com/locate/quaint

New insights on the relative sea level change during Holocene along the coasts of Tunisia and western Libya from archaeological and geomorphological markers

M. Anzidei^{a,b,*}, F. Antonioli^c, K. Lambeck^d, A. Benini^e, M. Soussi^f, R. Lakhdar^f

^a Istituto Nazionale di Geofisica e Vulcanologia, via di Vigna Murata 605, 00143 Roma, Italy

^b Università della Calabria, Dipartimento di Fisica, Cosenza, Italy

^c ENEA, Italy

^d Research School of Earth Sciences, The Australian National University, Canberra 0200, Australia

^e Università della Calabria, Dipartimento di Archeologia e Storia delle Arti, Cosenza, Italy

^f University of El Manar, Faculty of Sciences of Tunis, Department of Geology, Tunisia

ARTICLE INFO

Article history:

Available online 24 April 2010

ABSTRACT

New data of sea level changes for the Mediterranean region along the coasts of northern Africa are presented. Data are inferred from archaeological sites of Punic-Roman age located along the coast of Tunisia, between Tunis and Jerba island and along the western coast of Libya, between Sabratha and Leptis Magna. Data are based on precise measures of presently submerged archaeological markers that are good indicators of past sea-level elevation. Nineteen selected archaeological sites were studied in Tunisia and four in Libya, all aged between ~2.0 and ~1.5 ka BP. The functional elevations of significant archaeological markers were measured with respect to the sea level at the time of measurements, applying corrections for tide and atmospheric pressure values. The functional elevations of specific architectural parts of the sites were interpreted, related to sea level at the time of their construction providing data on the relative changes between land and sea. Observations were compared against sea level change predictions derived from the glacio-hydro-isostatic model associated with the Last Glacial cycle. The results indicate that local relative sea level change along the coast of Tunisia and Libya, has increased 0.2 ± 0.5 m since the last ~2 ka. Besides minor vertical tectonic movements of the land, the observed changes are produced by eustatic and glacio-hydro-isostatic variations acting in the Mediterranean basin since the end of the last glacial maximum.

© 2010 Elsevier Ltd and INQUA. All rights reserved.

1. Introduction

This paper provides new data and interpretations on the relative sea-level change since the last ~2 ka along the coastlines of North Africa, in Tunisia and western Libya, where the recent relative sea-level changes have not yet been adequately constrained. For this purpose, coastal geoarchaeological installations and markers provide a powerful source of information from which the relative motions between the land and the sea can be estimated. Results are interpreted taking into account that sea-level change is the sum of eustatic, glacio-hydroisostatic and tectonic factors. While the first is global and time dependent, the other two also vary according to location and can be influenced by tectonics.

Recent studies have proved that archaeological evidence from small tidal range areas such as the Mediterranean Sea provide

significant information for the estimation of relative sea-level changes since historical times, using ancient coastal structures (Schmiedt, 1965, 1974; Lambeck et al., 2004b; Antonioli et al., 2007). The latter are interpreted for their functionality, being precisely defined by their relationship to sea level at the time of construction. The Mediterranean shores are unique in the world in displaying a large number of archaeological remains, often well dated and sometimes very well preserved, that can be successfully used to provide constraints on relative sea level. Ancient fish tanks, piers and harbours constructions generally built around 2 ± 0.3 ka BP are the best indicators and provide a valuable insight of the regional variation in sea level in the last two millennia (Flemming, 1969; Schmiedt, 1974; Caputo and Pieri, 1976; Pirazzoli, 1976; Felici, 1998, 2000; Lambeck et al., 2004a, 2004b, in press; Antonioli et al., 2007, and references therein). Slipways and quarries carved along the coastlines and located near fish tanks and harbours or villas of the same age can provide additional data, both on the past water level and on their own functional elevation above sea level, although they are not very precise indicators (Flemming and Webb, 1986; Lambeck et al., 2004b).

* Corresponding author. Istituto Nazionale di Geofisica e Vulcanologia, via di Vigna Murata 605, 00143 Roma, Italy.

E-mail address: macro.anzidei@ingv.it (M. Anzidei).

Archaeological evidence was examined from the North African coasts of western Libya and Tunisia, where maritime constructions since the Phoenician and Punic times can still be found. During the Roman age, extensive development of coastal installations occurred, as North Africa was an important Roman province. Here, many well-preserved remains are still present today. The best preserved sites provide information on their constructional levels that can be accurately related to the local mean sea level between ~2000 and ~1500 BP. Unpublished archaeological markers are used as benchmarks recording the relative vertical motion between land and sea since their construction or formation. The heights of the significant markers were measured and compared with the present sea level, applying corrections for tide amplitude and pressure values at the time of the surveys. These data, together with their relative error estimation (elevation and age), are compared with sea-level predictions using the prediction model of Lambeck and Purcell (2005) for the Mediterranean coast, recently applied in Lambeck et al. (2004b) and Antonioli et al. (2007) for the Mediterranean region. This model uses a new equivalent sea-level (esl) function (the ice-volume esl change; Lambeck and Chappell, 2001) that assumes a small continuous melting of the Antarctic ice sheet until recent times. The accuracy of these predicted values is a function of the model parameter's uncertainties in defining the earth response function and the ice load history (esl). The results provide new insights on the rates of relative sea level rise and on the vertical tectonic stability in this region during the last ~2 ka.

2. Materials and methods

Nineteen archaeological markers were surveyed along the coasts of Libya (4 sites) and Tunisia (15 sites) (Table 1). Analysis was

performed through four subsequent steps: 1) measurements of the elevation of the significant archaeological markers of maritime structures with respect to the present sea level; 2) correction of the elevation measurements for tide and atmospheric pressure effecting the level of the sea surface at the time of surveys, using the data and algorithms adopted by the Permanent Service Mean Sea Level (PSMSL, www.pol.ac.uk, as well as Woodworth, 1991; Woodworth and Player, 2003) for the Mediterranean Sea (atmospheric corrections are based on the inverted barometer assumption using the closest available meteorological data obtained at www.metoffice.com); 3) error estimation for ages and elevation measurements of the archaeological markers, after their functional heights were evaluated on the basis of accurate archaeological interpretations (age errors are estimated from the architectural features; elevation errors derive from the measurements, corrections and estimates of the functional heights. For example, the lower limiting values for the quarries); 4) examination of the predicted and observed sea levels, by comparing the current elevations of the markers (i.e. the relative sea-level change at each location) with the sea-level elevation predicted by the last geophysical model for each location. Tectonic stability is hypothesized at the sites where the elevations of the markers are in agreement with the predicted sea-level curve. Conversely, an area has experienced tectonic subsidence or uplift when the elevations of the markers are below or above that of the predicted sea-level curve.

Field surveys were performed during September 2005 in Libya, and May 2007 and January 2008 in Tunisia. All elevation measurements were done by optical or mechanical methods during calm sea and they were related to the sea-level position for that particular moment. Since the investigated archaeological structures were originally used year round, the defining levels correspond to the

Table 1

(A) Site numbers (in brackets are listed according to our data base); (B) names as indicated in Figs. 4 and 5; (C) country; (D) type of archaeological remain; (E) and (F) are the WGS84 coordinates of the sites; (G) age estimates based on historical documentation; (H) functional elevation of the significant markers; (I) elevation error estimates; (K) limiting value of survey data: UL = upper limit, LL = lower limit; (L–O) are the predicted sea levels at 2 ka according to different parameters used in the model; (P) tectonic environment. Architectural features used to define sea level: P = pools; H = harbour; Q = quarry, N = notch, FT = fish tank, SW = slipway, S = sewerage, BW = breakwater, PV = pavement, RD = road, G = geology. The lowest cuttings of quarries are assumed to be at 0.30 m above high tide and the sidewalk (crepidinae) in the fish tanks at 0.20 m above high tide. For the pools of Sidi Mansour and Maamoura, perhaps dedicated to small flat fishes or production of *garum* (roman fish sauce), the minimum functional elevation corresponds to at least 0.3 m above the maximum local high tide. The current elevation of the road at Sidi Salem above the mean sea level is 0.43 m. For this marker, assuming a maximum tidal range of 0.90 m (from the Tide Gauge of Humtsuk) to keep the road always dry, indicates a sea level change of at least 0.45 m or, conversely, a relative sea level change < 0.45 m (if the road could be submerged during max high tides). Elevation data are the average values of multiple measurements collected at the best preserved parts of the investigated structures. All elevation data are corrected for tides and atmospheric pressure. The maximum tidal range in northern Africa is ~0.40 m with the exception of a limited part of the Gulf of Gabes that is subjected to tides up to 1.8 m. Tidal corrections have been performed using the algorithms of the PSMSL (http://www.pol.ac.uk). The atmospheric pressure correction is for the difference in pressure at the time of observation and the mean annual pressure for the site and is based on the inverted barometer assumption using nearby station data from http://www.metoffice.com. Columns K to N give predicted isostatic contributions for four earth models discussed in text. The tectonic rates assume uniform uplift since the time of construction of the archaeological markers. The uncertainty estimates include observational and model uncertainties.

A	B	C	D	E	F	G	H	I	J	K	L	M	N	O
Site No	Site name	Country	Marker	Latitude	Longitude	Age (ka)	Obs. rslc	σ obs.	Limit	ma3C	ma3A	ma2C	ma2A	Tectonic Rate
1 (9)	Gammarth	Tunisia	S	36.921	10.296	1.8 ± 0.05	-0.58	0.3	UL	-0.83	-0.61	-0.68	-0.49	0.12 ± 0.20
2 (8)	Carthage	Tunisia	SW	36.845	10.327	2.0 ± 0.1	-0.55	0.5	UL	-0.93	-0.69	-0.78	-0.56	0.17 ± 0.28
3 (10)	Mraissa	Tunisia	Q	36.976	10.868	2.0 ± 0.15	-0.48	0.2	UL	-1.09	-0.84	-0.89	-0.67	0.27 ± 0.16
4 (7)	Sidi Daoud	Tunisia	FT	37.002	10.894	1.8 ± 0.25	-0.28	0.1	LL	-0.97	-0.74	-0.78	-0.58	0.35 ± 0.14
5 (6)	Maamoura	Tunisia	P	36.455	10.804	1.5 ± 0.05	-0.46	0.2	UL	-0.62	-0.44	-0.52	-0.36	0.12 ± 0.18
6 (13)	Sidi Mansour	Tunisia	P	35.771	10.843	1.9 ± 0.1	-0.46	0.3	UL	-0.7	-0.47	-0.64	-0.44	0.13 ± 0.19
7 (11)	Salakta 1	Tunisia	P	35.388	11.042	1.7 ± 0.15	-0.55	0.3	LL	-0.6	-0.4	-0.55	-0.36	0.04 ± 0.21
8 (12)	Salakta 2	Tunisia	BW,P	35.388	11.041	1.7 ± 0.15	-0.58	0.3	UL	-0.6	-0.4	-0.55	-0.36	0.03 ± 0.21
9 (20)	El Grine	Tunisia	G	33.655	10.568	-	0.31	0.05	LL	-	-	-	-	-
10 (18)	Sidi Salem 1	Tunisia	RD	33.895	10.829	1.9 ± 0.1	-0.20	0.3	LL	-0.33	-0.12	-0.38	-0.19	0.11 ± 0.19
11 (14)	Lalla Hadria	Tunisia	PV	33.789	11.059	1.9 ± 0.1	-0.28	0.3	UL	-0.38	-0.17	-0.41	-0.22	0.09 ± 0.19
12 (16)	El Kantara (Meninx)	Tunisia	BW	33.683	10.920	2.0 ± 0.15	-0.31	0.3	UL	-0.33	-0.11	-0.39	-0.19	0.05 ± 0.19
13 (19)	Ersifet	Tunisia	Q	33.559	10.944	1.8 ± 0.1	-0.30	0.2	UL	-0.26	-0.06	-0.31	-0.13	0.02 ± 0.16
14 (17)	Rass Segala	Tunisia	H	33.532	10.925	1.8 ± 0.1	-0.34	0.3	UL	-0.25	-0.05	-0.30	-0.13	-0.00 ± 0.20
15 (15)	Gigtis	Tunisia	H	33.533	10.680	1.9 ± 0.15	-0.37	0.3	UL	-0.2	0.01	-0.28	-0.10	-0.04 ± 0.19
16 (1)	Sabratha	Lybia	P	32.808	12.486	2.0 ± 0.05	-0.48	0.2	LL	-0.43	-0.21	-0.44	-0.23	-0.00 ± 0.15
17 (5)	Fondough en Naggaza	Lybia	FT	32.717	14.100	2.0 ± 0.05	-0.24	0.2	UL	-0.75	-0.52	-0.66	-0.44	0.25 ± 0.15
18 (4)	Wadi Jabrum	Lybia	FT,Q	32.717	14.105	2.0 ± 0.05	-0.37	0.2	UL	-0.75	-0.52	-0.66	-0.44	0.19 ± 0.15
19 (3)	Villa Silin	Lybia	Q,N	32.709	14.178	2.0 ± 0.05	-0.38	0.2	UL	-0.76	-0.54	-0.67	-0.45	0.19 ± 0.15
20 (2)	Leptis Magna	Lybia	H	32.638	14.300	2.0 ± 0.05	-0.48	0.2	UL	-0.75	-0.52	-0.66	-0.44	0.13 ± 0.15

annual mean conditions at the time of construction. The measurements are therefore reduced to mean sea level applying tidal corrections at the surveyed sites, using the data of the nearby available tide gauges or the tidal predictions of the PSMSL. Corrections are generally within a few cm (the mean amplitude of Mediterranean tides is <45 cm) but, estimating and correcting for tide amplitudes are crucial for the central part of the Gulf of Gabes (Tunisia), as this area is affected by large tides (Sammari et al., 2006).

The *functional heights* of the archaeological benchmarks were defined in order to estimate the sea-level change in each location. This parameter has been extensively described in Lambeck et al., 2004b and applied in other studies (Auriemma and Solinas, 2009). It is defined as the elevation of specific architectural parts of an archaeological structure with respect to an estimated mean sea level at the time of their construction. It depends on the type of structure, on its use and on the local tide amplitudes. Functional heights also define the minimum elevation of the structure above the local highest tides. This information can also be deduced from previous publications (Schmiedt, 1965, 1974; Flemming, 1969; Flemming and Webb, 1986), from historical documents (Hesnard, 2004; Vitruvius), from the remnants of the Roman Age shipwrecks (which provided data on the size of the ships or boats and their draughts, as reported, for example, in Charlin et al., 1978; Steffy, 1990; Pomey, 2003; Medas, 2003) and through rigorous estimation of the functional heights of the piers, by using and interpreting different type of markers on the same location (Lambeck et al., 2004b). The use of these structures, their age and conservation, the accuracy of the survey and the estimation of the functional heights were all used in considering the observational uncertainties at each site. Concerning the functional height of quarries, found along the coast in Tunisia and Libya in proximity of coastal archaeological sites, a value of at least 0.3 m was used. This value was estimated by the relationships between the lowest elevation of the mining place and sea level as inferred by the quarry in Ventotene island (Italy), compared with the functional elevations of the fish tank and the pier located in close proximity (Lambeck et al., 2004b). The latter provide precise estimates of the elevation of the Roman markers related with sea level and were used to calibrate the elevation of the quarry. This value was successfully applied to the other quarries in the Mediterranean (Antonoli et al., 2007). Besides archaeological markers, in one case biological indicators such as *Strombus bubonius* and *Lithophaga* were used. The latter was found still in situ at El Grine, southeastern Tunisia. It was extracted from the limestone units and was chosen among those fossils placed at the highest elevations above sea level. Its elevation has been measured at +0.3 m with respect to the local mean sea level, after tidal and pressure correction were applied.

3. Data along the coast of Tunisia

The ~1300 km coastlines of Tunisia is abundant with archaeological installations whose ages date to the Punic age (Slim et al., 2004), although the best preserved sites are of Roman age of ~2 ka BP (Fig. 1a and 2). As the aim of this paper is to provide new analysis and interpretation on the sea level changes since the last 2 ka, the archaeological features of the investigated sites are discussed briefly; readers are referred to specific archaeological publications. The survey data show a general evidence of coastal submersion since Roman time, from the elevation of urban structures, fish tanks, harbours, quarries and roadways (Fig. 3). Some sites, such as the fish tank at Sidi Daoud equipped with channels tidal controlled for water exchange (see Lambeck et al., 2004b for description of channel systems of fish tanks), provide an excellent estimation of the intervening relative sea level rise since its construction 0.28 ± 0.10 m (Fig. 4b). Other significant sites are the harbours of Gigit

and Rass Segala (Fig. 4c) that provide relative sea level rise values of 0.37 ± 0.30 m and 0.34 ± 0.30 m, respectively, from the functional elevations of the pier surfaces (see Lambeck et al., 2004b, and Antonoli et al., 2007, for description of the functional elevations of piers). Valuable data came from the two submerged pools of Maamoura (Fig. 4a) and the seven pools of Sidi Mansour (Fig. 4d). These sites, perhaps used as fish tanks for small flat fishes or garum sauce (Slim et al., 2004), both provide relative sea level rise of 0.46 ± 0.20 m and 0.46 ± 0.30 m, respectively. Data are inferred from the functional elevations estimated from the relationships between the differential elevation among the pool floors, the narrow channels for water exchange and the presently submerged walking surfaces. The latter were dry and above the high tides at the time of their construction. Other data are from the submerged buildings walls of Salakta (Fig. 4i), El Kantara and the roadway of Sidi Salem (Fig. 4e). The latter is presently in the tidal range. The quarries of Ersifet and Mraissa (Fig. 4f) indicated relative sea level rises of 0.30 ± 0.20 m and 0.48 ± 0.10 m, respectively (see Lambeck et al., 2004b, and Antonoli et al., 2007, for description of the functional elevations of quarries). The pavement of Lalla Hadria, the slipways of Carthage and the sewerage of Gammarth, are additional archaeological markers that show a relative sea level rise ranging between 0.58 ± 0.50 m and 0.28 ± 0.3 m. These sites have been included in the analysis, although they are less precise due to less constrained functional elevations. All these sites along the coast of Tunisia, are in agreement to show a relative sea level rise since the last ~2 ka, in the range of 0.18 ± 0.2 m and 0.43 ± 0.3 m, with the exception of the less constrained markers as the slipway of Carthage (0.24 ± 0.5 m). The most precise data are from the fish tank of Sidi Daoud (0.05 ± 0.1 m) (Table 1).

Besides the archaeological remains, fossils of *Lithophaga* and *S. bubonius* were found. The first, placed at a corrected elevation of $+0.31 \pm 0.05$ m, was collected at El Grine, in SE Tunisia. The sample was dated through ^{14}C analysis and provided an age of 5846–5700 calibrated (CALIB 5.1, lab. N° DSH83). Its dating and position are in agreement with other biological data previously published (Jedoui et al., 2003; Morhange and Pirazzoli, 2005 and references therein). As regards the geological evidence of the Last Interglacial, a deposit containing *S. bubonius* at Monastir (Fig. 4g) occurs at 14 m above sea level. Elsewhere the elevation of similar Last Interglacial Aeolian and beach ridge deposits vary between 0 and 45 m above current sea level (Richards, 1996; Bouaziz et al., 2003; Elmejdoub and Jedoui, 2009).

4. Data along the coast of Libya

The Mediterranean coasts of western Libya show several coastal archaeological installations, such as urban structures, pools, harbours and quarries. Unfortunately, some are not well preserved, preventing their use for this study. Approximately 200 km of the western Libyan coast from the ancient cities of Sabratha to Leptis Magna was investigated (Fig. 2), where coastal installations such as the great harbour of Leptis Magna, the pools of Sabratha, and Villa Silin, can still be found. Other less precise sea level indicators, such as coastal quarries, provide additional information (Table 1).

The harbour of Leptis Magna is the most important archaeological site of this area and displays several sea level indicators consisting mainly in very well preserved piers with bollards (Fig. 5a). This harbour, which was abandoned after it was filled by sand caused by the failure of the dam placed at the mouth of the river which exits into the harbour basin, was surveyed for the first time in 1958 by Bartocchini (1960) who published exhaustive plans, including elevations of significant sea level indicators. In 2005, from the elevation of the piers (presently at 1.2 m above sea level) and the bollards, a relative sea level rise of 0.48 ± 0.2 m since the

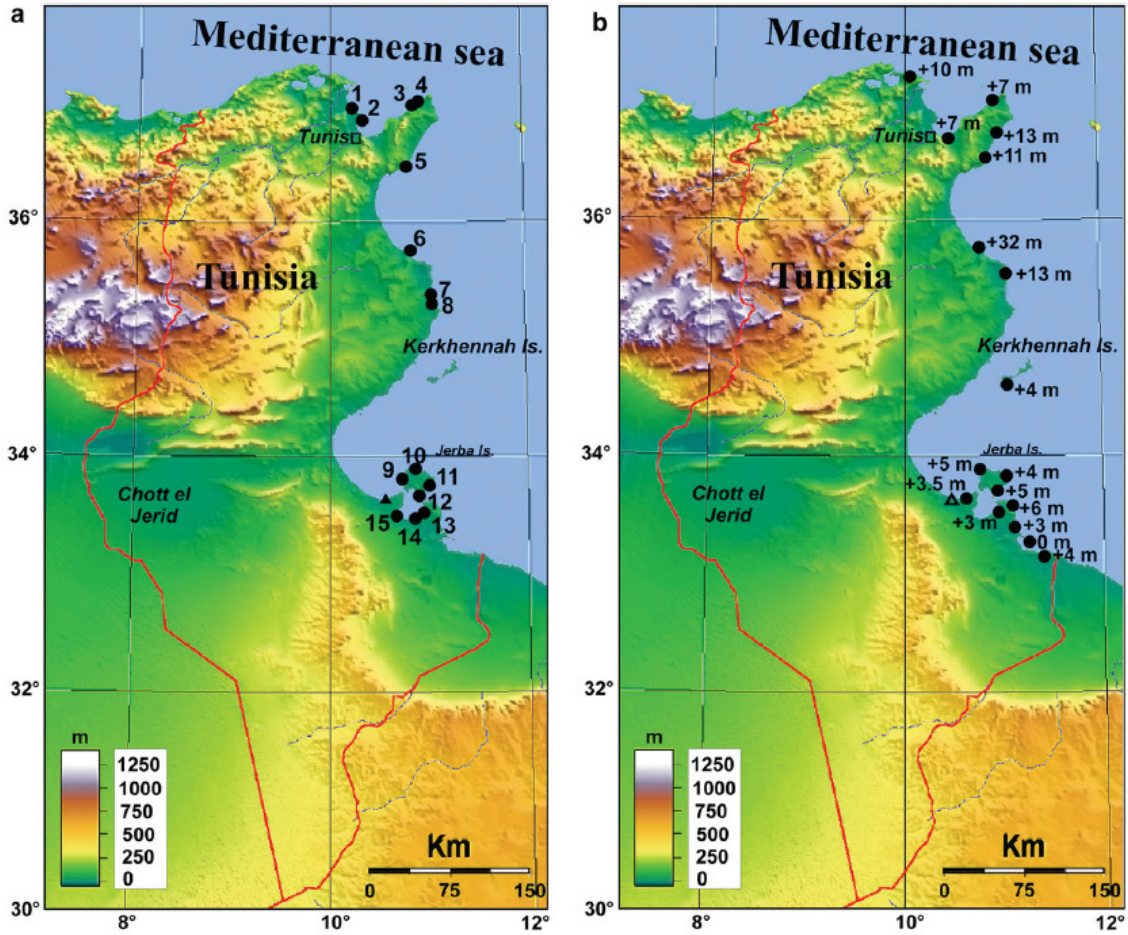


Fig. 1. (a) Map of the investigated archaeological sites in Tunisia; (b) elevation of the MIS 5.5 (modified from Bouaziz et al., 2003). The black triangle is the position of the *Lithophaga* sampled at El Grine.

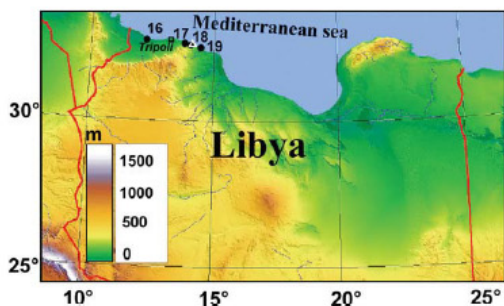


Fig. 2. Map of the investigated archaeological sites in Libya. The elevation of the MIS 5.5 at is also reported in the map. The white triangle is the position of the MIS 5.5 at +6 m above sea level (C. Faccenna, personal communication).

last 2 ka is estimated. This value is in agreement with the observation performed by Bartocchini in 1958. Other indicators include stairs and bollards, and reflect the commercial use of the harbour, planned for large commercial ships.

At Sabratha, the pools of the thermal area, equipped with channels opening toward the sea, indicate a sea level change of 0.48 ± 0.2 m (Fig. 5b). Minor relative sea level values are inferred from the coastal quarries of Villa Silin (Fig. 5c) as well as the fish tanks of Wadi Jabrum (Fig. 5d) and Foundoug en Nagazza. A tidal notch of 40 cm height is also present at Villa Silin, at an elevation corresponding to the current sea level.

Concerning the elevation of the MIS 5.5 transgression, fossil beaches are located between 5 and 10 m a.s.l., close to the fish tank of Fondoug En Nagazza (Claudio Faccenna, personal communication). Based on the elevation of the MIS 5.5 highstand this outcrop is assigned to the Last Interglacial (LIG).

5. The Isostatic model

The theory used here for describing the glacio-hydroisostatic process has been previously discussed in Lambeck et al., 2003 and its

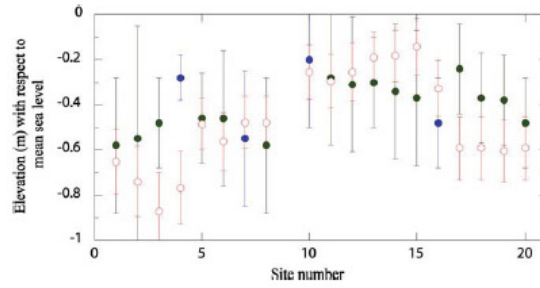


Fig. 3. Elevation (m) of the observed upper (green) and lower (blue) limits to sea level estimates from the archaeological sites compared with the predicted levels for the epoch of construction (open red circles). The predictions include the glacio-hydro isostatic contributions based on the mean of earth models discussed in the text and a contribution of recent increase in ocean volume at an equivalent sea level rate of 1.5 mm/year for the past 100 years (see Table 1 for data and Figures 1 and 2 for site location and numbering).



Fig. 4. The investigated archaeological sites in Tunisia: a) The pools of Sidi Mansour; b) the fish tank of Sidi Daoud. Note the two channels (front and right) for the exchange of water; c) the Roman age pier of Rass Segala; d) the pools at Maamoura, e) the roman road of Sidi Salem; f) the quarries at Mraissa; g) the MIS 5.5 fossil of *Strombus Bubonius* elevated at +5 m above sea level near Monastir; h) the submerged buildings and pools at Salakta; i) the submerged ruins of maritime installations at Salakta.

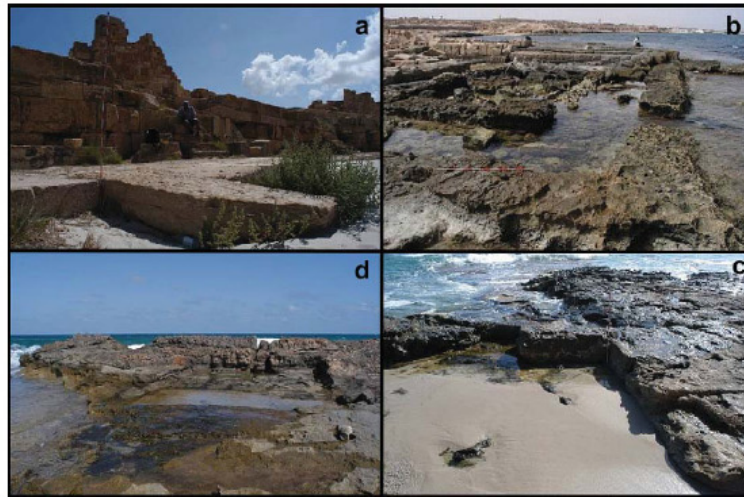


Fig. 5. The investigated archaeological sites in Libya: a) The Harbour of Leptis Magna. Front: the pier at 1.2 ± 0.2 m above current sea level. Back: the bollards and the stairways leading to the warehouses; b) the pools of the Baths of Oceanus (thermal installation) at Sabratha; c) the roman age coastal quarry at Villa Silin; d) the roman age fish tank at Wadi Jabrum.

applications to the Mediterranean region have been most recently discussed in Lambeck et al. (2004a, b) and Lambeck and Purcell (2005). The input parameters into these models are the ice models from the time of the Last Interglacial to the present and the earth rheology parameters. These have been established by calibrating the model against sea-level data from tectonically stable regions and from regions that are sensitive to particular subsets of the parameters: for example, data from Scandinavia to constrain the northern European and Eurasian ice models and data from far-field sites to improve the ice-volume equivalent sea-level function. Iterative procedures are used in which far-field data establish the global changes in ice volume and mantle rheology and near-field data constrain the local ice sheets and mantle rheology. The procedure is then re-iterated, using the near-field derived ice models to improve the isostatic corrections for the far-field analysis. The Mediterranean data, from the intermediate field, have been previously included in these analyses to establish constraints on regional mantle parameters and the eustatic sea-level function (Lambeck et al., 2004b) and on rates of tectonic vertical movements (Lambeck, 1995; Antonioli et al., 2006). This paper uses the most recent iteration results for the ice models (Lambeck et al., 2006; 2010) which include improved ice models for the major ice sheets of Europe, North America, Antarctica and Greenland back to the penultimate Interglacial, as well as mountain glaciation models including the Alps (Lambeck and Purcell, 2005). This last addition impacts primarily on the sea-level predictions for northern Italy and Slovenia. The time-integrated ice volumes are consistent with the ice-volume esl function previously established (Lambeck et al., 2002).

The solutions here and for other regions have indicated that three-layer rheological models largely suffice to provide a consistent description of the sea-level change due to the growth and decay of ice sheets. This comprises a high viscosity or elastic lithosphere defined by an effective elastic thickness of between 65 and 80 km, an upper mantle from the base of the lithosphere down to the 670 km seismic discontinuity with an average effective viscosity of between $(2-3) \times 10^{20}$ Pa s, and a lower mantle with an average effective viscosity of $(1-3) \times 10^{22}$ Pa s.

The Mediterranean data alone have so far not yet yielded solutions in which a complete separation of earth-model parameters

have been possible, nor in which these parameters can be separated fully from eustatic or ice-model unknowns. However, the combination used here provides a set of very effective interpolation parameters that describe well the observational data and that allow for an effective separation of tectonic and isostatic–eustatic contributions to sea level.

Table 1 gives the isostatic predictions for a subset of parameters within this model space. The second letter in the model name denotes lithospheric thickness but this parameter is not critical for these sites and the results are for a = 65 km lithosphere. The third character in the name refers to the upper mantle viscosity in units of 10^{20} Pa s, and the fourth character refers to the lower mantle viscosity with $A = 10^{22}$ and $C = 3 \times 10^{22}$ Pa s. A comparison between these model predictions and observations indicates that within the uncertainties of the latter agreement is satisfactory across this range of parameters and a mean model with uncertainties established from the spread of predictions at each site was adopted. To this a modern eustatic sea-level rise of 1.5 mm/year for the past 100 years was added, consistent with the inference previously drawn from the Roman period fish-tanks in Italy that the this rise started about 100 years ago (Lambeck et al., 2004b). Fig. 3 illustrates the comparison.

For most sites the predicted and observed values agree to within their respective uncertainties. Sidi Daoud (site 4) is one exception where the observed lower limit estimate lies well above the predicted value and is indicative of tectonic uplift. Table 1 gives the vertical rates inferred from the discrepancies between the observed and the mean-predicted (including the modern esl correction) values, with the estimate of the uncertainty taking into consideration the uncertainties of the observed and model values as well as an uncertainty of 0.09 m for the modern eustatic contribution (Lambeck et al., 2004b).

6. Discussion

The coastal archaeological sites of Punic-Roman age located along the coasts of Tunisia and Libya show that locally sea level has risen between 0.2 and 0.6 m during the last ~2 ka and that much of the region is consistent with vertical tectonic stability on this time

scale. Most of the variation observed from site to site appears to be a consequence of the glacio-hydro-isostatic response. In this part of the Mediterranean quite substantial changes in this response can be expected because of the coastal geometry which effectively provides a north-south section across the predominantly east-west trending contours of equal sea-level change (see Fig. 2 of Lambeck and Purcell, 2005). Thus these data can be expected to have some resolving power for mantle structure if the observational data is sufficiently accurate, and some of the regional differences that can be seen in Fig. 3 suggest that the isostatic model may overestimate this variability and that models with higher lithospheric thickness may be appropriate for what is effectively a continental lithosphere here. But since all of the observations are only limiting values this data alone is inadequate to establish the earth parameters from this data set alone.

As noted above, the only site with a systematic difference between the observed and predicted values occurs for Sidi Daoud (site 4) on the northwest side of Cap Bon. At the nearby site of Mraissa (site 3) the observed elevation is also above the predicted level and the average tectonic uplift rate for these two sites is ~ 0.3 mm/y and significant at 2 sigma level (Table 1). Both Burolet (1991) and Sebei et al. (2003) have previously suggested that faults on this peninsula may be active.

Sites 10–15 are all from the closely clustered area of Jerba Island and the eastern side of the Gabes Gulf and show very considerable consistency, although the upper limit estimates from the last three sites lie above (but within uncertainties) the predicted values. None of the indicators here have the intrinsic accuracy of fish tanks that are complete with their channels and sluice gates but their internal agreement indicates that the relative functional heights used are appropriate. Of note is that the *Lithophaga* sample, dated at ~ 5 ka BP, from nearby El Grine yielded an elevation of 0.3 m above sea level (corrected for barometric pressure and tides). This is a lower limit value since *Lithophaga* lives only underwater even during the lowest tides. Thus local sea level here was above present sea level whereas all isostatic predictions that are consistent with the results for the later periods indicate that highstands were not reached at this site and at this time. Hence, the current elevation of +0.3 m asl is not consistent with the sea level prediction valid for this stable region of the Mediterranean.

The sites from Libya also yield good agreement, with the lower limit value from Sabratha occurring below the predicted values and the upper limit observations from the other sites occurring above the predicted positions. It should be noted that the two fish-tanks are much less complete than those usually found along the coast of Italy and that their functions remain unclear, it having been suggested that they may have served as basins for the preparation of *garum* sauce or purple dye (reference) in which case the reference level may have been near the high tide level rather than mean sea level.

As illustrated in Figure 1b there is considerable evidence for raised shorelines during the last Interglacial, MIS 5.5 (Bouaziz et al., 2003; Jedoui et al., 2003; Elmejdoub and Jedoui, 2009) with reported elevations ranging from near zero to 45 m. Much of this evidence is in the form of successions of Aeolian and beach ridge deposits that are assigned Last Interglacial age because they contain the fossil *Strombus bubonius*. The more precise markers such as tidal notches and inner margins that are prevalent on the Italian coast (Ferranti et al., 2006) are not present here and it is generally not possible to relate these deposits with any accuracy to mean sea level.

For Jerba Island and the eastern end of the Gulf of Gabes (Sebkh el Melah), MIS 5.5 deposits are reported at elevations between 0 and 6 m above mean sea level (Jedoui et al., 2003) and the inference is that this is an area of long-term stability, consistent with the archaeological evidence from sites 10–15 but not with the mid-Holocene result from site 9.

At the southern end of the Gulf of Hammamet (Monastir) MIS 5.5 deposits occur between 0 and 32 m above sea level, and it has been suggested that this is indicative of vertical movements on the Sknes-Kmiss fault (Richards, 1986). If the higher value of 32 m reflects true uplift then the average rate for the past 125,000 years is ~ 2.5 mm/year, compared with an effectively zero rate indicated for the past 2000 years at Sidi Mansour (site 6 of figure 1a), near Monastir.

7. Conclusions

Earlier work has shown the complex pattern of sea level change within the Mediterranean region as a result of the decay of the last ice sheets, with long wavelength variations resulting from mantle deformation induced by the unloading of the northern hemisphere ice sheets and shorter wavelength variations from the loading of the ocean basins, including the Mediterranean, by the melt water (Lambeck and Purcell, 2005). This pattern is diagnostic of mantle rheology as well as of the former ice sheets themselves and observations of sea level change provide constraints on this rheology and on the time history of the ice melt. In the presence of tectonics the predicted isostatic pattern can be significantly disrupted and the challenge is to develop an accurate sea-level data base that is representative of both stable and unstable sites. The epoch ~ 2 ka BP is particularly significant because of the large amount of archaeological information around the Mediterranean shore line that can be precisely related to the position of sea level at that time, relative to the present. The significance of the new Tunisia-Libya data is that it fills a gap in the spatial pattern in an area where the sea-level response is particularly sensitive to mantle rheology. This is in contrast to the coast of Israel where this dependence is low (Anzidei et al., this volume) and, to a lesser degree, to the Tyrranean coast of Italy (Lambeck et al., 2004b). The present analysis is indicative of the potential of the coastal archaeological structures to constrain past sea level, thereby providing constraints on mantle rheology as well as a reference surface for quantifying rates of vertical tectonic motions.

This first analysis of archaeological data from a large section of coast from Tunis to the east of Tripoli reflects the spatial variability in sea level that is expected from the glacio-hydro-isostatic process as well as from superimposed tectonic signals. The archaeological data shows that the coast of Libya experienced a relative sea level rise in the past 2000 years of between 0.24 ± 0.10 m and 0.48 ± 0.10 m similar to the range seen along the coast of Tunisia of between 0.20 ± 0.10 m and 0.58 ± 0.30 m. Most of this signal is explained by the isostatic-eustatic process that also defines sea level in other parts of the Mediterranean. Thus estimates for the tectonic rates for this interval are mostly insignificant with the exception of the northwestern side of Cap Bon in Tunisia where the uplift rate of ~ 0.15 mm/year appears to be significant at the 2 sigma level in agreement with independent data (Burolet, 1991; Bouaziz et al., 2003).

Acknowledgments

This paper is dedicated to beloved Renato Funiello great geologist, athlete and fond of archaeology. We are thankful to Philip Woodworth, who provided tidal predictions using data and algorithms of the Permanent Service for Mean Sea Level (www.pol.ac.uk). Luisa Musso of University of Roma 3 who supported the archaeological surveys in Libya. Claudio Faccenna for the fruitful suggestions. The anonymous reviewers and Norm Catto who improved this paper with their suggestions. This study has been partially funded by MIUR – Prin 2006 (Grant Project “Il ruolo del riaggiustamento isostatico post-glaciale nelle variazioni del livello marino globale e Mediterraneo: nuovi vincoli geofisici, geologici ed archeologici”, directed by G. Spada), ENEA and INGV.

References

- Antonoli, F., Anzidei, M., Auriemma, R., Gaddi, D., Furlani, S., Lambeck, K., Orrù, P., Solinas, E., Gaspari, A., Karinja, S., Kovacic, V., Surace, L., 2007. Sea level change during Holocene from Sardinia and northeastern Adriatic (Central Mediterranean sea) from archaeological and geomorphological data. *Quaternary Science Reviews* 26, 2463–2486.
- Auriemma, R., Solinas, E., 2009. Archaeological remains as sea level change markers: a review. *Quaternary International*, 1–13. doi:10.1016/j.quaint.2008.11.012.
- Bartocchini, R., 1960. Il porto romano di leptis magna. 1958, Roma. *Boll Centro Studi per la storia dell'architettura* 13 (suppl.).
- Bouaziz, S., Jedoui, Y., Barrier, E., Angelier, J., 2003. Neotectonique affectant les depots marins tyrrhéniens du littoral sud-est tunisien: implications pour les variations du niveau marin. *Comptes Rendus Geoscience* 335, 247–254.
- Burrollet, P.F., 1991. Structures and tectonics of Tunisia. *Tectonophysics* 195, 359–369.
- Caputo, M., Pieri, L., 1976. Eustatic variation in the last 2000 years in the Mediterranean. *Journal of Geophysical Research* 81, 5787–5790.
- Charlin, G., Gassend, J.M., Lequément, R., 1978. L'épave antique de la baie de cavalière – le levandou. *Var. Archeonautica* 2.
- Elmejdoub, N., Jedoui, Y., 2009. Pleistocene raised marine deposits of the Cap Bon peninsula (N-E Tunisia): records of sea-level highstands, climatic changes and coastal uplift. *Geomorphology* 112 (3–4), 179–189.
- Felici, E., 1998. La ricerca sui porti romani in cementizio: metodi e obiettivi. In: Firenze (Ed.), *Archeologia Subacquea, Come Opera L'archeologo Sott'acqua*. All'insegna Del Giglio, pp. 275–340.
- Felici, E., 2000. Modern development and ancient maritime sites along the Tyrrhenian coast. In: *Focus on Alexandria*. UNESCO Publishing, Paris, pp. 81–88.
- Ferranti, L., Antonoli, F., Amorosi, A., Dai Prà, G., Mastronuzzi, G., Mauz, B., Monaco, C., Orrù, P., Pappalardo, M., Radtke, U., Renda, P., Romano, P., Sansò, P., Verrubbi, V., 2006. Elevation of the last interglacial highstand in Italy: A benchmark of coastal tectonics. *Quaternary International* 145–146, 30–54.
- Flemming, N.C., 1969. Archaeological Evidence for Eustatic Changes of Sea Level and Earth Movements in the Western Mediterranean in the Last 2000 years. *Geological Society of America, Special Paper* 109.
- Flemming, N.C., Webb, C.O., 1986. Tectonic and eustatic coastal changes during the last 10,000 years derived from archaeological data. *Zeitschrift für Geomorphologie NF* 62, 1–29.
- Hesnard, A., 2004. Vitruve, de architectura, V 12, et le port romaine de marseille. Eds. In: Gallina Zevi, Anna, Turchetti, Rita (Eds.), *Proceedings Anciennes Routes Maritimes Méditerranées. Le Structure Dei Porti e Degli Approdi Antichi*, Ostia, pp. 175–204.
- Jedoui, Y., Reyss, J.L., Jallel, N., Montacer, M., Ismail, H.B., Davaud, E., 2003. U-series evidence for two high last interglacial sea levels in southeastern Tunisia. *Quaternary Science Reviews* 22, 343–351.
- Lambeck, K., 1995. Late Pleistocene and Holocene sea-level change in Greece and south-western Turkey: a separation of eustatic, isostatic and tectonic contributions. *Geophysical Journal International* 122, 1022–1044.
- Lambeck, K., Chappell, J., 2001. Sea level change through the last glacial cycle. *Science* 29, 679–686.
- Lambeck, K., 2002. Sea-level change from mid-Holocene to recent time: an Australian example with global implications. In: Mitrovica, J.X., Vermeersen, B. (Eds.), *Glacial Isostatic Adjustment and the Earth System*. American Geophysical Union, Washington, DC, pp. 33–50.
- Lambeck, K., Purcell, A., Johnston, P., Nakada, M., Yokoyama, Y., 2003. Water-load definition in the glacio-hydro-isostatic sea-level equation. *Quaternary Science Reviews* 22, 309–318.
- Lambeck, K., Antonoli, F., Purcell, A., Silenzi, S., 2004a. Sea level change along the Italian coast for the past 10,000 yrs. *Quaternary Science Reviews* 23, 1567–1598.
- Lambeck, K., Anzidei, M., Antonoli, F., Benini, A., Esposito, E., 2004b. Sea level in Roman time in the central Mediterranean and implications for modern sea level rise. *Earth and Planetary Science Letters* 224, 563–575.
- Lambeck, K., Purcell, A., 2005. Sea-level change in the Mediterranean Sea since the LGM: model predictions for tectonically stable areas. *Quaternary Science Reviews* 24, 1969–1988.
- Lambeck, K., Purcell, A., Funder, S., Kjær, K., Larsen, E., Möller, P., 2006. Constraints on the Late Saalian to early Middle Weichselian ice sheet of Eurasia from field data and rebound modelling. *Boreas* 35, 539–575.
- Lambeck, K., C.D. Woodroffe, F. Antonoli, M. Anzidei, W.R. Gehrels, O. Van de Plassche, A.J. Wright, *Paleoenvironmental records, geophysical modelling and reconstruction of sea-level trends and variability on centennial and longer time scales*, Geological Society of London, in press.
- Medas, S., 2003. The late-Roman Parco di Teodorico Wreck, Ravenna, Italy: preliminary remarks on the hull and the shipbuilding. In: *Boats, Ships and Shipyards. Proceedings of the Ninth International Symposium on Boat and Ship Archaeology, Venice 2000*, C. Beltrame eds, Oxford, 42–48.
- Morhange, C., Pirazzoli, P.A., 2005. Mid-Holocene emergence of southern Tunisian coasts. *Marine Geology* 220, 205–213.
- Pirazzoli, P.A., 1976. Sea level variations in the northwest Mediterranean during Roman times. *Science* 194, 519–521.
- Pomey, P., 2003. Reconstruction of Marseilles 6th century BC Greek ships. In: C. Beltrame ed., *Boats, Ships and Shipyards. Proceedings of the Ninth International Symposium on Boat and Ship Archaeology, Venice 2000*. Oxford pp. 57–65.
- Richards, G.W., 1986. Late quaternary deformed shorelines in Tunisia. *Zeitschrift für Geomorphologie NF* 62, 183–195.
- Sammarì, C., Koutitonsky, V.G., Moussa, M., 2006. Sea level variability and tidal resonance in the Gulf of Gabes, Tunisia. *Continental Shelf Research* 26, 338–350.
- Schmiedt, G., 1965. Antichi porti d'Italia. *L'Universo* 45, 234–238.
- Schmiedt, G., 1974. Il livello antico del mar Tirreno. *Testimonianze da Resti Archeologici*, E. Olschki, Firenze, 323 pp.
- Slim, H., Pol, Trouset, Paskoff, R., Oueslati, A., 2004. Le littoral del la Tunisie. *Etude goarchéologique et historique*. Conseil National Recherche Editions, Paris, 310 pp.
- Steffy, J.R., 1990. The boat: a preliminary study of its construction. In: Wachsmann, S. (Ed.), *The Excavation of an Ancient Boat in the Sea of Galilee (Lake Kinneret)*. Israel Antiquities Authority, Jerusalem, pp. 29–47.
- Woodworth, P.L., 1991. The permanent service for mean sea-level and global sea-level observing system. *Journal of Coastal Research* 7, 699–710.
- Woodworth, P.L., Player, R., 2003. The permanent service for mean sea-level: an update to the 21st century. *Journal of Coastal Research* 19, 287–295. <http://www.pol.ac.uk/PSMSL/>.

Annex 6
(10 pages)

Abstract - Calabria is one of the most complex geological regions of the Mediterranean basin, which experienced large earthquakes and uplift and is still undergoing active tectonics. Along its coasts are located archaeological sites that can be used as powerful indicators of the relative vertical movements between land and sea since their construction. This paper presents and discusses data on the relative sea-level change as estimated from maritime archaeological indicators of the last ~2.0 ka BP existing along the Tyrrhenian coast of Briatico. These sites still show the remnants of a Roman age fish tank and a submerged breakwater about 320m long. The palaeo sea level has been obtained measuring the functional elevation of the significant archaeological markers. Their elevation was compared against the latest predicted sea level curve for the Holocene along the Tyrrhenian coast of Calabria. As this coastal area is affected by significant and continuous vertical tectonic uplift during Pleistocene, the data show the counterbalance between coastal uplift and relative sea level change caused by the glacio-hydro-isostasy, acting since the construction of these archaeological sites. The sum of these movements determined an about null relative sea level change for this location. These data are in contrast with other part of the tectonically stable areas of the Mediterranean and provide evidence that crustal uplift continued in the last 1806 ± 50 y at a rate of 0.65 mm/y.

Marco Anzidei, Fabrizio Antonioli, Alessandra Benini, Anna Gervasi, Ignazio Guerra (2012). Evidence of vertical tectonic uplift at Briatico (Calabria, Italy) inferred from Roman age maritime archaeological indicators. *Quaternary International*, in press (2012), doi:10.1016/j.quaint.2012.01.019



Contents lists available at SciVerse ScienceDirect

Quaternary International

journal homepage: www.elsevier.com/locate/quaint

Evidence of vertical tectonic uplift at Briatico (Calabria, Italy) inferred from Roman age maritime archaeological indicators

Marco Anzidei^{a,d,*}, Fabrizio Antonioli^b, Alessandra Benini^c, Anna Gervasi^{a,d}, Ignazio Guerra^d

^a Istituto Nazionale di Geofisica e Vulcanologia, via di Vigna Murata 605, 00143 Rome, Italy

^b ENEA – National Agency for New Technologies, Energy and Environment, Via Anguillarese, Casaccia, Rome, Italy

^c Università della Calabria, Dipartimento di Archeologia e Storia delle Arti, Rende (CS), Italy

^d Università della Calabria, Dipartimento di Fisica, Rende (CS), Italy

ARTICLE INFO

Article history:

Available online xxx

ABSTRACT

Calabria is one of the most complex geological regions of the Mediterranean basin, which experienced large earthquakes and uplift and is still undergoing active tectonics. Along its coasts are located archaeological sites that can be used as powerful indicators of the relative vertical movements between land and sea since their construction. This paper presents and discusses data on the relative sea-level change as estimated from maritime archaeological indicators of the last ~2.0 ka BP existing along the Tyrrhenian coast of Briatico. These sites still show the remnants of a Roman age fish tank and a submerged breakwater about 320 m long.

The palaeo sea level has been obtained measuring the functional elevation of the significant archaeological markers. Their elevation was compared against the latest predicted sea level curve for the Holocene along the Tyrrhenian coast of Calabria. As this coastal area is affected by significant and continuous vertical tectonic uplift during Pleistocene, the data show the counterbalance between coastal uplift and relative sea level change caused by the glacio-hydro-isostasy, acting since the construction of these archaeological sites. The sum of these movements determined an about null relative sea level change for this location. These data are in contrast with other part of the tectonically stable areas of the Mediterranean and provide evidence that crustal uplift continued in the last 1806 ± 50 y at a rate of 0.65 mm/y.

© 2012 Elsevier Ltd and INQUA. All rights reserved.

1. Introduction

Past sea levels are represented along the large part of the Earth's coasts from geomorphological indicators produced by the sea level stands during the interglacial periods. The Mediterranean coastlines during the Pleistocene were often displaced at various elevations, providing indications on sea level changes and tectonic activity (Pirazzoli, 1976). In Italy, this evidence can be found along most of the coasts, and particularly in southern Calabria, which is among one of the most seismic area of the Mediterranean (Antonioli et al., 2006, 2007; Ferranti et al., 2007; 2010). During the last decade, multidisciplinary surveys in coastal archaeological sites of the Mediterranean have allowed the estimation of the timing and trends of the vertical movements of the Earth's crust and the relative sea level changes since the late Holocene. Archaeological data as indicators of relative sea level change have been used since the 1970s (Flemming, 1969; Schmiedt, 1974; Flemming and Webb, 1986), to study the coasts of the Mediterranean settled by Romans or pre-roman civilizations that

built villas, harbors, piers and fish tanks. Recently, the integration of altimetric observations obtained in these classes of archaeological sites, with geological data and geophysical modeling has allowed the temporal and spatial reconstruction of the size and trends of the movements (Lambeck et al., 2004b). Sea level change along the coasts of the Mediterranean depends on the sum of eustatic, glacio-hydro-isostatic and tectonics (Lambeck and Purcell, 2005). The first one is mainly driven by climate changes and is time-dependent, while the latter two can also change in space and may vary from location. The glacio-hydro-isostatic component has been recently predicted and compared with direct observational data in deforming zones, after the Last Glacial Maximum (LGM) (Lambeck et al., 2004b, 2011; Antonioli et al., 2007; Anzidei et al., 2011b).

As the coasts of the Mediterranean are particularly rich in archaeological sites, there is the opportunity to obtain significant data for this study from maritime structures that nowadays are often submerged or emerged, even up to several m below or above the present sea level (Schmiedt, 1974; Pirazzoli, 1976, 1996; Flemming and Webb, 1986; Anzidei et al., 2003, 2011a, 2011b; Tallarico et al., 2003; Lambeck et al., 2004a, 2004b; Fouache and Pavlopoulos, 2005; Antonioli et al., 2007; Desruelles et al., 2009; Brückner et al., 2010).

* Corresponding author.

E-mail address: marco.anzidei@ingvit.it (M. Anzidei).

The presence of these archaeological indicators, located along the Tyrrhenian coast of Calabria, between the mouth of Trainiti creek and Briatico, allow estimation of the relative sea level changes and the vertical motion of the land over the last 2 ka in this area. This paper discusses data from these sites and the comparison of their elevations with the predicted sea level curves, calibrated at 40 sites in Italy (Lambeck et al., 2011) and, with the long term tectonic rates inferred from the elevation of the Quaternary marine terraces that are uplifted up to hundreds of metres in this area.

2. Geology and tectonics

The Calabrian arc is made up by Mesozoic and Cenozoic metamorphic and sedimentary units. Above these units are deposits aged from Miocene to Holocene. The extensional tectonics that have driven the geodynamics of the Calabrian arc since the late Pliocene have produced high and low structures, NW-SE and NE-SE trending. The northern sector of the arc (Fig. 1) shows, from west to east, the high of Capo Vaticano, the Mesima basin and the Serre relief, all bordered by transversal faults (Bianca et al., 2011).

The tectonics of this region are induced by the large scale movements of the African and Eurasian plates, that have produced regional uplift originated by re-equilibrium of isostatic movements (Westaway, 1990), crustal thickening (Ghisetti, 1981), or the intrusion of an asthenospheric hot body between the mantle and the crust (Miyachi et al., 1994). Uplift and extension have been interpreted as a response to slab retreat underneath the Calabrian arc and subsequent asthenospheric flow resulting from slab detachment (Westaway, 1993; Wortel and Spakman, 2000; Goes et al., 2004) or supported by asthenosphere wedging beneath the decoupled crust (Locardi and Nicolich, 1988; Miyachi et al., 1994; Gvirtzman and Nur, 1999; Doglioni et al., 2001). The consequence of the uplift in this region is the occurrence of Pliocene-Pleistocene marine sequences with terraces placed up to 1200 m above sea level (Ferranti et al., 2010 and references therein).

In the investigated area, between Vibo Valentia Marina and Briatico, the tectonic unit of Capo Vaticano is exposed (Tortorici et al., 2003). This is a structural NE-SW trending high, bordered toward the

SE by the Mesima basin, two main NW-SE trending antithetic faults (Mileto fault), in SSW by the Coccorino and Nicotera faults with WNW-ESE trends, and toward N-NW by a fault system, down-lifted northward (Fig. 1). Tortorici et al. (2003) found in the area of Briatico a typical morphological aspect of a bridge zone, placed between two fault planes (Ghisetti, 1979).

The current elevation of the Pleistocene marine terraces allowed estimation of the vertical tectonic rates in this area (Ferranti et al., 2006, 2010). These outcrops, which are approximately homogeneously distributed, show significant height differences (i.e. Salmoiraghi, 1884; Cosentino and Gliozzi, 1988; Carobene and Dai Prà, 1990; Anselmi et al., 1992; Miyachi et al., 1994; Bordoni and Valensise, 1998; Bianca et al., 2011). Ferranti et al. (2006) speculated that the large uplift values recorded by the Calabria-Peloritano arc can be related to the general uplift of the lithosphere above a subducting plate.

Miyachi et al. (1994) observed along the Tyrrhenian coast of southern Calabria twelve orders of Pleistocene terraces up to 1350 m above sea level. Among the areas where uplift is greater (Monte Poro, Le Serre and Aspromonte), the zone of Capo Vaticano promontory shows a large differential uplift. Here, the Tyrrhenian terrace of MIS 5.5 is at about 50 m above sea level near Vibo Valentia. At Capo Vaticano, it is up to 120 m above sea level, a difference of about 70 m (Fig. 2), in contrast with the recent ages published by Tortorici et al. (2003) who found an elevation even up to 285 m in this area.

Fig. 2 shows the seismicity of the Calabrian region according to the database of the Seismic Network of Calabria University. In black are plotted the events with $m_L \geq 2.5$ and focal depth to 50 km in the period 1981–2011 (Barberi et al., 2004). Red void squares indicate macroseismic epicentres of historical earthquakes in Calabria with $I_0 \geq VIII$ MCS from CPTI catalogue (CPTI Working Group, 2004). The inset shows a compilation of fault plane solutions for earthquakes shallower than 50 km in the Calabrian area and $m_L \geq 2.8$, obtained by the combination of: a) the EMMA database by Vannucci et al. (2004); b) the Global and Italian CMT Catalogs (<http://www.globalcmt.org/>; Pondrelli et al., 2006); c) original computations performed in the framework of the SyNaRMA Interreg III B Project (Guerra, 2007) using the PPFIT algorithm by Reasenber and Oppenheimer (1985); d) specific papers published more recently (e.g. D'Amico et al., 2010; D'Amico et al., 2011).

In historical times, the city of Vibo Valentia was destroyed by the catastrophic earthquake ($m = 7.0$, $I_0 = XI$ MCS) of September 8th, 1905. The location of the source of this shock, and consequently the identification of the major tectonic structure from which it was generated, is still debated since Mercalli (1906) and Baratta (1906). Several authors have studied more recently or are presently studying the problem, by using different approaches (e.g. Piatanesi and Tinti, 2002; CPTI Working Group, 2004; Michelini et al., 2005; Loreto et al., 2011), but a sound solution has not yet been reached.

The Capo Vaticano promontory and its surrounding sea are characterized by a very low level of surface seismicity (Chiarabba et al., 2005). On the basis of the knowledge of the historical seismicity and of the instrumental data for the last decades, the existence of coseismic differential displacements between different domains inside the Monte Poro complex in historical times can be excluded.

3. Materials and method

Between Vibo Valentia marina, at the mouth of the Trainiti creek and the village of Briatico, are located two archaeological structures of Roman age (Fig. 1). The first is represented by a breakwater built at the mouth of Trainiti creek near Porto Salvo village (Fig. 3a, b). The second is a fish tank, excavated on the Scoglio Galera, a small rocky islet near the small village of Santa Irene (Briatico) (Figs. 4a and 5a, b). With the goal to estimate the vertical motion of the

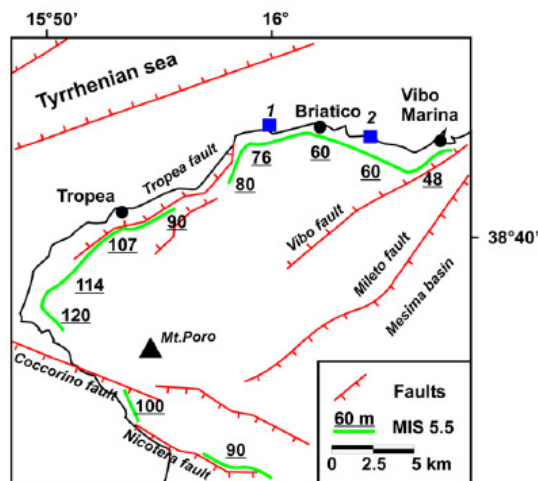


Fig. 1. The MIS 5.5 terrace (green line with elevation in meters) and the main faults at Capo Vaticano promontory (from Miyachi et al., 1994). Numbered blue squares are 1) the location of the Scoglio Galera fish tank and 2) the pier at the mouth of Trainiti creek. (For interpretation of the references to colour in this figure legend, the reader is referred to the web version of this article.)

Please cite this article in press as: Anzidei, M., et al., Evidence of vertical tectonic uplift at Briatico (Calabria, Italy) inferred from Roman age maritime archaeological indicators, Quaternary International (2012), doi:10.1016/j.quaint.2012.01.019

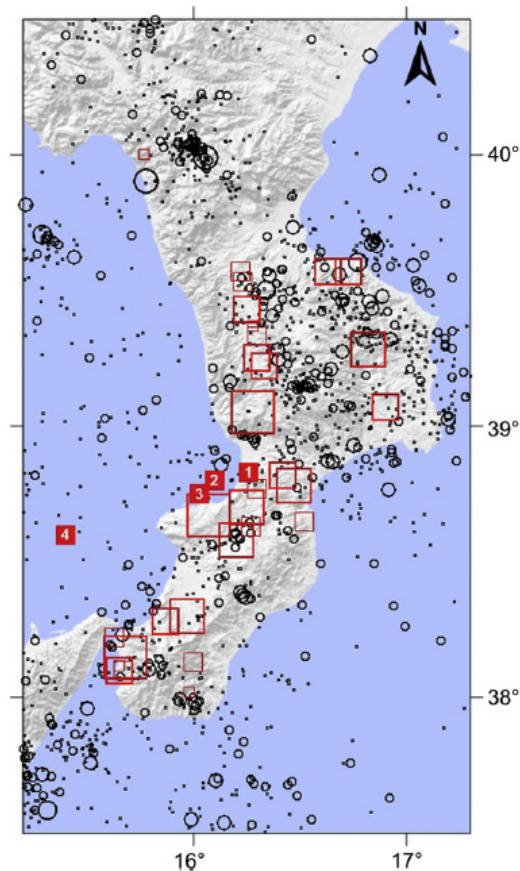


Fig. 2. Seismicity of Calabria. See text for description. Red squares are the epicenters of the historical earthquake (size is proportional to Magnitude). The locations of the 1905 earthquake are from: 1 = Rizzo (1907), 2 = Ruscetti and Schick (1974); 3 = Camassi and Stucchi (1997), 4 = Michellini et al. (2005). (For interpretation of the references to colour in this figure legend, the reader is referred to the web version of this article.)

land and the relative sea level changes along this coast, these archaeological sites were analyzed, taking into account their former use and the functional elevations, following the guidelines described in Lambeck et al. (2004b).

To account for tides that can affect the measurements of the elevation of the archaeological markers, observational data have been reduced for tide values at the time of surveys, using tidal data from the nearest tide gauge stations of ISPRA (<http://www.mareografico.it/>). The time series of the near tide gauge data of Reggio Calabria was analyzed to estimate the sea level trend and the tidal range for this area. To account for the long term vertical land movements, the elevation of the inner margin of the marine terrace of MIS 5.5 (Miyachi et al., 1994) was used. The normal elevation of the MIS 5.5 is 7 m for tectonically stable areas, but in the vicinity of the Scoglio Galera it is at 65 m above sea level, thus indicating a marked uplift of this area (Miyachi et al., 1994; Ferranti et al., 2010 and references therein).

Data included a terrestrial and marine topographic survey. The latter was performed by a single beam survey, across the pier and

around the fish tank of Scoglio Galera, to get an overview of the morphology of the seafloor, to help in interpretation (Fig. 4).

3.1. Bathymetric and topographic surveys

Bathymetric and topographic data were collected during two distinct surveys, using the Differential Global Positioning System technique (DGPS). Data allowed producing an accurate bathymetric and topographic map of the investigated area. This method is normally used to perform rapid and accurate bathymetric surveys in very shallow waters where conventional surveys performed from large boats cannot be carried out (Anzidei, 2000).

The topography of Scoglio Galera was obtained using two DGPS Trimble 4000ssi receivers equipped with radio modems and collecting data at 1 s sampling rate (Fig. 4). The reference station was located on a benchmark previously established on the islet while the rover was moved along defined paths. Bathymetry was obtained using two DGPS receivers: one located on the Scoglio Galera while the second was installed on a small boat and connected to an echo sounder and navigation software running on a portable Personal Computer (Fig. 4). The GPS antenna of the rover receiver and the echo sounder transducer were mounted at the ends of a rigid pole, which was installed on the right side of the boat. The latter was sailing at a constant speed of 2 knots during surveys. Positioning data were collected by GPS Novatel receivers equipped with an Omnistar correction system, while depth measurements used an Odom echo sounder (standard accuracy of $0.5\% \pm 1$ cm). All data were collected at 1 s sampling rate. At the beginning of the survey a calibration of the transducer was performed, and sound speed values were estimated and applied during data analysis. Tidal corrections were neglected due to the small values of tide amplitudes during surveys (≤ 15 cm) and depths were measured with respect to the instantaneous sea level. During data analysis, the noise due to pitch and roll of the boat were removed to correct the observations.

The final accuracy of each planar coordinate collected along the routes was ± 30 cm. Seafloor coordinates and depths were computed and converted in an ASCII file suitable to be managed by numerical and graphic software. Data were collected along ~ 8 nautical miles and were used to construct several cross sections and a Marine Digital Terrain Model of the sea bottom. Bathymetric data were also combined with the topographic data provided by the terrestrial GPS survey on the islet and with the available digital aerial images, providing valuable information on the overall morphology of the area. Fig. 3b show the area of the pier at the mouth of Trainiti and Fig. 4 is the plot of the MDTM for the Scoglio Galera. The Marine Digital Terrain Models and the Digital Terrain Models were computed by the triangulation interpolation method.

3.2. Piers at the mouth of the Trainiti creek

This archaeological site consists of a submerged structure, approximately rectangular in shape, about 320 m long and 40 m wide (Fig. 3a, b). It extends NW-SE (330° N), oblique with respect to the coastline to which is connected. Another smaller wing was previously found by Mariottini (2001), but it was not found during these investigations. Both wings formed a typical harbor entrance named *faucis*, by their position suitable to protect an inner harbor. These structures can be interpreted as offshore breakwaters pertaining to a large harbor, likely belonging to the ancient port of *Hippionion/Valentia*, which presently is completely buried by coastal sediments (Schmiedt, 1966).

The structure was built with large blocks of concrete that contain several fragments of amphorae dated to Roman age (2 ka BP). The constructional features of the main wing show at least three

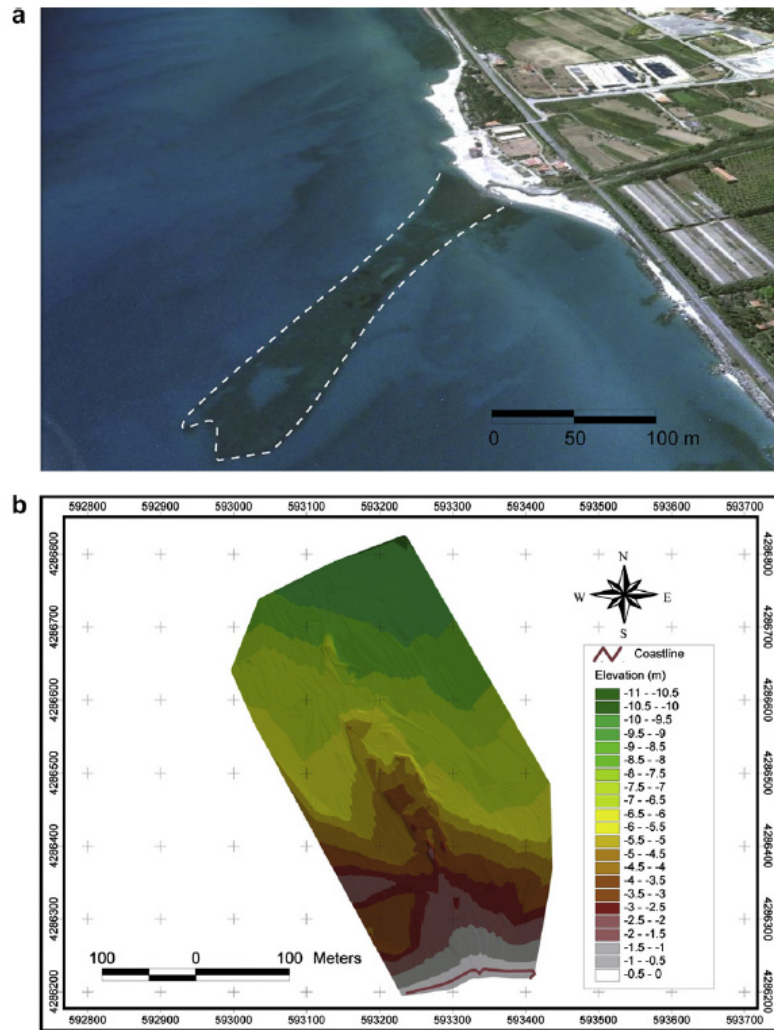


Fig. 3. a) Aerial view of the pier at the mouth of Trainini creek (image from Google Earth, <http://www.earth.google.com>); b) bathymetric map across the pier (see color scale for depth values); c) cross section of the seafloor across the pier. (For interpretation of the references to colour in this figure legend, the reader is referred to the web version of this article.)

homogenous building sectors of: i) strongly cemented material containing abundant fragments of archaeological remains, ii) dissolved material, with poor archaeological remains and finally, iii) breakwater material, with elements partially built but without archaeological material.

The surface of the structure is rough, and its base follows the irregular topography of the seafloor, which is tilted toward offshore. It begins from the shore at an elevation of -1 m and extends offshore up to -9 m at its end. The surface of this structure was likely covered by pavements, now destroyed. Similar structures are found in other areas of the Mediterranean settled since Roman or pre-roman times, such as at Tharros, in Sardinia (Melis, 1998).

Previous geomorphological and palaeogeographical studies determined that this area suffered from significant changes of the coastline, which have caused the modification of the coastal plan

that evolved toward a coastal environment with marshes and lagoons, separated by the sea from sand dunes (Lacquaniti, 1952; Cucarzi et al., 1995). Hence, this transitional zone underwent continuous flooding and silting caused by the Trainiti and S. Anna creeks (Medici and Principi, 1939; D'Alessandro et al., 1987). The progradation of the coastline and its timing is confirmed by Cucarzi et al. (1995) from the migration toward north of several phases of human settlements.

The old topographic maps of the Italian Istituto Geografico Militare (IGMI) show some ruins that could match the ancient harbor structures as reported in XVIII century by Priest Fiore. The description made by G. Schmiedt (1966) is the same as left by Fiore in 1680, when the harbour was "destroyed under the order by the Roman pope to give to the barbarians a poorhouse" and that this harbour was "built with cut stones from the ancient inhabitants of

Please cite this article in press as: Anzidei, M., et al., Evidence of vertical tectonic uplift at Briatico (Calabria, Italy) inferred from Roman age maritime archaeological indicators, Quaternary International (2012), doi: 10.1016/j.quaint.2012.01.019

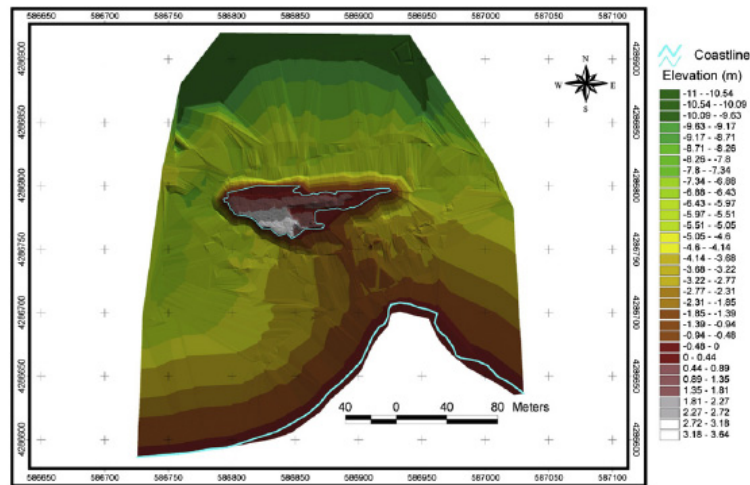


Fig. 4. Bathymetry and topography of Scoglio Galera (see color scale for depth values). (For interpretation of the references to colour in this figure legend, the reader is referred to the web version of this article.)

Hipponion, in a shape similar to a bended arm", in a time when most of its parts could still be seen.

Schmiedt (1966) cites previous descriptions "Even today in the low and calm tide can be observed large remains of a big construction composed by very large blocks with arches and pillars of concrete and even the moorings to tie ships" and "the Harbour of Hipponium was placed in the bay in front of the castle of Bivona, at that time partly in a lagoon and connected with sea; near the shore of the lagoon there were large squared pillars built with bricks, distributed in regular intervals, that were outcropping from the sand and likely holding arcades circling the whole harbor".

Schmiedt himself (1966) observes that "on the shore, in the same zone indicated by the aerial photographs, are present structures built with bricks that seem to be ancient... it is not an hazard to collocate the ancient basin of the harbour of Hipponium in the bay where a lagoon was existent in the previous century".

All these information support the hypothesis that during the Roman time the current coastal plain was the site of the ancient port. The submerged structures, in particular those placed at the mouth of Trainiti creek, are likely part of the ancient Harbour which had two entrances: the first at the mouth of Trainiti creek, and the second in the eastern side of the lagoon. The underwater structure can be interpreted as a system to facilitate the outflow of the debris transported by creeks that exit in the basin, preventing its progressive infilling.

3.3. Scoglio Galera

Scoglio Galera is located near the village of Briatico, about 100 m distant from the coast. It is ~120 m long and ~40 m wide, extending east-west (Figs. 4 and 5a, b). This small islet was known from historical tradition to be used by Arabs to jail the Christians, sinking them in the pools.

Recently, marine archaeologists classified this site as a fish tank and a fish processing plant (Mariottini, 2001). The islet was excavated and cut at its surface, thanks to the softness of the biolimestone and limestone of Miocene age (Fig. 5c).

Along the NNW side of the islet, which is the most exposed to the sea, the remnant of a wall and traces of the formworks used for the

concrete, are still present. The fish tank consists of four nearby pools, E-W aligned, that follow the natural morphology of the islet (Fig. 5c, d, e). The pools have a total length of about 28 m and a constant width of 2.5 m. The two main pools are subdivided into minor pools and their inner walls show some holes at ~1 m above sea level, that were likely used to host horizontal wooden beams and a roof. The pools are crossed by two main channels, A and B, which link the inner basin with the open sea (Fig. 5b, e). The latter is protected and suitable for the moorings of ships. In particular, channel B crosses the islets by a tunnel. Two additional minor channels, C and D, connect the pools 2 and 3 with the inner basin. The pools are all connected by channels and separated by partition sects (Fig. 5c, d).

All the channels show the signs of the grooves used to operate the sluice gates, similar to those found in the fish tanks along the Tyrrhenian coasts of central Italy and other localities (Lambeck et al., 2004b; Anzidei et al., 2011b). These were used to provide an effective water exchange in the basin but without letting the fish escape. The inner side of the basin shows i) the crepidini, narrow sidewalks used to walk around the pools without getting wet, ii) the surface of a dock, and iii) ten bollards of different size, all rock cut in the islet. The inner side of the pools show a present day notch about 40 cm high and 30–60 cm deep. Its lower part shows an organic platform typical of environments at high hydrodynamics, which is in agreement with the amplitude of the local tides (Fig. 5c, d, e).

The underwater part of the islet, particularly inside the mooring basin, shows a selective erosion process, acting in coincidence with the different level of local stratigraphy, separated each other by 40 cm (Fig. 5f). The surface of the islet shows an additional squared small pool of ~1.5 × 1.5 m in width, crossed by a channel without sluice gates.

The geology of Scoglio Galera belongs to the outer limits of the youngest marine terrace of Upper Pleistocene (Miyachi et al., 1994) that is exposed between 0 and 30 m above sea level. It consists of littoral deposits formed by alternating clastic facies with variable size of strongly cemented conglomerates, sands and bio-limestone. The thickness of the strata ranges from 20 to 250 cm and those aligned N 260°–290° are tilted 10°–15° toward NNE. The thickness of the bio-limestones is about 200 cm in the islet.

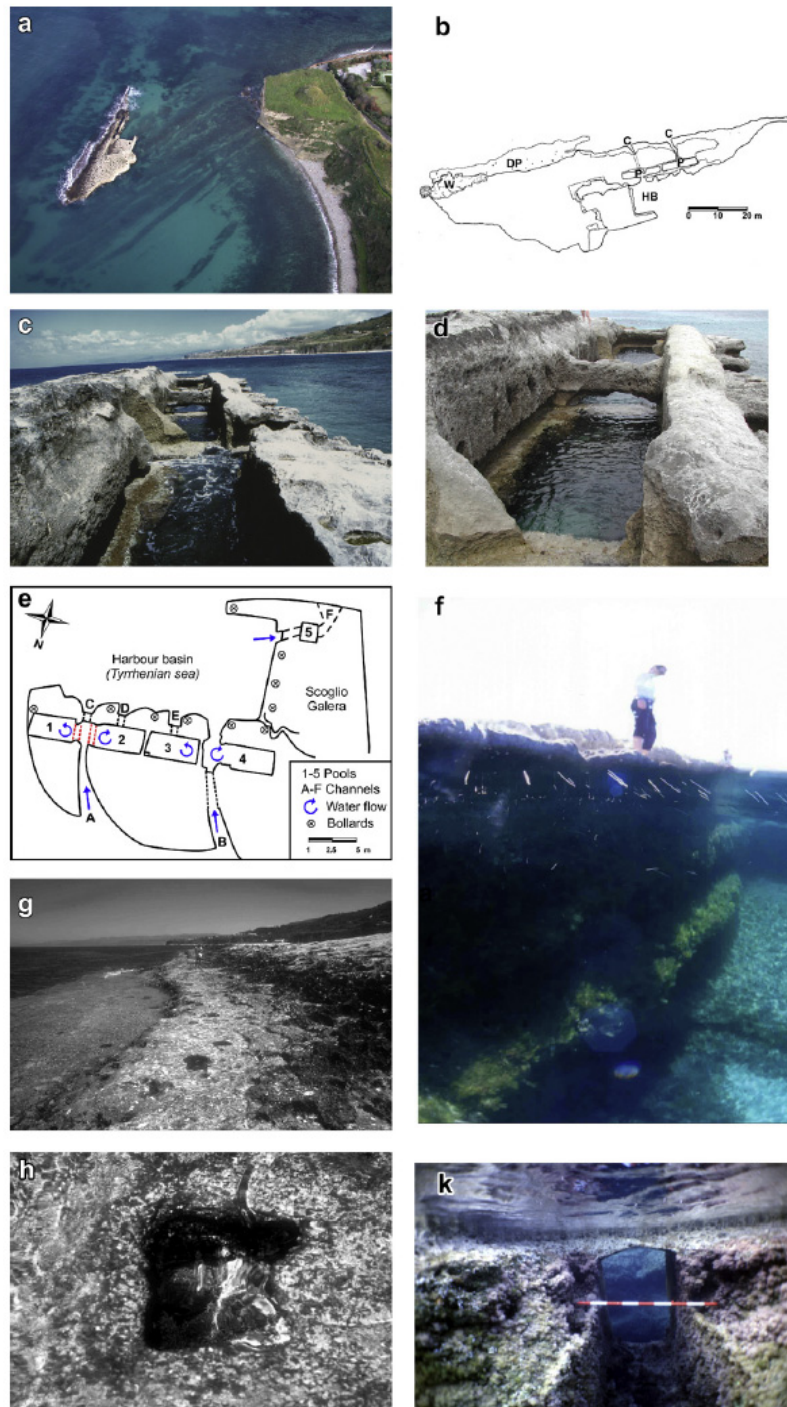


Fig. 5. a) Aerial view of the Scoglio Galera and b) its topographic map (modified from Mariottini, 2001) c) the pools of the fish tanks and d) their partition sects and the erosion notch. Below the sects run the channels that link the nearby pools. e) Particular of the Scoglio Galera: Black dots are the bollards excavated in the rock; pools are numbered 1–5; the main (A, B) and secondary (C,D,E,F) channels, are also reported in the map. f) An underwater view of the islet from inside the harbor basin. These notches are caused by selective

Please cite this article in press as: Anzidei, M., et al., Evidence of vertical tectonic uplift at Briatico (Calabria, Italy) inferred from Roman age maritime archaeological indicators, *Quaternary International* (2012), doi:10.1016/j.quaint.2012.01.019

As the strata are all tilted NNE, the islet has an asymmetric morphology. Its southern part is indented and with a vertical coastline up to 3 m high, while the northern part shows a linear trend and is gently tilted NNE.

Along the southern border, inside the pools and in the mooring basin, a present day erosion notch 30–60 cm wide and 50–100 cm high, is present (Fig. 5c, d). The northern border displays an abrasion platform up to 6 m wide, characterized by *Dendropoma petreum*. These gastropods usually live in the lower intertidal environment (Antonoli et al., 1999).

The northern border shows also relics of a marine terrace ~60–80 cm above sea level, at the same level of the walking surface (crepidine) that runs along the mooring basin. The crepidine was partially excavated on the surface of the marine terrace.

The cross section (Fig. 6) shows the cliff running along the northern coast of the islet whose bottom ends in the seafloor at a depth of 6–7 m. The elevation of the intertidal abrasion shows a level of 7–8 cm of *Dendropoma petreum* (Antonoli et al., 1999) which is in agreement with the current sea level. This platform includes several squared holes, excavated in the islet to support the wooden poles that made up the reinforcements of high concrete walls, built to protect the islet from the waves. The platform ends with a small scarp 80 cm high, over which were developed a small terrace 3.5 m wide (Fig. 5g). The latter ends with an additional small scarp, and its surface shows other squared holes where parts of the walls are still remaining. Although this may appear as natural terrace, it appears to have been excavated to adapt the surface of the islet to the wall foundations. Along the opposite side of the islet the seafloor is up to 4–5 m deep and shows an erosion-smoothed marine notch. The present day erosion notch has a size a few cm larger than the tidal range.

4. Results

The goal of this paper is to provide quantitative data on the relative sea level changes during the late Holocene and of the vertical land movements in an area of high tectonic deformation rate. For this purpose, direct measurements of archaeological and geomorphological markers connected to sea level were used. To correlate the archaeological structures to sea level at the time of their construction, the functional elevations of the observed architectural features are defined as significant parameters to estimate the local relative sea level change. These are specific parts of an archaeological site which were constructed at specific elevations for functional purposes, defining the minimum elevation above high tide (Lambeck et al., 2004a, 2004b).

4.1. Trainiti creek

Surveys have determined that the depth of the main pier ranges between –1 and –9 m from its attachment along the coast towards the offshore (Fig. 3b). This structure, a breakwater or an outer pier, was built to ensure that at least 1 m remained emerged in the part close to the shore, to function properly and to guarantee good protection to the harbor basin, which today is silted (Lena, 1989; Mariottini, 2001). Excluding any large vertical movement, this structure was intentionally built at these depths to create an artificial barrier against waves and currents. The bathymetry support this hypothesis, as the pier is tilted toward offshore, following the

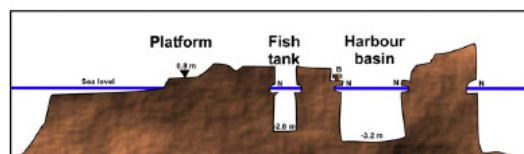


Fig. 6. Sketch of a cross section of Scoglio Galera (not in scale) with i) present day abrasion platform placed at the same elevation of the ii) present day erosion notches placed inside the pools, iii) mooring basin, iv) bollard and crepidine. All the analyzed archaeological and geomorphological markers are in agreement with an unchanged relative sea level since 1806 ± 60 years BP.

surface of the seafloor. The latter is gently deepening, and does not show any relevant first order morphological signatures. In absence of precise constructional and morphological elements in the shallow part of the pier, precise estimation of the intervening relative sea level changes since the time of its construction cannot be determined, mainly due to a lack of more precise information on the harbor, that today is completely buried under the recent sediments of the coastal plain (Schmiedt, 1966).

4.2. Scoglio Galera

The fish tank of Scoglio Galera shows significant features that allow the precise estimation of past sea level positions in this area. In particular, as also reported in Lambeck et al. (2004b), from the elevation of the channels used for water exchange within the basin, it is possible to determine the relative sea level change since its construction at this site. Latin writers, as Columella (*De Re Rustica XVII*), suggest for basin constructions a depth up to 2.7 metri *...in pedes novem defondiat piscina... even depending from the fish species to breed. Moreover, the pools were protected from waves ...Mox praeiaciuntur in gyrum moles, ita ut complectantur sinu suo et tamen excedant stagni modum...* In the fish tank of Scoglio Galera, the pools show average depths of 2.8 m, while channels for water exchange of the inner basin show maximum depths of 1.9 m, with elevations compatible for a good functioning of the pools driven by the typical tides of the Mediterranean Sea, normally ~50 cm high. Therefore the pools and the channels of the fish tank are tidally controlled, even today.

To date the fish tank, whose age was still unknown, a piece of wooden pole found in one of the squared holes along the northern side of the islet was dated (Fig. 5h). ¹⁴C AMS analysis dated this sample as Roman age, precisely at 1806 ± 50 BP (calibrated age, Calib 4, Stuiver et al., 1998).

5. Discussion

The sea level curve estimated by Lambeck et al. (2011) (that models the crustal response to the glacio-hydro-isostatic signal) predicts a sea level change for this location of –113 cm since the last 1806 ± 50 years, at a mean rate of –0.63 mm/y (Fig. 7). Observations have estimated that the relative sea level has changed only 7 cm since the construction of the archaeological site (Table 1). Therefore, the recent tectonic uplift inferred from the fish tank exceeds by ~0.18 mm/y the previous estimates of Miyauchi et al. (1994) obtained from the elevation of the MIS 5.5 marine terrace,

erosion processes occurring along the different levels of the geological unit. g) The abrasion platform with the *Dendropoma petreum* which is drilled with several squared holes used to host wooden poles. A relic of wood allowed us to date by ¹⁴C AMS this site at 1806 ± 60 years BP. h) One of the holes for the wooden poles of 20 × 20 cm size. k) One of the channels used for water exchange in the pools. Their functional elevations still correspond to those at the time of the construction of the fish tank. The openings of the channels were originally closed by fixed gates to avoid the escape of fish.

Please cite this article in press as: Anzidei, M., et al., Evidence of vertical tectonic uplift at Briatico (Calabria, Italy) inferred from Roman age maritime archaeological indicators, Quaternary International (2012), doi:10.1016/j.quaint.2012.01.019

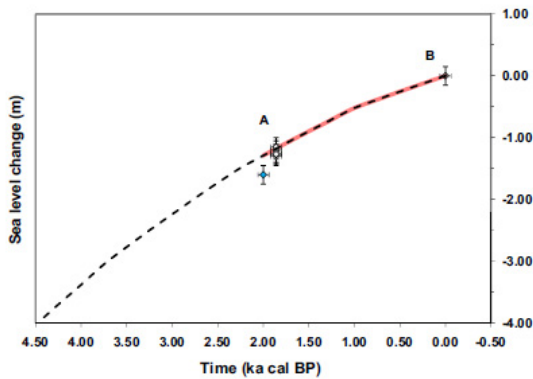


Fig. 7. Plot of the predicted sea level curve (from Lambeck et al., 2011) compared with the elevation of the archaeological markers of the fish tank (diamonds with error bars for age and elevation). The archaeological indicators remained at the same elevation with respect to local sea level since 1806 ± 60 ka BP. The data at the top right of the curve show the current mean elevation value of the markers, as listed in Table 1, still matching the local sea level.

which infers an uplift rate of 0.47 mm/y at Briatico. Bianca et al. (2011) found the MIS 5.5 terrace at 216 m of elevation, in contrast to the value of about 60 m reported in Miyauchi et al. (1994) (Fig. 1), thus inferring a long term uplift rate up to 1.74 mm/y. As this value is in large contrast with the previous measurements of Miyauchi et al. (1994), who dated this terrace through the *Strombus B.*, the latter is preferred for comparison here.

Besides the long term geological data, recent geodetic observations are available in Calabria which show the present day uplift of this region. The tide gauge of Reggio Calabria has recorded a sea level trend of 0.28 mm/y during the time span 1999–2007 (Fig. 8). Although the duration of the sea level recordings for this station is still too short to provide a robust estimation, this value can be considered a preliminary indication that should correspond to a deficit of ~ 0.8 mm/y in the sea level increase with respect to tectonically stable coastlines of Italy. This result is in agreement with Braitenberg et al. (2011). Moreover, the available GPS data show a variable uplifting trend for southern Calabria (Devoti et al., 2010). Therefore, the rate of crustal uplift inferred from the marine archaeological site of Scoglio Galera provides the evidence of a continuous uplift, whose trend is in agreement with the recent instrumental observations. The archaeological data fills a gap between geological and instrumental data, providing new estimations on the tectonic trend of this region during historical times.

In Table 1, the predicted and observed data of sea level change are shown and compared against the tectonic signal, using the predicted sea level curve of Lambeck et al., 2011 for this location (Fig. 7). The vertical uplift rate is based on the elevation of the Quaternary terraces of MIS 5.5 (124 ka, elevated at 65 m according to Miyauchi et al. (1994)) (Fig. 1) and a uniform uplift since the last 1806 ± 50 yr BP, which is the age of the archaeological site, is assumed.

Column L of Table 1 contains the average value of f the relative sea level change inferred from the archaeological site, estimated at -106 cm for the last 1806 ± 50 y (radiocarbon age of the wooden pole). In column K of the same table, the predicted sea level curve for the last 1806 y gives a value of -113 cm.

The difference of only 7 cm between predicted and observed data results from the sum of the opposite movements of uplift and subsidence that counterbalance each other. This estimation includes the uncertainties from the model and field observation. This result is in good agreement with the tectonic rate inferred by

Table 1
 (A) marker number; (B) type of marker; (C) Age based on radiocarbon dating for site 1 and also on radiocarbon dating for site 2; (D) and (E) are the WGS84 coordinates of the sites; (F) and (G) are the upper and lower limiting values of the significant markers; (H) relative sea level change based on the functional elevations of the markers; (K) predicted sea levels at 2 ka for this location according to Lambeck et al., 2011. (L) Difference between predicted and observed sea level. (M) is the geological vertical rate based on the elevation of the Quaternary terraces of MIS 5.5 (124 ka, elevated at ~ 60 m according to Miyauchi et al., 1994). (N) is the uplift rate inferred from the archaeological site assuming a uniform tectonic uplift since the last 1806 ± 50 BP; time of construction of the archaeological site. A functional elevation of 0.20 m is assumed. Elevation data are the average values of multiple measurements collected at the best preserved parts of the structures. All elevation data are corrected for tides and atmospheric pressure using the tidal data from the Reggio Calabria and Palinuro stations of ISPRA (<http://www.mareografico.it/>). The maximum tidal range for this coast is 0.60 m. The estimates include observational uncertainties.

A	B	C	D	E	F	G	H	K	L	M	N
N.	Site and Type of marker	Age (ka)	Lat N	Lon E	Ul. (cm)	LL. (cm)	Obs. RSLC (cm)	Pred. RSLC (cm)	Pred. - Obs. SIC (cm)	Geo. Tect. rate (mm/y)	Arch. Tect. rate (mm/y)
1	T Pier	2 ± 0.1	$38^{\circ}43'18''$	$16^{\circ}04'22''$	-1	-9	-	-129 (at 2000 BP)	-93	0.47	-
2 a	SG Channel B	1.86 ± 0.05	$38^{\circ}43'31''$	$15^{\circ}59'57''$	30	-70	20	-113 (at 1806 yr BP)	-99	-	0.60
2 b	SG Channel E				40	-68	14		-96.5		0.61
2 c	SG Channel D				40	-73	16.5		-113		0.60
2 d	SG Bollards				-	50	0		-113		0.69
2 e	Dock surface				50	-	0		-113		0.69
2 f	SG notch				40	0	0		-113		0.69
					Mean	Mean	Mean	Mean	Mean		
					46.7	-26.8	7.21	0.63 mm/y in 1806 \pm 50 y	-106		
											Uplift is 85 cm in 1806 \pm 50 y
											Mean 0.65 mm/y in 1806 \pm 50 y

Please cite this article in press as: Anzidei, M., et al., Evidence of vertical tectonic uplift at Briatico (Calabria, Italy) inferred from Roman age maritime archaeological indicators, Quaternary International (2012), doi:10.1016/j.quaint.2012.01.019

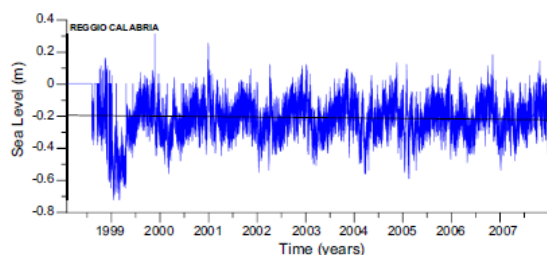


Fig. 8. Plot of the tide gauge recordings at Reggio Calabria station from 1999 to 2007. Data show a sea level trend at 0.28 ± 0.1 mm/y (linear fit shown by the black line). The maximum tidal range is 0.63 m for this location, in agreement with the height of the erosion notch at Scoglio Galera.

the elevation of the terraces of MIS 5.5, located at 60 m above sea level, that infer a vertical uplift of 0.47 mm/y (Miyachi et al., 1994), that caused a displacement of about 85 cm since the last 1806 ± 50 years at the studied site. This estimate, which differs by 21 cm from the present study's results, could result from the measurements of the MIS 5.5 elevation in this region, which shows large spatial variability. Finally, the flat surface at 80 cm above sea level on the northern side and in the harbor of Scoglio Galera, is interpreted as entropic (Fig. 5g).

6. Conclusions

The timing of the relative sea level changes along the Tyrrhenian coast of Calabria, at Briatico, can be inferred from the elevation of the Quaternary marine terrace and the coastal archaeological sites of Roman age. As the pier located at the mouth of Trainiti creek does not provide any precise data, the only available indicator along this coast is the Scoglio Galera. Analysis used: i) functional elevations of channels used for water exchange within the pools; ii) functional elevation of crepidine and bollards; iii) elevation of the erosion notch in the pools, correlated with the *Dendropoma* platform placed along the northern side of the islet, and iv) the elevation of the marine terrace of the upper Holocene, excavated at 80 cm above sea level along the northern side of the islet.

As the age of the fish tank is 1806 ± 50 cal BP, the present day erosion notch in the inner side of the pools formed only after the fish tank was excavated. This geomorphological indicator, strictly related to the recent sea level, developed during this time, reaching a size related to the mean tidal range for this location, as estimated from tidal data (Fig. 8). Excluding any uplifting coseismic displacement, these observations imply that the fish tank, since the time of its construction, underwent continuous uplift with the same value of the subsidence signal caused by the glacio-hydro-isostasy. The erosion notches formed in this tectonic environment and developed under a constant tidal range amplitude, since the relative sea level remained steadily at the same relative level while it was continuously rising together with the Earth's crust (Fig. 7). The pools do not show any morphological evidence of submerged erosion notches, supporting the hypothesis that relative sea level has not changed since their construction.

Assuming a constant rate of uplift since the late Quaternary, including the last 1806 years, then the current elevation of the Scoglio Galera is due to the glacio-hydro-isostatic signal that counterbalances the tectonic signal. Therefore, the uplifting rate for this location can be estimated at ~ 0.65 mm/y for the last 1806 ± 50 BP.

The present day biological marker, the *Dendropoma* platform, is in agreement with these observations as well as with the tidal notch along the inner side of the pools of the fish tank. These markers

developed in an environment characterized by a relative null vertical motion, and consequently are at the same elevation. This balance also includes the recent eustatic increase of 13 cm, as estimated for the Mediterranean by Lambeck et al. (2004b), Anzidei et al. (2011a, 2011b).

On the base of these data, the archaeological markers at Scoglio Galera did not record coseismic significant displacements along the vertical, including the December 8th, 1905 $M_s = 7$ earthquake, which is the largest in this region in the last centuries, in agreement with the dislocation model proposed by Piatanesi and Tinti (2002). However, coseismic movements may have occurred before the construction of the fish tank.

Acknowledgments

This study has been partially funded by INGV and CNR-Agenzia2000. We are thankful to Carlo Del Grande of the University of Bologna, who provided the bathymetric maps.

References

- Antonoli, F., Chemello, R., Improta, S., Riggio, S., 1999. The *Dendropoma* (Mollusca Gastropoda, Vermetidae) intertidal reef formations and their paleoclimatological use. *Marine Geology* 161, 155–170.
- Antonoli, F., Ferranti, L., Lambeck, K., Kershaw, S., Verrubbi, V., Dai Pra, G., 2006. Late Pleistocene to Holocene record of changing uplift rates in southern Calabria and eastern Sicily (southern Italy, Central Mediterranean Sea). *Tectonophysics* 422, 23–40.
- Antonoli, F., Anzidei, M., Lambeck, K., Auriemma, R., Gaddi, D., Furlani, S., Orru, P., Solinas, E., Gaspari, A., Karinja, S., Kovacic, V., Surace, L., 2007. Sea level change during Holocene from Sardinia and northeastern Adriatic (Central Mediterranean sea) from archaeological and geomorphological data. *Quaternary Science Reviews* 26, 2463–2486.
- Anzidei, M., 2000. Rapid bathymetric surveys in marine volcanic areas: a case study in Panarea area. *Physics and Chemistry of the Earth* 25 (1), 77–80.
- Anzidei, M., Lambeck, K., Antonoli, F., Baldi, P., Benini, A., Esposito, A., Nobili, A., Surace, L., 2003. Sea level change from Roman time up to the present in Central Mediterranean. In: Mastroruzzi, G., Sansò, P. (Eds.), *Puglia 2003-Final conference. Quaternary Coastal Morphology and Sea Level Changes, IGCP 437 Project, Otranto/Taranto - Puglia (Italy) 22–28 September 2003*, pp. 27–39.
- Anzidei, M., Antonoli, F., Lambeck, K., Benini, A., Soussi, M., Lakhdar, R., 2011a. New insights on the relative sea level change during Holocene along the coasts of Tunisia and western Libya from archaeological and geomorphological markers. *Quaternary International* 232, 5–12.
- Anzidei, M., Antonoli, F., Benini, A., Lambeck, K., Sivan, D., Serpelloni, E., Stocchi, P., 2011b. Sea level change and vertical land movements since the last two millennia along the coasts of southwestern Turkey and Israel. *Quaternary International* 232, 13–20.
- Anselmi, B., Dai Prà, G., Galletti, M., Myauchi, T., 1992. Età dei depositi a *Strombus bubonius* di Vibo Valentia Marina (Italia meridionale). *Il Quaternario* 6, 139–144.
- Baratta, M., 1906. Il grande terremoto calabro dell'8 settembre 1905. *Atti della Società Toscana di Scienze Naturali, Pisa, Memorie* 22, 57–80.
- Barberi, G., Cosentino, M.T., Gervasi, A., Guerra, I., Neri, G., Orecchio, B., 2004. Crustal seismic tomography in the calabrian arc region, south Italy. *Physics of the Earth and Planetary Interiors* 147, 297–314.
- Bianca, M., Catalano, S., De Guidi, G., Gueli, A.M., Monaco, C., Ristuccia, G.M., Stella, G., Tortorici, G., Tortorici, L., Troja, S.O., 2011. Luminescence chronology of Pleistocene marine terraces of Capo Vaticano peninsula (Calabria, southern Italy). *Quaternary International* 232, 114–121.
- Bordoni, P., Valensise, G., 1998. Deformation of the 125 Ka marine terrace in Italy: tectonic implications. In: Stewart, I.S., Vita-Finzi, C. (Eds.), *Coastal Tectonics*. Geol. Soc. London, Spec. Publ., vol. 146, pp. 71–110.
- Braitenberg, C., Mariani, P., Tunini, L., Grillo, B., Nagy, I., 2011. Vertical crustal motions from differential tide gauge observations and satellite altimetry in southern Italy. *Journal of Geodynamics* 51, 233–244.
- Brückner, H., Kelterbaum, D., Marunchak, O., Porotov, A., Vöth, A., 2010. The Holocene sea level story since 7500 BP – Lessons from the Eastern Mediterranean, the Black and the Azov Seas. *Quaternary International* 225 (2), 160–179.
- Camassi, R., Stucchi, M., 1997. NT4.1: un catalogo parametrico di terremoti di area italiana al di sopra della soglia di danno. <http://emidius.mi.ingv.it/NT/>.
- Carobene, L., Dai Prà, G., 1990. Genesis, chronology and tectonics of the quaternary marine terraces of the Tyrrhenian coast of northern Calabria. *Il Quaternario* 3 (2), 75–94.
- Cosentino, D., Gliozzi, E., 1988. Considerazioni sulla velocità di sollevamento dei depositi eolitici dell'Italia meridionale e della Sicilia. *Memorie della Società Geologica Italiana* 41, 127–143.
- Chiarabba, C., Jovane, L., Di Stefano, R., 2005. A new view of Italian seismicity using 20 years of instrumental recordings. *Tectonophysics* 395, 251–268.

- CPTI-Working Group, 2004. Catalogo Parametrico dei Terremoti Italiani. Ver. 2004 (CPTI04). INGV, Bologna. <http://emidius.mi.ingv.it/CPTI04/>.
- Cucarzi, M., Iannelli, M.T., Rivolta, A., 1995. The coastal site of Bivona. Its detection and its environmental changes through geoarchaeological explorations. In: Egypt, T.G.S.O. (Ed.), Proceedings of International Conference "Geosciences and Archaeology in the Mediterranean Countries", Cairo 28–30 November 1993, pp. 149–168.
- Columella, De Re Rustica, XVII, 50 BC.
- D'Alessandro, L., Raffi, R., Catizzone, A., 1987. Il litorale del Golfo di S. Eufemia (Calabria): indagini sulle variazioni della spiaggia nell'ultimo secolo. Ministero Pubbl. Istruz., Prog. Naz. "Dinamica e Tutela delle Coste", Roma.
- D'Amico, S., Orecchio, B., Presti, D., Zhu, L., Herrmann, R., Neri, G., 2010. Broadband waveform inversion of moderate earthquakes in the Messina Straits, southern Italy. *Physics of the Earth and Planetary Interiors* 179, 97–106.
- D'Amico, S., Orecchio, B., Presti, D., Gervasi, A., Zhu, L., Guerra, I., Neri, G., Herrmann, R., 2011. Testing the stability of moment tensor solutions for small earthquakes in the Calabro-Peloritan arc region (southern Italy). *Bollettino di Geofisica Teorica ed Applicata* 52 (2), 283–298.
- Desruelles, S., Fouache, E., Ciner, A., Dalongeville, R., Pavlopoulos, K., Kosun, E., Coquinot, Y., Potdevin, J.L., 2009. Beachrocks and sea level changes since Middle Holocene: comparison between the insular group of Mykonos-Delos-Rhenia (Cyclades, Greece) and the southern coast of Turkey. *Global and Planetary Change*. ISSN: 0921-8181 66 (1–2). ISSN: 0921-8181, 19–33. doi:10.1016/j.gloplacha.2008.07.009. Quaternary sea level changes: records and processes.
- Devoti, R., Pietrantonio, G., Pisani, A., Riguzzi, F., Serpelloni, E., 2010. Present day kinematics of Italy. In: Beltrando, M., Peccerillo, A., Mattei, M., Conticelli, S., Doglioni, C. (Eds.), *The Geology of Italy: Tectonics and Life along Plate Margins*. J. Virtual Explorer, Electronic Edition. ISSN: 1441-8142, vol. 36. doi:10.3809/jvirtex.2010.00237. paper 2.
- Doglioni, C., Innocenti, F., Mariotti, G., 2001. Why Mt Etna? *Terra Nova* 13, 25–31.
- Ferranti, L., Antonoli, F., Mauz, B., Amorosi, A., Dai Pra, G., Mastroruzzi, G., Monaco, C., Orrù, P., Pappalardo, M., Radtke, U., Renda, P., Romano, P., Sansò, P., Verrubbi, V., 2006. Markers of the last interglacial sea level highstand along the coast of Italy: tectonic implications. *Quaternary International* 145–146, 30–54.
- Ferranti, L., Monaco, C., Antonoli, F., Maschio, L., Kershaw, S., Verrubbi, V., 2007. The contribution of regional uplift and coseismic slip to the vertical crustal motion in the Messina Straits, southern Italy: evidence from raised late Holocene shorelines. *Journal of Geophysical Research* 112, B06401. doi:10.1029/2006JB004473.
- Ferranti, L., Antonoli, F., Anzidei, M., Monaco, C., Stocchi, P., 2010. The timescale and spatial extent of vertical tectonic motions in Italy: insights from relative sea-level changes studies. *Journal of the Virtual Explorer* 36 (Paper 30). <http://virtualexplorer.com.au/>.
- Hemming, N.C., 1969. Archaeological evidence for eustatic changes of sea level and earth movements in the Western Mediterranean in the last 2000 years. *Special Paper – Geological Society of America* 109, 1–125 pp.
- Hemming, N.C., Webb, C.O., 1986. Tectonic and eustatic coastal changes during the last 10,000 years derived from archaeological data. *Zeitschrift für Geomorphologie, N.F. (Suppl. 62)*, 1–29.
- Fouache, E., Pavlopoulos, K. (Eds.), 2005. Sea Level Changes in Eastern Mediterranean during Holocene. Indicators and Human Impacts. *Zeitschrift für Geomorphologie, Supplementbände*, vol. 137, p. 193.
- Ghisetti, F., 1979. Evoluzione neotettonica dei principali sistemi di faglie della Calabria centrale. *Bollettino della Società Geologica Italiana* 98, 387–430.
- Ghisetti, F., 1981. L'evoluzione strutturale del bacino plio-pleistocenico di Reggio Calabria nel quadro geodinamico dell'arco Calabro. *Bollettino della Società Geologica Italiana* 100, 433–466.
- Goes, S., Giardini, D., Jenny, S., Hollenstein, C., Kahle, H.G., Geiger, A., 2004. A recent tectonic reorganization in the south-central Mediterranean. *Earth and Planetary Science Letters* 226, 335–345.
- Gvirtzman, Z., Nur, A., 1999. The formation of Mount Etna as the consequence of slab rollback. *Nature* 401, 782–785.
- Guerra, I., 2007. Earthquakes in Calabria Databases. SyNaRMA Interreg IIIB Project ARCHIMED (2000–2006), Technical Report. Physics Dept., Calabria University.
- Lacquaniti, L., 1952. Variazioni di linee di spiaggia nei golfi di S. Eufemia e Gioia (Calabria Tirrenica). *Atti XV Congresso Nazionale della Società Geologica Italiana* 1, 278–283. I.T.E.R., Torino.
- Lambeck, K., Antonoli, F., Purcell, A., Silenzi, S., 2004a. Sea level change along the Italian coast for the past 10,000 yrs. *Quaternary Science Revue* 23, 1567–1598.
- Lambeck, K., Anzidei, M., Antonoli, F., Benini, A., Esposito, E., 2004b. Sea level in Roman time in the Central Mediterranean and implications for modern sea level rise. *Earth and Planetary Science Letters* 224, 563–575.
- Lambeck, K., Purcell, A., 2005. Sea-level change in the Mediterranean Sea since the LGM: model predictions for tectonically stable areas. *Quaternary Science Reviews* 24, 1969–1988.
- Lambeck, K., Antonoli, F., Anzidei, M., Ferranti, L., Leoni, G., Scicchitano, G., Silenzi, S., 2011. Sea level change along Italian coast during Holocene and a projection for the future. *Journal of Quaternary International* 232.
- Lena, G., 1989. Vibo Valentia. Geografia e morfologia della fascia costiera e l'impianto del porto antico. *Annali della Scuola Normale Superiore di Pisa* 19 (2), 583–607. Pisa.
- Locardi, E., Nicolich, R., 1988. Geodinamica del Tirreno e dell'Appennino Centro-Meridionale: la nuova carta della Moho. *Memorie della Società Geologica Italiana* 41, 121–140.
- Loreto, M.F., Zgur, F., Pettenati, F., Facchin, L., Fracassi, U., Tomini, L., 2011. Active tectonics and potential seismogenic behavior of newly imaged structures in the Gulf of Santa Eufemia (southern Italy). *EGU 2011, Vienna (Austria)*, 4–8 April, vol. 13.
- Mariottini, S., 2001. Volontariato e archeologia subacqua: esperienze di ricerca in Calabria. In: *Lezioni Fabio Faccenna*. Edipuglia, Bari.
- Medici, G., Principi, P., 1939. Le bonifiche di S. Eufemia e Rosarno. Zanichelli, Bologna.
- Melis, S., 1998. Variation des rivages aux environs de la ville de Nora (Sardaigne Sud-Ouest – Italie) d'après les données géoarchéologiques. In: Vertmeuller, F., De Dapper, M. (Eds.), *Géochéologiques des Paysages de l'antiquité classique*, pp. 127–135.
- Mercalli, G., 1906. Alcuni risultati ottenuti dallo studio del terremoto calabrese dell'8 settembre 1905, vol. 36. Acc. Pontaniana, Napoli. 1–9.
- Michellini, A., Lomax, A., Nardi, A., Rossi, A., Palombo, B., Bono, A., 2005. A modern re-examination of the locations of the 1905 Calabria and the 1908 Messina Straits earthquakes. *Geophysical Research Abstracts* 7, 07909. European Geosciences Union.
- Miyauchi, T., Dai Pra, G., Sylos Labini, S., 1994. Geochronology of Pleistocene marine terraces and regional tectonics in the Tyrrhenian coast of southern Calabria, Italy. *Il Quaternario* 7 (1), 17–34.
- Piatanesi, A., Tinti, S., 2002. Numerical modelling of the September 8, 1905 Calabria (southern Italy) tsunami. *Geophysical Journal International* 150, 271–284.
- Pirazzoli, P.A., 1976. Sea level variations in the northwest Mediterranean during Roman times. *Science* 194, 519–521.
- Pirazzoli, P.A., 1996. *Sea-level Changes – the Last 20,000 Years*. Wiley, Chichester.
- Pondrelli, S., Salimbeni, S., Ekström, G., Morelli, A., Gasperini, P., Vannucci, G., 2006. The Italian CMT dataset from 1977 to the present. *Physics of the Earth and Planetary Interiors* 159 (3–4), 286–303.
- Reasenber, P.A., Oppenheimer, D., 1985. FPFIT, FPLOT and FPPAGE: FORTRAN computer programs for calculating and displaying earthquakes fault plane solutions. U.S. Geological Survey. Open File Rep., 85–739.
- Riuscetti, M., Schick, R., 1974. Earthquakes and tectonics in southern Italy. *Bollettino di Geofisica Teorica ed Applicata* 17, 59–75.
- Rizzo, G.B., 1907. Contributo allo studio del terremoto della Calabria del giorno 8 settembre 1905. *Atti della Accademia Peloritana dei Pericolanti* 22 (1), 3–86.
- Salmoiraghi, F., 1884. Terrazzi quaternari sul litorale tirrenico della Calabria Citra. *Bollettino del R. Comitato Geologico d'Italia* XVII, 281–316.
- Schmidt, G., 1966. Antichi porti d'Italia. I porti delle colonie greche. *L'Universo* XLVI, 253–296.
- Schmidt, G., 1974. Il livello antico del mar Tirreno. *Testimonianze da Resti Archeologici*. E. Olschki, Firenze, pp. 323.
- Stuiver, M., Reimer, P.J., Bard, E., Beck, J.W., Burr, G.S., Hughen, K.A., Kromer, B., McCormac, G., Van der Plicht, J., Spurk, M., 1998. Intcal 98 radiocarbon age calibration, 24,000–0 cal BP. *Radiocarbon* 40 (3), 1041–1083.
- Tallarico, A., Dragoni, M., Anzidei, M., Esposito, A., 2003. Modeling long-term ground deformation due to the cooling of a magma chamber: case of Basiluzzo island, Aeolian Islands, Italy. *Journal of Geophysical Research* 108 (B12), 2568. doi:10.1029/2002JB002376.
- Tortorici, G., Bianca, M., de Guidi, G., Monaco, C., Tortorici, L., 2003. Fault activity and marine terracing in the Capo Vaticano area (southern Calabria) during the Middle-Late Quaternary. *Quaternary International* 101–102, 269–278.
- Vannucci, G., Pondrelli, S., Argnani, A., Morelli, A., Gasperini, P., Boschi, E., 2004. An atlas of Mediterranean seismicity. *Annals of Geophysics* 47, 1. Suppl. with CDR.
- Westaway, R., 1990. Present-day kinematics of the plate boundary zone between Africa and Europe, from the Azores to the Aegean. *Earth and Planetary Science Letters* 96, 393–406.
- Westaway, R., 1993. Quaternary uplift of southern Italy. *Journal of Geophysical Research* 98, 21741–21772.
- Wortel, M.J.R., Spakman, W., 2000. Subduction and slab detachment in the Mediterranean-Carpathian region. *Science* 290, 1910–1917.